

2007

THE IMPACTS OF ATMOSPHERICALLY DERIVED METALS ON COASTAL MARINE SYSTEMS

Orif, Mohammed

<http://hdl.handle.net/10026.1/1839>

<http://dx.doi.org/10.24382/4272>

University of Plymouth

All content in PEARL is protected by copyright law. Author manuscripts are made available in accordance with publisher policies. Please cite only the published version using the details provided on the item record or document. In the absence of an open licence (e.g. Creative Commons), permissions for further reuse of content should be sought from the publisher or author.

**THE IMPACTS OF ATMOSPHERICALLY DERIVED METALS ON COASTAL
MARINE SYSTEMS**

by

Mohammed Orif

A thesis submitted to the University of Plymouth

in partial fulfilment for the degree of

DOCTOR OF PHILOSOPHY

School of Earth, Ocean and Environmental Sciences

Faculty of Science

January 2007

Univ	200
Item No	91007630078
Sh	THESIS 557.5113 OR1

THE IMPACTS OF ATMOSPHERICALLY DERIVED METALS ON COASTAL MARINE SYSTEMS

Mohammed Orif

Abstract

The total concentrations of trace metals (Al, Fe, Mn, Co, Na, Cu, Zn, Mo, Ni, V, Cd, Pb) have been determined in the marine aerosol at two contrasting coastal sites, Plymouth UK, (December 2001 to April 2003) and Jeddah, Saudi Arabia (August 2002-January 2004). Trace metal concentrations in the Plymouth urban aerosol were lower (2-13 times) than those observed at other comparative UK urban locations and generally comparable with those observed at European coastal non-urban locations. Statistically significant differences were found in aerosol metal concentrations associated with populations of contrasting air mass sources (i.e. Atlantic and UK/European), being greatest in the UK/European air mass sector for Al, Fe, Mn, Cd, Mo and Pb, owing to enhanced source emission rates from continental Europe. Based on the current work, refined budgets for Ni and Pb for the English Channel were presented. The budgets clearly indicated the importance of the English Channel sediments as both a sink (Ni) and a source (Pb). Aerosol concentrations in the Red Sea Marine Aerosol (RSMA) for the crustally sourced elements Al, Mn and Fe were higher (typically 2.7-3.1 times) than those detected at other comparative sites (i.e. Eastern Mediterranean). The aerosol population associated with the Middle and Southern Saudi Arabia (SSA) air mass had the greatest concentrations of Al, Fe, Mn and Co, whereas, the lowest were found associated with the open Red Sea (RS) marine aerosol. Summer enhancement of aerosol metals was attributed to seasonal dust re-suspension as documented in the literature. Red Sea trace metal budgets were presented and would suggest that the sediments are an important source for all elements to the Red Sea water column except for Co and Cd. This work has, therefore, provided unique insights into influences on the air/sea exchange of trace metals and their subsequent impacts and fates in two contrasting marine systems.

ACKNOWLEDGEMENTS

Firstly, I would like to thank Dr Malcolm Nimmo, Prof Paul Worsfold and Dr Eric Achterberg for their relentless support, guidance and advice during my research at Plymouth. I must also thank the University of Liverpool for their helpful support to let me use their sampler in Plymouth station, also for King Abdul Aziz University for purchasing the second sampler located at the Jeddah station. I must also thank the Ministry of Higher Education (Saudi Arabia) for the financial support.

I would like to acknowledge all of those in the School of Earth, Ocean and Environmental Sciences, especially Debbie, Tamsin, Donella, Elaine, Jo, Lee and the technical support group – Ian, Sally, Andrew, Andy, Jeremy and Adrian. A sincere thanks to Dr Andy Fisher for all his advice and help in the laboratory. In addition, a big thanks to Dr Sultan Al lihaibi, Dr Radwan Al frawati, Dr Mohammed El sayed and Mohamed Al hayeg from King Abdul Aziz University for their support during sampling at Jeddah station.

To the “106” group, a sincere thanks to Rich, Phil, Paulo, Grady, Omaka, Laura, and Marie and to all of those past members. Thanks to all of the “106” neighbours, especially to Nui, my Thai friend.

I am especially grateful to my wife who helps me through the whole process. Without you this would have never been possible. You will always be in my mind. My two sons “my two precious sons”.

Dad and Nana I wish you could be here.

Finally, my loving thanks to Mom, Papa for your never ending support and guidance throughout the years. I am truly grateful.

AUTHOR'S DECLARATION

At no time during the registration for the degree of Doctor of Philosophy has the author been registered for any other University award. The work was financed with the aid of a studentship by the Ministry of Higher Education, Saudi Arabia.

A programme of advanced study was undertaken, which included aerosol sampling at the Red Sea coast, Jeddah, Saudi Arabia using a dedicate sampler and another sampling station was located at Plymouth. Relevant scientific seminars and conferences were regularly attended at which work was presented.

All other data presented in this thesis was prepared by the author, whom the ownership rests with. Before using this data in any presentation or printed publication, please contact the author and include full acknowledgements.

Training programmes attended

A programme of training was undertaken, which included training in aerosol trace metal total digestion and detection at University of Plymouth and experience of collecting high-volume aerosol samples from Jeddah, Saudi Arabia (King Abdul Aziz University).

Presentations and conferences attended

Attended meeting: 'Formation and fate of aerosols from road vehicles and gas turbines' at University College London. 18th September 2001.

Poster presentations:

- 'Atmospheric Input of Trace Elements', at UMIST (Manchester), The RSC meeting 2001.

- ‘The Impacts of Atmospherically Derived Metals on Coastal Marine Systems’, at University of Plymouth, Challenger conference 2002.
- ‘The Impacts Of Atmospherically Derived Metals On Coastal Marine Systems’, at UEA (Norwich), Progress in Chemical Oceanography 2003.

Oral presentation:

- ‘Characteristic of Plymouth Aerosol Trace Elements’, University of Plymouth, Departmental presentation 2001.
- ‘Atmospheric Input of Trace Elements to two contrasting sites; Jeddah (South West Asia) and Plymouth (South West UK)’, University of Plymouth, Departmental presentation 2002.
- ‘Atmospheric Input of Trace Elements’, University of Plymouth, Beach 2003.
- ‘The Trace Metal Chemical Character of the Red Sea Marine Aerosol’, University of Plymouth, Beach meeting 2005.

LIST OF CONTENTS

Abstract

Acknowledgements

Author's declaration

Chapter 1 <i>Introduction</i>	1
1.1 Importance of atmospheric transport to marine metal cycles	2
1.2 Aims and objectives	3
1.3 Structure of the thesis	4
Chapter 2 <i>Trace metals in the marine atmosphere</i>	6
2.1 Introduction	7
2.2 Global marine biogeochemical cycles of aerosol associated trace metals	7
2.3 The trace metal composition of the marine aerosol and its sources	13
2.3.1. Natural background aerosol material	18
2.3.2 Anthropogenically derived aerosols	20
2.4 Methods of aerosol trace metal source identification	20
2.4.1 Aerosol particles size distribution	21
2.4.2 Air mass movement	24
2.4.3 Use of the Enrichment Factor to identify sources	25
2.5 Modes of deposition of atmospheric trace metals to the sea surface	27
2.5.1 Dry deposition	27
2.5.2. Wet deposition	33
2.6 Aerosol fate in seawater and rainwater	35
2.7 Solubility of aerosol associated trace metals in seawater and rainwater	37
2.7.1 Solid state speciation of aerosol associated elements	38
2.7.2 Dissolved organic ligands	40

3.4. Application of the sequential leach procedure to determine the trace metal solid state speciation in aerosol samples	71
3.4.1 Reagents preparation	72
3.4.2 Sequential leach procedures	72
3.5 Air mass back trajectory calculations	73
 Chapter 4 <i>Aerosol trace metal concentrations at a western English Channel urban coastal site (Plymouth)</i>	 76
4.1 Introduction	77
4.2. Background	77
4.2.1. The English Channel coastal environment	77
4.2.2 Aerosol trace metal concentrations in the English Channel	79
4.2.3 Meteorological characteristics of the English Channel	81
4.3 The chemical composition of the Plymouth coastal and semi-urban aerosol	82
4.3.1 The overall chemical characteristics of the aerosol trace metals in the Plymouth coastal and semi-urban aerosol.	82
4.3.2 Comparison of the aerosol trace metal concentrations with literature data	85
4.3.3. Evaluation of the Plymouth aerosol trace metal sources; Application of the crustal enrichment factor (EF_{crust})	89
4.3.4 The percentage of crustal source contribution of trace metals to the Plymouth aerosol	91
4.3.5 Temporal variability in the trace metal composition of the Plymouth coastal and semi-urban aerosol population	94
4.3.6 Trace metal aerosol chemical composition in contrasting air masses influencing the Plymouth atmosphere	104
4.3.7 Aerosol trace metal EF_{crust} for different wind sectors	112

4.4 Inter-elemental relationships in the Plymouth aerosol	113
4.5 The solid state speciation signal of aerosol associated trace metals (Al, Fe, Mn, Co, Mo, Ni, Cd, Pb) in the Plymouth aerosol populations	117
4.5.1 Elemental solid state speciation signal associated with aerosol populations derived from different wind sectors	122
4.6 Total atmospheric dry depositional fluxes to the English Channel	123
4.7 Conclusions	132
 Chapter 5 <i>Aerosol trace metal trace metal concentrations at a Red Sea coastal site (Jeddah)</i>	 137
5.1 Introduction	138
5.2. Background	138
5.2.1. Red sea coastal environment	138
5.2.2. Regional Climatology	140
5.2.3. Aerosol trace element concentration and cycle in the RSMA	141
5.2.4. Aerosol sampling location	143
5.3 The trace metal chemical composition of the Jeddah Red Sea aerosol	144
5.3.1 The overall chemical characteristics of the aerosol trace metals in the Jeddah urban aerosol	144
5.3.2 Evaluation of the Jeddah aerosol trace metal sources; Application of the crustal enrichment factor (EF_{crust})	148
5.4 Temporal variations in the trace metal concentration in the RSMA	151
5.5 Impact of air mass source on the aerosol trace metal concentrations in the RSMA	162
5.5.1 Seasonality of aerosol trace metal concentration associated with different air masses	169
5.6 Inter-elemental relationships within the RSMA	170

5.7 The elemental solid state speciation of the RSMA	174
5.8 Atmospheric dry deposition of trace metal to the Red Sea	178
5.8.1 Atmospheric trace metal total dry deposition and bioavailable inputs into the Red Sea	183
5.9 Trace metal budget within the Red Sea	186
5.10 Conclusions	192
 Chapter 6 <i>Conclusions and Future work</i>	195
6.1 The aerosol trace metal chemical characteristics of the Plymouth urban aerosol and RSMA	196
6.1.1 The Plymouth urban aerosol population	196
6.1.2 The Red Sea Marine Aerosol (RSMA)	198
6.2 Future work	202
 References	205
 Appendices	229
Appendix A. Samples concentrations and date collected at Plymouth and Jeddah	230
Appendix B. The ICP-AES, ICP-MS operating conditions	247
Appendix C. The equations used to calculate the trace metal budget in the Red Sea.	248

LIST OF TABLES

Table 2.1. Comparison of atmospheric and riverine inputs of metals to the total ocean surface (10^9 g/yr) (After Duce et al., 1991)	8
Table 2.2. Literature data for geometric mean concentrations and ranges for trace elements in aerosols from a number of representative marine environments. concentrations expressed as ng m^{-3} of air	14
Table 2.3. Average concentration (pmol m^{-3}) of aerosol associated trace metals at Mace Head (Ireland) in two contrasting air masses; a polluted south easterly air mass and a marine dominated air mass (From Spokes et al., 2001).	17
Table 2.4. Estimates of the global emissions of particulate material to the atmosphere (units, 10^{12} g yr^{-1}) (Chester, 2000).	19
Table 2.5. Global atmospheric emissions of trace metals (adapted from Duce et al. 1991).	20
Table 2.6. EF_{crust} values for some anomalously enriched crustal (AEE) elements in marine aerosols of contrasting locations.	29
Table 2.7. Atmospheric flux of mineral aerosol to the ocean (After Duce et al., 1991) (Brackets show the % contribution of dry and wet to the total).	30
Table 2.8 Elemental flux (wet dry and total) expressed as $\mu\text{g m}^{-2}\text{yr}^{-1}$.	30

Table 2.9. Summary of the elemental settling velocities (cm s^{-1}) used to calculate elemental dry deposition fluxes in recent studies	32
Table 2.10. Concentrations ($\mu\text{g l}^{-1}$) of trace metals in rainwater from different marine sites.	36
Table 2.11. Range of literature seawater solubilities of aerosol associated trace metals.	38
Table 3.1 Typical elemental concentrations (mg kg^{-1}) (except for Al, Fe and Pb expressed as percentage) and recoveries using the total acid digestion procedure (n=9). Recoveries assessed using the CRM (NIST 1648).	62
Table 3.2 Summary of the elemental standard solution concentration ranges for the contrasting sampling sites in the current study. Al, Fe and Na concentrations are expressed in mg L^{-1} , whereas the remaining elements are expressed in $\mu\text{g L}^{-1}$.	67
Table 3.3. The calculated and reported ICP-AES elemental instrumental limits of detection (p.p.m.) for correspondent emission line (using ICP-AES).	67
Table 3.4 Calculated and reported ICP-MS elemental instrumental limits of detection expressed in $\mu\text{g L}^{-1}$.	67
Table 3.5. Determined operational aerosol blank values compared with the average trace metal concentrations observed in the sample acid	

digest extracts (expressed in $\mu\text{g ml}^{-1}$ for ICP-AES and flame photometry / ng ml^{-1} for ICP-MS).	71
Table 3.6 The range of standards used for the calibration in $\mu\text{g mL}^{-1}$ (Al and Fe in mg mL^{-1}), for each of the sequential leach stages.	75
Table 4.1. The annual direct industrial discharges (tonnes yr^{-1}) to the English Channel from both the British and French (Seine) coastlines.	77
Table 4.2. Mean trace metals concentration (ng m^{-3}) detected in contrasting air sectors of the English Channel aerosol (Wells 1999)). (significant intervals represent ± 1 s.d.).	80
Table 4.3. Wet and dry trace elemental fluxes ($\text{ng cm}^{-2} \text{yr}^{-1}$) to the western English Channel sea surface.	80
Table 4.4. Geometric and arithmetic mean of aerosol trace metal concentrations (ng m^{-3}) observed at Plymouth between 24 th May and 20 th December 2002.	83
Table 4.5. Geometric mean concentrations (ng m^{-3}) of aerosol associated trace metals at different UK urban sites.	84
Table 4.6. Comparison of trace elemental aerosol concentrations (ng m^{-3}) in coastal European atmospheres.	87

Table 4.7. EF_{crust} for the Plymouth urban aerosol (in samples collected between 24 th May and 18 th December 2002).	89
Table 4.8. Comparison of EF_{crust} values from the current study with values from Western Europe coastal atmospheres.	90
Table 4.9. Statistical summary of the calculated percentage crustal contribution to elements in the Plymouth Urban aerosol (for samples collected between 24 th May and 18 th December 2002, i.e. samples 41-195).	91
Table 4.10. Aerosol trace metal concentrations (expressed as ng m^{-3}) in the Plymouth urban aerosol collection between (i) 10 th December 2001 – 8 th May 2002 and (ii) 8 th May -18 th December 2002.	95
Table 4.11. Comparison of aerosol associated trace element concentrations (geometric mean, ng m^{-3}) at Plymouth (samples 1-40), with those observed at Liverpool and Preston.	96
Table 4.12. The geometric mean concentration (ng m^{-3}) of trace metals in the Plymouth Urban environment during day and night-time sampling (sample 1-40) 10 th December 01 – 9 th May 02.	96
Table 4.13. The geometric mean aerosol trace metal concentrations in the Plymouth Urban aerosol population (n=91) between 24 th May-18 th December 2002.	98
Table 4.14. Seasonal variability of aerosol trace metal concentrations (ng m^{-3})	

Table 4.15. Aerosol associated trace elements concentrations (ng m^{-3}), range and standard deviation in the contrasting air masses reaching the sampling site at (Plymouth).	107
--	-----

Table 4.16. Comparison of air mass trace metal concentrations for the current study with defined air mass trace metal concentrations from other studies.	109
---	-----

Table 4.17. Crustal Enrichment factors in total sampling.	111
--	-----

Table 4.18 Pearson correlation coefficients between log transformed aerosols trace metal concentrations in the Plymouth atmosphere. *indicates a significant correlation ($p < 0.05$).	113
--	-----

Table 4.19. Statistical summary of the aerosol trace metal solid state speciation signature for the overall Plymouth aerosol population.(Each stage expressed as a % of the total metal aerosol concentration; $n=20$).	118
---	-----

Table 4.20. Comparison of sequential leach result of the Plymouth aerosol with other European marine aerosols in wt %.	123
---	-----

Table 4.21. Statistical summary of the three stage sequential leach (standard deviation in parentheses) for the different wind sources, Geometric mean in % for all elements.	124
--	-----

Table 4.22. Elemental settling velocities used in the calculation of (V_d) dry deposition adopted from the literature for the current study (Spokes et al., 2001 and Duce et al., 1991).	126
Table 4.23. Literature elemental settling velocities (cm s^{-1}) for European coastal regions.	129
Table 4.24. The flux (expressed as $\mu\text{g m}^{-2} \text{yr}^{-1}$ except for Al, Fe, Mn and Na which are expressed as $\text{mg m}^{-2} \text{yr}^{-1}$) of aerosol associated trace metals to the English Channel. Presented data are weighted according to air mass influence (see text for further discussion).	130
Table 4.25. A comparison of dry deposition fluxes from Plymouth (current study) with other European regions (fluxes are expressed as $\mu\text{g m}^{-2} \text{yr}^{-1}$ except for Al, Fe, Mn and Na which are expressed as $\text{mg m}^{-2} \text{yr}^{-1}$).	130
Table 4.26. Bio-available and air mass weighted fluxes (expressed as $\mu\text{g m}^{-2} \text{yr}^{-1}$ except for Al, Fe, Mn and Na which are expressed as $\text{mg m}^{-2} \text{yr}^{-1}$).	131
Table 4.27. Dry and dissolved trace metal inputs to the English Channel (t yr^{-1}).	131
Table 4.28. Geochemical budget of Ni and Pb (t y^{-1}) in the English Channel.	131
Table 5.1 Concentration of trace metal in aerosol from samples collected in the Arabian Sea (Chester et al., 1985; expressed as ng m^{-3}) and trace metal in dust fall from Red Sea Behairy et al., (1985; expressed as $\mu\text{g g}^{-1}$)	

Table 5.2. The trace metal concentrations (ngm^{-3}) in the Red Seas Marine Aerosol (RSMA); Comparison with values from the literature of coastal systems boarded by arid regions	146
Table 5.3. A comparison of the EF_{crust} (calculated using $(\text{E}/\text{Al})_{\text{crust}}$ ratios from Taylor 1964) for the RSMA with those determined at other Marine Systems	149
Table 5.4. Geometric mean aerosol trace metal concentrations (expressed as ng m^{-3} except for Al, Fe and Mn expressed as $\mu\text{g m}^{-3}$) in the RSMA for winter and summer period.	156
Table 5.5. The % influence of each air mass back trajectory category during the sampling period.	159
Table 5.6. Geometric means (arithmetic means \pm standard deviation) of the characteristic air mass sector trace metal aerosol concentrations (ng m^{-3}).	164
Table 5.7 Statistical differences between air sector elemental aerosol concentrations are highlighted with an “*”. (SSA = Middle and Southern Saudi Arabia; N= Northern Saudi Arabia; E= Egyptian; RS= Red Sea).	166
Table 5.8. Statistical difference (at 95 % confidence level) between summer and	

Table 5.9. Pearson correlation coefficients between log transformed aerosols

trace metal concentrations in the RSMA. *indicates a

non-significant correlation ($p < 0.05$).

171

Table 5.10. Summary of the elemental aerosol solid state speciation in the RSMA

175

Table 5.11. Summary of the three stage sequential leach for the different

wind sources, mean in % for all elements.

176

Table 5.12. Comparison of trace metal dry deposition fluxes expressed as $\mu\text{g m}^{-2}$ yr^{-1} ($\text{mg m}^{-2} \text{yr}^{-1}$ for Al, Fe and Mn) to European coastal zones.

183

Table 5.13. The atmospheric total dry inputs (tons y^{-1}) of trace metals to the Red

Sea. The "bioavailable" fraction is quoted in brackets for selected

elements. (* after Koçak et. al., 2006; § Saharan samples carried out

in this study).

185

Table 5.14. Dissolved trace metal concentration ($\mu\text{g L}^{-1}$) in surface and deep waterof The Red Se, expressed as $\mu\text{g L}^{-1}$ (nM).

186

Table 5.15. Estimate of the layer transport (surface, sub-surface and deep layer)at Bab Al-mandeb in the literature (inflow +, Outflow -, in 10^{-4} $\text{m}^3 \text{s}^{-1}$).

191

Table 5.16. Elemental flux in the Red Sea (t yr^{-1}).

192

LIST OF FIGURES

- Figure 2.1.** Vertical profile of Al at (a) station 11 and (b) station 35 (c) the location of sampling stations, (after Kramer et al., 2004). 10
- Figure 2.2.** Lead emission (tonnes/annum) from traffic and industrial sources in Switzerland against time (BUWAL, 1995) 17
- Figure 2.3** Aerosol particles distribution according to particle size and formation (from Whitby 1977). 23
- Figure 2.4** SEM Photomicrographs of airborne particles (a) a fly ash particle (b) solid-driven kaloinite agglomerates (c) soot aggregates (d) cubes of sea salts. Images a, b and c after Xie et al., (2005). Image d is from Moreno et al., (2004). 23
- Figure 2.5.** The influence of particle size on modelled deposition velocity (after Slinn and Slinn, 1980). 31
- Figure 2.6.** Relationship between enrichment factors and dry deposition velocities of elements in aerosol (Cawse 1981). 31
- Figure 2.7.** Schematic representation of alternatives for the fate of trace metals at the air-sea interface (After Lion & Leckie, 1981). 35
- Figure 2.8.** Solid state speciation of (a) urban aerosol and (a) saharan Aerosol, (crustal) (after Chester et al. 1989). 40

Figure 3.1 The Sierra Anderson –TSP Hi-Vol.GS2312 sampler, as used in The current study at Jeddah (excluding cascade impactor attachment).	53
Figure 3.2 Location of aerosol sampling site to the north of Jeddah city, Saudi Arabia	56
Figure 3.3 Location of aerosol sampling sites at Plymouth, Devon UK.	57
Figure 3.4 The designated HF fume cupboard	61
Figure 3.5 The major components of the ICP-AES	65
Figure 3.6 The major components of the ICP-MS	65
Figure 3.7 The main instrumental components of a flame photometer.	69
Figure 3.8. An example of a 3 day back-trajectory arriving at Jeddah, starting on the 23 rd August 2003 ending on 25 th August 2003 (lines with triangles represent an altitude of 100 m at the sampling site whereas lines with squares represent an altitude of 500 m; lastly the line with circles represent an altitude of 1000 m altitude).	75
Figure 4.1. Location of sampling site (Plymouth).	78
Figure 4.2. Air masses influencing the British Isles (after Barry and Chorley 1992).	83

Figure 4.3. % Crustal contribution against EF_{crust} (a) Mn and (b) Co.	93
Figure 4.4. Temporal variability of (a) Al (b) Fe (c) Mn and (d) Co concentrations (log10) in the Plymouth aerosol	100
Figure 4.5. Temporal variability of (a) Ni (b) V and (c) Zn concentrations (log10) in the Plymouth aerosol	101
Figure 4.6. Temporal variability of (a) Cd (b) Mo (c) Pb and (d) Na concentrations (log10) in the Plymouth aerosol	102
Figure 4.7. Na concentration (ng m^{-3}) vs wind speed (m s^{-1}) for onshore wind during the winter ($r^2=0.5$; $P=0.038$; $n=17$).	104
Figure 4.8. Wind sectors of Atlantic (1) and Europe and UK (2).	105
Figure 4.9. Wind rose for the period 1991-2000 at Plymouth	106
Figure 4.10. (a) European and UK air mass (sample 117) and (b) Atlantic air mass (sample 114).	107
Figure 5.1. Temporal variability of (a) Al (b) Fe (c) Mn and (d) Co concentrations (log10) in the Red Sea marine aerosol.	153
Figure 5.2. Temporal variability of (a) Ni (b) Cu (c) Mo and (d) V concentrations	

(log10) in the Red Sea marine aerosol.	154
Figure 5.3. Temporal variability of (a) Pb (b) Zn and (c) Cd concentrations (log10) in the Red Sea marine aerosol.	155
Figure 5.4. Monthly mean TOMS AI ($\times 10$) (1980–1992). After Engelstaedter et al., (2006).	157
Figure 5.5. Comparison of seasonal of dust (Tegen et al., 1996 and Mahowald et al., 1999) and remotely sensed absorbing Aerosol Index from the Total Ozone Mapping Spectrometer (TOMS AI) average of 5 years (1986-1990).	158
Figure 5.6. Air mass sectors of (i) Egyptian (E) (ii), Northern Saudi Arabia (N) (iii), Southern + middle Saudi Arabia (SSA) (iv) and Red Sea (RS).	162
Figure 5.6. Air mass sectors of (i) Egyptian (E) (ii), Northern Saudi Arabia (N) (iii), Southern + middle Saudi Arabia (SSA) (iv) and Red Sea (RS).	162
Figure 5.7. Comparison of the elemental solid state speciation signal for the RSMA population and that of the Saharan aerosol end member population (Chester <i>et al.</i> , 1989).	176
Figure 5.8. Simplified model of the trace metal fluxes in the Red Sea	187

Chapter 1

Introduction

1.1 Importance of atmospheric transport to marine metal cycles

Up until recently it was thought that rivers were quantitatively the most important source of trace metals from land into the oceans. However, from recent studies it is now accepted that trace metal atmospheric inputs are large enough to be equal to or exceed those of rivers (Duce et al., 1991; Martin et al., 1989; and Chester et al., 1993). In addition, atmospheric deposition of trace metals in surface open ocean waters has resulted in surface seawater concentration enrichments. Classic examples of this have been documented for Pb (Veron et al., 1993) and P (Migon et al., 2001). Over the last decade it has also become apparent that the deposition of atmospheric mineral dust to the oceans may play an important role in primary productivity (Coale et al., 1996; Millero, 1996; Martin et al., 1991; Martin et al., 1990; Martin and Gordon 1988). More recently Spokes et al., (2001) demonstrated that the atmosphere is a source of trace metal nutrient constituents (e.g. Fe) to remote oceanic regions.

The quantitative evaluation of trace metals fluxes and their fate are essential to our understanding of their impact on marine biogeochemical cycles. The flux of aerosol associated trace metals to the sea surface is controlled by 'dry' and 'wet' deposition modes. These fluxes will be influenced by the variability of aerosol trace metal concentrations, therefore it is important to define aerosol trace metal concentrations and to understand the processes which lead to both a high degree of spatial and temporal variability. Factors influencing aerosol trace metal concentrations include (i) aerosol source, (ii) aerosol emission strength, (iii) removal processes during aerosol transport from source to sampling site and (iv) air mass transport of aerosol material. These influences have been confirmed by a large body of work defining aerosol concentrations both in coastal and open ocean environments (e.g. Duce et al., 1991; Yaaqub et al. 1991; Spokes et al. 2001; Chester et al., 2000).

In terms of European coastal systems, there are literature sources which describe aerosol concentrations in the Western Mediterranean (e.g. Chester et al., 1990; Guieu et al., 1997; Ridame et al., 1999), Eastern Mediterranean (e.g. Kubilay and Saydam 1995; Kubilay et al., 1997; Herut et al., 2001), the North Sea (e.g. Yaaqub et al., 1991; Chester et al., 1993), with additional findings for the Irish Sea marine atmosphere (Fones, 1996; Williams et al., 1998). However there is relatively little known about the aerosol trace metal characteristics of the Western English Channel marine atmosphere, although Bertho et al. (1998) considered the lead content of the atmosphere above the Eastern Channel in terms of its seasonal variability and subsequent solubility in coastal seawater. Deboudt et al., (1999) subsequently assessed the sources of pollutant aerosols above the Straits of Dover using lead isotopes. The only reported extended work carried out in the Western English Channel was that carried out by Wells (1999).

As one moves eastwards from the English Channel to the Western and Eastern Mediterranean aerosol elements, particularly those derived from crustal sources (Al, Fe, Mn and Co) are enhanced (Ridame et al., 1999; Herut et al., 2001). These coastal regions are influenced by seasonal air masses originating from North Africa which are heavily loaded with Saharan desert material. Moving even further east to the Red Sea region one would anticipate an even greater impact on the marine aerosol of these inputs. Limited amount of work has previously been carried out to measure the aerosol trace metal concentrations in the Red Sea aerosol.

1.2 Aims and objectives

Owing to the limited knowledge of aerosol trace metal concentrations in the Western English Channel and Red Sea atmospheres the following work was instigated. Aerosol sampling stations were established at Plymouth (December 2000- July 2002) and Jeddah (August 2002- January 2004) at which collection of high volume samples was carried out

to; (i) define the temporal concentrations of aerosol associated trace metals (Al, Fe, Mn, Cd, Cu, Zn, Pb Ni, Mo and Na) over a prolonged period of time (in excess of 1 year), (ii) determine the factors influencing the variability in concentrations and (iii) determine the dry deposition, flux and inputs of metals to the associated coastal zones (English Channel and Red Sea) and compare these inputs with other sources, (iv) determine the likely contrasting fates of trace metals post dry deposition, (v) model trace metal budgets in the English Channel and Red Sea. These aims will be further placed into context in Chapter 2.

1.3 Structure of the thesis

Chapter 2 reviews the recent literature, describing the trace metal composition of the marine aerosol and its sources; applied methods for the determination of aerosol trace metal sources (e.g. EF_{crust} , back trajectory analysis); modes of atmospheric deposition of trace metals to the sea surface; seawater solubility of aerosol associated trace metals and their impact post-deposition. Chapter 3 describes and appraises the sampling and analytical procedures adopted for the current study.

Chapter 4 presents the trace metal aerosol concentrations observed at the Plymouth coastal and semi-rural sampling site and the factors influencing their temporal variability (e.g. type and proximity of aerosol source contributions, air mass origins). Dry deposition fluxes and inputs to the English Channel were then calculated, along with the “bioavailable” fraction based on data derived from solid state speciation analyses of selected samples.

Chapter 5 describes for the first time the trace metal aerosol composition of the Red Sea marine aerosol. Factors influencing its variability will be presented along with estimates of dry deposition fluxes and inputs to the Red Sea.

Finally, Chapter 6 will highlight the main conclusions of the study and will compare and contrast the trace metal aerosol characteristics of the two marine systems considered in the current study, the English Channel and Red Sea. Suggestions for future work will also be presented.

Chapter 2

Trace metals in the marine atmosphere

2.1 Introduction

The biogeochemical cycling of trace metals is of great importance in the marine environment. The compartment of this cycle that involves aerosol associated trace metals is the focus of the current work. This chapter summarises the importance of atmospheric metal inputs to marine biogeochemical processes. The magnitude and effects of atmospheric metal inputs from contrasting sources to the marine aerosol are presented, along with approaches to identify these sources. Different factors affecting the concentration of aerosol associated trace metals are discussed in conjunction with methods and procedures used in the calculation of atmospheric dry and wet deposition to the sea surface. Finally, the fate and impact of aerosol associated trace metals, post-deposition, is considered in relation to their bioavailability. Factors affecting the bioavailability of aerosol trace metals are briefly discussed.

2.2 Global marine biogeochemical cycles of aerosol associated trace metals

It was highlighted in Chapter 1 that atmospheric inputs of trace elements, up until the last two decades, was assumed to be quantitatively of minor importance. However numerous studies have now firmly established the significance of such inputs (Patterson and Settle, 1987; GESAMP 1989; Martin et al., 1989; Duce et al., 1991). This is further highlighted in Table 2.1, which illustrates the global deposition of dissolved and particulate trace metals to the ocean from both atmospheric and riverine sources. The importance of atmospheric inputs is particularly apparent for coastal seas bordered by arid / industrialised regions. These include European marine systems such as the Irish Sea, North Sea, Western and Eastern Mediterranean (Chester et al., 1984; Yaaqub et al., 1991; Guieu et al., 1997; Guerzoni et al., 1999; Kubilay et al., 2000; Kocak et al., 2004).

Table 2.1. Comparison of atmospheric and riverine inputs of metals to the total ocean surface (10^9 g/yr), (after Duce et al., 1991).

Element	Atmospheric Input		Riverine Input	
	Dissolved	Particulate	Dissolved	Particulate
Cd	1.9-3.3	0.4-0.7	0.3	15
Cu	14-45	2-7	10	1500
Ni	8-11	14-17	11	1400
Zn	33-170	11-60	6	3900
As	2.3-5.0	1.3-2.9	10	80
Fe	3.2×10^3	29×10^3	1.1×10^3	110×10^3

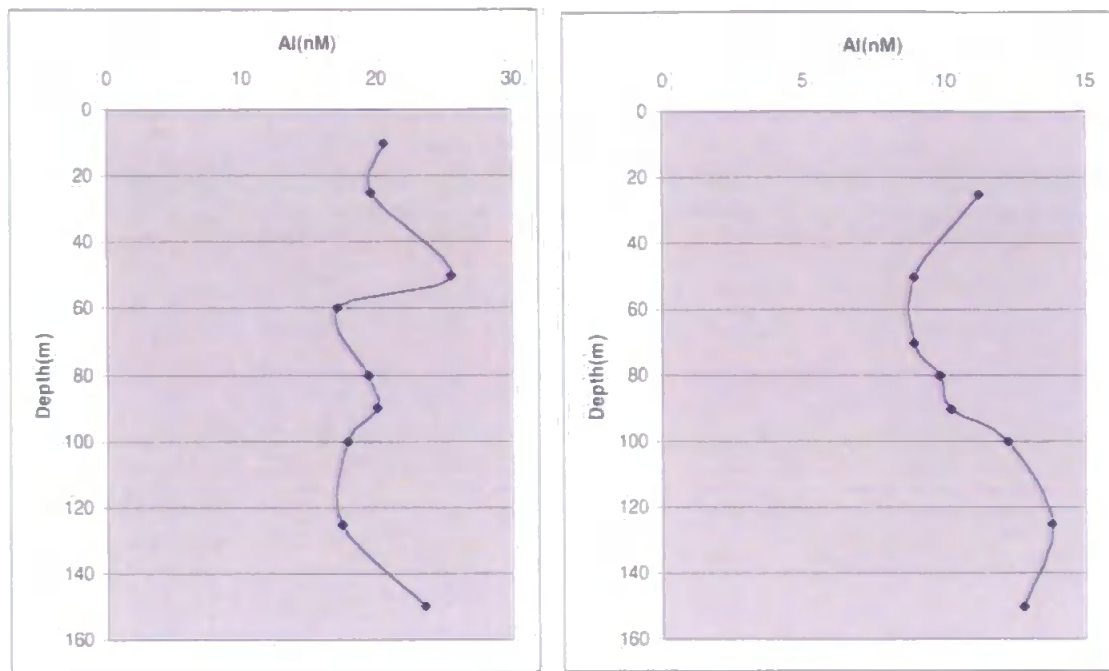
The flux of aerosol associated trace metals to the sea surface is controlled by ‘dry’ and ‘wet’ deposition modes. In the dry deposition mode, aerosols are delivered directly to the sea surface by gravitational settling. The extent and rate of trace metal dissolution from aerosol material post-deposition and hence their potential bioavailability (i.e. fate and impact) from dry deposition depends upon their particle-seawater reactivity (Chester et al., 1993; Spokes, 1994; Guerzoni et al., 1999). Likewise the impact of the trace metals deposited by wet deposition is constrained by the degree to which aerosol associated trace metals are soluble in rain water prior to deposition in seawater (Lim et al., 1994; Spokes et al., 1994). Further details of the importance of each of these atmospheric modes of input are presented in sections 2.5.1 and 2.5.2. Atmospheric inputs can influence marine metal biogeochemical cycles by (i) modifying the surface dissolved (e.g. Kramer et al., 2004) and particulate (Dixon, 1998) trace metal concentrations and (ii) impacting upon the rate of primary productivity and phytoplankton community structure.

The former effect has been illustrated for Al and Fe in the open ocean environment (Sarhou et al., 2003; Kramer et al., 2004). For example, Kramer et al., (2004) noted an increase in the dissolved Al concentration (up to 25 nM) in the surface waters off the

Canary Islands owing to atmospheric inputs from the Saharan desert. This is illustrated by Figure 2.1 which presents depth profiles highlighting a higher surface Al concentration (20.5 nM) at Station 11 (Figure 2.1 (a)) compared with that measured at station 35 (Figure 2.1 (b)) (11.2 nM), which is less influenced by surface dust deposition during intense Saharan dust events.

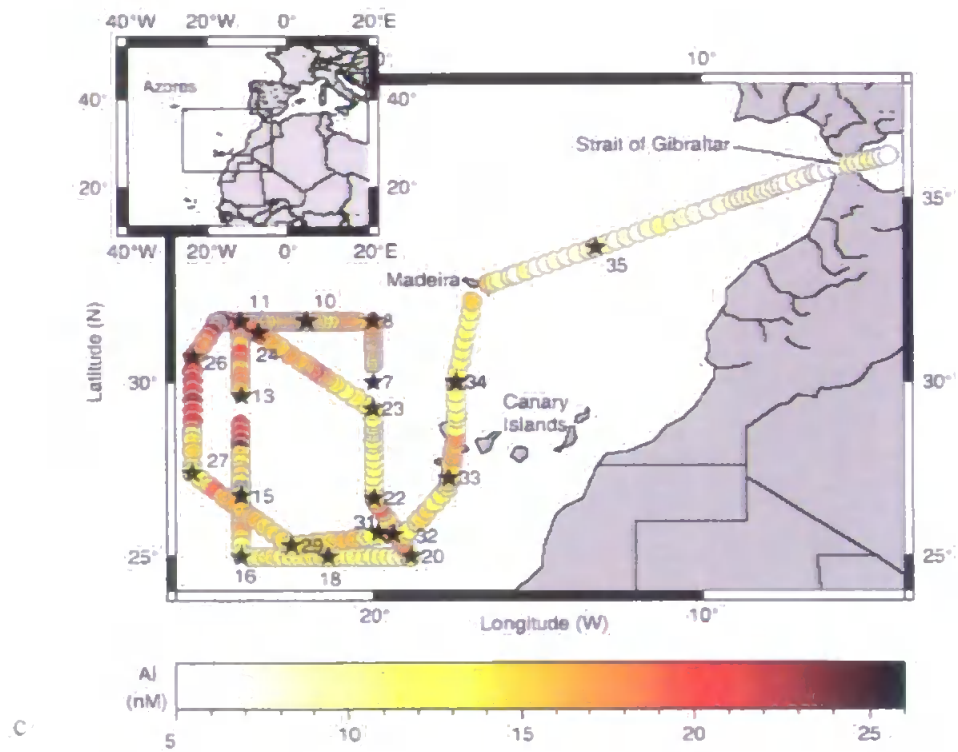
Some trace elements (e.g. Fe, Cd, Co, Cu, Zn) are crucial for the healthy growth of phytoplankton. These elements are required in trace amounts for proteins (e.g. ferredoxin (Fe protein) and enzymes (e.g. carbonic anhydrase; Cu, Zn, Co; Millero, 1996). The biological importance of these elements is illustrated by their open ocean depth profiles which generally exhibit a nutrient type behaviour (Saito and Moffet 2002; Morel and Price 2003; Chen et al., 2005; Norisuye et al., 2007). Therefore in open ocean systems the atmosphere may be the only major source of these essential nano-nutrients. One extensively studied element is iron which has been found to be a limiting factor for primary production in extensive areas of the world oceans (e.g. equatorial Pacific and Northeast Pacific; Martin and Gordon, 1988; Coale et al., 1996). Iron plays an important role in phytoplankton metabolism where it is essential for photosynthetic and respiratory electron transport, nitrate reduction, chlorophyll synthesis and detoxification of reactive oxygen species (Sunda and Huntsman, 1995).

Experiments to test the hypothesis that Fe limits primary production in high nutrient low chlorophyll (HNLC) regions have been conducted (de Barr et al., 1990, 1995; Martin et al., 1990, 1991; Buma et al., 1991). Fe enrichment experiments being performed in the equatorial Pacific (IronEx I, II), the Southern Ocean (SOIREE, SOFEX, EisenEx) and Subarctic Pacific (SEEDS, SERIES).



a

b



c

Figure 2.1. Vertical profile of Al at (a) station 11, (b) station 35 and (c) location of the sampling stations, (after Kramer et al., 2004).

By definition, the biomass of chlorophyll remains low in such regions regardless of the abundant amount of the major nutrients (nitrate, phosphate and silicate). Such iron experiments have illustrated that the enrichment of HNLC regions with iron can stimulate phytoplankton growth in the short term. The findings from these experiments have caused global climate change modellers to seek ways in which to incorporate marine biogeochemical cycles into climate models. However, critical questions remain unanswered about the cycling of iron in seawater, in particular the different effects of chemical speciation on the availability of Fe to competing autotrophs, and thus its effects on ecosystem structure impacting upon the ultimate fate of the Fe. In remote surface ocean the atmospheric inputs (wet or dry) are the dominant external source of trace metals (Jickells and Spokes, 2001). Recently for example, Sarthou et al., (2003) observed a correlation between mean sea surface dissolved iron and total atmospheric deposition fluxes, confirming the importance of atmospheric deposition on the iron cycle in the Atlantic.

The above discussion highlights the importance of Fe in terms of primary productivity (de Barr et al., 1995; de Barr et al., 1999; Morel and Price, 2003). However, recent studies have also shown that the phytoplankton community structure may also be affected (Baker et al., 2003; Mills et al, 2004). For example, Baker et al., (2003) have examined the role of the three nutrient elements N, P and Fe in the Atlantic Ocean and concluded that atmospheric inputs from the Saharan Desert drive the system to be dominated by N₂ fixing diazotrophs (*Trichodesmium* sp.). Although the N:P ratio in aerosol inputs was considerably higher than the Redfield ratio (16:1), the overall water column ratio suggested N limitation. Once the phytoplankton had consumed the N, excess P and Fe allowed productivity to continue with the proliferation of diazotroph communities via N₂ fixation, providing their own N requirements for primary productivity.

A similar affect was also observed off the coast of Florida in October 1999, when a huge bloom of toxic red algae developed following a dust cloud, originating from the west coast of Africa (17 June 1999), arriving at the coast of Florida on the 1st of July 1999. The surface water was enriched by 300 percent with iron. As a result *Trichodesmium* counts increased 10 times, dominating the phytoplankton community. The *Trichodesmium* would have developed at low N concentrations as it has the competitive advantage over other species, being a diazotroph, of fixing its own nitrogen requirements from the atmosphere. As P was still available and Fe was in plentiful supply owing to the dust event, the species had ideal conditions for growth.

In addition to Fe, other transition metals play important roles in marine biological cycles. Whitfield (2001), for example, described Co as an essential growth factor for phytoplankton, as it is an active metal centre of vitamin B₁₂. Cobalt is also known to substitute for Zn in enzyme carbonic anhydrase (Sunda and Huntsman, 1995; Yee and Morel, 1996).

Copper plays a major role in photosynthesis as a structural and electron exchange component of plastocyanin (the protein which takes part in photosynthetic electron transfer). Copper exhibits a nutrient type behaviour in the open ocean with surface depletion, followed by regeneration at depth through biotic uptake together with in-situ sub-surface scavenging onto SPM (both biogenic and lithogenic in origin) (Chester, 2000).

Nickel shows a typical nutrient profile with surface depletion and deep water enrichment (Millero, 1996). This behaviour is due to surface consumption by biota and regeneration in the sub-surface. Chester (2000) described the Ni vertical profile as a dual nutrient behaviour where it has surface depletion and a maximum concentration at a shallow sub-surface depth (comparable to P and N) and another maximum concentration at deeper

depths (comparable to Si). This is a result of the involvement of Ni in soft and hard tissues (labile and refractory carriers) which decompose at deeper depths. Therefore the atmospheric input of these metals in remote open ocean systems may also be of importance.

2.3 The trace metal composition of the marine aerosol and its sources

Aerosols are defined as “A suspension of solid and liquid material in a gaseous medium” (Chester, 2000). Trace metals present in an aerosol population will be derived essentially from a mixture of anthropogenic and natural sources (see sections 2.3.1 and 2.3.2), however the predominant sources will influence the aerosol trace metal concentrations at any one time and location. Prospero et al., (1983) classified atmospheric aerosols into natural (sea spray residues, windblown mineral dust, volcanic effluvia, biogenic materials, smoke from the burning of land biota and natural gas-to-particle conversion products) and anthropogenic aerosols (direct emission and anthropogenic gas-to-particle conversion products).

Elements such Al and Fe are primarily associated with naturally derived aerosol particles (e.g. Kocak et al., 2005; Chester 2000; Duce et al., 1991). This material is a result of low temperature physical and chemical weathering processes on crustal particles.

Elements such as Pb and Cd are associated primarily with anthropogenically derived aerosol particles (e.g. Var et al., 2000; Kocak et al., 2005). Table 2.2 presents the geometric mean aerosol trace metal concentrations observed in different marine systems. It is apparent from Table 2.2 that there is a high degree of spatial variability between contrasting sampling locations. Studies carried out at individual sites have also highlighted the great temporal variability in aerosol trace metal concentrations. This is illustrated by the high range of observed aerosol metal concentrations presented in Table 2.2 at any one

Table 2.2. Literature data for geometric mean concentrations and (ranges) for trace elements in aerosols from a number of representative marine environments. Concentrations expressed as ng m⁻³ of air.

Element	Coastal seas				Open ocean		
	Irish Sea (Fones, 1996)	North Sea (Chester and Bradshaw, 1991)	Western Mediterranean (Chester et al., 1990)	Eastern Mediterranean (Kocak et al., 2004)	Arabian Sea (Chester et al., 1991)	Tropical North Atlantic (Buta-Menard & Chesselet 1979)	North Pacific (Duce et al, 1983)
Al	210 (101-586)	219(21-887)	370(40-2033)	567 (15-8278)	1227(317-5148)	160	21(1.3-150)
Fe	159(65.1-486)	230.5((2.0-1565)	320(122-1184)	407 (8-5601)	790(317-3074)	100	18(0.66-91)
Mn	4.42(0.40-31.6)	9.1(0.2-84.5)	11(2.3-50)	7.9 (0.1-92)	17(6.3-59)	2.2	0.29(0.025-1.7)
Ni	3.71(1.12-12.3)	2.5(0.04-13)	2.8(0.4-8.9)	-	2.0(0.39-9.4)	0.64	-
Co	0.14(0.05-0.5)	0.19(0.01-0.79)	0.17(0.003-0.78)	-	0.38(0.037-1.9)	0.08	0.008(0.001-0.044)
Cr	-	3.1(0.1-25)	2.5(0.8-5.2)	3.9 (0.1-39)	3.0(0.77-14)	0.43	0.091(0.034-0.390)
V	-	-	-	-	6.3(0.91-30)	0.54	0.082(0.019-0.270)
Cu	4.57(1.27-14.9)	4.4(0.4-37.5)	6.2(1.1-19)	8.9 (1.0-65)	2.6(0.96-12)	0.79	0.044(0.005-0.29)
Zn	25.3(6.72-100)	26(0.7-250)	41(6.1-210)	15.9 (0.7-744)	10(4.2-29)	4.4	0.180(0.031-0420)
Pb	15.1(3.59-82.4)	20(0.6-189.5)	58(15-255)	21.5 (0.3-586)	4.3(1.1-12)	9.9	0.120(0.030-0.320)
Cd	0.19(0.04-0.85)	-	0.36(0.02-1.5)	0.17 (0.01-2.36)	0.045(0.024-0.099)	-	0.004(0.001-0.017)

sampling location (e.g.; Buat-Menard and Chesselet, 1979; Duce et al., 1983; Arimoto et al., 1987; Chester et al., 1990; Chester and Bradshaw, 1991; Fones, 1996; Kocak et al., 2004). The general trend for crustally derived aerosol trace metals (Al, Fe, Mn) is an increase in concentration from western Europe (Irish Sea, North Sea) to the eastern Mediterranean, whereas elements dominated by anthropogenic sources (e.g. Pb, Cd) generally decrease from Europe as one moves westwards. Crustal element concentrations (e.g. Al and Fe) are clearly much higher in the Eastern Mediterranean (owing to the close proximity of the Saharan desert belt to the south) and frequent seasonal desert dust events (Gehlen et al., 2003; Sarthou et al., 2003; Kocak et al., 2004). Whereas marine systems such as the tropical Pacific (a remote pristine area located far from continental industrialized areas and the influence of crustal inputs) experiences comparatively lower aerosol trace metal concentrations (typically one or two orders of magnitude lower).

Generally, the overall composition and concentration of trace elements in a sampled aerosol population is controlled by (i) the predominating type of aerosol source, (ii) the emission strengths of the contributing sources, (iii) chemical and physical (wet and dry deposition) modifications of the aerosol population during transport from source to sink and (iv) atmospheric transport processes.

The source type influence can be seen from the data in Table 2.2. One can divide the Marine systems (Duce et al., 1983; Chester and Bradshaw, 1991; Fones, 1996; Sarthou et al., 2003 Kocak et al., 2004) into three categories; (i) coastal seas close to anthropogenic sources (North Sea and Irish Sea) (ii) coastal seas influenced by crustal and anthropogenic sources (i.e. western and eastern Mediterranean) and (iii) open oceans influenced by crustal sources (i.e. Atlantic ocean, affected by the northeast trades off West Africa and Arabian Sea). The use of air mass back-trajectories are important to trace such sources and to assess how contrasting aerosol sources might impact on variations in aerosol trace metal

concentrations. Table 2.3 illustrates this point by highlighting the observed differences in the aerosol associated trace metals concentrations at Mace Head (Ireland) (Spokes et al., 2001). Air masses originating from the marine environment which have not recently passed over continental regions have comparatively very low trace metals concentrations (e.g. Al of marine source represent 19% of Al derived from the SE flow). In contrast, a southeasterly air mass which has passed over populated and industrialised areas has much higher (by typically 5-50%) trace metals concentrations.

The potential effect of source emission strengths and their impact on aerosol metal concentrations is best described by Pb, a predominantly anthropogenically derived aerosol element emitted to the atmosphere mainly as a result of vehicular traffic. Over the last few decades in different regions of the world there has been a diminished usage of leaded fuel (Spokes et al., 2001). This has impacted upon aerosol Pb concentrations and has created difficulties when making comparisons between literature datasets. Lead has been extensively studied due to its toxicity and long range atmosphere transport as it is mainly associated with the fine fraction anthropogenic aerosol (e.g. Pacyna et al., 1991; Injuk et al., 1992, 1993; Boutron, 1995; Shotyk, 1996). For example, Injuk et al., 1992 using a well equipped aircraft to collect atmospheric aerosol samples (total and size fractionated samples) concluded that Pb was primary associated with submicrometre size (in contrast to Zn). Lead was first introduced as a fuel additive in the 1920s with its maximum input to the atmosphere around 1970 (Aberg et al., 2001). The increase during this period is exemplified by Figure 2.2 illustrating the chronological changes in lead emissions to the atmosphere of Switzerland, peaking in the 1970's followed by a decrease from traffic exhausts and industrial processes in Switzerland during the 1990's. Environmental legislation has subsequently been introduced as part of a strategy to reduce emissions from road traffic for the purpose of improving air quality, leading to a ban on the domestic sale of leaded fuel in the USA in the mid 1970s (Spokes et al., 2001). Its use in Europe was

later reduced by the introduction of unleaded fuel in 1978 and then banned in Europe (and Saudi Arabia) around 2000.

Table 2.3. Average concentration (pmol m^{-3}) of aerosol associated trace metals at Mace Head (Ireland) in two contrasting air masses; a polluted south easterly air mass and a marine dominated air mass (From Spokes et al., 2001).

Air-mass Back Trajectory	Al	Pb	Zn	Mn
SE flow	1300	140	486	100
marine air masses	248	2.0	45	6.0

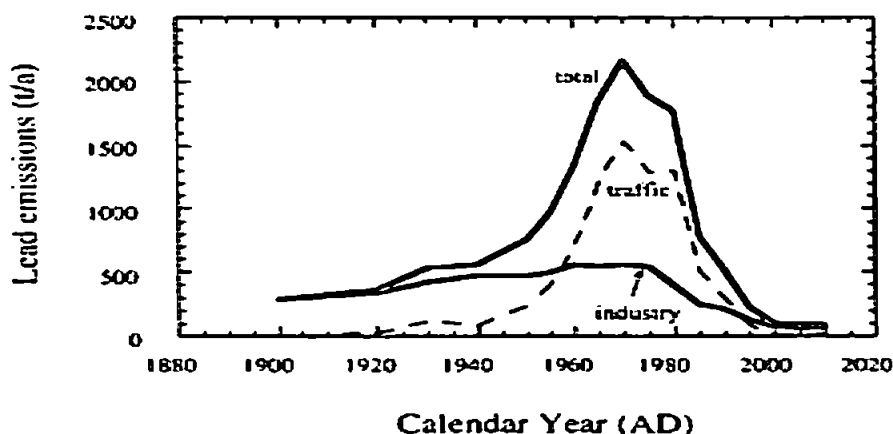


Figure 2.2. Lead emission (tonnes/annum) from traffic and industrial sources in Switzerland against time (BUWAL, 1995).

As a result of this environmental legislation there has been a clear decline in lead aerosol concentrations. For example this has amounted to a 30-40% decline in the North Atlantic Ocean (Veron et al., 1993) between 1979 and 1989, and a similar decrease (30%) was found in the surface ocean waters near Bermuda between 1979 and 1993 (Wu and Boyle 1997). Cave et al., (2005) also showed a decrease in the wet deposition of lead from 97 tonnes/year in 1994 to 57 tonnes/year in 1999 to the entire Humber catchment (UK) (a decrease of 40%). As the European ban on leaded fuel was introduced after that introduced in the USA, the decline in European atmospheric Pb exhibited a similar time lag in its decline. Diminished aerosol Pb concentrations have been observed in European coastal

atmospheres (Ligurian Sea, 25-30%; 40% in the Levantine Basin of the Eastern Mediterranean, Migon and Nicolas, 1998; Ridame et al., 1999; Lammel et al. 2002; Kocak et al., 2004). In addition Huang et al., (1996) suggested that 25% of lead inputs to the Sargasso Sea can be attributed to European sources in the mid 1990s. The above trend was also reported by Wu and Boyle (1997) who observed a decrease in lead concentrations in the surface ocean waters near Bermuda from around 150 p mol kg⁻¹ (in the 1970s) to 50 p mol kg⁻¹ (in the 1990s).

The deposition of aerosol material during transport may also greatly impact on measured aerosol metal concentrations. Both wet and dry deposition are mechanisms by which air masses can be stripped of their associated aerosol population, the wet depositional mode being the more effective but more sporadic, the dry depositional mode being a constant mechanism. Chester et al., (1990) for example, investigated the influence of rainfall on trace metal concentrations in the Western Mediterranean marine aerosol. They observed a decrease in Zn, Cu and Pb by up to 60% between just before and after a rain event, with a two to three day recharge. This also confirmed the conclusions made by Bergametti et al., (1989) that a period of around two days is required to reload the atmosphere over the Western Mediterranean with aerosol from continental sources.

2.3.1. Natural Background Aerosol material

In the previous section contrasting sources were briefly discussed in terms of their impact on trace metal aerosol concentrations. Literature estimates of natural aerosol sources exhibited a wide range of values, which reflects the uncertainty of the applied assumptions in the calculations. Tables 2.4 and 2.5 illustrate the global emission estimates of particulate material and trace metals from natural and anthropogenic background sources. Natural sources include; (i) sea salts generated in the atmosphere by mechanical action (bubble bursting at the sea surface), (ii) crustal material (e.g. soil, desert dusts etc) transported by air mass movement from arid regions following the natural weathering of rocks and (iii)

volcanic activity resulting in the production of particulate (e.g. ash) and gaseous phases formed from high-temperature volatilisation processes. Moreover, volcanoes (major volcanic eruptions) can contribute aerosol material to the stratosphere (altitude from 11-50 km). It is clear from Table 2.4 that natural background aerosol sources are far higher than anthropogenic sources. Although there is variability in terms of which source is the more important (within the natural sources), however Table 2.4 clearly shows that the generation of sea salts and the re-suspension of crustal material are by far the most important sources to the global aerosol.

Table 2.4. Estimates of the global emissions of particulate material to the atmosphere (units, 10^{12} g yr⁻¹) (Chester, 2000).

Source		Global production		
		Prospero et al., (1983)	Nriagu (1979)	Lantzy & Mackenzie (1979)
Anthropogenic	Direct particle production	30		
	Particles formed from gases			
	Converted sulphates	200		
	Other	50		
	Total anthropogenic	280		200
Natural	Direct particle production			
	Forest fires	5	36	
	Volcanic emission	25	10	
	Crustal eathering	250	500	
	Sea salt	500	1000	
	Particles formed from gases			
	Converted sulphates	335		
	Other	135		
	Total Natural	1250		
Total		1530		

Table 2.5. Global atmospheric emissions of trace metals (adapted from Duce et al., 1991).

Elements	Global Emissions 10^9 g yr^{-1}	
	Anthropogenic	Natural
Pb	289-376	1-23
Cd	3.1-7.6	0.15-2.6
Cu	20-51	2.3-54
Ni	24-87	3-57
Zn	70-132	4-86

2.3.2 Anthropogenically derived aerosols

Anthropogenic contributions to the aerosol population are about 20 % of the natural source contributions (see Table 2.4). However, anthropogenic sources are geographically concentrated. Industrial and social activities leading to the injection into the atmosphere of anthropic aerosol material include fossil fuel burning, mining and the processing of ores, waste incineration, and the production of chemicals. In the case of some elements (Pb, Cd, Cu, Ni, Zn) anthropogenic source inputs may be equivalent to or exceed the natural sources (Duce et al., 1991; see Table 2.5).

2.4 Methods of aerosol trace metal source identification

The source type of aerosol associated trace metals can significantly impact upon their concentrations. It is also apparent that when attempting to make dry deposition calculations, knowledge of the predominant elemental source facilitates the assignment of the most appropriate settling velocities (see section 2.5.1 for more details).

A combination of approaches can be adopted to evaluate the contribution made by different sources to an aerosol population. These include the following; (i) particle size determination, (ii) the calculation of air mass back trajectories and (iii) the calculation of

the elemental enrichment factor (EF). Each of these approaches is discussed in the following sections.

2.4.1 Aerosol particles size distribution

The type of source contributing to an aerosol population might, in addition to influencing the trace metal concentration, impact upon the particle size spectrum of an aerosol population. Aerosols particle sizes may can be divided into two broad categories; fine particles ($d < 2 \mu\text{m}$) and coarse particles ($d > 2 \mu\text{m}$) (see Figure 2.3). The fine particle category can be further sub-divided into transient nuclei or Aitken nuclei range and accumulation modes (Whiteby, 1977).

Particles in the transient nuclei (Aitken nuclei $d < 100\text{nm}$) range originate predominantly from high temperature combustion processes, which are mainly derived from anthropogenic processes although volcanic emissions and biomass burning are also included. The accumulation mode is thought to result primarily from the coagulation of Aitkin nuclei into larger aggregates. In contrast, particles in the coarse mode have been formed by mechanical action (low and high temperature processes) and are mainly natural in origin (e.g. sea salts, crustal material). Coarse mode particles have shorter residence times in the atmosphere, in contrast to fine mode particles, owing to their comparatively higher settling velocities (e.g. Arimoto and Duce, 1986).

Defining the aerosol particle size spectrum of an aerosol population is important because this information allows; (i) more representative settling velocities to be assigned to the aerosol population and hence more accurate calculation of aerosol dry deposition (see further section 2.5.1) and (ii) a better evaluation of the contributions made to the aerosol population of contrasting sources (Chester et al., 1993; Spokes et al., 1994; Paoletti et al., 2003; Conner and Williams, 2004).

A number of researchers have used scanning electron microscopy (SEM) to identify the physico-chemical properties of aerosol material such as grain size and, morphology (e.g. Kasparian et al., 1998; Ebert et al., 2000; Biscombe 2004; Dordevic et al., 2004; Hoffman et al., 2004; Niemi et al., 2004; Desboeufs et al., 2005). SEM can be coupled with energy dispersive X-ray analysis (EDX) to yield a rapid, easy and nondestructive approach to surface elemental analysis (Toyoda et al., 2004).

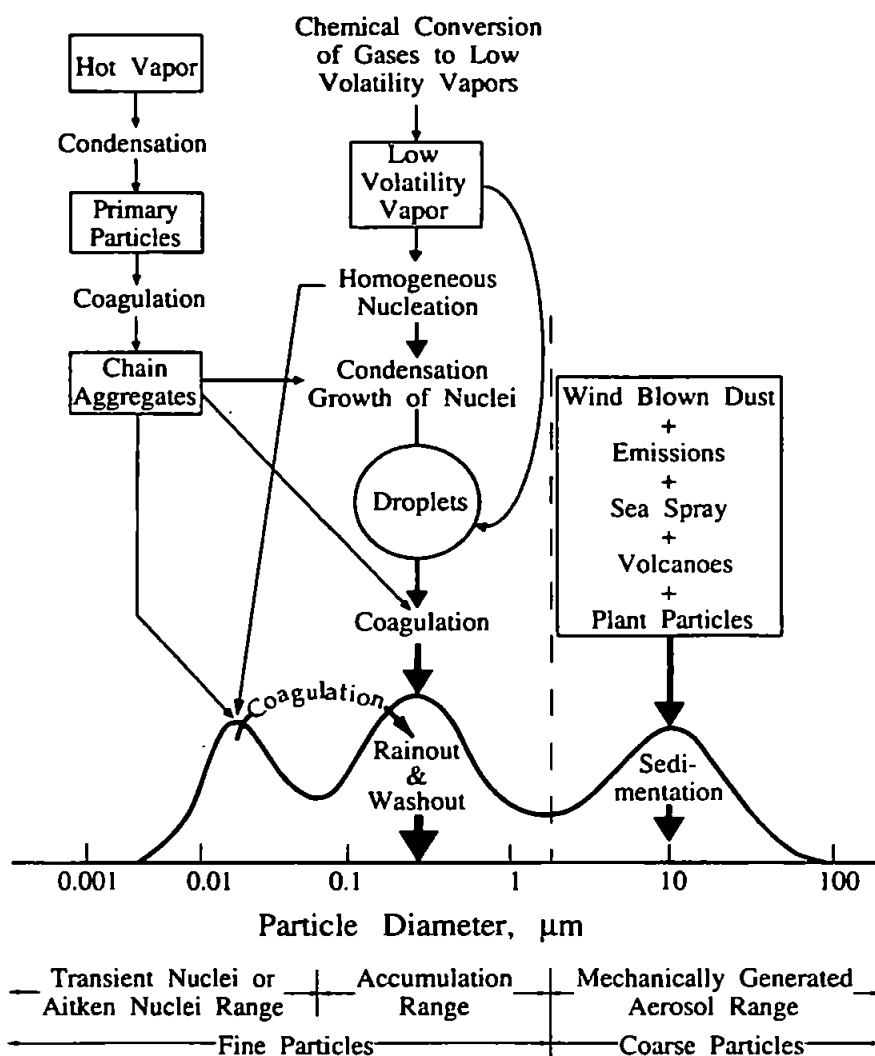


Figure 2.3. Aerosol particles distribution according to particle size and formation (from Whitby 1977).

The dust samples are fixed on a carbon tape then either coated with carbon or gold before SEM observation. SEM images can highlight the size and shape of airborne particles. Figure 2.4a, for example, illustrates a fly ash particle as being spherical in shape and comparatively small ($\sim 0.5 \mu\text{m}$), whilst soot aggregates form irregular shaped, comparatively larger particles ($> 1 \mu\text{m}$). In addition naturally derived particles are larger than anthropogenic particles as is clear from images (Figure 2.4) of sea salts ($\sim 5 \mu\text{m}$) and soil derived kaolinite agglomerates, both being larger than $2 \mu\text{m}$ (Figure 2.4 b and d). Therefore, it is clear that SEM can provide useful guideline information of the physical characteristics of aerosol populations.

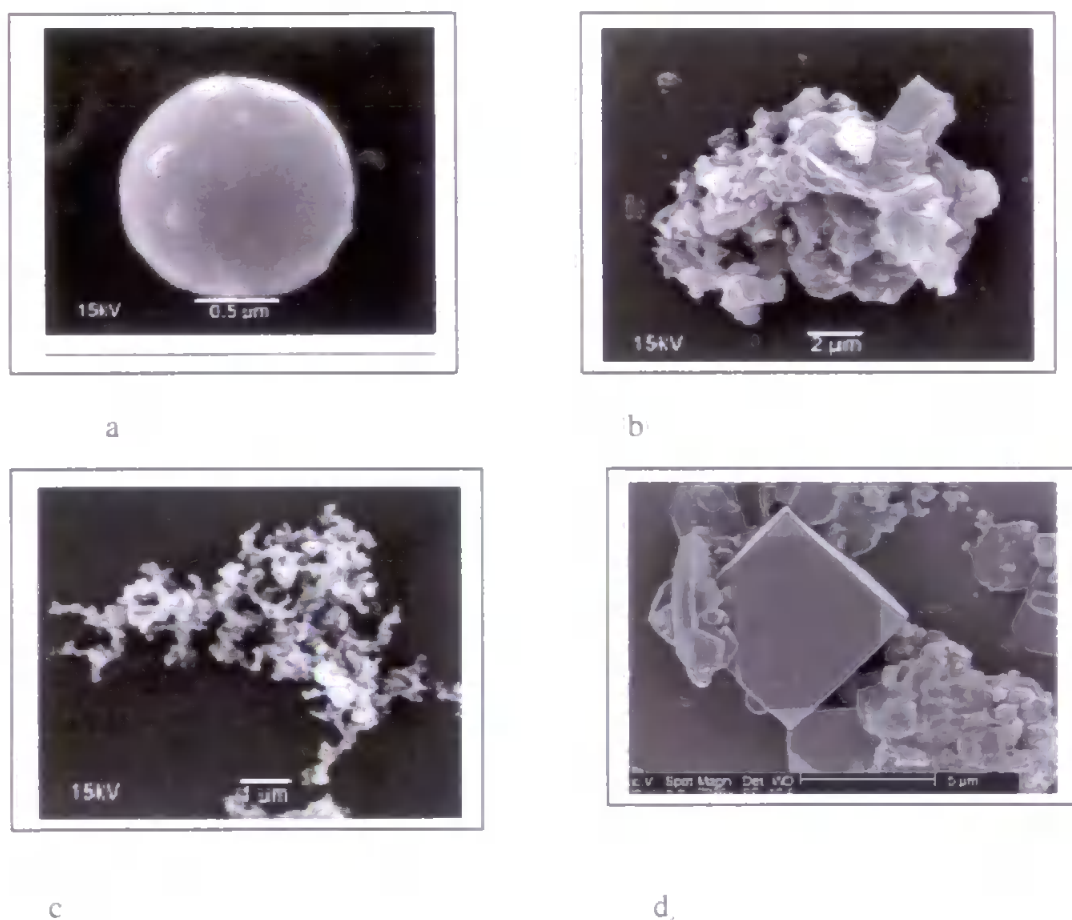


Figure 2.4. SEM Photomicrographs of airborne particles. (a) a fly ash particle (b) solid-driven kaolinite agglomerates (c) soot aggregates (d) cubes of sea salts Images (a), (b) and (c) after Xie et al., (2005). Image d is from Moreno et al., (2004).

2.4.2 Air mass movement

Knowledge of air mass movement is of great importance in enhancing our understanding of source contributions to aerosol populations and hence trace metal aerosol concentrations (Methven et al., 2001). Simple and complex models (HY-split4, CAPITA Monte Carlo) have been used to predict air mass movement. The trajectory model is useful for (1) determining the possible history of a given air parcel using back trajectories (2) studying mixing and transport processes in the atmosphere (3) combining observations made over a wide variety of places into a consistent map representing the state of the atmosphere at any one period (i.e., a synoptic map), and (4) providing a dynamic component to a photochemical box model so that the chemical evolution of an air parcel can be reliably studied.

Trajectory models are important tools for studying transport phenomena in the atmosphere (Stohl, 1998) and establishing the relationship between air mass origin and chemical composition (Kubilay and Saydam, 1995; Methven et al., 2001). Interpreting the chemical composition of atmospheric aerosols is a key factor in understanding their atmospheric cycling. Mathematical models have been widely used to evaluate the transport of aerosols in the atmosphere (Chiapello et al., 1997; Spokes et al., 2001; Baker et al., 2003; Jickells et al., 2003; Oikonomou et al., 2003;), but few offer the flexibility, broadness and accuracy the user requires. Accuracy is the most important factor for aerosol studies. Errors in trajectory calculations result from a number of factors (see Stohl, 1998): numerical truncation (e.g. Seibert, 1993), interpolation (Kuo et al., 1985; Rolph and Draxler, 1990; Stohl et al., 1995), treatment of the vertical velocity (for instance, use of isobaric or isentropic approximation) (Stohl and Seibert, 1998), errors in the underlying wind fields (Kahl et al., 1989; Pickering et al., 1994, 1996) and sometimes inaccurate specification of the starting positions and times which lead to subsequent growth of errors (Merrill et al., 1985).

The model used in this study is HYSPLIT (Hybrid Single-Particle Lagrangian Integrated Trajectory) which was designed by ARL-NOAA in the USA and the Bureau of Meteorology in Australia. This model can:

- Compute Single or multiple simultaneous trajectories
- Project forward and backward in time
- Incorporate other options which are not of particular interest for this project

Moreover, this model is free to use and has been adopted by many researchers (e.g.; Baker et al., 2003; Caputo et al., 2003; Oikonomou et al., 2003; Sarthou et al., 2003; Li et al., 2004) in the field of aerosol study.

2.4.3 Use of the Enrichment Factor to identify sources

A classical way in which the source has been determined is by invoking the use of the enrichment factor (e.g. Guieu et al., 1997; Chester et al., 1999; Kocak et al., 2004). The enrichment factor is generally defined in the following manner:

$$EF_{\text{source}} = (E/I)_{\text{air}} / (E/I)_{\text{source}} \quad 2.1$$

Where $(E/I)_{\text{air}}$ is the ratio of the concentration of the element of interest and the concentration of an indicator element I in the aerosol sample and $(E/I)_{\text{source}}$ is the ratio of their equivalent concentrations in the precursor source material. The most appropriate indicator element will vary depending upon the type of enrichment factor to be calculated. The most commonly applied enrichment factor is the crustal enrichment factor (EF_{crust}). The indicator element usually adopted is aluminium. Hence the EF_{crust} can be defined as:

$$EF_{\text{crust}} = (E/Al)_{\text{air}} / (E/Al)_{\text{crust}} \quad 2.2$$

where $(E/Al)_{\text{crust}}$ is taken from the global elemental concentrations in the crust (Taylor, 1964; Wedepohl, 1995). Because Al is used as the crustal reference element the contribution of anthropogenic Al should theoretically be negligible for an accurate determination of EF_{crust} . Moreover, the chemical composition of the continental crust will vary from one location to another and the average concentration in the crustal rock is an approximation of the regional value. It is demonstrated that the concept of normalizing element concentrations to an average total crust value is of doubtful merit, for theoretical considerations alone serious flaws with EFs have been discussed by Reimann and De Caritat (2000). More recently Kocak et al., (2005) calculated the EF_{crust} for the Eastern Mediterranean aerosol using elemental ratios taken from an end-member Saharan dust, to better represent the regional crustal elemental /Al ratios and hence obtain a more accurate representation of the EF_{crust} for the Eastern Mediterranean aerosol. Guieu and Thomas (1996) also used the local abundance of elements from the source to calculate a more representative EF_{crust} . Therefore, considering the various limitations involved in the calculation of EF_{crust} , values should be treated only as order of magnitude indicators of the crustal source (Chester 2000). Once the EF_{crust} has been calculated, elements having an EF_{crust} of > 10 are assumed as having a predominantly non-crustal source (e.g. Pb and Cd) whereas elements having an $EF_{\text{crust}} < 10$ are assumed to have a predominantly crustal source (e.g. Fe and Al). Elements having $EF_{\text{crust}} < 10$ are referred to as “non-enriched” elements, whereas elements having EF_{crust} of > 10 are referred to as “enriched” elements. Having said that some authors (e.g. Guieu and Thomas 1996; Chester 2000) treat this assumption with reservation as elements may have an EF_{crust} of 10 or less but still have a significant anthropogenic source contribution (e.g. Kocak et al., 2005).

In addition, “enriched” elements under special conditions may exhibit “non-enriched” behaviour (i.e. $EF_{\text{crust}} < 10$). This has been observed when an aerosol population is heavily loaded with crustally derived material (e.g. Saharan dust pulses see Chester et al., 1996). In

contrast it is also possible that non-enriched elements may apparently become enriched, Mn being a recent example. Spokes et al., (2001) sampled manganese in the fine ($<2\mu\text{m}$ diameter) and coarse ($>2\mu\text{m}$ diameter) modes and found that in some events the fine mode exceeded the coarse mode. Fine mode ($d<2\mu\text{m}$) manganese would be generated from high-temperature combustion of manganese rich fuel enhancers or smelting and this suggestion was supported with a high crustal enrichment factor value (i.e. southeasterly air; $EF_{\text{crust}} \sim 45$).

Table 2.6 highlights typical EF_{crust} values in marine aerosols at contrasting locations and it is apparent that the EF_{crust} are generally higher in marine systems in the vicinity of industrialised regions (e.g. North Sea). This is due to the effect of dominating anthropic sources. However, in the case of the North Atlantic, EF_{crust} for elements in samples collected during the North East Trade winds are lower than for samples collected from westerlies due to the domination by crustal material from the western Sahara desert.

2.5 Modes of deposition of atmospheric trace metals to the sea surface

Atmospheric trace metal deposition to the sea surface occurs by dry and wet deposition. Wet deposition comprises of dissolved constituents together with insoluble particles contained therein. Both modes of deposition (wet and dry) plus the gas phase make up the total deposition.

2.5.1 Dry deposition

Dry deposition is simply the gravitational settling of aerosol particulate associated trace metals to the receptor surface, being either terrestrial or marine. Table 2.7 highlights the spatial variability in the aerosol mineral flux and deposition to the global ocean system. The relative importance of wet and dry fluxes varies (Table 2.7) from region to region and from metal to metal. Where arid regions influence open ocean systems, dry deposition of

mineral dust becomes increasingly more important, such that in these regions it becomes the predominant deposition transport mechanism.

This is apparent for the N Atlantic, which experiences periodic intense pulses of Saharan dust events leading to, on average, three times greater dry deposition rates for mineral dust compared with wet depositional rates. Moreover, in arid regions and surrounding areas rain events are rare and consequently the dry flux will dominate in these regions (see Table 2.8). As a result elements such as Al and Fe have high aerosol concentrations and dry depositional rates.

The dry removal of particles from the atmosphere is a continuous process that is affected by a number of factors, which include particle size, wind speed, relative humidity and particle concentration (Cawse, 1981; Fitzgerald, 1991; Wesely and Hicks 2000). Table 2.8 shows the wet/dry elemental daily flux in different regions influenced by diverse sources.

Elemental dry deposition is generally calculated from the following equation 2.3 (Duce et al., 1991):

$$F (\mu\text{g cm}^{-2} \text{ s}^{-1}) = V_d (\text{cm s}^{-1}) \cdot C (\mu\text{g cm}^{-3}) \quad 2.3$$

where V_d is the elemental deposition or settling velocity, F is the rate of dry deposition and C is the concentration of the element in the air. The deposition velocity (V_d) comprises of all processes of dry deposition including gravitational settling (which is affected by particle size), impaction, and diffusion. As presented in Figure 2.5 (Slinn and Slinn, 1980), particle size would influence the modelled dry deposition velocity. This is also emphasised by Cawse (1981) (Figure 2.6) who defined the relationship between enrichment factor and dry deposition velocity (cm s^{-1}). A mean value of 0.025 cm s^{-1} was found for a SO_4^{2-} aerosol with a size range of $0.1\text{-}1 \mu\text{m}$, whilst larger particles ($1\text{-}20 \mu\text{m}$) showed a higher velocity, from $0.06\text{-}2.5 \text{ cm s}^{-1}$.

Table 2.6. EF_{crust} values for some anomalously enriched crustal (AEE) elements in marine aerosols of contrasting locations.

Element	North Atlantic Ocean Westerlies	North Atlantic Ocean N.E Trade	North Sea Chester et al., (2000)	W. Med. Chester et al., (2000)	W. Med. (Spain) Chester et al., (1993)	Corsica (W. Med.) Bergametti et al., (1989)	Cap Ferrat (Med.) Chester et al., (1990)	Vignola (W. Med.) Migon et al., (1993)	Sardinia (W. Med.) Migon et al., (1993)	E. Med. (Erdemli) Kubilay and Saydam, (1995)	Jeddah (S.W. Asia) El Sayed et al., (2004)
Cu	120	1.2	58.5	22	29	18	24	26	-	-	49
Zn	110	3.8	280	155	148	133	130	130	52	33	27
Cd	730	9.4	-		628	1633	676	423	260	116	22
Pb	2200	9.1	1825	955	837	635	1045	550	194	294	6

Table 2.7. Atmospheric flux of mineral aerosol to the ocean (After Duce et al., 1991) (Brackets show the % contribution of dry and wet to the total).

Ocean	Flux, $10^{-3} \text{ g m}^{-2} \text{ yr}^{-1}$			Deposition, $10^{-9} \text{ g yr}^{-1}$		
	Wet	Dry	Total	Wet	Dry	Total
North Pacific	3.8 (72)	1.5 (28)	5.3	340	140	480
South Pacific	0.23 (63.9)	0.13 (36.1)	0.35	25	14	39
North Atlantic	1.1 (27.5)	2.9 (72.5)	4	61	160	220
South Atlantic	0.27 (57.4)	0.20 (42.6)	0.47	14	10	24
North Indian	5.1 (71.8)	2.0 (28.2)	7.1	73	29	100
South Indian	0.60 (73.2)	0.22 (26.8)	0.82	32	12	44
Global Total	1.5 (60)	1.0 (40)	2.5	550	360	910

Table 2.8. Elemental flux (wet dry and total) expressed as $\mu\text{g m}^{-2}\text{yr}^{-1}$.

Element	South Pacific ¹		Med. Sea ²		North Sea ³		Med. Sea ⁴	
	Wet	Dry	Wet	Dry	Wet	Dry	Wet	Dry
Al			749	1200				
Fe	3300	2800			89000	22000		
Mn	44	38			1730	890		
Cu	20	2.6	14.6	11.9	880	420	584	1606
Cd	3.9	0.51					32.85	32.85
Zn	22	2.9			5030	1470	38690	41610
Pb	31	4.1	19.1	18.5	3200	490	584	2555
Ni			3.6	3.3	880	330	693.5	657
Co			0.6	0.24			32.85	94.9
V					880	170		

(1- Halstead et al., 2000, 2- Chester et al., 1999, 3- Injuk et al., 1998 , 4- Migon et al., 1997)

The dry deposition velocity has been calculated using different approaches; (i) models (Hicks and Williams, 1980; Dulac et al., 1987; and Slinn and Slinn 1980) (ii) experimental cascade impactor (Bergametti, 1987) (iii) surrogate surfaces (Dolske and Gatz, 1985; Baeyens et al., 1990; Kim et al., 2000) (iv) calculated difference between total and wet deposition field data (Migon et al., 1997). Table 2.9 gives a summary of the settling velocities used in the literature. The results are very different and hence their comparability is generally invalid due to the uncertainties in the applied approaches.

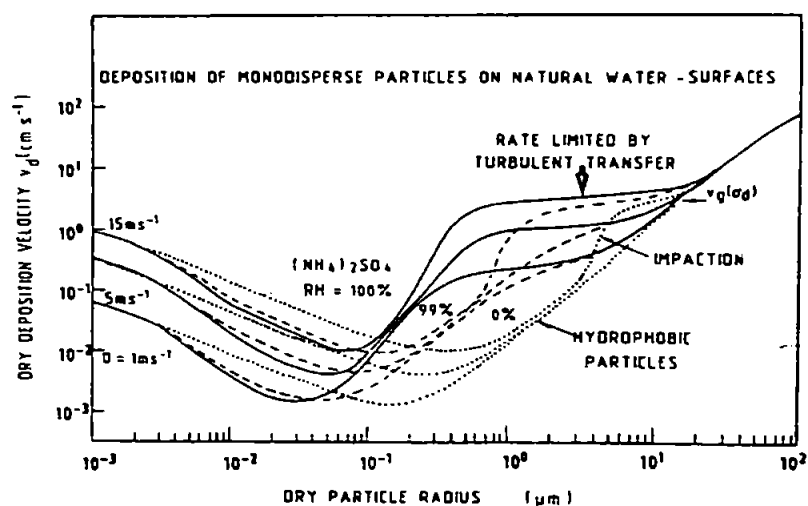


Figure 2.5. The influence of particle size on modelled deposition velocity (after Slinn and Slinn, 1980).

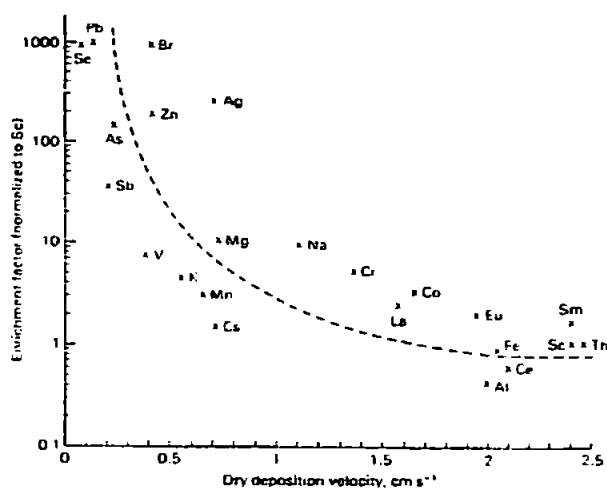


Figure 2.6. Relationship between enrichment factors and dry deposition velocities of elements in aerosols (Cawse, 1981).

Table 2.9. Summary of the elemental settling velocities (cm s^{-1}) used to calculate elemental dry deposition fluxes in recent studies

Element	Flamant (1985)	Dulac et al., (1989)	Remoudaki (1990)	Guieu et al., (1991)	Ottley and Harrison (1993)	Rojas et al., (1993)	Injuk et al., (1998)	Migon et al., 1997	Guerzoni et al., (1999)	Wells (1999)	Spokes et al., (2001)
Al	-	0.69-3.8	-	-	0.46	-	-	-	2	1.08	1.3
Fe	-	-	-	-	0.45	-	0.32-0.55	-	2	-	-
Mn	-	-	-	-	-	-	0.21-0.53	-	-	0.69	1.1-1.4
Cu	0.49	-	1.1	0.8	0.7	0.48	0.21-0.5	1.19	-	0.44	-
Zn	0.5	-	-	5	0.52	0.35	0.20-0.4	4.38	-	0.09	0.71-0.92
Pb	0.17	0.041	1.9	0.1	0.17	0.25	0.07-0.11	0.19	0.2	0.02	0.36-0.63
Cd	0.49	0.053	-	7	0.38	0.39	-	0.42	0.2	0.04	-

For example, Duce et al., (1991) used three categories of aerosol particles and calculated the deposition velocity based on the Slinn and Slinn (1980) model. Category one was the sub-micrometer aerosol particles and the calculated deposition velocity was 0.1 cm s^{-1} (\pm a factor of 3). The second category was super-micrometer crustal particles (not associated with sea salts) and the calculated deposition velocity was 1.0 cm s^{-1} (\pm a factor of 3). The third category was large sea salt particles and material carried by them with a calculated deposition velocity of 3.0 cm s^{-1} (\pm a factor of 2). Anthropogenic sources are the dominant source of metals such as zinc and therefore the dry deposition velocity for zinc using the Slinn and Slinn (1980) model should be $0.1\text{-}0.3 \text{ cm s}^{-1}$. Whereas, Migon et al., (1997) calculated the zinc deposition velocity to be 4.4 cm s^{-1} for the western Mediterranean, using the difference between total bulk deposition and wet deposition. Moreover, Rojas et al., (1993) estimated the dry deposition velocities for Cd, Cu, Pb and Zn using a modified version of the two-layer of Slinn and Slinn (1980) and the particle size distribution obtained from size-fractionated samples (see Table 2.9).

Generally it is assumed however that elemental gravitational settling velocities for elements associated with natural particles (e.g. Al, Cu, Fe) ($EF_{\text{crust}} < 10$) have higher settling velocities than those elements associated with anthropogenic particles (e.g. Pb, Zn) ($EF_{\text{crust}} > 10$). Therefore, knowledge of trace metals aerosol sources (as defined by the EF_{crust}), as well as their aerosol concentrations, is essential in order to accurately assess quantitatively dry deposition fluxes (Figure 2.6).

2.5.2. Wet deposition

Wet deposition is when particulate matter (solid aerosols) is removed from the atmosphere by collision with, and capture by, falling precipitation (below-cloud), or via the particles themselves acting as condensation nuclei (in-cloud). Table 2.10 presents the trace metal concentrations in rainwater from different marine sites. Aerosol concentration and rainfall

intensity are the prominent factors controlling the wet deposition flux. Aerosol concentrations may vary by orders of magnitude over short time scales, which will lead to a high variability in the trace metal concentration in rainwater (Lim, 1991). In view of this some authors quote their trace elements concentration data as a volume-weighted mean (VWM) (e.g. Kane et al., 1991). The VWM is defined in equation 2.4:

$$\text{VWM} = \sum C_s V_s / V_t \quad (\text{ng m}^{-3}) \quad 2.4$$

Where C_s is the concentration of each sample, V_s is the volume of each collected sample and V_t is the total volume of collected samples.

Wet deposition is a major contributor to the atmospheric deposition of trace metals (Table 2.10). Table 2.10 presents the regional trend of elemental rainwater concentrations with mainly crustal sourced elements (e.g. Al and Fe) being comparatively high in the vicinity of arid regions (North Atlantic) and lower in remote areas (e.g. Bermuda), whereas elements with a predominately anthropogenic source (e.g. Cd and Pb) are higher in the vicinity of industrial areas (e.g. Irish Sea). Both dissolved and particulate trace metals are deposited to the sea surface during precipitation events.

The wet deposition flux can be calculated as follows (Duce et al., 1991):

$$F_r = P \cdot C_r \quad (\text{ng cm}^{-2} \text{ yr}^{-1}) \quad 2.5$$

Where P is the precipitation rate, C_r is the concentration of the substance of interest in rain and F_r is the wet deposition trace metal flux. It is often expressed as a scavenging ratio (washout factor), instead of C_r :

$$F_r = P \cdot S \cdot C_{p_a} \cdot \rho^{-1} \quad 2.6$$

where S is the scavenging ratio (unitless), C_{p_a} is the concentration of particles in air ($\mu\text{g cm}^{-3}$) and ρ is the density of air (air density at STP is 1.2929 kg m^{-3}). In the literature the scavenging ratio is defined either as C_r / C_{p_a} or $C_r / C_{p_a} \cdot \rho$ (Chester 2000).

The scavenging ratio is affected by several factors, which include the size of the particles being scavenged, their chemical and physical form and cloud properties (droplet size, temperature and cloud type).

2.6 Aerosol fate in seawater and rainwater

The post-depositional behaviour of aerosol associated trace metals has been studied (e.g. Duce et al., 1991; Jickells 1995) in order to predict both their impact and fate. Both are constrained by the degree to which they undergo dissolution in seawater (through biotic or physiochemical processes) and rainwater, pre-deposition. The dissolution reaction is crucial in the extent to which atmospheric inputs can influence surface marine trace metal biogeochemical processes (Martin et al., 1989; Bowie et al., 2002; Sarthou et al., 2003). Figure 2.7 represents the alternative fates of aerosol trace metals in both the sea surface microlayer and the bulk seawater, post-deposition. This is a model outlined by Lion and Leckie (1981) to emphasize the enrichment of the microlayer with trace elements.

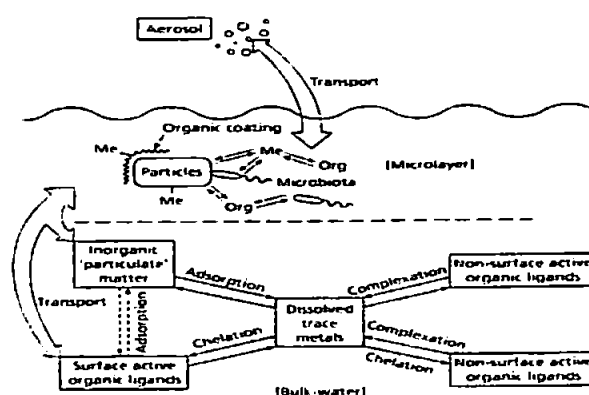


Figure 2.7. Schematic representation of alternatives for the fate of trace metals at the air-sea interface (After Lion & Leckie, 1981).

Table 2.10. Concentrations ($\mu\text{g l}^{-1}$) of trace metals in rainwater from different marine sites.

Element	North Atlantic	Bermuda	North Atlantic	South Atlantic	Mount Etna volcano vicinity	Irish Sea	North Sea
	Lim & Jickells	Church et al,	Church et. al.,	Helmers and Schrems	Cimino and Toscano (1998)	Fones (1996)	Chester et al., (1990)
	(1990)	(1984)	(1991)	(1995)			
Al	1.14-35.2		8.1-110	1.30-131		43.5	105
Cd	0.009-0.18	0.034-0.155	0.003-1.8	0.016-0.196			
Co				0.71-1.72		0.06	0.017
Cu	0.03-0.36	0.23-0.53	0.1-1.2	0.070-0.91	11	2.4	15
Fe	0.18-133	0.99-7.86	1.5-85	1.70-63.5	320		84
Mn	0.06-5.25	0.06-0.51	0.4-4.1	0.11-3.43	45		<12
Ni		0.023-0.32	7.9	0.63-1.42		1.2	
Pb	0.050-0.83	0.48-1.34	0.02-3.1	0.091-1.03		1.2	
Zn	0.09-2.21	0.82-3.49	0.3-5.0	0.359-3.93	640		35

Metals may occur dissolved in seawater, adsorbed onto particles or complexed with organic ligands. The following sections discuss the factors impacting upon the seawater and rainwater dissolution of aerosol associated metals.

2.7 Solubility of aerosol associated trace metals in seawater and rainwater

Much research has been carried out to define aerosol trace metal solubility in seawater but these studies have mainly focused on laboratory simulations whereby either “end-member” aerosol material (Saharan / anthropogenic) or filter collected mixed aerosol samples have been equilibrated with seawater, followed by analytical detection of the dissolved fraction of the aerosol trace metal. Table 2.11 summarises the observations made by different researchers (Walsh and Duce 1976; Hodge, et al., 1978; Crecelius 1980; Graham and Duce 1982; Wollast and Chou 1985; Moore, et al., 1984; Maring and Duce 1987; Maring and Duce 1989; Maring and Duce 1990; Zhuang et al., 1990).

From these studies it is apparent that elements predominantly associated with the crustal aerosol (e.g., Al, Fe and Si) are generally less soluble (Al (0.6-10%); Si (5-10%); Fe (< 1-50%)) in seawater than those elements associated with anthropogenic aerosol components (e.g., Pb (13-90%), Cd (81-84%) and As (48-78%)).

It is also apparent that the range of elemental solubilities in sea water is variable. Such variability might be explained by one or more of the following factors; (i) solid state speciation of the aerosol associated trace metals (Chester et al., 1993; Spokes et al., 1994) (ii) dissolved organic ligands (composition and concentration) in the seawater (Maring and Duce, 1990) (iii) seawater temperature (iv) the presence of micro-organisms in seawater (Biscombe, 2004) (v) the particle concentration in seawater (vi) photochemical processes (Statham and Chester, 1988) (vii) aerosol modification during atmospheric transport (Spokes et al., 1994; Desbocufs et al., 2001).

Table 2.11. Range of literature seawater solubilities of aerosol associated trace metals.

Element	Solubility %	References
Al	0.6-10	1,2
Si	5-10	3
P	21-51	4
Fe	<1-50	2,5,6,9
Mn	25-49	2,6,7
V	31-85	2,6,8
As	48-78	5,6
Cd	81-84	2
Cu	15-86	2,6,10
Ni	29-47	2
Pb	13-90	2,11
Zn	24-76	2,5

References are as follows: 1, Maring and Duce (1987); 2, Hodge, *et al.*, (1978); Wollast and Chou (1985); 4, Graham and Duce (1982); 5, Crecelius (1980); 6, Moore, *et al.*, (1984); 7, Statham and Chester (1988); 8, walsh and Duce (1976); 9, Zhuang *et al.*, (1990); 10, Maring and Duce (1989); 11, Maring and Duce (1990).

2.7.1 Solid state speciation of aerosol associated elements

Sequential leach procedures have been used to determine the solid state speciation (or solid phase associations) of aerosol associated metals, (e.g. Chester *et al.*, 1989). Sequential leach techniques may involve many stages (3, 5 and 6 stages) (e.g. Lum *et al.*, 1982) depending upon the solid state species which the researcher is interested in and constrained by the amount of sample available for processing. Chester *et al.*, (1989) described a three stage sequential leach scheme evaluating the characterisation of the sources and environmental mobility of aerosol trace metals in the marine aerosol. It was designed to establish the partitioning of the metals between; (i) loosely-held (environmentally mobile), (ii) carbonate and oxide, and (iii) refractory (environmentally immobile) associations. This experimental procedure was adopted and used in the current study to determine the solid-state speciation of trace metals in filter-collected aerosols samples. In high temperature processes metals can become associated with the surfaces of ambient aerosol particles by processes such as adsorption, impaction and condensation. These processes usually occur on small particles surfaces more than large particle surfaces as a result of the smaller particles having a relatively greater surface area.

In the first stage of the Chester et al., (1989) procedure, ammonium acetate (at pH 7) is used to determine the loosely held fraction (bioavailable). In the second stage, 25% v/v acetic acid and 0.25 M hydroxylamine hydrochloride is used to leach all carbonate and oxide associated metals into solution. The third and final stage uses a combination of nitric and hydrofluoric acids, used to leach trace metal associated with the organic and refractory fractions. Nitric acid is a strong oxidising agent which oxidises the organic matter resulting, in a release of associated trace metals whereas the hydrofluoric acid attacks the lattice material (e.g. aluminosilicate). This sequential leaching procedure was used to determine the solid-state speciation of trace metals in Liverpool Urban Aerosol Population (LUAP) and Saharan particulates (Figure 2.8), it is clear that when the dominant source is urban (anthropogenic), the exchangeable fraction (stage 1) dominates the solid state speciation (except for Al and Fe which are mainly associated with the residual fraction). However, in the Saharan aerosol the refractory phase becomes increasingly important. Chester et al., (1993) have identified three different groups of elements according to their seawater solubility. Group 1 elements are crustally-controlled (Si, Al and Fe) and generally have very low seawater solubilities (< 10%) from both crustal and urban aerosol populations. The solid state speciation showed that < 10% of Al and Fe occurred in the exchangeable fraction in the LUAP aerosol population and < 1% of Al and Fe occurred in the Saharan (crustal) population (Figure 2.8). The second group of elements (Cr, Mn and Co) are similarly crustally-controlled but have intermediate seawater solubility values (~ 10-50%) from both crustal and urban populations. This could be due to the solid state speciation (Figure 2.8) of which 22-44% of Mn is associated with stage 1 (exchangeable fraction). Group 3 elements (Zn, Cu, Ni and Pb) have higher seawater solubilities in the urban populations than that in the crustal populations. This could also be explained by their solid state speciation characteristics.

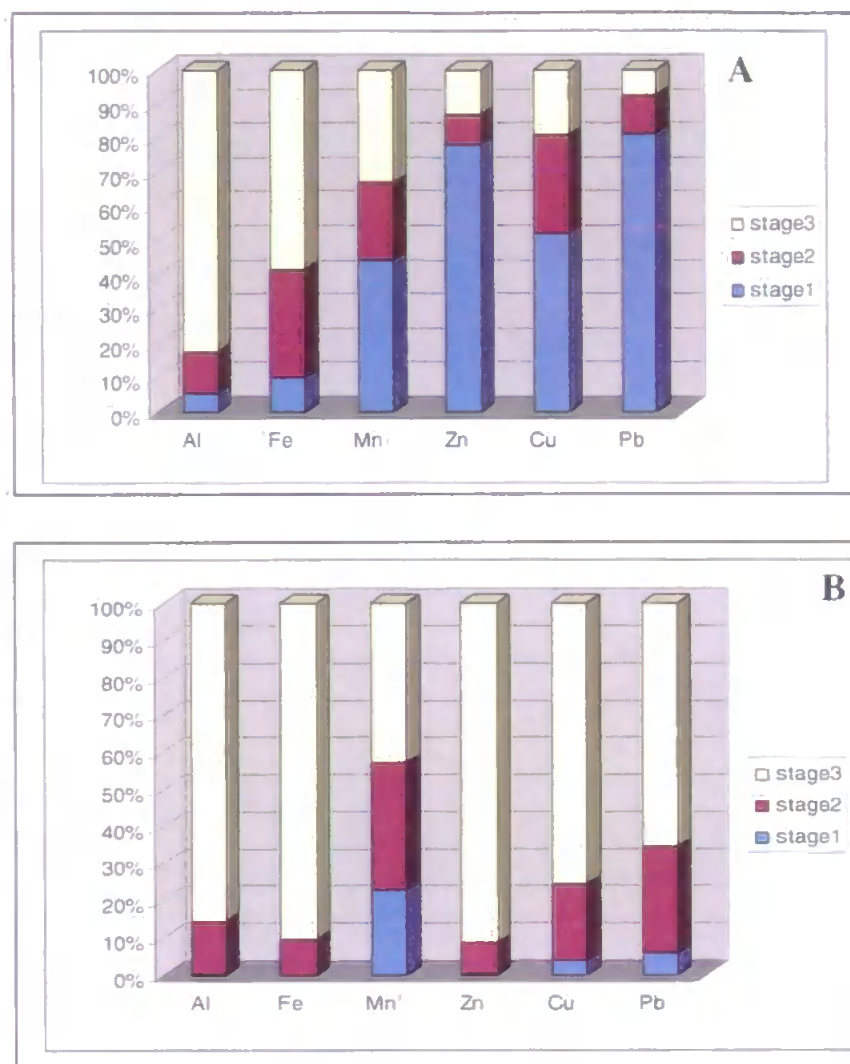


Figure 2.8. Solid state speciation of (A) LUAP (urban) aerosol and (B) Saharan (crustal) aerosol, (after Chester et al., 1989).

2.7.2 Dissolved organic ligands

Many metals are likely to be organically complexed in seawater (van den Berg 1985; Nimmo et al., 1989; Zhang et al., 1990; Bruland, 1992; van den Berg 1995). Spokes et al., (1994) speculated that organic complexation plays a role in increasing the solubilisation of trace metals. The organic complexation of metals is a key factor in oceanic metal cycling, and because the reaction ligands acts to maintain metals in the dissolved form they will also increase metal solubility (Kuma et al., 1996; Wu et al., 2001). Metal-organic complexation may also retard the removal of the metal by scavenging on particulates.

According to van den Berg (1995), the stability of natural organic complexes increases in the following order: $Zn < Pb < Cu < Co < Ni < Fe$. The stability of the metal organic complexes formed will affect the extent of metal organic complexation and hence its seawater solubility but will also be controlled by the organic ligand concentration in seawater.

2.7.3 Seawater temperature

The temperature of the seawater surface will vary from one location to another; for instance the Red Sea has an average temperature of about 30 °C whereas in the polar regions the temperature is around -2 °C. Previous studies to investigate the effect of temperature on the aerosol associated trace metal solubility in seawater are scarce. Biscombe (2004) has reported the effect of temperature on the seawater solubility of trace metals associated with a Standard Reference Material purchased from the National Institute of Standards and Technology (NIST) (SRM 1648). Seawater solubility increased with temperature from 10.8-25.2 °C as follows: Cd (61.1-72.5%), Cu (19.6-24.2%), Pb (17.8-22.8%) and Zn (17.4-22.6%).

2.7.4 Micro-organisms

Bacteria play a key role in the cycling of trace elements in seawater (Azam 1998). About 50% of oceanic primary production is channelled via bacteria into the microbial loop. Gordan et. al., (2000) reported that marine bacteria could produce organic ligands that had a strong complexing capacity with copper in chemostat cultures using estuarine water. Biscombe (2004) also carried out solubility experiments for trace metals in seawater in the presence of bacteria. This study reported a significant increase in aerosol seawater solubility of Cu, Pb and Zn in the presence of bacteria.

2.7.5 Photochemical processes

Statham and Chester (1988) reported the effect of photochemical processes on Mn dissolution. Using Saharan dust, Mn solubility was enhanced under light (ca 3000 lux) as compared to dark conditions. A similar conclusion for Fe has been reported by Spokes and Jickells (1996). Saydam and Senyuva (2002) recently reported an increase in dissolved Fe (II) concentration after the irradiation of 10 g sieved soil sampled mixed with 500 mL distilled deionized water with a UV lamp (1500 W) with the highest concentration being reached after 210 minutes. Borer et al., (2005) illustrated in their laboratory experiments that adding siderophores and a second organic ligand (acting as electron donor) accelerated the light-induced dissolution of crystalline iron oxides to produce a dissolved form of iron (Fe(II)). The ligand-to-metal charge transfer initiated by light absorption by the surface complex (Fe-complex) in the presence of a reductant (e.g. oxalate) will lead to the reduction of Fe(III) to Fe(II), eventually the Fe(II) would dissociate from the complex to an aqueous form (Sulzberger and Laubscher, 1995). Rijkemberg et al., (2005) have also shown that Fe (II) is produced from Fe (III) in seawater at different wavelengths (280-315, 315-400 and 400-700nm) of light and found that wavelengths between 280-314 nm were responsible for the highest production of Fe (II). However, in contrast Ozturk et al., (2004) did not observed any particular wavelength of light which were more effective in the reduction of Fe (III).

2.7.6 Aerosol modification during atmospheric transport

The solubility of trace metals in rainwater has been studied by the direct determination of dissolved and particulate metal fractions in collected rainwater, as well as in laboratory simulation experiments. Factors impacting upon the degree of metal dissolution in rainwater include those highlighted above (see Figure 2.8) and rainwater pH. Many authors have related the solubility of trace metals in aerosols with pH in cloud droplets (Borg et al., 1989; Spokes et al., 1994; Spokes and Jickells, 1996; Desboeufs et al., 2001). It is known

that the pH of rainwater is governed by a balance between the acid and neutralising species present in the atmosphere. Strong acid species, e.g. H_2SO_4 and HNO_3 , have a predominantly anthropogenic origin, the precursors being SO_2 and NO_x (Jickells et al., 1982; Losno et al., 1991). Conversely, the major neutralising agents have a mixed source with mineral dust from crustal weathering (Losno et al., 1991) and NH_3 from natural and/or anthropogenic sources (Apsimon et al., 1987). Moreover, weak organic acids and inorganic acids (neutralising) in aerosols could affect the pH of rain-water.

The proportion of the dissolved form of a metal depends on the pH of the rain (Spokes et al., 1994; Desboeufs et al., 2001) as the solubility increases with lower pH and decreases with higher pH (Losno et al., 1988). During atmospheric transport an aerosol may be subjected to repeated wetting and drying cycles during cloud formation and dissipation prior to its integrating into hydrometers. During these cycles particles could experience very low pHs (Jickells, 1995). A laboratory study conducted by Spokes et al., (1994) examined aerosol associated trace metal solubility during repeated cycling of pH (high-low), simulating cloud processes. For some species (e.g. dissolved nitrogen) the relationship between solubility and pH is simple (Jickells, 1995) but the behaviour of trace metals is likely to be more complex. For example, the solubility of manganese and barium from Saharan aerosol remains high after the initial acidification regardless of the subsequent pH alteration, which is very different behaviour to that of Al and Fe. Whereas in urban aerosols Al and Fe results are slightly different, with not only higher percentage dissolution during the low pH stages, but also incomplete solution phase removal at high pH. These results were suggested to be due to organic complexation (Spokes et al., 1994).

2.8 Context of the current study

This chapter has reviewed the biogeochemical processes which influence the aerosol trace metal fluxes to the marine atmosphere and their subsequent fate in seawater. This has been

done by discussing the possible contrasting sources, source emission strengths and removal processes during transport from source to sink of aerosol associated trace metal, all of which may strongly influence the aerosol metal concentrations and their variability at any one location over time. Factors impacting upon the fate of deposited trace metals in the marine environment have also been discussed.

The current study will embrace these processes and, using two contrasting locations, will investigate their importance in the transport of trace metals to and within the marine aerosol.

The two areas of focus will be:

- 1- Jeddah (South West Asia).
- 2- Plymouth (Western Europe).

These two sites potentially contrast strongly in terms of source types, emission strengths and subsequent removal processes.

Jeddah is a marine site situated on the western side of Saudi Arabia surrounded by arid desert regions. With a population of c.a 2.5 millions and various industries located within its environs, aerosol metals concentrations will be influenced by both crustal and industrial inputs, although the natural crustal source is likely to be a dominant feature.

Plymouth is also a marine influenced sampling site, situated on the south west of the UK surrounded by rural agricultural areas. However, contrasting influences include westerly air masses bringing pristine marine dominated aerosol and easterlies which may transport long range anthropogenically derived trace metal from western European industrialised regions. Plymouth is a city with a population of around 250,000.

These two sites contrast in the type of aerosol sources and removal processes and little work has been carried out to identify the aerosol associated trace metals concentrations and factors influencing their fate in seawater, especially in Jeddah (e.g. Berry, 1990; Behairy et al., 1985 and El-sayed et al., 2004).

Chapter 3

Sampling procedures and analytical techniques

3.1 Introduction

This chapter reports on the various sampling methods, sample treatment and applied analytical techniques used in the current study. These approaches were applied to a series of aerosol samples collected from the following two contrasting sampling locations:-

- 1) Jeddah, Saudi Arabia (representative of a “coastal and arid” influenced site,)
- 2) Plymouth, Devon, UK (representative of a “coastal and semi-rural” influenced site)

Further detailed information on each of these sites is provided in sections 4.1 and 5.1. The collected aerosol samples were typically analysed for the following metals; Al, Fe, Mn, Na, V, Co, Ni, Zn, Cu, Mo, Cd, Pb after total acid digestion with nitric and hydrofluoric acid (Jeddah $n = 203$, Plymouth $n = 131$) and a selected number of aerosol samples (Jeddah $n = 40$, Plymouth $n = 25$) were processed through a three stage sequential leach procedure to determine the aerosol trace metal solid state speciation characteristics.

3.2 Aerosol sampling procedures

3.2.1 Mesh collection

Early methods of sampling the marine aerosol used nylon meshes (Murphy 1985; Saydam 1981; Sanders 1983). These were typically made from cross-weaved terylene fibres (with typical diameters of 0.33mm), covering a surface area of 1 m² (Murphy 1985). During their deployment aerosol particles can adhere to the fibres, a tendency that is enhanced by inertial and electrostatic effects and also by a thin layer of saline moisture on the fibres during collection at sea. Although this means that the meshes are capable of retaining particles which are considerably smaller than the openings between the fibres, their collection efficiency falls off for sub-micron sized particles. Therefore mesh collection results in a size biased aerosol sample, with preferential collection of naturally derived

coarse material (i.e. sea salt and crustal material). Another limitation of the use of meshes is the inaccuracy of the calculation of the volume of air sampled and hence inaccuracies in the calculation of the aerosol chemical constituent concentrations. Therefore, for the collection of total aerosol populations and the subsequent evaluation of aerosol trace metal concentrations, the use of meshes is not appropriate. However, they have been recently used to collect bulk Saharan dust which was subsequently used in metal seawater solubility studies and solid state speciation studies (e.g. Biscombe, 2004; Koçak et al., 2007).

3.2.2 Active aerosol collection systems

The most common and accurate approach (used extensively in atmospheric aerosol collection (e.g. Yaaqub et al., 1991; Spokes et al., 2001; Chester et al., 1999; Guerzoni et al., 1999; Baker et al., 2003; Koçak et al., 2004; Koçak et al., 2005; Baker et al., 2006a) for the collection of aerosol material involves the use of filter media. This method of collection requires forcing the sampled air through the filter substrate over a specific recorded time period using an air pump. Such an approach requires a sampler from one of the following three categories: (i) high volume systems (Wieprechat et al., 2004; Spokes et al., 2001; Chester et al., 1999; Koçak et al., 2004; Koçak et al., 2007; Baker et al., 2006a) which generally operate at an approximate flow rate of 1000 L min^{-1} ; (ii) medium volume systems which operate at 100 L min^{-1} ; (iii) low volume systems (Wieprechat et al., 2004; Spindler et al., 2004; Fones 1996) which operate at 20 L min^{-1} . Such samplers have been used to collect total suspended particulate (TSP) or adapted to collect a selective size spectrum of particles (specified aerodynamic diameter) using cascade impactor attachments (SEAREX (program) 1977-1986; Duce 1989; Chester et al., 1993; Chester et al., 1999; Chan et al., 2000; Kwon et al., 2003; Muller et al., 2004). Cascade impactor attachments may have up to six different stages, and are used to separate different particle diameter ranges (typically 7.2, 3.0, 1.48, 0.96, 0.48 and $<0.48 \mu\text{m}$) or PM_{10} and $\text{PM}_{2.5}$ (Yin et al., 2005) where the particulate material has a diameter less than $10 \mu\text{m}$ and $2.5 \mu\text{m}$

respectively. Differentiation of particulate matter into size fractions (using cascade impactor, PM₁₀ or PM_{2.5} collectors) is crucial if (i) the impact of aerosol particulate material on human health in urban areas is to be assessed and (ii) the evaluation of the dominant aerosol trace metal sources is needed for accurate metal dry deposition and fate predictions and calculations. Recent studies (Yip et al., 2004; Samet et al., 2000; Pope et al., 1995; Dockery et al., 1993) would suggest that there is an association between ambient PM and mortality rates. Harrison and Yin (2000) suggested that for each 10 µg m⁻³ increase in concentration of PM₁₀, there is an associated increase of approximately 1% in the daily all-cause mortality. Therefore, regulatory and environmental bodies have embraced this issue in their priorities and imposed regulations for urban air quality. This is mainly in regard to acceptable levels of PM₁₀ but in some countries a maximum level of PM_{2.5} has recently been introduced (for example the EPA has set national ambient air quality standards in the USA for PM_{2.5} as 15 µg m⁻³ as an annual mean and 65 µg m⁻³ as a 24 hour mean), (Tucker 2000 and Hoffmann 2000).

Being able to define the size distribution of an aerosol population also aids assessment of the source contributions to an aerosol population (see section 2.4.1 for further details). Aerosol populations can be separated into two broad categories; the coarse mode aerosol fraction (>1 µm) which is primarily generated during low temperature processes (e.g. soil erosion, sea salt aerosols) and the fine mode fraction (<1 µm) which is primarily generated during high temperature processes (gas-phase precursor). Spokes et al., (2001); Baker et al., (2003); Alfaro et al., (2003) and Koçak et al, (2005) have all used two stages or multiple stage cascade impactors to differentiate between the coarse and fine modes to assign appropriate elemental settling velocities when calculating dry depositional fluxes (see section 2.5.1).

However, using multi-stage impactor systems is costly and requires longer sample collection times. Such collection times for each sample may be up to five or six times longer than that for total aerosol collection (Chester et al., 1999). This is to ensure that a sufficient quantity of aerosol associated trace metals have been collected on each of the cascade impactor stages such that, after total dissolution into the acid digest solution, they are present at concentrations well in excess of the analytical detection limits. Having longer collection times, however, reduces the temporal resolution compared with that which can be adopted for total aerosol collection (i.e only one stage). For example, aerosol sampling at sea or at coastal stations may require a typical sample resolution of one week instead of 24 hours (Chester et al., 1999). Owing to the dynamic nature of the atmosphere (see section 2.4.2) and the changing aerosol trace metal concentrations over very short time periods, having to adopt a lower temporal resolution sampling strategy will result in the loss of essential information. For example, Koçak et al., (2004) found that just three Saharan dust events (spanning over only several days) occurring over the Eastern Mediterranean in 2001 contributed to about 25 % of the total annual dry deposition fluxes for crustally derived elements (Al, Fe and Mn) and, hence, such events could easily be missed if a low temporal resolution sampling approach was adopted, leading to significant errors in elemental dry deposition flux calculations. This limitation has also been stated by Koçak et al., (2005).

Ideally, total aerosol collection and cascade sample collection should be carried out simultaneously using two samplers, with the total aerosol sampler having a high temporal resolution of sampling (typically daily). However cost often prohibits this option. For the current study only total aerosol samplers were available. These were used to collect aerosol samples at a high temporal resolution over an extend period of time e.g. in Plymouth for a selected period twice daily and in Jeddah one sample per day over the whole sampling period, except at weekends, when one integrated sample was collected. This sampling

strategy provided a large library of aerosol samples which enabled subsequent classification of each sample into different air mass sectors based on three day back trajectories (see section 3.5 for further details on back trajectory calculation).

The total volume of filtered air has been calculated after calibration of the high volume samplers. The calibration kit was purchased from the sampler manufacturer (Andersen Instrument Inc.) and the calibration procedure was taken from the sampler manual. The manometer (Plymouth sampler) or the continuous flow recorder readings taken during the calibration needed to be corrected for prevalent meteorological conditions as prescribed in the sampler manual. The readings from the calibrating kit during calibration were converted to standard air flow (m^3/min).

Following calibration five readings of the corrected manometer or the continuous flow recorder readings taken during the calibration would be drawn against the converted readings (standard air flow) from the calibrating kit. Where the calibration kit readings would be the 'x' values and the manometer or the continuous flow recorder readings will represent the 'y' values. From the equation of the correlation line the manometer or the continuous flow recorder readings during sampling will be converted to standard air flow (m^3/min).

3.2.3 Collection media

Contrasting filter materials have been used for the collection of the marine aerosol. These include cellulose membrane ($0.45\mu\text{m}$) filters (e.g. Yaaqub et al., 1991), fibrous glass fibre filters (e.g. Herut et al., 2001) and Whatman 41 fibrous cellulose acetate filters (e.g. Chester et al., 1993; Fones, 1996; Herut et al., 2001; Koçak et al., 2004; Sarthou et al., 2007).

For the current study, aerosol samples were collected using Whatman 41 cellulose acetate filters, which is the most commonly used filter medium for the sampling of trace metals associated with marine aerosol populations. This type of filter material is most suitable for the following reasons; (i) low metal contamination of filter blanks (in contrast to the high level of impurities present in quartz filters); (ii) easily digested in mineral acids (in contrast to quartz filters); (iii) cause minimal restriction to air flow, allowing high volume collection to be carried out (in contrast to cellulose nitrate membrane filters which greatly restrict flow rates and are brittle); (iv) reasonably inexpensive and readily available; (v) high retention efficiency (>95%) of all particulates, particularly at $<1\mu\text{m}$ in size (Lowenthal and Rhan 1987; Wells, 1999); (vi) mechanical stability as it is flat in the sampler, remains in one piece and gives a good seal with the filter holder to minimize air leaks; and (vii) high temperature stability, which is important because filters must maintain their physical properties (porosity and structure) over ambient temperature ranges.

Clearly all of the above factors are of importance, however in terms of collection of a representative sample, factor (v) is the most important. Whatman 41 filter collection efficiencies have been tested by Stafford and Ettinger (1972), who found that at low filter face velocities, their efficiency never dropped below 95% for particles down to $0.18\mu\text{m}$ diameter. In the natural environment during the course of a sample collection the filters are likely to become loaded with material which will further enhance the collection efficiency of the filters. The main limitation of the Whatman 41 filters is their hygroscopic nature, leading to errors in gravimetric analysis, if required. Accurate measurements of TSP concentrations are therefore unreliable with Whatman 41 filters (e.g. Herut et al., 2001).

3.2.4 High volume TSP sampler used in the current study

Total suspended particulate (TSP) aerosol samples for the current study were collected using commercially bought high-volume samplers (Sierra Anderson –TSP Hi-Vol.

GS2312) having a typical flow rate of $0.8 \text{ m}^3 \text{ min}^{-1}$ (Figure 3.1). Two variations of this sampler were used in the current study. The type used in Jeddah, Saudi Arabia had a brushless motor and a mass flow controller. There are two advantages of this type of system; (i) maintains a constant flow rate throughout the sampling period; (ii) allows the determination of copper in aerosol samples. Earlier models of the Sierra Anderson high volume TSP samplers (similar to the one used at Plymouth) were found to be unsuitable for the determination of aerosol Cu owing to contamination of the samples arising from particle generation from the wearing of the electric motor brushes. Cu determinations were not carried out on the samples collected from Plymouth. This sampler was kindly provided, on temporary loan, by the Oceanography Laboratories, University of Liverpool.

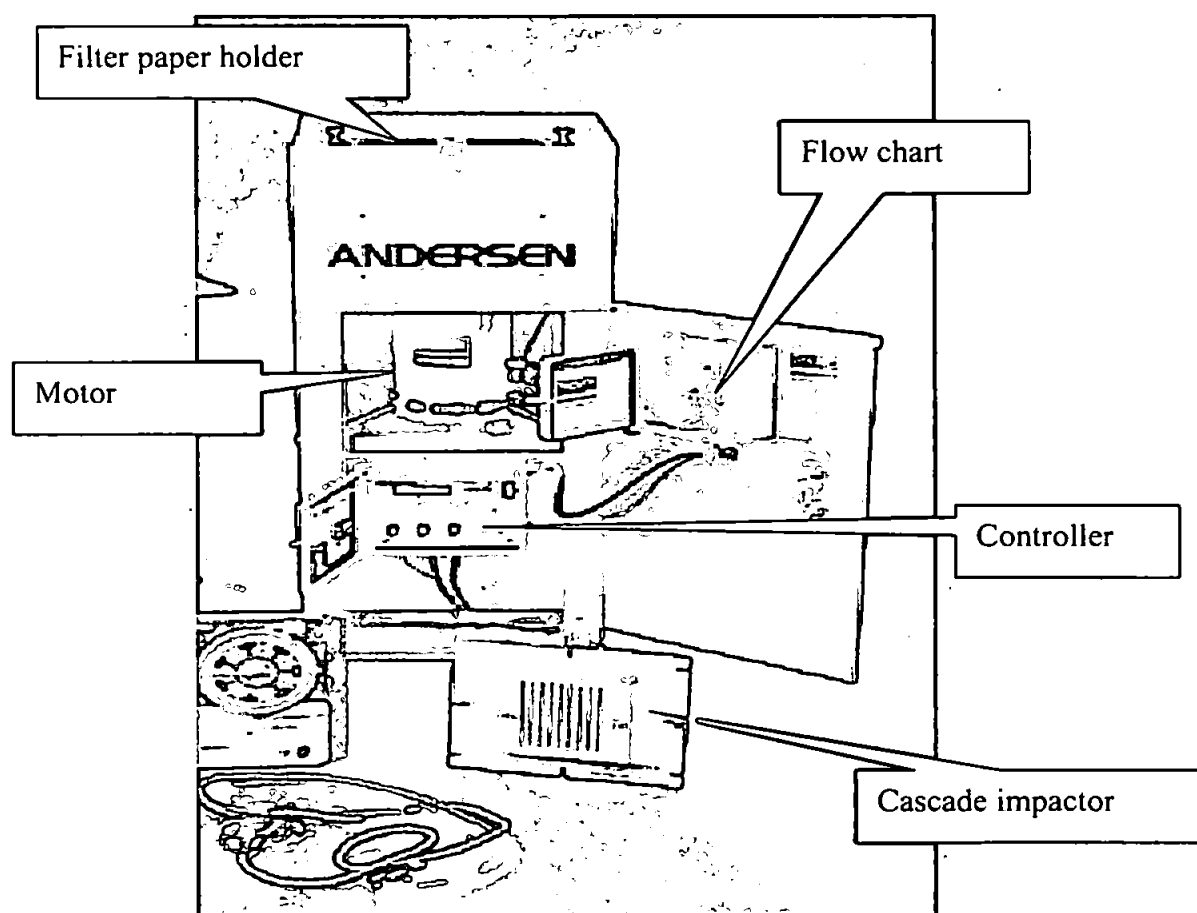


Figure 3.1. The Sierra Anderson –TSP Hi-Vol.GS2312 sampler, as used in the current study at Jeddah (excluding cascade impactor attachment).

3.2.5 Sampling locations adopted in the current study

Collections have been accomplished at two contrasting sites, the first was an urban site in the south-west of Britain (Plymouth) whereas the second site was located in the south-west of Asia (Saudi Arabia: Jeddah). Jeddah is located on the coast of the Red Sea (west coast of Saudi Arabia), being the country's major port and the second largest city with a population of around three million. Figure 3.2 illustrates the sampling location in Jeddah, being to the north of the city in the vicinity of the Obhor lagoon close the Faculty of Marine Science, University of King Abdulaziz campus.

The main areas of business, commerce, industry and urban development lie to the south of Jeddah city and these potential influences are further discussed in section 5.3. The prevailing climatologically influences at the site are also discussed in section 5.2.

The second sampling location was in the south-western region of England. Plymouth is the largest city in Devon with a population of around 275,000. Located in the western region of the English Channel, Plymouth is characterised by a maritime climate, predominantly influenced by North Atlantic westerlies (with a frequency of 30-33% of wind blown on Plymouth; Wells, 1999; for further details see section 4.1.1). The high volume sampler was located on the roof of the Fitzroy building at the University of Plymouth campus (ca. 15m above sea level) as shown in Figure 3.3.

The sampling resolution at Plymouth was initially two samples per day commencing at 10th December 2001 and terminating at 29th July 2002 after which one per day was collected up to 19th April 2003, with a total number of 208 samples being collected over the whole sampling period. There were periodic gaps in the sample coverage owing to motor malfunctions and the requirement to regularly replace the motor brushes. When day and night differentiated samples were collected, the exchange times between samples were

typically 19:00 and 07:00. Whereas, at Jeddah, a sampling resolution of one sample per day was adopted commencing at 10th August 2002 and terminating at 11th January 2004. A total of 313 aerosol sample filters of daily samples were collected. Full details of sampling dates; collection period flow rate and air volumes sampled are presented in Appendix A.

3.2.6 Sampling Protocol

As stated previously Whatman 41 filters were used for aerosol collection in the current study. During manipulations, new and used filters were stored in re-sealable plastic bags to minimise sample contamination. During filter handling on site and in the laboratory the operator always wore disposable plastic gloves. In the laboratory environment all filter handling was carried out in a “Bassaire” Class 100 laminar flow cabinet. Sampler flow rates were measured at the start and at the end of all sampling periods at Plymouth, whereas at Jeddah continuous flow rate measurements were recorded. The flow rates of the samplers were calibrated using a commercial calibration kit. The mean flow rate was 0.8 (± 0.1) m³ min⁻¹ for Jeddah and 0.8 (± 0.2) m³ min⁻¹ for Plymouth. This is in the same range of flow rates previously reported in the literature (e.g. Koçak et al., 2005; Herut et al., 2001). Filter samples, once collected, were divided into two equal sections and stored in air tight plastic containers after labelling with all the relevant information, i.e. dates, start and finish of the sampling period, flowrates, meteorological conditions and any other important observations which might have impacted upon the aerosol trace metal concentrations (e.g. any possible sources of contamination during sample handling or sampling).



Figure 3.2. Location of aerosol sampling site to the north of Jeddah city, Saudi Arabia.



Figure 3.3. Location of aerosol sampling sites at Plymouth, Devon UK.

Operational filter blanks were carried out during every week of sampling by adopting the same procedures as that for the sample filter, except that no air was processed through the filter. These operational blank filters were passed through the acid digestion and analytical stages to assess the levels of contamination in the whole sampling, sample treatment and analytical process.

The outer frame of the sampler and around the filter holder was cleaned regularly, rinsing with Milli-Q water, to remove any potentially contaminating particulate material.

3.3 Adopted analytical approach

Total aerosol associated trace metals were brought into solution by acid digestion using a mixture of concentrated acids (HNO_3/HF). Analysis for trace elements was then carried out using either inductively coupled plasma-atomic emission spectrometry (ICP-AES) or inductively coupled plasma-mass spectrometry (ICP-MS) depending upon the elemental digest concentrations (for Al, Fe and Mn determinations typically ICP-AES was used and for the rest of the considered elements, except Na, ICP-MS was typically the preferred technique, Na was determined by flame atomic emission spectrometry).

3.3.1 Total acid digestion of the aerosol samples

Total acid digestions were carried out in batches on both the aerosol samples and an urban aerosol CRM (NIST 1648) (Certified Reference Material). This CRM probably best represents the collected aerosol samples analysed in the current study if they are anthropogenically dominated in terms of source contributions. Indeed, for some published works reporting aerosol trace metals in the marine aerosol, sediment digests have been used as CRMs which clearly are less representative of aerosol material. The main limitation of the currently available aerosol CRM is that it is less likely to represent aerosol populations dominated by crustal material.

Therefore a combined acid digest was carried out (i.e. both concentrated HNO_3 and HF) to ensure metals which are associated with crustal material, and hence likely to be incorporated within the resistant crystalline lattices of aluminosilicate and quartz phases, undergo complete acid dissolution. Total metal digestions are important when considering aerosol trace metals, as information on the constituent's concentration associated with the whole aerosol population is provided and hence allows for the calculation of the EF_{crust} (see section 2.4.3 for further details on the importance of the EF_{crust}).

The digestion method applied during the current study, was that adapted from Fones (1996), with minor modifications. The digestion method required the use of clean PTFE (polytetrafluoroethylene) vessels (30 mL; Cowie Ltd). The digestion vessels prior to use were washed in detergent followed by rigorous rinsing with Milli-Q water (resistivity of $18 \text{ M}\Omega \text{ cm}^{-1}$) and left in a 20% HCl ('AnalaR' grade) acid bath for 7 days. They were then removed and further washed with copious amounts of Milli-Q water and dried in a laminar flow (Class 100) cabinet and stored in clean re-sealable plastic bags ready for use in the digestion procedure. Full COSHH and risk assessments were completed prior to the first acid digestion batch along with appropriate training in the use of HF.

3.3.2 The total acid digestion procedure

The acid digestion procedure consisted of firstly placing one half section of the Whatman 41 filter sample into a clean PTFE digestion vessel (30 mL; Cowie Ltd.). To this was added 15 mL of concentrated 'Aristar' (VWR) HNO_3 then the digestion tube cap was closed firmly and the mixture was refluxed on a hotplate (Hotplate SH3D, Stuart Scientific) at $80\text{-}90^\circ\text{C}$ for 24 hours in a fume cupboard. After the concentrated HNO_3 digestion, the samples were placed on a hot plate, which was located in a specially designed and constructed HF fume cupboard within a dedicated laboratory annex (see Figure 3.4). This fume extraction system consisted of a continuous water spray at the back

of the cupboard to capture HF fumes. The re-circulated water spray was continually monitored for pH to ensure complete neutralisation of the absorbed acidic fumes. Two mL of “Aristar” HF (BDH) was then added to all samples, CRM (3 replicates) and blanks (3 replicates). The lids were then replaced and the mixture was allowed to reflux for a further two days at 120 °C to dissolve any remaining material. The lids were then removed and the mixture evaporated down to near dryness (to a small bead of solution). Two mL of the concentrated “Aristar” nitric acid was added, followed by a second evaporation to near dryness stage. This last step was repeated twice to remove any residual volatile fluorides. To the final evaporation residue 10 mL of ‘Aristar’ (VWR) nitric acid (2%) was added. The lids were replaced and vessels were transferred to a laminar flow cabinet where the samples were made up to volume (25 mL) in 2% nitric acid (‘Aristar’ in Milli-Q water) using acid washed 25 mL volumetric flasks (grade A). Digest solutions were then placed in 30 mL Sterilin vials (polycarbonate) (Patterson Scientific) and labelled to await analysis by ICP-AES, ICP-MS or flame photometry (see section 3.3.3.1 and 3.3.3.2). Recoveries of elements after digestion of the CRM were > 85% (see Table 3.1). The recoveries presented on Table 3.1 were calculated using the arithmetic mean of the determined metal concentrations in the CRM digestions arising from nine separate acid digestion batches and the certified value provided by the supplier. In every batch the urban aerosol CRM was digested in triplicate, ensuring analytical accuracy and efficient digestion for all batches of samples. Generally the recoveries for the considered elements were acceptable (>85%). However the recoveries calculated for cobalt tended to be higher than 100%, probably owing to the relatively low detected concentrations. However it must also be acknowledged that the value quoted for the cobalt concentration for the CRM is a non-certified value, as it has been analysed by only one technique (NAA; Neutron Activation Analysis), and hence the comparative value may be in error. Sodium also had high recoveries ($115 \pm 5\%$). This might have been due to the fact that Na has been determined using flame photometry which has a relatively poor reproducibility. The final consideration

for the obtained aerosol associated trace metal concentrations is that of quality control and quality assurance. By including the CRM during every digestion it was possible to assess the accuracy and precision of all sample analyses. In cases where there were generally low or excessively high recoveries, the analyses /digests were re-done. Routine verification of the accuracy of sample treatment and analyses represents good analytical practice, ensuring reliable environmental datasets are produced.

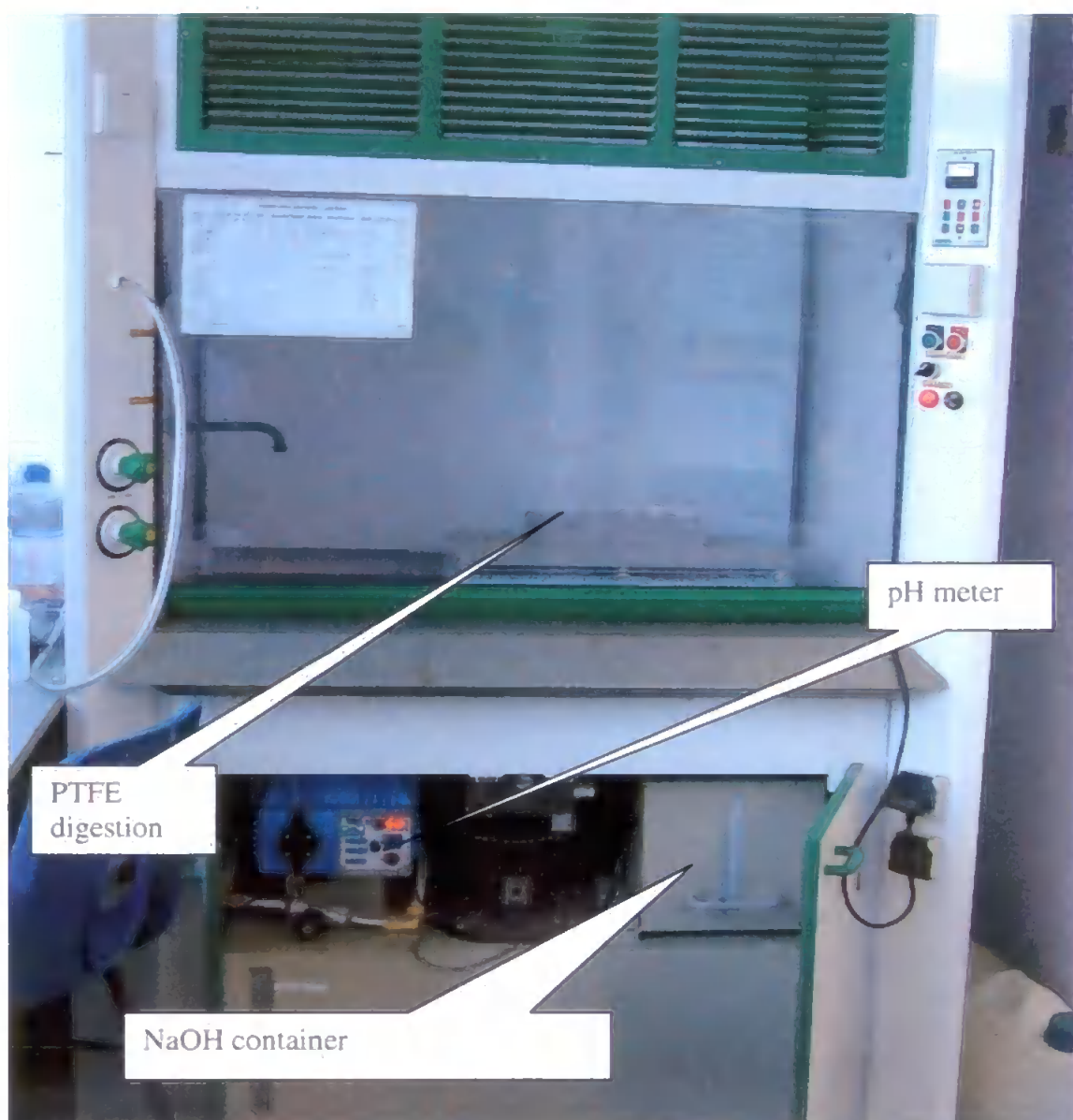


Figure 3.4. The designated HF fume cupboard.

This problem usually affects some of the isotopes determined (the ones that can have interferences). That may therefore affect analytes such as Cu, Zn and other transition elements. Other elements e.g. Pb may not have been affected so badly, because they have fewer interferences.

Table 3.1. Typical elemental concentrations (mg kg⁻¹) (except for Al, Fe and Pb expressed as percentage) and recoveries using the total acid digestion procedure (n=9). Recoveries assessed using the CRM (NIST 1648).

Element	Mean Concentrations (2sd)	Certified Concentrations NIST 1648 (2sd)	Recovery %
Ni	90.0 (20.)	82(3)	109
Pb	0.576 (0.09)	0.655(0.008)	87.9
Al	3.37 (0.14)	3.42(0.11)	98.5
Mn	754 (66)	786(17)	95.9
Fe	3.45 (0.19)	3.91(0.10)	88.2
Na	4920 (430)	4250 (20)	115.7
V	123 (15)	127(7)	96.8
Zn	4140 (60)	4760 (0.14)	86.9
*Cu	554 (21.2)	609(27)	91.0
Co	21.9 (4)	18	121
Cd	64.4 (8.8)	75(7)	85.8

CRM (n=4) value for copper has been analysed only in conjunction with Jeddah samples.

* CRM value for cobalt is a non-certified value.

* Analysis carried out by Flame Photometry.

3.3.3 Analytical techniques

3.3.3.1 Inductively Coupled Plasma-Atomic Emission Spectrometry (ICP-AES) and Inductively Coupled Plasma-Mass Spectrometry (ICP-MS)

ICP-AES and ICP-MS were the analytical techniques selected for the determination of trace metals (except for Na) in the total aerosol acid digests. ICP-AES was used to determine Al, Fe and Mn in aerosol samples collected from both Plymouth and Jeddah, whereas ICP-MS was used for the determination of Cd, Ni, Co, Zn and Pb in samples collected from Plymouth and Jeddah.

ICP-AES is a well-established technique for routine analysis for a wide range of elements. It is used extensively in environmental science owing to its wide dynamic range (10 ng mL⁻¹ up to 100 µg mL⁻¹), comparatively low detection limits (sub-µg mL⁻¹), high selectivity and its ability to carry out multi-elemental analysis.

The ICP-AES instrument employed for the analysis in the current study was the Liberty 516 (Varian). Detailed operating conditions are presented in Appendix B. The ICP-MS used was the V.G. Plasmaquad PQ2 (Fisons Instruments). Similarly, detailed operating conditions are also presented in Appendix B.

The sample compartments and plasma source for ICP-MS and ICP-AES are similar. The basic components of ICP-AES and ICP-MS instruments are shown in Figures 3.5 and 3.6 respectively. During ICP-AES operation the optical spectrum (ca. 165-800 nm) is viewed either sequentially (which was the one used during the current work) or simultaneously (faster in measurement). The analyte emission lines are detected using a photomultiplier (PMT) (or by charge-coupled and charge-injection devices).

For ICP-MS ions are produced in the plasma and passed through the interface (sampler cone and skimmer cone) to reduce the pressure, allowing passage into the mass spectrometer (MS), having a relatively lower pressure. Then the ions pass through the ion optics through the mass filter (quadrupole, double focusing magnetic sector) and then eventually into the detector. In general, the ion beam passes through the entrance slit to the analyzer and then through the exit slit to the detector.

ICP-MS is a powerful and rapidly developing technique for multi-elemental determination at sub- $\mu\text{g L}^{-1}$ concentrations. Therefore, determination of some elements is difficult because of interferences (spectral and isobaric spectral overlaps) but these can often overcome by high resolution ICP-MS.

3.3.3.2 Reagents and Standards

All reagents were Aristar[®] grade or equivalent unless otherwise stated and were used as received, with the exception of acetic acid (which was used for the sequential leach) for which Romil Ultra Pure Acid was used to reduce contamination.

Stock solutions of the reagents were prepared as described below and working solutions were prepared by serial dilution as required. Milli-Q water ($18.2 \text{ Mohm cm}^{-1}$, Elagastat Maxima), which was low in trace metals and fitted with UV treatment (and thus also low in dissolved organic carbon (DOC)) was used for solution preparation and labware rinsing throughout this work.

Standards were prepared freshly on the day of analysis using an ICP standard (10,000 / 1,000 mg L^{-1} in 2.0 % (v/v) HNO_3 , Spectrosol, BDH) by making up a multi-element stock solution in 25 mL (in a glass volumetric flask, grade A) with 2 % nitric acid. Serial dilutions were then made, allowing a series of six mixed standards to be prepared, which

were then used to construct a calibration line for the ICP-MS and ICP-AES. In addition, the standards used to calibrate the ICP-MS contained two internal standards (In and Th at concentrations of $100 \mu\text{g L}^{-1}$ and 1 mg L^{-1} respectively).

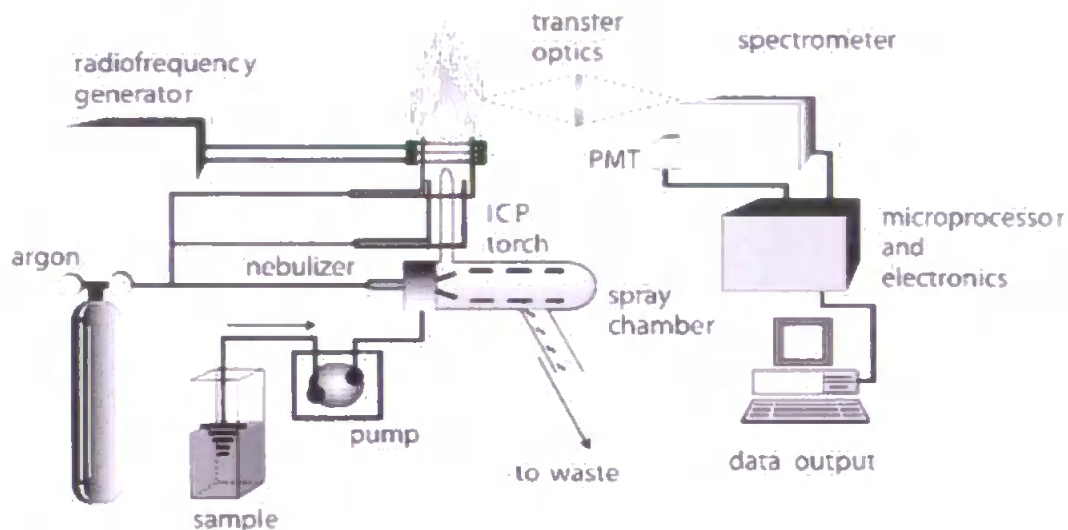


Figure 3.5. The major components of the ICP-AES (Source: [http:// www.balticuniv.uu.se/environmentalscience/ch12/chapter12_g.htm](http://www.balticuniv.uu.se/environmentalscience/ch12/chapter12_g.htm)).

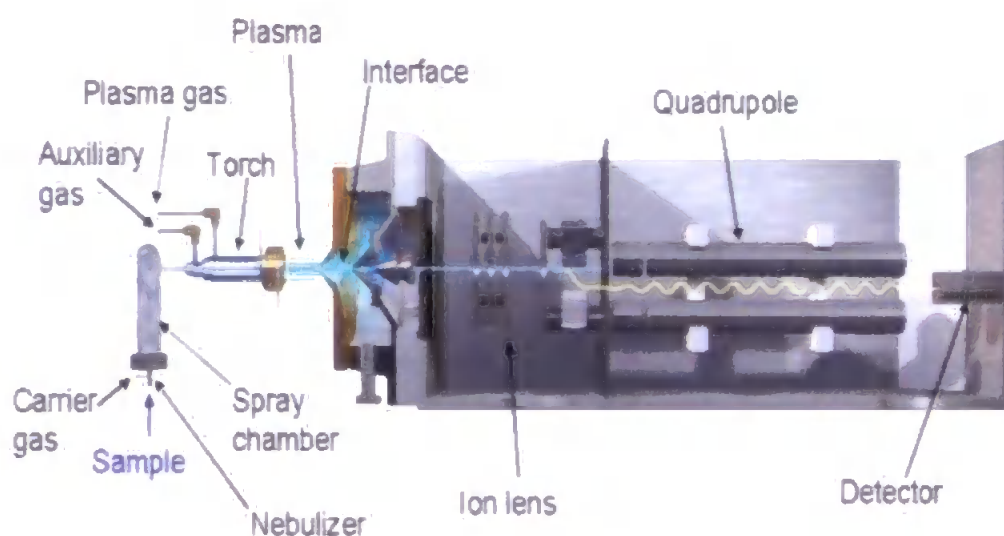


Figure 3.6. The major components of the ICP-MS (Source: [http:// www.esslab.com/agilent icpms. htm](http://www.esslab.com/agilent_icpms.htm)).

Depending upon the sample type (Jeddah or Plymouth) different mixed elemental standard concentrations were prepared. The adopted standard solution concentration ranges are summarised in Table 3.2. Any sample digest solution which gave a signal above the highest standard was diluted and re-analysed.

3.3.3.3 Analytical performance

Table 3.3 highlights the instrumental limits of detection for ICP-AES, along with the corresponding applied elemental emission line.

The linear ranges are also quoted. Analytical limits of detection were calculated from the following equation:

$$\text{Instrumental limits of detection} = \text{blank} + 3\sigma, \text{ (Miller and Miller, 2001)} \quad (3.1)$$

Where σ is the standard deviation of the blank replicates. In this case the blank is represented by the trace elemental concentrations in 2 % nitric acid. Although the calculated limits of detection were greater than the reported limits of detection, they were adequate for the current study for the determination of Al, Fe, Mn, and Zn in all aerosol sample types.

For the current study the linearity of the techniques was not specifically defined, instead calibrations were tailored to approximate the concentrations expected in the sample. However the calibration graph was rejected if the correlation coefficient (r^2) was < 0.995 , ensuring that the linearity of the instruments response was maintained for the range of elemental concentrations encountered in the samples analysed.

Table 3.2. Summary of the elemental standard solution concentration ranges for the contrasting sampling sites in the current study. Al, Fe and Na concentrations are expressed as mg L⁻¹, whereas the remaining elements are expressed as µg L⁻¹.

Element	Jeddah acid digest solutions	Plymouth acid digest solutions
Al	5-150	5-20
Cd	5-150	1-30
Co	5-150	1-30
Cu	100-2000	-
Fe	5-150	5-20
Mn	0.5-6	0.5-6
Mo	5-150	3-100
Na	1-10	1-10
Ni	5-150	3-100
Pb	100-2000	30-500
V	100-2000	3-100
Zn	100-2000	30-500

Table 3.3 also highlights the wide linear range (typically between 10 µg L⁻¹- 100 mg L⁻¹) exhibited by ICP-AES.

Table 3.3. The calculated and reported ICP-AES elemental instrumental limits of detection (p.p.m.) for correspondent emission line (using ICP-AES).

Element (wavelength nm)	LOD (Calculated)	Linear range
Al (308.215)	0.1	0.1-450
Cu (324.754)	2.9	2.9-1000
Mn (257.610)	0.044	0.044-150
Fe (259.940)	0.05	0.05-750
**Na	1	1-10

****Na** has been measured using flame photometer.

A number of elements were present in the aerosol acid digestion solutions at concentrations below the limits of detection for ICP-AES (i.e. Co, Cd, Mo, Pb, V and Ni) and hence these were subsequently determined using ICP-MS.

The limits of detection for ICP-MS were calculated in the same manner as those for the ICP-AES and are presented in Table 3.4. The linearity for ICP-MS lies in the range 0.1 $\mu\text{g L}^{-1}$ to 20 mg L^{-1} . Similar criteria for rejection / acceptance of the calibration line were adopted as were applied for ICP-AES analyses.

Table 3.4. Calculated and reported ICP-MS elemental instrumental limits of detection expressed in $\mu\text{g L}^{-1}$.

Element	LOD (experimental)	Linear range
V	3	3-20
Co	0.4	0.4-30
Mo	1.0	3.8-10
Pb	3.8	0.8-8
Cd	0.16	1.6-10
Ni	1.1	1.1-20
Zn	15	15-50
Cu	10	10-20

3.3.3.4 Flame photometry

Flame photometry (flame atomic emission spectrometry) was chosen for the determination of Na in aerosol digests. It is a rapid, simple, and sensitive analytical method for the determination of alkali and alkaline earth metal ions in solution (e.g. Na, K, Li). Owing to the very narrow and characteristic emission lines from the gas-phase atoms in the flame, the method is relatively free of interferences from other elements. Typical precision and accuracy for analysis of dilute aqueous solutions are $\pm 1-5\%$. This method is used to

determine metals which are easily excited to higher energy levels at the temperature of a flame. A diagram of the main components is highlighted in Figure 3.7.

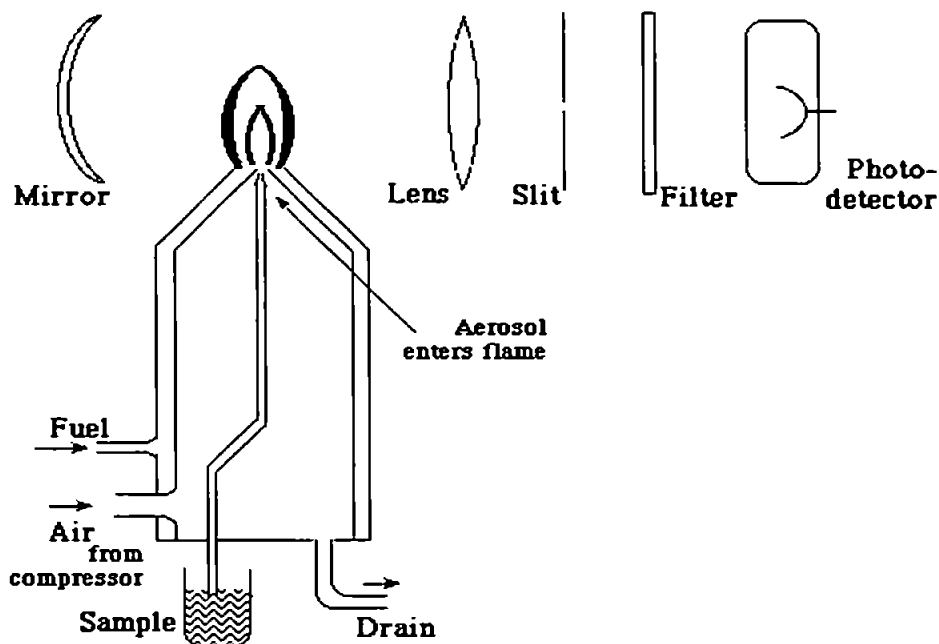


Figure 3.7. The main instrumental components of a flame photometer.

3.3.4 Measurement of trace metal in aerosol digest solutions; operational blanks

Analytical blank values which were obtained directly from the analysis of Milli-Q water were used to calculate the limits of detection. However, the operational blank is also essential to define and assess the contribution of contamination during sample handling and processing. The operational blank was defined by processing a filter paper which has been passed through the same process as the samples. The values of the operational blanks were expected to be higher than those observed in the reagents blanks, but should be significantly lower than the mean values of the sample digests. Table 3.5 highlights the mean operational blank elemental concentrations for each sample type (Jeddah and Plymouth) along with the average elemental concentration in the sample digest solutions.

Table 3.5 Determined operational aerosol blank values compared with the average trace metal concentrations observed in the sample acid digest extracts (expressed in $\mu\text{g ml}^{-1}$ for ICP-AES and flame photometry / ng ml^{-1} for ICP-MS).

Element	Instrument	Plymouth		Jeddah	
		Average Whatman 41 Filter blank (\pm s.d.)	Average concentration in acid digestion (blank contribution %)	Average Whatman 41 Filter blank (\pm s.d.)	Average concentration in acid digestion (blank contribution %)
Al	ICP-AES	0.71 (0.56)	39 (1.8)	0.59 (0.39)	119 (0.5)
Mn	ICP-AES	0.09 (0.15)	2.5 (3.7)	n.d.	2.4 (0.6)
Fe	ICP-AES	0.14 (0.16)	41 (0.35)	0.33 (25)	130 (0.3)
Na	Flame	1.42 (1.5)	54 (2.6)	2.3	240 (1.0)
Cu	ICP-MS	-	-	23 (25)	400 (5.8)
V	ICP-MS	4.1 (4.8)	102 (4)	6.9 (11)	910 (0.8)
Co	ICP-MS	0.71 (0.98)	25 (2.8)	3.4 (3.7)	111 (3)
Ni	ICP-MS	9.9 (5.7)	69 (14)	33 (66)	460 (7)
Zn	ICP-MS	46 (40)	620 (7.2)	44 (42)	1390 (3)
Mo	ICP-MS	1.2 (0.73)	12 (9.0)	2.4 (3.3)	16.0 (15)
Cd	ICP-MS	0.22 (0.09)	85 (0.26)	0.70 (0.52)	8.7 (8.0)
Pb	ICP-MS	3.8 (4.6)	800 (1.0)	5.5 (5.5)	457 (1.2)

In addition, Table 3.5 also highlights the typical % contribution of the operational blank to the digest solution concentration. Generally for all the aerosol samples collected from Plymouth and Jeddah the contribution of the operational blanks were <10% of the aerosol digest concentrations, with the exception of Ni (Plymouth) and Mo (Jeddah) which for both was 15%.

3.4. Application of the sequential leach procedure to determine the trace metal solid state speciation in aerosol samples

The application of a three stages sequential leach procedure is described, which has been adapted from that of Chester et al., (1989). These authors described a three stage sequential leaching scheme allowing the characterisation of sources and environmental mobility of aerosol associated trace metals in the marine aerosol. It was designed to establish the partitioning of metals between loosely-held (environmentally mobile), carbonate and oxide and refractory (environmentally immobile) solid phase associations. This experimental procedure was adopted and used in this study to determine the solid-state speciation of aerosol trace metals in samples collected from both the Plymouth and Jeddah sites. Samples were chosen based on their air mass origin. In high temperature processes metals can become associated with the surfaces of ambient aerosol particles by processes such as adsorption and condensation. These processes usually occur on small particle surfaces more than large particles surfaces and are represented by the exchangeable fraction. If a metal is predominantly associated with this phase, then it is easy to release into solution. The first stage in the sequential scheme was defined by equilibration of the filter sample with ammonium acetate (at pH 7). The second stage of 25% of acetic acid and 0.25 M hydroxylamine hydrochloride was used to leach all carbonate and oxide associated metals into solution. The third and final stage use a combination of concentrated nitric and hydrofluoric acids to leach trace metal associated with organic and refractory solid fractions. Nitric acid is a strong oxidising agent which will oxidise the organic matter

whereas the concentrated hydrofluoric acid will attack the residual lattice material (aluminosilicate) and release the associated trace metals. The sequential leach solution blank contributions (expressed as a percentage of the average trace metal concentration in the leach solution after equilibration with aerosol loaded filter portions) amounted to (i) for stage 1 < 10 % for all elements with the highest value being observed for Fe (9.8%) and lowest for Co (0.1%) (ii) for stage 2 < 10% for all elements except for Ni (23%), Mo(17%) and Cd (17%) and Cu (16%) (iii) for stage 3 < 10% for all elements with the highest being for Ni (3.3%) and the lowest for Al and Fe (0.1%). With the lack of certified reference material (CRM) for this particular sequential leach procedure the alternative was to compare the sequential leach analysis with the literature which illustrate geochemically consistent trends (when compared with the literature e.g. see table 4.20).

3.4.1 Reagents preparation

Ammonium acetate (1.0 M): This reagent was prepared by dissolving high purity (99.999%) ammonium acetate in Milli-Q water to yield a 1.0 M solution (77.08 g ammonium acetate in 1 L de-ionised water). The pH was then measured in a small aliquot of the solution and if the pH was not 7, it was adjusted with Aristar[®] grade nitric acid or ammonium hydroxide to pH 7.

Hydroxylamine hydrochloride + 25% acetic acid: A 69.49 g of hydroxylamine hydrochloride (Aristar[®] grade or equivalent) was dissolved in 750 mL of Milli-Q water, then 250 mL of ultra high purity acetic acid was added to the solution to make the final volume 1 L. All reagents were prepared fresh on the day of analysis and stored in acid washed high density polyethylene containers.

3.4.2 Sequential leach procedures

Stage 1: Half a filter paper was folded and placed in a 50 mL centrifuge tube, then 15mL of 1.0 M ammonium acetate (pH 7) was added. Extraction was then carried out at room

temperature with constant agitation on a shaker for 15 min. Lastly the tubes were centrifuged at 3000 rpm for 15 min. The supernatant was then pipetted out and stored in sterilin containers for analysis.

Stage 2: Filter residue from stage 1 was extracted at room temperature for 6 h with 15 mL of 1.0 M hydroxylamine hydrochloride in 25 % acetic acid. After leaching the suspensions were centrifuged for 15 min at 3000 rpm. The supernatant was then pipetted out and stored in a sterilin for analysis.

Stage 3: Residue was transferred to a PTFE vessel and total digestion using HNO₃ (15 mL) and HF (2 mL) was carried out (see section 3.3.1 for the description of total digestion).

Standards were prepared using a matching matrix for all stages. Al, Fe and Mn were analysed using ICP-AES and the rest of the elements were measured in all stages using ICP-MS. To control and minimise contamination plastic gloves were worn at all times and preparation of standards and reagent preparation took place in a class 100 laminar flow hood. The range of standard used for each element for each of the three stages is presented in Table 3.6.

3.5 Air Mass Back Trajectory Calculations

To aid in aerosol source evaluation and aerosol trace metal variability air mass back trajectories for each sample were calculated at different atmospheric altitudes. A trajectory is the time integration of the path transported by an air parcel. The air parcel trajectory is calculated using a meteorological model called HYSPLIT (NOAA Air resources Laboratory, FNL data set). However, trajectories can be integrated both forward and backward in time. Trajectories should primarily be used as a tool to help evaluate the source of the sampled aerosols (Stohl et al., 2002).

The longer the time backward or forward used to calculate the air mass trajectories, the larger the error becomes. Moreover, it is useful to calculate different pressure levels of trajectories (e.g 899, 845, 700 hP) as this information may help in the interpretation of

Table 3.6. The range of standards used for the calibration in $\mu\text{g mL}^{-1}$ (Al and Fe in mg mL^{-1}), for each of the sequential leach stages.

Element	Plymouth	Jeddah
Al	1-0.5-5	1-0.2-2
	2-0.5-5	2-1-15
	3-1-20	3-30-300
Fe	1-0.5-5	1-0.2-2
	2-0.5-5	2-1-15
	3-1-20	3-30-300
Mn	1-80-800	1-200-2000
	2-4-50	2-5-60
	3-10-200	3-40-600
V		1-30-500
		2-6-70
		3-10-200
Co	1-1-20	1-3-30
	2-0.5-5	2-2-20
	3-1-10	3-5-50
Ni	1-10-200	1-30-500
	2-4-50	2-
	3-10-200	3-10-200
Zn	1-100-2000	1-200-2000
	2-10-200	2-10-150
	3-50-600	3-20-300
Mo	1-1-20	1-3-30
	2-0.5-5	2-1-10
	3-2-30	3-1-10
Cd	1-1-20	1-3-30
	2-0.5-5	2-1-10
	3-1-10	3-1-10
Pb	1-30-500	1-30-500
	2-4-50	2-5-50
	3-10-200	3-10-200

aerosol trace metal results because mixing between different air masses may occur during transport. In this study the model HYSPLIT (HYbrid Single-Particle Lagrangian Integrated Trajectory) developed by NOAA (National Oceanic and Atmospheric Administration) was used. Three day back trajectories were calculated at three different pressure levels (100,

500, 1000 m) or (1000, 955, 850 hPa) for each of the samples at each sites. This information was then used to evaluate the effect of air mass movement on aerosol trace metal characteristics (at all collection sites). Samples were then categorised into groupings (e.g. Plymouth: 1-Atlantic, 2- UK and Europe). Samples which did not stay for 50% of the time in one category were defined as being “mixed”. An example of a back trajectory diagram is presented in Figure 3.8.

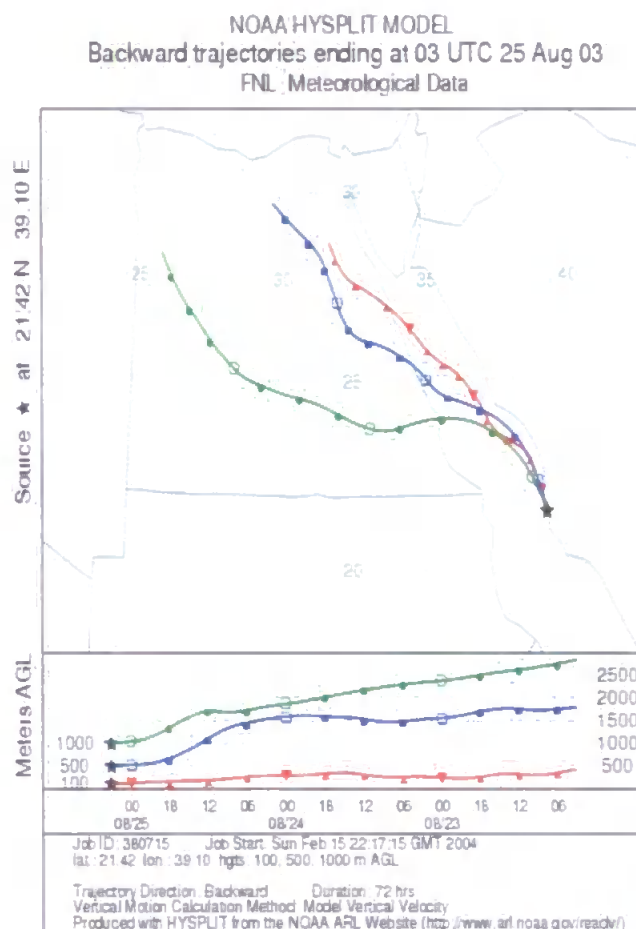


Figure 3.8: An example of a 3 day back-trajectory arriving at Jeddah, starting on the 23rd August 2003 ending on 25th August 2003 (lines with triangles represent an altitude of 100 m at the sampling site whereas lines with squares represent an altitude of 500 m; lastly the line with circles represent an altitude of 1000 m).

Chapter 4

Aerosol trace metal concentrations at a western English Channel urban coastal site (Plymouth)

4.1 Introduction

This chapter discusses the variability in the aerosol trace metal concentrations (Al, Fe, Mn, Ni, Co, Cd, Pb, Zn & Na) observed at an urban western English Channel coastal site (Plymouth), over a fifteen month sampling period (December 2001 to April 2003). Long (seasonal) and short (inter- and intra- daily) term variability in the aerosol chemical composition will be defined. The observed variability will be discussed in the context of the following factors; (i) aerosol source types, (ii) aerosol emission strengths, (iii) proximity of aerosol source, (iv) air mass transport processes and (v) removal processes. In addition, this Chapter will present atmospheric total and bioavailable trace elemental dry deposition fluxes to the western English Channel. Full details of the sampling and analytical methods employed have previously been discussed (sections 3.2 and 3.3).

4.2. Background

4.2.1. The English Channel coastal environment

Plymouth is a city with a population of around 250,000 situated in the south west of England (see Figure 4.1) on the western English Channel coastline. The English Channel connects the North Sea to the Atlantic Ocean and is bordered by 650 km of English and 1100 km of French coast line, covering a surface area of some 77,000 km² (Reid et al., 1993). The whole coastline of the English Channel is inhabited by about nine million people of whom about forty four percent live along the British coast (Reid et al., 1993). The British side of the Channel possesses a wide variety of industries which are chiefly concentrated around urban centres and ports such as Plymouth, Southampton, Portsmouth, Folkestone and Dover. Plymouth and Portsmouth each have a naval base and passenger ferry connections to Europe.

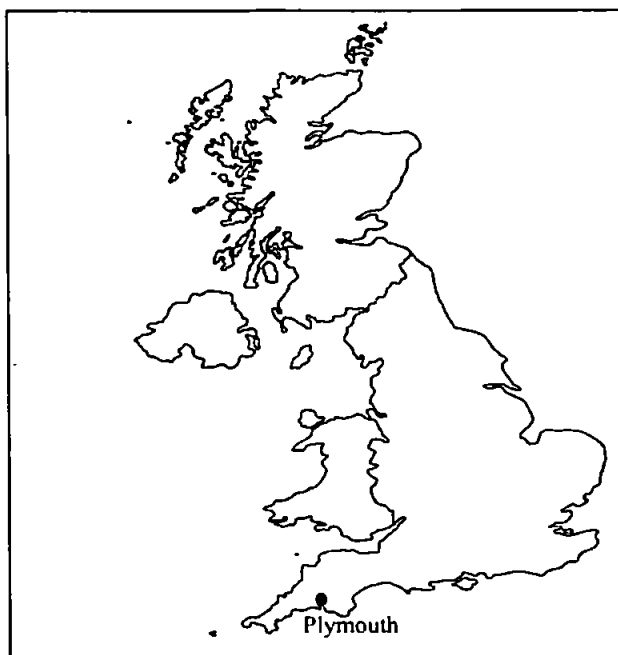


Figure 4.1. Location of sampling site (Plymouth).

The hinterland of Southampton is arguably the most industrialised region along the southern England coastline with oil refineries and an oil fired power station which contributes significantly to atmospheric emissions (Reid et al., 1993). The majority of the French industry in the region is located on the Seine estuary and its hinterland, including TiO_2 processing plants (discharging acid iron waste) and three phosphate manufacturing plants (discharging phosphogypsum) (Reid et al., 1993). Three nuclear power stations are in operation along the French coastline, moreover, a major petrochemical complex is sited within the industrial region of Le Harve. Table 4.1 highlights the annual direct industrial discharges of trace metals to the English Channel (Reid et al., 1993).

Table 4.1. The annual direct industrial discharges (tonnes yr^{-1}) to the English Channel from both the British and French (Seine) coastlines.

Region	Cd	Cu	Pb	Zn
Britain	1.2-2.7	47-51	15-27	384
France (Seine)	7.4	166	236	676

4.2.2 Aerosol trace metal concentrations in the English Channel

A limited amount of research has been carried out on defining the aerosol trace metal concentrations in the English Channel marine atmosphere. Some of the earliest work was that carried out by Austin and Millward (1986) who defined As and Sb inputs to the English Channel and the Atlantic Ocean. In this study three sampling stations were established. These were; (i) at Plymouth (50° N 22.54'; 004° N 08.33' W), (ii) on board the Channel Light vessel (49° N 54'; 2° 54' W), and (iii) on board an Ocean Weather ship at Ocean Station Lima (57° N; 20° N). The observed concentrations at Plymouth and the Channel Light vessel were respectively As: 0.83 ng m⁻³ and 1.70 ng m⁻³; Sb: 0.45 ng m⁻³ and 0.80 ng m⁻³. These concentrations were an order of magnitude higher than those measured at Ocean Station Lima, being As: 0.075 ng m⁻³; Sb: 0.086 ng m⁻³, which was suggested to be due to multiple local sources (mineralised land masses of the South West Peninsula). Austin and Millward (1986) also contradicted the then conventional perspective that riverine inputs are the dominant external source for trace metals to coastal waters; suggesting that atmospheric transport could dominate, particularly in the vicinity of large industrial and urban areas. More recently Otten et al., (1994) showed that the observed concentrations of atmospheric aerosol trace metals decrease moving from east to west (towards the South West Peninsula) through the English Channel. For instance, chloride concentrations (which is indicative of the maritime influence) ranged from < 600 ng m⁻³ off the Normandy coast up to 3560 ng m⁻³ off Land's End. Moreover, S (non sea salt; indicator of anthropogenic emission) and Fe (indicator of crustal material input) concentrations fell from 1360 ng m⁻³ to 410 ng m⁻³ and from 48 ng m⁻³ to 7.3 ng m⁻³ respectively in aerosol samples collected from off the Kent coast (high) to the Land's End (low), representing a decrease of more than a factor of 3. A more detailed study was carried out by Wells (1999) over a period in excess of one year. This study employed a coastal / rural site (Slapton in South Devon) aiming to understand the factors influencing the geochemistry of aerosol/rain water associated trace metals, the magnitude of trace

metal fluxes and an assessment of the marine fate of atmospherically derived trace metals. Wells (1999) collected aerosol samples using a high volume air filtration system and then carried out a total digestion on the samples ($\text{HNO}_3 + \text{HF}$) with the analyses being carried out using FAAS, GFAAS and flame photometry. Ten trace metals (Al, Cd, Co, Cu, Fe, Mn, Na, Ni, Pb and Zn) were investigated. The following geometric mean concentrations were observed: Al:229, Cd:0.11, Co:0.12, Cu:2.34, Fe:115, Mn:7.94, Na:2570, Ni:15.1, Pb:1.20 and Zn:20.9 ng m^{-3} respectively. Wells (1999) concluded that the long range transport of European aerosol appeared to influence the chemical character of the western English Channel aerosol. Also, suspended regional terrestrially derived material had a significant influence on the western English Channel aerosol, particularly for Ni. Aerosol trace metal concentrations were dependent upon the meteorological conditions; particularly the wind direction, aerosol source (see Table 4.2) and wet deposition (see Table 4.3). A clear enhancement of trace elemental concentrations (Fe, Mn, Na, Pb and Zn) were detected in air masses travelling from the east and presumably passing over UK and Western European aerosol sources (both natural and anthropogenic), compared with those concentrations detected in air masses derived from the west, having passed over the more pristine Atlantic environment. For example, the geometric mean concentrations of Fe and Mn were 325 and 16.1 ng m^{-3} respectively, being associated with the UK (and long range European) air sector whereas they were 219 and 13.3 ng m^{-3} within the Atlantic maritime (non-anthropogenic) air sector. Therefore, the overall mean trace metal concentrations observed in this region will be dependent on the influence of contrasting air masses at the collection site over the applied sampling period. Wet deposition flux calculations indicated a higher flux for all the considered trace metals, compared with the equivalent dry deposition flux, except for Al (Table 4.3). This clearly highlights the relatively more efficient removal effect of rain events compared with the continuous dry depositional mechanism. The Al dry depositional flux is often calculated to be higher than its wet depositional flux, owing to a predominant association with the larger particle size fraction

of the aerosol population (see section 2.4.1). The percentage contribution of dissolved trace metal flux to the total flux was 1.18 and 84.7 for the two contrasting sourced elements, Al and Pb respectively.

Table 4.2. Geometric mean trace metals concentration (ng m^{-3}) detected in contrasting air sectors of the English Channel aerosol (Wells 1999) (significant intervals represent ± 1 s.d.).

Wind direction	Fe	Mn	Na	Pb	Zn
(N,NE,E)	286 \pm 411	7.7 \pm 14.9	85700 \pm 28967	7.3 \pm 7.88	8 \pm 171
(S,SW,W)	190 \pm 200	4.3 \pm 14.4	6670 \pm 73993	3.8 \pm 5.41	10 \pm 29.6

Table 4.3. Wet and dry trace elemental fluxes ($\text{ng cm}^{-2} \text{ yr}^{-1}$) to the western English Channel sea surface.

Element	Dry deposition flux	Wet deposition flux	Total deposition flux	Total dissolved flux
Al	7830	6450	14280	167
Co	1.45	83.8	85.3	80.2
Cu	32.1	986	1018	946
Ni	33.0	320	353	200
Pb	0.86	301	302	138

4.2.3 Meteorological characteristics of the English Channel

The daily weather charts for the British Isles have been classified by authors such as Lamb (1950) and Barry and Chorley (1992). Two dominant types of weather systems have been defined; (1) low pressure cyclonic (C) depression and (2) high pressure anticyclonic (A). The airflow direction or isotropic patterns may be placed into one of five major categories: southerly (S), westerly (W), north westerly (NW), northerly (N) and easterly (E). On an annual basis, the most frequent airflow type is typically westerly (including cyclonic and anticyclonic subtypes) with a 35% frequency between December and January and 33% between July and September. The frequency reaches a minimum of 15% in May when northerly and easterly airflow types reach their maximum ($\sim 10\%$ for each type). Pure

cyclonic patterns are most frequent (13-17%) in July and August and anticyclonic patterns in June and September (20%), cyclonic patterns have $\geq 10\%$ frequency in all months and anticyclonic patterns $\geq 13\%$ (Barry and Chorley, 1992).

Consequently, air masses which affect the UK can be divided into the following categories. The tropical continental (TrC) air mass, tropical maritime (TrM), arctic maritime (ArM), arctic continental (ArC), polar continental (PC), returning polar maritime (rPM) and polar maritime (PM) as shown in Figure 4.2 (Barry and Chorley, 1992). The polar maritime (rPM and PM) air masses dominate all the months with a frequency of 30% except during March (with PM having a maximum frequency of 33% and a further 10% contribution from rPM in July).

4.3 The chemical composition of the Plymouth coastal and semi-urban aerosol

4.3.1 The overall chemical characteristics of the aerosol trace metals in the Plymouth coastal and semi-urban aerosol.

Table 4.4 shows the geometric and arithmetic mean, standard deviations and ranges of the overall aerosol trace metal concentrations Al, Fe, Mn, Ni, Co, Na, Zn, Cd and Pb for the Plymouth atmosphere. The dataset represents samples collected from 24th May- 20th December 2002, even though the sampling campaign commenced December 2001. Initial aerosol samples were excluded from the overall dataset, as it was felt that temporary construction work in close proximity to the sampling site had impacted upon the detected aerosol concentrations. Further details are presented in section 4.3.5, where the temporal variations in the aerosol trace metal concentrations are discussed.

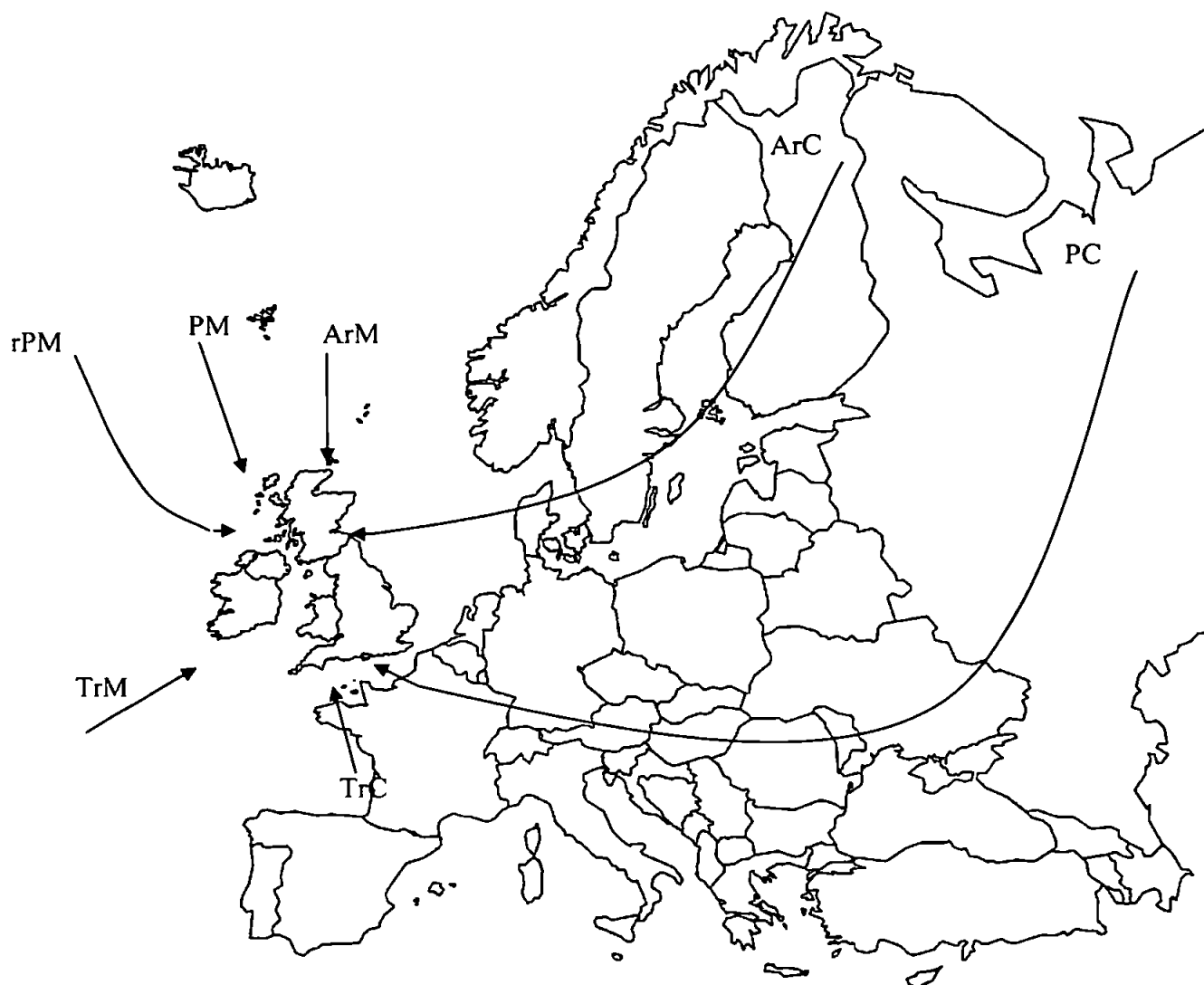


Figure 4.2. Air masses influencing the British Isles (after Barry and Chorley, 1992).

As is apparent from Table 4.4, the minimum and maximum aerosol trace metal concentrations, as well as the standard deviations, indicate a high variability in all the datasets. Such a high variability has been observed previously in other aerosol datasets describing European aerosol populations (e.g. Eastern Mediterranean; Kubilay and Saydam, 1995; Herut et al., 2001 Koçak et al., 2004; and Western Mediterranean; Chester et al., 1990; Chester et al., 1992).

Table 4.4. Geometric and arithmetic mean (± 1 sd) of aerosol trace metal concentrations (ng m^{-3}) observed at Plymouth between 24th May and 18th December 2002.

Element	Geometric mean	Arithmetic mean	Standard deviation	Range
Al	187	246	166	2.0-783
Cd	0.11	0.18	0.18	0.01-1.14
Co	0.18	0.25	0.24	0.03-1.86
Fe	250	298	154	33-685
Mn	6.2	8.1	6.4	1.1-36.8
Mo	0.47	0.56	0.34	0.08-1.82
Na	5700	15800	19000	50-64600
Ni	2.4	4.1	6.5	0.1-53.6
Pb	5.4	7.7	6.6	0.5-31.1
V	2.1	3.6	3.7	n.d.-19.9
Zn	10.0	23.3	35.4	0.42-169

Previous studies have shown that the log normal distribution best describes aerosol datasets (e.g. Fones, 1996; Koçak, 2001). The current aerosol datasets were tested for their log normality using the Kolmogorov-Smirnov test. This is a non-parametric t-test for independent samples. However, unlike the parametric t-test for independent samples, the Kolmogorov-Smirnov test is sensitive to differences in the general shapes of the distributions in the two sample populations, and hence was applied to assess the goodness of fit of the data to lognormal distributions. The Kolmogorov-Smirnov test involves the whole distribution of the studied variable and compares the empirical cumulative distribution function to that of the hypothesized distribution. After application of the Kolmogorov-Smirnov test, using the statistical software Minitab, the distribution of the aerosol trace metal concentrations were found to be lognormal within the 95% confidence

interval. Owing to the log normality of the population distribution the geometric mean would be the more representative mean to describe the aerosol trace metal concentration datasets. Therefore when comparing the aerosol data from the current study with those from the literature, comparisons with the geometric mean will be made. The mathematical definition of the geometric mean is as follow: The n-th root of the product of n numbers of samples.

4.3.2 Comparison of the aerosol trace metal concentrations with literature data

Table 4.5 compares the concentrations of the trace metals in the urban aerosol for Plymouth (SW England), with those observed at Liverpool, Preston (NW England) and Edinburgh (Scotland), which are all UK urban atmospheres with varying degrees of maritime air mass influence. Aerosol samples collected from Liverpool (n=60) were analysed using flame atomic absorption spectrometry and graphite furnace atomic absorption spectrometry whereas those collected at Preston (n=90) were analysed using either flame atomic absorption spectrometry or ICP-MS (Chester et al., 2000).

Table 4.5. concentrations (ng m⁻³) of aerosol associated trace metals at different UK urban sites.

Element	Preston* (n=90)	Liverpool* (n=60)	Edinburgh [#]		London [#] (n=12)	Plymouth [§] (n=90)
			PM ₁₀ (n=354)	PM _{2.5} (n=362)		
Al	365	317				187
Co	0.68	0.42				0.18
Fe	589	340	183	27.6	870	250
Mn	21	8.4	2.9	0.7	12	6.2
Ni	16	3.0	3.4	1.0	5	2.4
Pb	45	43	14.1	13.6		5.4
V	7.7	7.3	1.1	0.7	4	2.1
Zn	153	36	13.3	7.5	41	10.0

*Chester et al., 2000; [#]Heal et al., 2005; [§] current study.

Aerosol samples collected at Edinburgh were analysed using ICP-MS, whereas aerosol samples collected at London were analysed by XRF and INAA (Heal et al., 2005).

Generally, the Plymouth coastal and semi-urban aerosol concentrations for all elements were lower than the aerosol concentrations observed at other urban sampling locations in the North West (Liverpool and Preston) and London. The degree of enhancement varied between UK locations. For example comparison between Liverpool, Preston and the Plymouth coastal and semi-urban aerosols clearly highlighted concentration enhancements for Al and Fe (typically 2x) at Liverpool and Preston. However for V, Zn and Pb greater concentration enhancements were detected ranging from around 3.3x for V at Liverpool to 13x for Zn at Preston higher than Plymouth concentration. Zinc is mainly influenced by anthropogenic processes such as transportation (i.e. car tyre wear; Koçak et al., 2004), coal combustion, smelting operations, incineration (Pacyna et al., 1984; Lee et al., 1994) and as a result of the North West of England being an industrial area, Liverpool and Preston are likely to have local sources of Zn emissions, leading to their elevated Zn concentrations. V and Ni are tracers for oil combustion (Niragu, 1979; Lee et al., 1994; Siefert et al., 1999) and again the elevated concentrations observed in the north-west would be a result of regional sources. Therefore it is likely that for the enhanced elements local and regional source influence the North Western aerosol population (Chester et al., 2000), leading to both higher variability and background aerosol trace metal concentrations. Regional and local sources are likely to include; (1) emission from the industrial activities from the South Wirral peninsula, (2) enhanced aerosol trace metals derived from the burning of fossil fuel for transport and heating, and (3) relatively closer proximity to regional anthropogenic sources in the NE, E (Teeside), SE (Midlands).

However, in contrast, with the exception to the mineralised catchment in the vicinity of the city (Austin and Millward 1986), the Plymouth coastal and semi-urban aerosol population

has no major industrial regions in its proximity, and is more likely to be influenced by long range transported anthropogenically derived material from the UK and Western Europe. In addition “dilution” by more pristine maritime air masses from the west and south-west would also lead to lower observed trace elemental concentrations.

It is interesting to note that Pb concentrations are generally much lower in Plymouth than any of the other sites (up to 7.5 and 7.8x higher at Liverpool / Preston respectively). This difference is likely to be due to the fact that the sampling at the two main comparative urban sites (Liverpool and Preston) were carried out in the early nineties of the 20th century, whereas at Plymouth sampling commenced at the end of 2001.

Leaded gasoline was banned from use in the UK in 2000 (Spokes et al., 2001) and concentrations of aerosol Pb are clearly diminishing as a consequence. Diminished aerosol Pb concentrations have been noted in the literature over the last decade. For example, Hassanien et al., (2001) indicated that urban Pb concentrations in Cairo have decreased by 40% between 1994 and 1997. Furthermore, it is apparent that diminished aerosol Pb concentrations have been observed in European coastal atmospheres: Ligurian Sea, 25-30% and North Sea, 50%, decrease respectively (Migon and Nicolas 1998; Ridame et al., 1999; Flament et al., 2002; Lammel et al., 2002).

Table 4.6 further compares the Plymouth coastal and semi-urban aerosol trace elemental concentrations with those observed at Western European coastal sampling sites. It is clear that the Plymouth aerosol concentrations are generally comparable with those observed in coastal non-urban locations (Chester et al., 1990; Chester and Bradshw, 1991; Yaaqub et al., 1991; Fones, 1996; Chester et al., 2000) which could further indicate that the Plymouth background urban atmosphere, as regards trace elements, is perturbed by local anthropic activities significantly less than other urban UK and European atmospheres. Nickel, however, exhibits a contradictory behaviour, being significantly lower at the urban

Plymouth site compared with that reported by Wells (1999) for a rural site to the east of Plymouth. The higher Ni concentrations observed by Wells (1999) was attributed to Ni rich natural material derived west of the sampling station at the Lizard peninsular, Cornwall, an area rich in the mineral serpentine. However if this was the case one would also have expected to observe a similar enrichment in the Plymouth atmosphere. One possible explanation for the discrepancy is that the air masses which influenced the Plymouth site during the sampling period compared with those influencing the sampling site of Wells (1999), might have taken different westerly trajectories. The significant impact on trace elemental aerosol concentrations of air mass origin will be discussed further in section 4.3.6.

Table 4.6. Comparison of trace elemental aerosol geometric concentrations (ng m^{-3}) in coastal European atmospheres.

Element	Plymouth ^a	Western English Channel ^b	Irish Sea ^c	North Sea ^d	Irish Sea ^e	Western Mediterranean ^f
Al	187	229	210	219	264	370
Co	0.18	0.12	0.14	0.19	-	-
Fe	250	115	159	230	226	320
Mn	6.2	7.94	4.42	9.1		11
Mo	0.48	-	-	-	-	-
Na	5609	2570	1140	-	-	-
Ni	2.4	15.1	3.7	2.5	6.5	2.8
Pb	5.4	1.2	15.1	20	31	58
V	2.1	-	-	-	-	-
Zn	10.0	20.9	25.3	26	15	41

^aCurrent study; ^bWells (1999); ^cFones (1996); ^dChester and Bradshaw (1991);

^eMurphy, (1985); ^fChester et al., (1990)

4.3.3. Evaluation of the Plymouth aerosol trace metal sources; Application of the crustal enrichment factor (EF_{crust})

Calculation of the EF_{crust} has been used previously to help define aerosol elemental sources (Chester et al., 2000). For a crustal source, Al is normally used as the source indicator element and the earth's crust as the source material. The EF_{crust} value is then calculated according to the equation:

$$EF_{\text{crust}} = (C_{\text{xp}}/C_{\text{Alp}})/(C_{\text{xc}}/C_{\text{Alc}}) \quad (4.1)$$

Where (C_{xp} and C_{Alp}) are the concentrations of a trace metal x and Al, respectively, in the aerosol, and (C_{xc} and C_{Alc}) are their comparable concentrations in “average” crustal material. By convention, an arbitrary average EF_{crust} value of <10 is an indication that an element in an aerosol population has a predominantly crustal source and would be referred to as a “non-enriched” element. In contrast, $EF_{\text{crust}} > 10$ indicates that a significant proportion of an element has a non-crustal source and is referred to as an “enriched” element (Chester 2000). Although enrichment factors are a useful method of rationalising the data, they should be interpreted cautiously as they do not take into account regional variations in the mineralogy of the crustal precursor material. Guieu and Thomas (1996) recently used different selected soil samples from the origin of the air masses to ensure that the calculated EF_{crust} values were more representative by taking into account the regional geological characteristics. However, the current study has applied the average concentration of metals in the crust (their ratios to Al) from Taylor (1964) as these data are widely used by other researchers. This pattern is derived principally from the hypothetical mixing of basic and acidic igneous rock patterns, from which elemental abundances in the continental crust can be calculated on the basis of a 1:1 mixture of granite and basalt abundances. Wedepohl (1995) has also proposed a modified Al/elemental ratio. More

details and discussion of the application and the limitations of the elemental source crustal enrichment factor have already been presented in section 2.4.3.

Table 4.7 presents the crustal enrichment factor for elements determined in this study. From the values (average) of EF_{crust} one can categorise the elements into two groups (i.e. “enriched” and “non-enriched” elements; see discussion above) according to their potential sources. Cd, Pb Zn and Ni, are likely to have predominately anthropogenic sources as their average EF_{crust} are >10 . They decrease in the order of Cd (227) $>$ Pb (187) $>$ Zn (65) $>$ Ni (14). In contrast Fe, Mn, V and Co all have $EF_{crust} < 10$ and hence are categorised as “non-enriched” elements and have a progressively greater crustal source influence (in the order V $<$ Co $<$ Mn $<$ Fe). Mo and Na have relatively high EF_{crust} values (115 and 135 respectively) and hence have a predominantly non-enriched source, but have been shown to be present in the aerosol as a result of sea salt generation (Chester et al., 1984; Chester, 2000).

Table 4.7. EF_{crust} for the Plymouth coastal and semi-urban aerosol (in samples collected between 24th May and 18th December 2002).

Element	Geometric Mean	Arithmetic Mean	Standard Deviation	Range
Cd	227	311	241	21-1022
Co	3.08	4.23	4.45	0.8-23.4
Fe	1.87	2.09	1.02	0.20-5.24
Mn	2.77	3.19	1.92	0.60-12.6
Mo	134	162	104	17-556
Na	98.2	293	2780	0.4-2780
Ni	14.2	28.0	37.9	0.1-208
Pb	187	229	161	23-1003
V	6.74	14	18.6	0.02-121
Zn	64.9	199	415	5.0-2665

Table 4.8 highlights a comparison of the EF_{crust} for current study site (Plymouth) and those observed at other sites from Western European atmospheres. Generally, the EF_{crust} ’s for

Plymouth are comparable with the western European data and hence the same general elemental categorisations applied to the Plymouth aerosol are consistent. Nickel, however has a lower value compared with that of Wells (1999) whose sampling site was located in a rural site to the east of the Plymouth site (for further details see section 4.3.1).

Table 4.8. Comparison of EF_{crust} values from the current study with values from Western Europe coastal atmospheres.

Element	North Sea ¹	English Channel ²	Cap Ferrat ³	Blanes ⁴	Tour du Valet ⁵	NE Irish Sea ⁶	English Channel ⁷	Plymouth (40-195)
Al	1.0	1.0	1.0	1.0	1.0	1.0	1.0	1.0
Cd	-	-	-	-	-	-	214	230
Co	-	-	-	-	-	-	2.09	3.1
Fe	1.75	1.3	1.3	1.2	1.1	2.0	0.79	1.9
Mn	4.2	-	2.6	2.2	2.9	3.2	3.02	2.5
Mo	-	-	-	-	-	-	-	135
Na	-	-	-	-	-	-	43.7	115
Ni	-	-	8.4	15.5	6.7	28.5	77.6	14.7
Pb	781	683	1054	838	982	775	39.8	187
V	-	-	-	-	-	-	-	6.8
Zn	164	215	130	150	186	281	107	61.6

¹ Chester and Bradshaw (1991); ²Flament et al. (1987); ³Chester et al. (1990); ⁴Chester et al. (1992); ⁵Guieu et al. (1997); ⁶Chester et al. (2000); ⁷Wells (1999); ⁸Current study.

4.3.4 The percentage of crustal source contribution of trace metals to the Plymouth aerosol

The percentage of crustal source contribution is another approach which has been applied to estimate the importance of crustal/non-crustal contributions to the aerosol (Arimoto et al., 2003; Koçak et al., 2005; Koçak et al., 2006). The crustal contribution percentage of an element in an aerosol population is calculated according to the equation:

$$\% \text{ of the crustal contribution} = [\{ (C_{Alp}) * (C_{xc}/C_{Alc}) \} / (C_{xp})] * 100 \quad (4.2)$$

where (C_{xp} and C_{Alp}) are the concentrations of a trace metal x and Al, respectively, in the individual aerosol samples, and (C_{xc} and C_{Alc}) are their comparable concentrations in average crustal material (Taylor, 1964).

The % crustal contribution calculations presented above used the same ratio of element to Al in the crust as that used for the EF_{crust} calculations, taken from the Taylor (1964) ,

therefore, as has been stated previously that the Enrichment Factor (EF) has its flaws. The % crustal contribution suffers from the same drawback as that associated with the calculation of the EF. This calculation was carried out for all measured elements within each sample and the statistical summaries are highlighted on Table 4.9. It was apparent that for a number of samples for the elements Fe (n=5) and Mn (n=3), the calculated crustal contributions were higher than 100%. This would arise from the applied elemental ratio to Al not being completely representative of the elemental ratio in the local crust, i.e. the elemental/Al ratio being lower than the global average. In such cases the crustal contribution was assumed to be 100 %. From Table 4.9 it is apparent that percentage crustal contribution for elements follows broadly the order of their EF_{crust} values. Fe, Mn, Co, V and Ni have the highest calculated crustal contributions with an average of 57, 41, 38, 22 and 12 % respectively. The rest of the elements have percentages <5%, i.e. for these elements the non-crustal sources represents $\geq 95\%$ of the total contributions.

Table 4.9. Statistical summary of the calculated percentage crustal contribution to elements in the Plymouth coastal and semi-urban aerosol (for samples collected between 24th May and 18th December 2002, i.e. samples 41-195).

Element	Geometric Mean	Arithmetic Mean	Standard Deviation	Range
Cd	<1	1	<1	<1-4.9
Co	28	38	22	<1-100
Fe	52	57	23	19-100
Mn	36	41	21	8-100
Mo	<1	1	<1	<1-6
Na	<1	4	14	<1-100
Ni	6	12	18	<1-100
Pb	<1	1	<1	<1-4.3
V	13	22	24	<1-100
Zn	2	4	4.2	<1-20

Elements having EF_{crust} values <10 have a greater crustal contribution than those elements with EF_{crust} value > 10. However, the cut off point between predominately crustal and non-crustal sources contributions which has traditionally been adopted in the past (i.e. $EF_{crust}=10$, e.g. Chester, 2000) is misleading as it is clear from the calculated crustal contributions

(Table 4.9) some elements which have $EF_{\text{crust}} < 10$, (Mn, Co, V and Ni) also have predominately non-crustal sources and not, as implied by the historic use of the EF_{crust} , non-crustal sources. To serve as an example, Figure 4.3 highlights the relationship between the % crustal contribution and the enrichment factor for two elements (Mn and Co). It is clear that for the 10 cut off (EF_{crust}) represents a 10% crustal contribution to Mn and Co. Therefore the manner in which the EF_{crust} has been used universally in the atmospheric science literature is misleading. EF_{crust} values < 2 would represent the transition between predominantly non-crustal contributions ($> 50\%$) to predominantly crustal contributions, and hence is a more logical value to use.

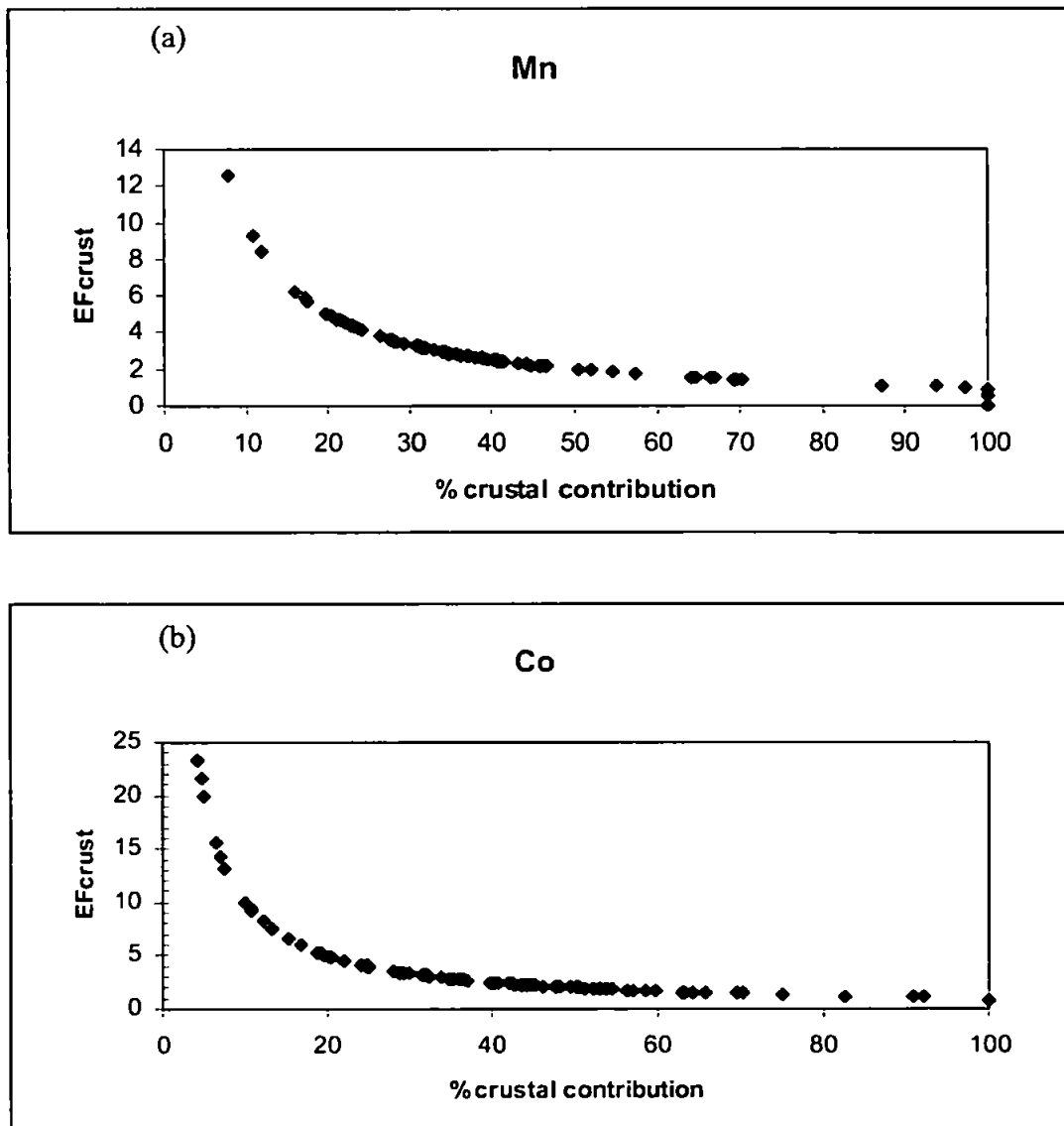


Figure 4.3. % Crustal contribution against EF_{crust} (a) Mn and (b) Co.

4.3.5 Temporal variability in the trace metal composition of the Plymouth coastal and semi-urban aerosol population

Temporal variations (including both seasonal and daily) in aerosol trace metal concentrations have been well studied by many authors (e.g. Kubilay and Saydam 1995; Kubilay et al., 1997; Kubilay et al., 2000; Wang and Shooter 2002; Koçak et al., 2004). For example seasonal differences have been discussed by Koçak et al. (2004) who reported that the crustally derived elements (Al, Fe, and Mn), at an Eastern Mediterranean site, exhibit trends in their concentrations in the following order: transitional (March-May, October) period > summer (June-September) > winter (November-February), owing to the greater frequency and intensity of Saharan dust events. In contrast, in the winter, due to the higher rainfall compared with the summer, scavenging of the aerosol associated trace metals is more prevalent and hence lowers the aerosol concentrations compared with those observed in the summer.

Diurnal variation of chemical components (nss (non sea salt)-K, nss-Cl⁻, nss-Ca²⁺, nss-SO₄²⁻, NO₃⁻ and NH₄⁺) of atmospheric aerosols have also been reported, for example, by Wang and Shooter (2002) which was explained by the intensive coal and wood burning for home-heating, the sheltered geographic location and the relatively calm atmospheric conditions. Observed temporal variations generally relate to the emission strength of inputs from local, regional and distant natural and anthropogenic sources along with meteorological conditions (such as wind speed, wind direction, rainfall and relative humidity) and the effects of removal processes during transport.

The current section will investigate, define and explain the temporal variability in the Plymouth coastal and semi-urban aerosol trace metal concentrations (i) over the whole sampling period (which includes samples 1-195, covering the sampling period between 10th December 2001 – 18th December 2002) (ii) between night and day collected samples

(which includes samples numbers 41-101, covering the sampling period 24th May – 29th July 2002).

Initial consideration of the aerosol trace metal concentrations over the whole sampling period clearly indicated comparatively elevated concentrations of all the trace metals in the early period of sampling (i.e. sample numbers 1-40, covering the sampling period between 10th December 2001–9th May 2002). This is illustrated by Table 4.10, which presents all the statistical information on the aerosol characteristics during and after this initial sampling period. It is apparent that the enhancement of the aerosol trace metal concentrations was typically 2-3x (e.g. for Al the geometric means were 603 ng m⁻³ and 187 ng m⁻³ respectively for the two sampling periods). To evaluate the statistical significance between the two populations the Mann-Whitney test (the equivalent non-parametric t-test) at the 95% confidence limits was applied, owing to the log-normal distribution characteristics of the two populations (see section 4.3). From this, statistical differences were detected for all elements between the two defined sampling periods. Comparison of the elevated concentrations with those encountered at the other UK urban environments (Table 4.11) also clearly indicates that the detected values during the initial sampling period were unusually high for an urban UK environment. It is likely that local construction work around the University campus close to the sampling site was the predominant cause. The main construction work was carried out during the collection of the samples 1-40 and would have included, for example, the use of natural materials, welding activities etc. as well as extensive vehicle traffic. Further comparison of trace metal geometric night and day time collected samples during this period (Table 4.12) generally highlighted elevated daytime trace metal concentrations, providing further evidence of the local source influence rather than meteorological conditions (i.e. rainfall and air mass transport). Meteorological conditions are likely to vary during both the night and day sampling periods. The concentration enhancement factor was highest for Al and Mn, being between 3 and 4 (Table 4.12), whereas, for Cd and Pb, there were lower and

close to unity (0.8 and 1.01 respectively). This behaviour is likely to be due to the different size fractions association of the elements produced from the local activities, with those associated with the largest particle size fractions (i.e. natural material) being deposited the quickest after daily work had ceased and hence exhibiting a clearer diurnal variation. Whereas, elements associated with smaller particle size fraction (Pb and Cd) would stay longer in the air therefore would not exhibit a distinct diurnal variations compared to those exhibited by elements associated with the larger particle size fraction.

Table 4.10. Aerosol trace metal concentrations (expressed as ng m^{-3}) in the Plymouth coastal and semi-urban aerosol collection between (i) 10th December 2001 – 9th May 2002 and (ii) 24th May -18th December 2002.

Element	Sampling period (i)		Sampling period (ii)		Enhancement factor
	Arithmetic mean	Geometric Mean	Arithmetic mean	Geometric mean	
Al	992±1127	603	313±508	187	3.2
Cd	0.52±0.74	0.3	0.19±0.21	0.11	2.7
Co	29.1±101	2.9	0.3±0.4	0.19	15.3
Fe	957±858	651	355±396	250	2.6
Mn	27.6±37.8	16	9.8±15.1	6.2	2.6
Mo	19.6±86.9	1.4	4.1±33.7	0.48	2.9
Na	105200±203900	27500	29400±93000	(5609)	4.9
Ni	4.2±6.7	1.8	4.56±7.3	2.4	0.8
Pb	23.8±28.9	15.6	8.4±7.8	5.4	2.9
V	4.9±4.7	3.2	4.1±4.5	2.1	1.6
Zn	76±122	36	56±146.4	10	3.6

Table 4.11. Comparison of aerosol associated trace element concentrations (geometric mean, ng m⁻³) at Plymouth (samples 1-40), with those observed at Liverpool and Preston.

Element	Plymouth ¹	Liverpool ²	Preston ²
Al	603	317	365
Co	2.9	0.42	0.68
Fe	651	340	589
Mn	16	8.4	21
Ni	1.8	3.0	16
Pb	15.6	43	45
V	3.2	7.3	7.7
Zn	36	36	153

¹ Current study; ² Chester et al., 2000.

Table 4.12. The geometric mean concentration (ng m⁻³) of trace metals in the Plymouth coastal and semi-urban environment during day and night-time sampling (sample 1-40); 10th December 01 – 9th May 2002.

Element	Samples 1-40		Ratio of Day/Night concentrations
	Day	Night	
Al	1091	280	3.9
Cd	0.28	0.35	0.8
Co	3.24	2.47	1.3
Fe	872	463	1.9
Mn	23	7.26	3.2
Mo	1.36	1.45	0.94
Na	14,300	58,800	0.24
Ni	2.37	1.19	1.99
Pb	15.7	15.5	1.01
V	3.47	2.80	1.2
Zn	41.2	30.3	1.4

Owing to the likely local contamination of the initially collected samples, to ensure subsequent accurate environmental interpretations, it was decided to omit the initial 40 samples from the dataset used for environmental interpretation.

Figures 4.4-4.6 illustrate the temporal variation of all detected aerosol trace metal concentrations in the collected samples numbers 41-195 (24th May-18th December 2002). These Figures represent the variation in concentration against day of sampling (with day 1 on the x-axis representing the first day of the sampling campaign). For the period day 140 – 220, day and night time samples were collected. From Figures 4.4-4.6 (and Table 4.13) it is apparent that for all elements there are substantial variations, with typical RSDs, being > 100%. As discussed in section 4.3.1, this is characteristic of atmospheric chemical datasets, exhibiting very dynamic changes in concentrations ranging up to several orders of magnitude for some elements at certain sites (Guerzoni et al., 1997; Jickells 1995; Koçak et al., 2004 and Lee et al., 1994).

As was apparent with local construction work (Table 4.12), the influence of local sources might be characterised by diurnal differences in aerosol trace metal concentrations. This was investigated by comparison of the trace metal aerosol datasets during night-time and day-time sampling for the three month sampling period post sample number 40 (i.e. between 24th May- 18th December 2002). Figures 4.4-4.6 also highlight the diurnal variations in trace metal concentrations and a statistical summary is presented in Table 4.13. There is no statistical difference between the datasets derived from day / night sampling for any of the trace metals (Mann-Whitney; 95% confidence level). This indicates that local immediate sources are not predominantly impacting upon the general variability of the aerosol trace metal dataset. In addition, seasonal variability was investigated by separating the trace metal aerosol concentrations observed into two broad seasonal categories; (i) Summer (May to September, 2002), and (ii) Winter (December - March 2001; October to December 2002).

Table 4.13. The geometric mean aerosol trace metal concentrations (ng m^{-3}) in the Plymouth coastal and semi-urban aerosol population (n=91) between 24th May- 18th December 2002.

Element	Samples 40-101		
	Day	Night	Day/Night
Al	187	214	0.87
Cd	0.07	0.09	0.78
Co	0.18	0.16	1.1
Fe	242	268	0.90
Mn	5.64	4.58	1.2
Mo	0.42	0.55	0.76
Na	2190	2760	0.79
Ni	2.66	2.38	1.1
Pb	4.3	5.1	0.84
V	1.87	1.35	1.4
Zn	37.1	29.9	1.2

The statistical description of these two populations is exhibited in Table 4.14. Applying the Mann–Whitney test shows that some elements had a statistically significant difference (95% confidence) between the two seasons. These were Na, Cd, Co, Mo and Zn, with winter : summer ratios of geometric means being 10, 2.2, 1.7, 1.5 and 0.22 respectively. To investigate the correlation between Na and Mo a Pearson statistical test was applied with a 95% confidence limit and there was a statistically significant correlation. Na will predominantly associate with sea salts, the entrainment of which in the atmosphere is controlled by wind speed across the sea surface with onshore winds.

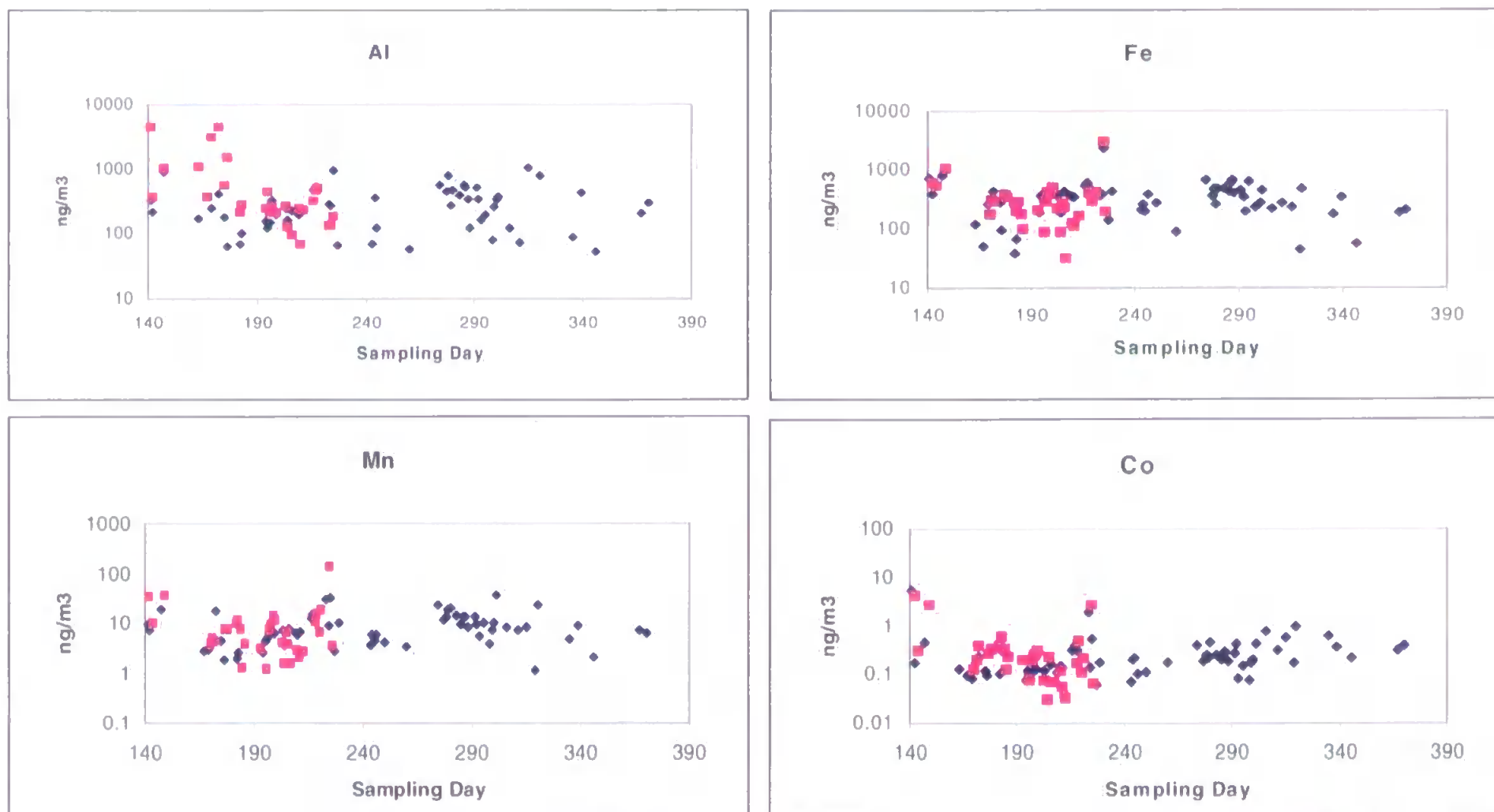


Figure 4.4 Temporal variability of (a) Al (b) Fe (c) Mn and (d) Co concentrations (log₁₀) in the Plymouth aerosol; Red legends represent samples collected during the day time (during sampling days 140-226) whereas the blue legends represent samples collected at night (during sampling days 140-370). All the above elements have $EF_{\text{crust}} < 4$.

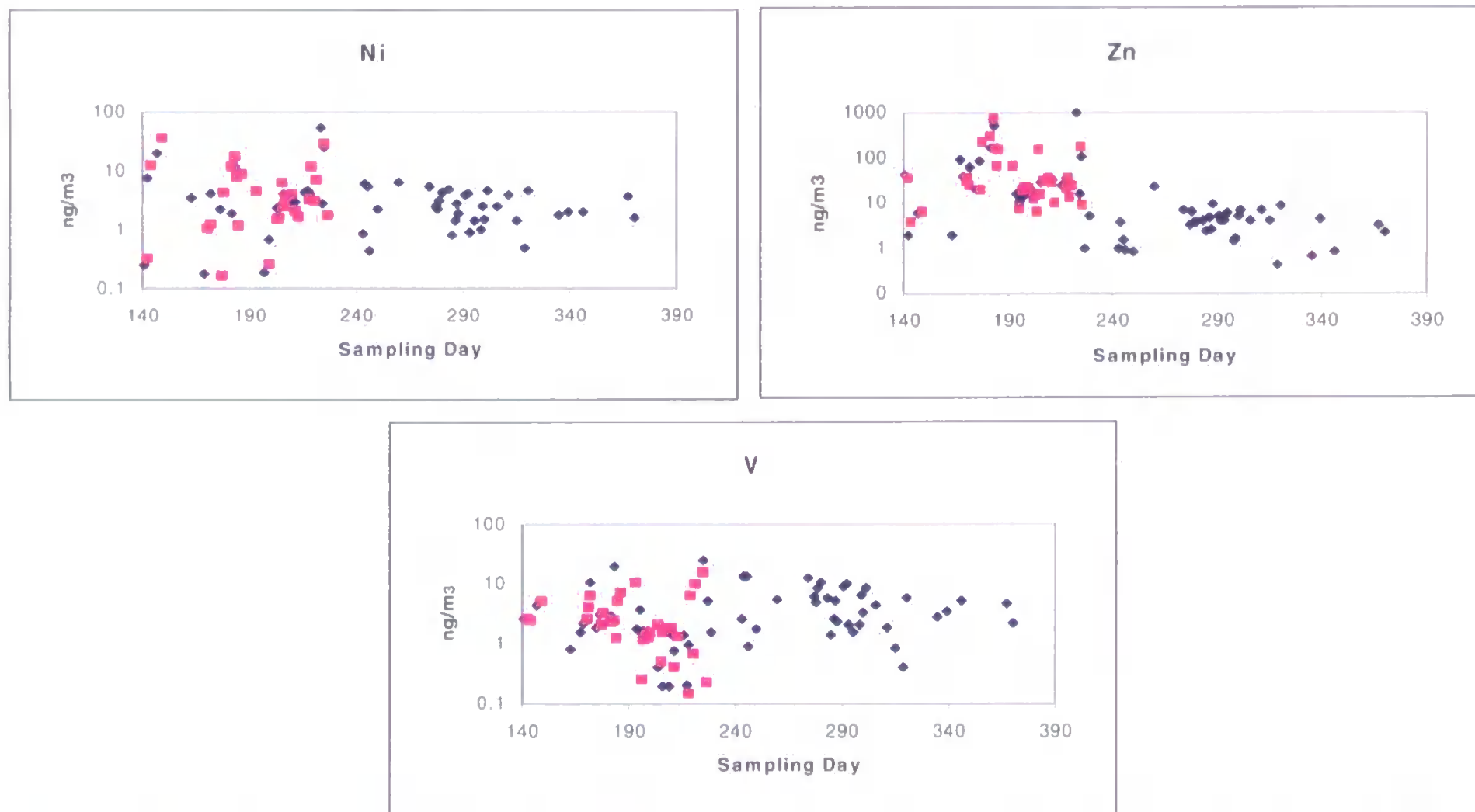


Figure 4.5 Temporal variability of (a) Ni (b) V and (c) Zn concentrations (log10) in the Plymouth aerosol; Red legends represent samples collected during the day time (during sampling days 140-226) whereas the blue legends represent samples collected at night (during sampling days 140-370). All the above elements have EF_{crust} between 6.8 and 65.

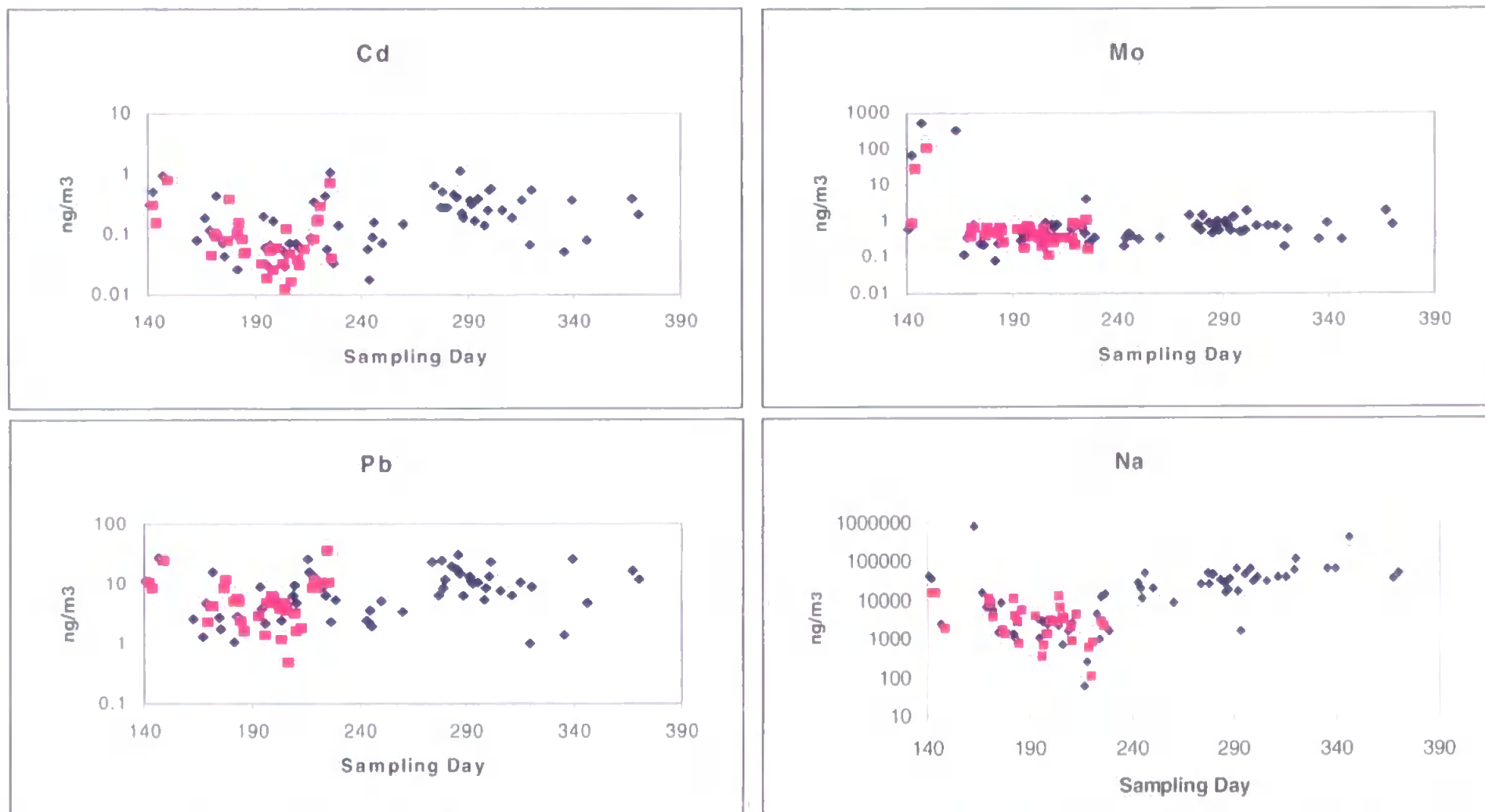


Figure 4.6 Temporal variability of (a) Cd (b) Mo (c) Pb and (d) Na concentrations (log₁₀) in the Plymouth aerosol; Red legends represent samples collected during the day time (during sampling days 140-226) whereas the blue legends represents samples collected at night (during sampling days 140-370). All the above elements have EF_{crust} between 98 and 227.

Table 4.14. Seasonal variability of aerosol trace metal concentrations (ng m⁻³) at Plymouth.

Element	Winter				Summer			
	Geometric Mean	Arithmetic Mean	Standard Deviation	Range	Geometric Mean	Arithmetic Mean	Standard Deviation	Range
Al	124	218	207	2.03-764	202	251	158	29.5-738
Cd	0.21	0.27	0.169	0.05-0.56	0.1	0.16	0.18	0.01-1.14
Co	0.30	0.38	0.257	0.08-0.94	0.17	0.22	0.23	0.03-1.86
Fe	217	266	163	46.6-641	257	304	153	32.5-685
Mn	6.70	9.48	9.43	1.14-36.8	5.5	7.8	5.7	0.003-30.3
Mo	0.68	0.81	0.506	0.197-1.82	0.44	0.51	0.28	0.08-1.46
Na	45000	75140	100243	1531-412000	4270	10900	14400	57.3-64500
Ni	1.88	2.27	1.38	0.49-4.63	2.57	4.46	7.09	0.07-53.6
Pb	7.55	10.3	7.34	0.99-26	5.10	7.15	6.32	0.49-31.1
V	2.50	3.22	2.20	0.40-8.57	2.0	3.7	3.93	0.01-19.9
Zn	2.75	3.79	2.54	0.46-8.32	12.6	26.1	38.2	0.81-223

In winter the onshore wind speeds are higher than those of other seasons which explains the higher concentration of Na in winter. Figures 4.7 highlights the relationship of Na concentrations in samples collected during onshore winds in the winter with their speed. Clearly there is an increase in concentration with increasing wind speed, highlighting the impact of wind speed on seasalt generation. This effect has also been observed by e.g. Wai and Tanner 2004 and Nair et al., 2005).

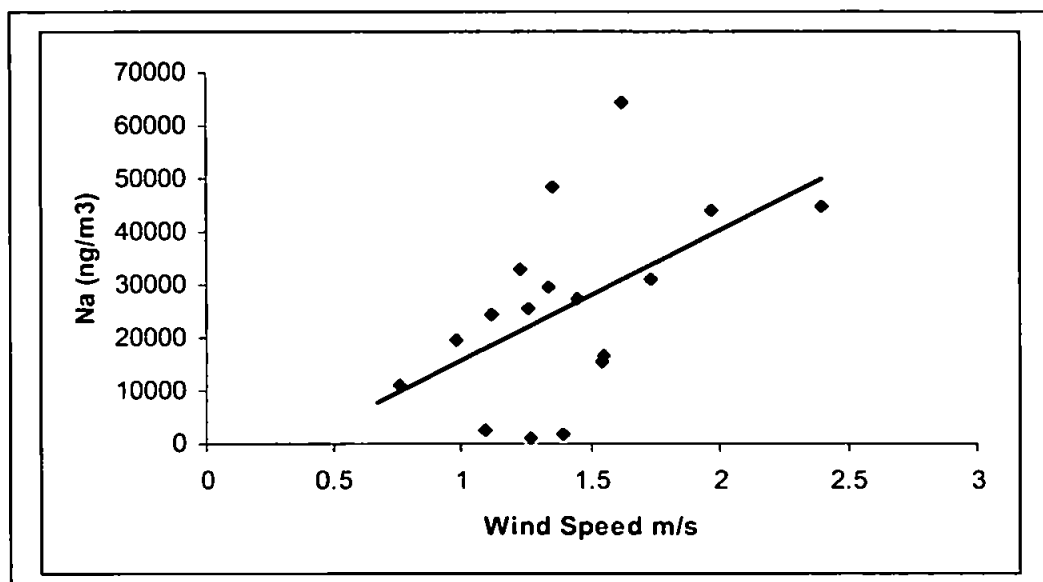


Figure 4.7. Na concentration (ng m^{-3}) vs wind speed (m s^{-1}) for onshore wind during the winter ($r^2=0.5$; $P=0.038$; $n=17$).

4.3.6 Trace metal aerosol chemical composition in contrasting air masses influencing the Plymouth atmosphere

The influence of contrasting air masses arriving at a sampling site on aerosol associated trace concentrations has been studied previously (see for example Koçak et al., 2005, Spokes et al., 2001 and Chester et al., 2000; Wells, 1999 and Fones 1996 also see sections 2.3 and 2.4.2). For the current study it was decided to apply to each collected sample a simple air mass categorisation, i.e. air masses which have travelled over (i) the North Atlantic and (ii) the UK mainland and Europe (including both Western and Eastern Europe); see Figure 4.8. Similar classifications have previously been adopted by Yaaqub

1991, Chester et al., 1999, Chester et al., 2000, Spokes et al., 2001 and Arimoto et al., 2003. From the Meteorological office official site the prevailing wind direction influencing the Plymouth atmosphere over the ten year period 1991-2001 is derived from the south west (see Figure 4.9). Using these data the ratio of influencing wind direction from the North Atlantic compared with the UK mainland and Europe was 1.4. To aid sample categorisation back trajectories were calculated for each of the collected aerosol samples (see section 3.5 for more details).

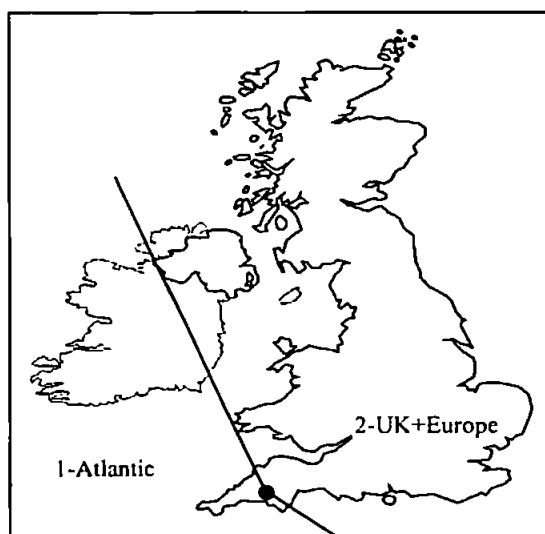


Figure 4.8. Wind sectors of Atlantic (1) and Europe and UK (2).

The classification criteria of any particular back trajectory was that it had to reside in that air mass sector at all three considered pressure levels (100, 500 and 1456 m; 1001, 955 and 850 hPa) for >50% of its travel time (over a 72 hour trajectory period) this in conjunction with the literature (e.g. Koçak et. al., 2004).

Examples of back trajectories representing both of the two air mass sectors are presented on Figures 4.10 (a) (European and UK) and 4.10 (b) (Atlantic). Table 4.15 summaries the statistical characteristics of the aerosol concentrations of trace elements for the two different air mass sectors. Considering Table 4.15 it is apparent that the majority of the

considered elemental concentrations are enhanced in air masses associated with the UK and European air mass sector with the exception of Zn, Ni and V.

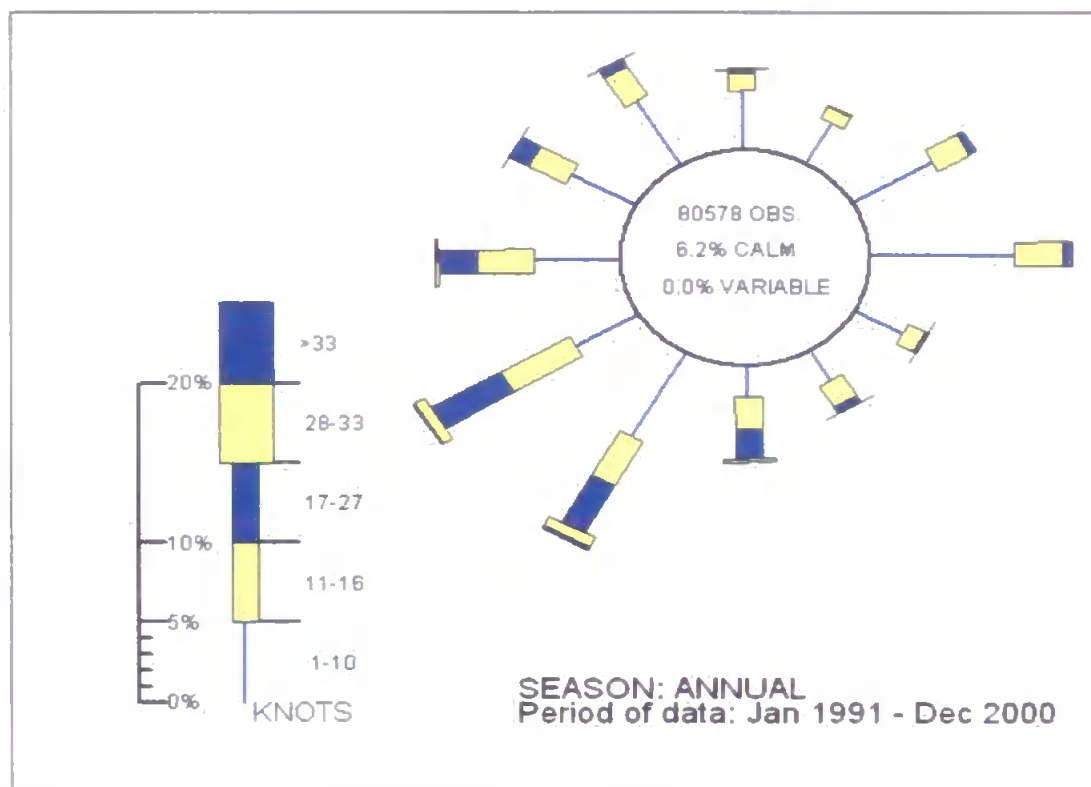


Figure 4.9. Wind rose for the period 1991-2000 at Plymouth (50 m above mean sea level). <http://www.metoffice.com/climate/UK/location/southwestengland/wind.html>

The non-parametric Mann-Whitney test was applied to the datasets (Atlantic and UK+European samples) at the 95% confidence limit to verify whether the differences were statistically significant between the two populations for each element. Statistical differences were found for Al, Fe, Mn, Cd, Mo and Pb whereas Na, V, Co, Ni and Zn showed no significant differences.

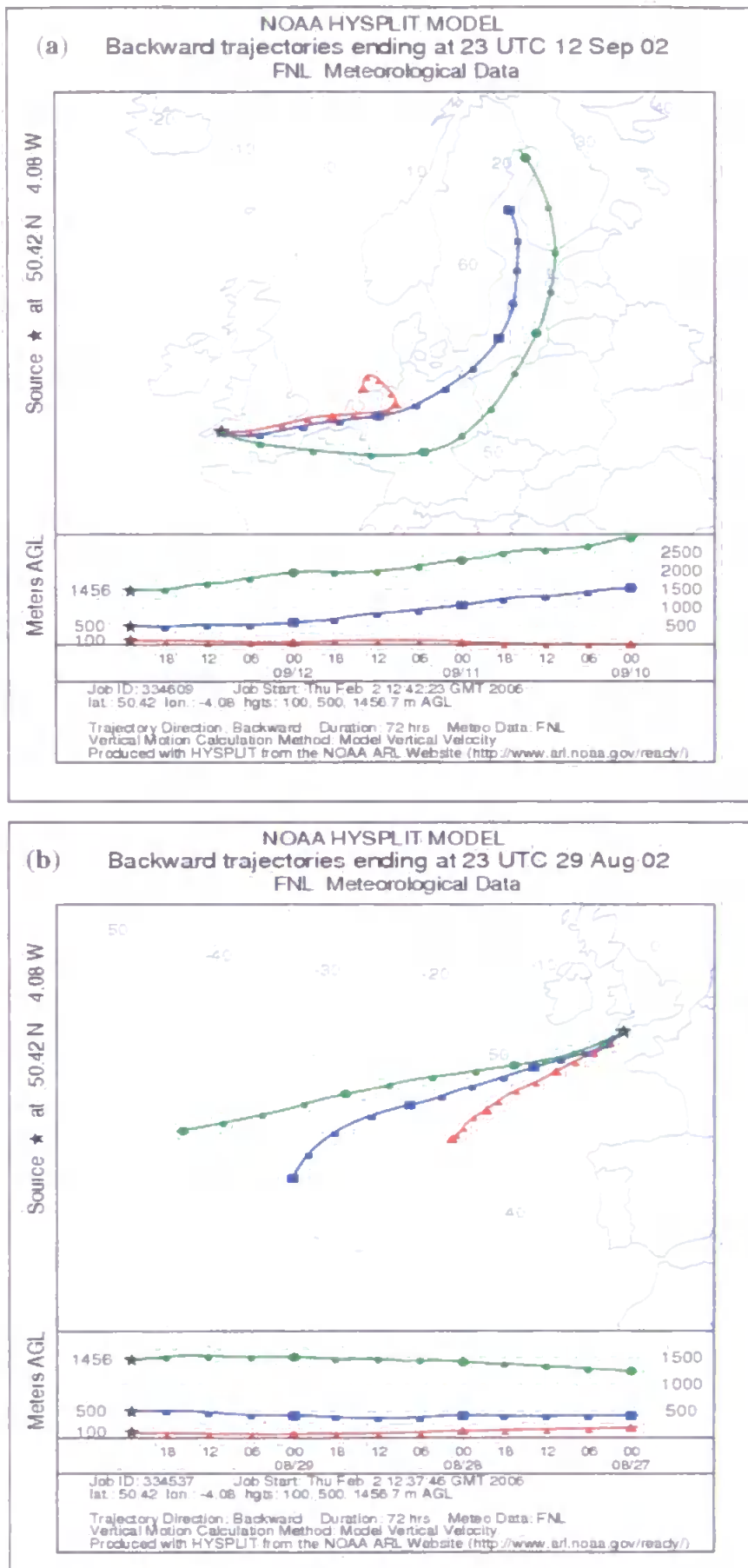


Figure 4.10. (a) European and UK air mass (sample 117) and (b) Atlantic air mass (sample 114).

Table 4.15. Aerosol associated trace elements concentrations (ng m^{-3}), range and standard deviation in the contrasting air masses reaching the sampling site at (Plymouth).

Element	Atlantic Wind Source (n=41,44.5%)				Europe+UK Wind Source (n=39,42.3%)				
	Geometric Mean	Range	Standard deviation	EF _{crust}	Geometric Mean	Range	Standard deviation	EF	Ratio of Geometric mean UK+Europe/ Geometric mean Atlantic
Al	123	2.0-361	88	-	216	29.5-783	176	-	1.8
Cd	0.08	0.02-0.39	0.1	245	0.15	0.01-1.14	0.23	272	1.9
Co	0.16	0.1-0.60	0.1	4.2	0.18	0.03-0.75	0.16	2.6	1.1
Fe	190	39.0-641	128	2.1	286	32.5-685	156	1.9	1.5
Mn	4.30	1.1-15.5	3.3	2.7	7.7	1.58-36.8	8.24	3.0	1.8
Mo	0.46	0.1-322	51.4	166	0.62	0.12-1.82	0.43	153	1.3
Na	6670	351-778400	137700	157	8700	101-64600	21620	114	1.3
Ni	2.51	0.17-18	4.4	1.6	2.7	0.82-7.2	1.5	13.6	1.1
Pb	3.8	1.0-11.7	3.1	191	7.3	0.49-31.1	8.0	220	1.9
V	2.5	0.23-25.0	5.3	9.1	2.1	0.01-12.6	3.52	5.2	0.8
Zn	10.9	0.42-223	56	126	8.0	0.66-151	25.0	50.1	0.7

Table 4.16 highlights the comparison of aerosol trace metal concentrations associated with similar air mass types with values from the literature relating to sampling stations within the UK. Three sites were considered in the comparison; (i) Mace Head, Ireland (Spokes et al., 2001), (ii) North West England (Chester et al 2000), (iii) East Anglia (Yaaqub et al. 1991), although for the latter only European air mass types were defined.

Enhanced concentrations of the crustally derived elements Al, Fe and Mn were detected in UK+European air mass types at both Mace Head and the North West as was the case at Plymouth. This is to be expected as UK+European air masses will be loaded with crustal material both locally generated and transported from distant sources both within the UK and from continental Europe, whereas aerosol populations associated with the Atlantic air mass types will have lost a significant proportion of their aerosol material via removal processes during transport.

Interestingly, the relative enhancement in the UK+European air mass type (relative enhancement = concentration in UK+European air mass / concentration in Atlantic air mass) was greater at Mace Head (Al=5.2 and Mn=6.4) compared with those observed at Plymouth (Al=1.8; Fe=1.5; Mn=1.9) and the North West site (Al=1.3; Fe=1.9; Mn=2.6). This is probably due to their more easterly locations, with the defined “Atlantic” air masses arriving at both Plymouth and the North West containing a contribution of crustal material transported from westerly located terrestrial areas (Plymouth – Lands End and Ireland; North West - Ireland). Thus the sampled Atlantic air masses at Mace Head will be the most representative of the Atlantic marine aerosol.

Table 4.16. Comparison of air mass trace metal concentrations (ng m^{-3}) for the current study with defined air mass trace metal concentrations from other studies.

Element	Atlantic ^a	Europe + UK ^a	W.Europe+UK ^b	W.Europe ^b	Atlantic ^c	Europe + UK ^c	Atlantic ^d	Europe + UK ^d
Al	123	216			186	249	6.69	35.1
Cd	0.08	0.15	1.2	1.3				
Co	0.16	0.18			0.12	0.26		
Fe	190	286	269	351	132	250		
Mn	4.30	7.7	14.3	20	2.9	7.6	0.66	4.45
Mo	0.46	0.62						
Na	6670	8700						
Ni	2.51	2.7			3.7	5.45		
Pb	3.8	7.3	47	62	12	23.5	1.45	19.1
V	2.5	2.1			2.1	4.35		
Zn	10.9	8.0	58.5	84	18	45.5	3.99	36.6

^acurrent study ; ^bYaaqub et al., (1991) ; ^cChester et al., (2000); ^dSpokes et al., (2001).

Pb also exhibited enhancement in the UK+European air mass types compared with the Atlantic air masses at Plymouth, Mace Head and the North West. Again this enhancement, as for the crustally derived trace elements, is attributed to sources being located in the UK, east of the sampling sites, and longer range transported anthropogenically emitted material from continental Europe. The relative enhancement was lowest at Plymouth (1.9) and the highest was observed at the North West site (13). A lower average Pb concentration was found at Plymouth for the UK+European air mass type compared with the other locations. This is likely to be due to the Plymouth sample dataset being more recent compared with those at Mace Head (Spokes et al. 2001) and North West (Chester et al. 2000). As has already been stated, more recent aerosol data will reflect the diminishing Pb anthropic emissions within continental Europe (see section 2.3).

Of the other elements for which there is comparative literature data, V exhibits contrasting air mass sector behaviour. At Plymouth there is no statistical difference between the V concentrations whereas at the North West an enhancement of about 2x is apparent, which might indicate local sources.

At Plymouth, zinc was enhanced in the Atlantic air mass category compared with that in the UK category, but was not statistically different at the 95% confidence level. A high variation in the Atlantic air mass population was observed for zinc, as a result of a number of high concentration events, accounting for the lack of statistical difference (95% confidence) between the two populations. It is unlikely that these high zinc episodes are marine derived, and therefore are probably due to the re-suspension of material from disused and abandoned mine wastes from historical mining activities in the South West. Zinc is widely found in such wastes, being present in the mineral spheralite. In addition in the Plymouth atmosphere, compared with the other UK locations, the UK+European air mass is comparatively lower. This might be due to the fact that the UK+European air masses arriving from Europe at Mace Head and the North West take a different path from

those arriving at Plymouth, with those arriving at Mace Head / North West having passed through more industrialised locations. Ni concentrations are not statistically different (95% confidence) in the two sectors which indicates a local influence.

4.3.7 Aerosol trace metal EF_{crust} for different wind sectors

In an attempt to establish the dominant source in the different wind sectors the investigation of the proportion of crustal (NEE) and non-crustal (AEE) material as a source for a certain trace metals, crustal enrichment factors (EF_{crust}) have been calculated for the different elements in the different wind sectors (Table 4.17). For the two different wind sectors a prominent variation in EF_{crust} occurs for Cd, Na, Zn and Ni. This observation is consistent with the concentrations of those elements. Cd has dominant intense anthropogenic sources in the UK+European wind sector. Zn and Ni may be affected by local sources with enhanced EF_{crust} for the Atlantic air mass sectors. As mentioned previously this might be due to historic mine waste located in the region being a source for Zn whereas the main source for Ni is from the Lizard peninsula (Wells 1999) to the west of Plymouth.

Table 4.17. EF_{crust} for the Atlantic and European and UK aerosol populations influencing the Plymouth atmosphere.

Element	Atlantic wind source (n =67)	UK+Europe wind source (n =40)
Cd	205	727
Co	4.45	10.3
Fe	2.00	1.68
Mn	2.54	3.01
Mo	155	133
Na	135	4.40
Ni	12.7	6.13
Pb	165	133
V	6.81	6.04
Zn	130	52.9

4.4 Inter-elemental relationships in the Plymouth aerosol

Atmospheric sciences uses correlation coefficients matrices (e.g. Huang et al., 1999; Huang et al., 2001; Lim et al., 2006; Xie and Berkowitz 2006) to define patterns of relationship between several variables (e.g. sources) in large and complex datasets. Here Pearson's correlation test has been used (using the statistical package Minitab) to investigate relationships between elements. In aerosol data sets, high correlation coefficients between two aerosol species may be due to one or more of the following common processes; (a) similar sources (b) similar generation and/or removal mechanisms and/or (c) similar transport patterns. The statistical significance of the correlation coefficient depends on the number of samples in the population and the confidence level imposed. For the current study the number of samples ($n=91$) was such that a correlation of > 0.185 would suggest a statistical significance at the 95% confidence level (i.e. $p<0.05$), whereas a correlation coefficient of > 0.361 would suggest a statistical significance at the 99% level. Since the aerosol trace metals indicated log-normal distributions (see section 4.2), correlation coefficients between the trace elements were produced after taking their logarithms.

Statistical analysis (Pearson's correlation) was applied to the Plymouth data set. It is important to bear in mind that the results of such a test are not an absolute indication of causes/effects between the two variables (Owen and Jones 1990) but a tool to aid in data interpretation. This type of statistical approach has been used extensively in trace metal aerosol studies (Fones 1996; Yuan et al., 2004; Hodzic et al., 2005; Gong et al., 2005; Koçak 2007). All of the sample population correlation coefficients are presented in Table 4.18a. The correlation coefficients with * represent statistically significant relationships with a p value <0.05 .

Table 4.18 Pearson correlation coefficients between log transformed aerosols trace metal concentrations in the Plymouth atmosphere. *indicates a significant correlation ($p < 0.05$).

(a) -All aerosol samples

	Al	Mn	Fe	Na	V	Ni	Co	Zn	Mo	Cd
Mn	0.736*									
Fe	0.740*	0.806*								
Na	0.014	0.123	-0.067							
V	0.151	0.158	-0.023	0.349*						
Ni	0.076	0.278	-0.019	-0.092	0.222					
Co	0.421*	0.686*	0.391*	0.201	0.343*	0.409*				
Zn	0.142	-0.088	-0.052	-0.624	-0.173	0.198	-0.087			
Mo	0.528*	0.695*	0.690*	0.250*	0.255*	0.214	0.542*	-0.133		
Cd	0.481*	0.676*	0.508*	0.379*	0.314*	0.186	0.567*	-0.275*	0.644*	
Pb	0.659*	0.778*	0.741*	0.122	0.140	0.143	0.520*	-0.155	0.702*	0.733*

(b)-Atlantic air mass samples

	Al	Mn	Fe	Na	V	Ni	Co	Zn	Mo	Cd
Mn	0.604*									
Fe	0.604*	0.745*								
Na	-0.211	-0.092	-0.179							
V	0.342	0.078	-0.015	-0.067						
Ni	0.316	0.456*	-0.033	-0.324	0.443*					
Co	0.246	0.569	0.180	-0.110	0.314	0.625				
Zn	0.418*	0.054	-0.016	-0.617*	0.193	0.346	0.242			
Mo	0.292	0.669*	0.258	0.377*	-0.077	0.123	0.207	-0.124		
Cd	0.157	0.467*	0.299	0.250	-0.015	0.004	0.367*	-0.042	0.213	
Pb	0.467*	0.662*	0.635*	-0.079	-0.007	0.195	0.359*	-0.003	0.229	0.620*

(c) UK-European air mass samples

	Al	Mn	Fe	Na	V	Ni	Co	Zn	Mo	Cd
Mn	0.804*									
Fe	0.837*	0.824*								
Na	0.293	0.335*	0.119							
V	0.318	0.461*	0.167	0.578*						
Ni	0.148	0.437*	0.247	-0.110	0.209					
Co	0.543*	0.738*	0.539*	0.508*	0.467*	0.386*				
Zn	-0.239	-0.221	-0.125	-0.733*	-0.507*	0.441*	-0.373*			
Mo	0.678*	0.810*	0.714*	0.429*	0.401*	0.383*	0.675*	-0.206		
Cd	0.768*	0.859*	0.738*	0.448*	0.557*	0.557*	0.212	0.724*	-0.405*	0.764*
Pb	0.835*	0.833*	0.821*	0.326*	0.416*	0.159	0.639*	-0.291	0.787*	0.919*

It is clear that the crustally influenced trace elements Al, Fe ($EF_{\text{crust}}=1.87$) and Mn ($EF_{\text{crust}}=2.77$) have highly statistical significant inter-correlations (e.g. Al / Fe = 0.740; Al / Mn = 0.736; Fe / Mn = 0.806 all with $p<0.01$). This is not surprising owing to their common crustal source (see section 4.3.2). Similar observations have been noted by e.g. Koçak (2007); Fones (1996); and Wells (1999). These relationships become more significant the greater the influence of natural sources on aerosol populations.

Pb and Cd, being predominantly sourced from anthropogenic activities, also exhibit a strong correlation (0.733). However what is surprising is that they statistically co-vary with the crustally derived elements Al, Mn, Fe, Co (with Cd and Pb) as well as Mo (with Pb). This clearly suggests that not only is the source (either crustal or anthropogenic) impacting upon the variability of the aerosol trace metal concentrations but air mass transport and associated removal mechanisms are also important. There are two distinctly different chemical characteristics of the Atlantic and UK+European air masses (section 4.3.6), it is not surprising that there may be correlations between elements having different sources. Another interesting feature in Table 4.18a is the lack of any relationship between Zn concentrations and other metals except for Na (showing an inverse correlation, -0.624).

This indicates that there is a unique, terrestrially dominating source for this metal. This source is also likely to be regionally located as no inter-element relationship suggests limited air mass influence on its variability. As mentioned in section 4.3.1 local sources may originate from the re-suspension of Zn enriched waste from local, historically contaminated mining sites.

Sodium is correlated (95% confidence level) with Cd, V and Mo. Previous studies have shown that most Cd in surface seawater is complexed with natural organic ligands (Bruland, 1992; Wen et al., 2006). Therefore correlations between Na and Cd may be due to enhanced concentrations of Cd in the sea surface microlayer, followed by injection into the atmosphere from the generation of marine aerosol. A more likely explanation is be that Cd enhanced air masses from Western Europe may have taken a longer marine route to reach the sampling site. Regarding V and Mo, both elements have been shown to have a contribution from the marine aerosol (Chester et al., 1984), although owing to their relatively lower correlation coefficient, factors other than the marine source are also likely to influence their variability.

Similar correlation matrices to that presented in Table 4.18a were prepared for both the Atlantic (Table 4.71b) and UK+European (Table 4.71c) trace metal datasets. It is apparent that the inter-elemental correlation coefficients are generally greater in the UK+European air masses compared with those from Atlantic air masses. For example Al and Fe have correlation coefficients of 0.837 and 0.604 for the UK+European and Atlantic air masses respectively. Correlation coefficients between Pb and Cd also show differences between the two categories; the UK+European air mass dataset being greater (0.919) than the Atlantic air mass (0.620). A similar trend was apparent for correlation coefficients between crustal and anthropic sourced elements. This could be due to the fact that the elements in the Atlantic air mass have been transported for a significantly longer distance than in the

UK+European air masses. During transport over the Atlantic Ocean crustally derived elements (e.g. Al and Fe) will be affected more by sequential dry and wet deposition than anthropogenic source elements (e.g. Cd and Pb) due to the elements being associated with particles of different sizes, which will result in a deviation between the concentration variation between the different sourced elements. In contrast the comparatively shorter distances over which the elements associated with the UK+European air masses will have been transported will mean that the effects of deposition processes on the variation of aerosol elemental concentrations will be less effective than on those for the Atlantic air mass. Moreover, some elements may appear correlated for the whole data set (Table 4.18 a) due to strong correlations in one population. For example, Na and V did not correlate with each other in the Atlantic air mass population whereas a statistical correlation was detected in the UK+Europe population and in the whole data set

4.5 The solid state speciation signal of aerosol associated trace metals (Al, Fe, Mn, Co, Mo, Ni, Cd, Pb) in the Plymouth aerosol populations

The impact of atmospheric inputs on marine biogeochemical cycles will not only be determined by the quantity of total atmospheric inputs (See section 2.6) but also on the degree to which the aerosol associated trace metals undergo dissolution in both rainwater (during wet deposition events) and seawater, post dry deposition.

Studies have been carried out by previous workers to define the aerosol trace metal solubility / bioavailability in a variety of aqueous media (e.g. Chester et al., 1994, 2000; Lim et al., 1994; Fernandez et al., 2000, 2002; Dabek-Zlotorzynska et al., 2002, 2003, 2005; Voutsas and Samara, 2002; Chen and Siefert, 2003; Bonnet and Guieu, 2004; Hand et al., 2004; Desboeufs et al., 2005; Heal et al., 2005; Al-Masri et al., 2006; Baker et al., 2006a, b). As stated in section 2.7 the processes which influence seawater and rainwater dissolution of trace metals from aerosol material are varied and act simultaneously in a

complex manner. Chemical, biotic and physical processes such as pH, presence of dissolved organic complexing ligands, particle concentrations, bacteria, phytoplankton, and temperature may influence the extent of metal dissolution. The trace metal solid state speciation of aerosol material from contrasting sources will also markedly affect the potential availability of trace metals for seawater/rainwater dissolution (Chester et al., 1989, 1994). The solid state speciation has, in the past, been defined by applying operational sequential leach schemes on aerosol material. Different schemes have been applied depending upon the environmental application of the generated data (Chester et al., 1989; Zatka et al., 1992; Spokes et al., 1994; Fernandez et al., 2000, 2002; Fuchtjohann et al., 2000; Slejkovec et al., 2000; Dabek-Zlotorzynska, 2003; Profumo et al., 2003; Al-Masri et al., 2006). One of the first schemes applied to aerosol collected on filter material was that proposed by Chester et al. (1989) and has been used in the current study. The measured “exchangeable” fraction generally represents the upper limit of the soluble or bioavailable fraction of the aerosol associated trace metals (Chester et al., 1994). Hence carrying out solid state speciation studies of aerosol populations yields essential information on the potential reactivity of the associated metals with seawater, post-deposition or during wet deposition events, and hence their impact on marine biogeochemical cycles. Therefore, this section describes the application of an established operational three stage sequential leach scheme of Chester et al., (1989) to aerosol populations sampled from the Plymouth coastal and semi-urban aerosol. The three stage sequential leach (see section 3.5 for the full experimental details) was applied to twenty selected samples representing different wind sectors to assess the effect of different possible sources. The air mass diagrams for each of the twenty samples are on the supplied data CD. Table 4.19 summarises the statistical characteristics of aerosol trace metal solid state speciation signatures for the Plymouth populations.

Considering the general trends in the Plymouth dataset (Table 4.19) and by comparison with literature data (Table 4.20), it is apparent that different metals exhibit contrasting solid state speciation signatures.

(i) Al and Fe are present predominantly (> 98% of their total concentrations) in the combined “refractory” and oxide / carbonate fractions (Stages 2 and 3) with 1-2.2% being found in the “exchangeable” fraction (Stage1). This is consistent with literature values (see Table 4.20) with the “refractory” fraction, which is the most important phase for both Al and Fe, found in European aerosol material in the typical ranges of 82-96% and 58-93% respectively (Chester et al., 1989, 1994; Fernandez et al., 2002).

Table 4.19. Statistical summary of the aerosol trace metal solid state speciation signature for the overall Plymouth aerosol population. (Each stage expressed as a % of the total metal aerosol concentration; n=20).

Element (EF _{crust})	Stage 1		Stage 2		Stage 3	
	% (S.D)	Range	% (S.D)	Range	% (S.D)	Range
Al (1)	1.5 (1.18)	0.17-4.5	15.4 (7.2)	4.4-34.1	84.2 (8.3)	61.4-98.5
Cd (227)	71.7 (10.2)	53.9-93	0.9 (0.46)	0.3-1.6	27.8 (10.5)	6.2-46.1
Co (3.08)	39.6 (18)	8-90.1	2.5 (2.1)	0.1-6.99	58.1 (18.6)	9.9-92
Fe (1.87)	2.2 (1.9)	0.6-7.1	41.8 (14.9)	4.8-68.7	55.9 (15.3)	24.2-94.0
Mn (2.77)	66.2 (15.4)	32.9-95.7	3.3 (2.7)	0.3-8.7	30.5 (15.8)	3-67.1
Mo (134)	36.8 (20.6)	11.5-93.8	2.13 (1.4)	0.3-4.2	61.2 (20.6)	5.8-88.3
Ni (14.2)	57.3 (16)	27.6-87	13.1 (5.9)	5.2-25.5	29.6 (12.3)	3.5-58.1
Pb (187)	80.8 (7.84)	60.7-93.8	2.0 (0.5)	0.1-2.6	17.3 (8.1)	3.8-39.1

A relatively high association of an element with the oxide/carbonate and residue phase would indicate low temperature generation of the aerosol material, i.e. predominantly natural sources, which is consistent with their lower EF_{crust} (1 by definition and 1.9, for Al and Fe respectively; Chester et al., 1989).

Owing to the role played by the atmospheric deposition of Fe in stimulating primary productivity in HNLC regions of the world's oceans, there have been a number of recent studies (e.g. Zhu et al., 1992; Chen and Siefert, 2003; Bonnet and Guieu, 2004; Hand et al., 2004; Desboeufs et al., 2005; Baker et al., 2006a, b) focussed on defining the “solubility” of aerosol associated Fe. These studies have considered “end-member” aerosol populations in controlled laboratory simulations (e.g. Bonnet and Guieu, 2004; Desboeufs et al., 2005) whilst other workers have used mixed, typically filter collected, aerosol populations (e.g. Chen and Siefert, 2003; Hand et al., 2004; Baker et al., 2006 a,b). For a more detailed critical summary see Mahowald et al. (2005). Comparison of these values with those from the current study is difficult owing to the contrasting experimental approaches applied. However, from the summary, the extent of “soluble” Fe is generally lower for crustally derived aerosols, and lowest in systems which apply extraction solutions buffered at higher pH (8.2, seawater; Bonnet and Guieu, 2004; Chen et al., 2006; compared to ca 4.7 ; Baker et al., 2006a, b), although the literature does exhibit a wide range of values. Highest Fe solubilities tend to be quoted for marine rainwaters, e.g. Jickells and Spokes (2001) quoted iron rainwater solubilities of 14% in regions close to industrial activity and Kieber et al. (2003) observed dissolved iron concentrations of about 50% for marine rains collected off Bermuda. The observed range of % “exchangeable” Fe fractions for the current study (0.6-7.1 %) for the Plymouth aerosol falls within the range of values observed in recent studies (Table 4.20). What is interesting is that the observed “carbonate / oxide” fraction was generally higher than literature quoted values except for that quoted by Chester et al (1989) for Liverpool urban aerosol material in which the “oxide / carbonate” fraction amounted to 32% of the total aerosol. Fe is expected to be primarily associated with the residual fraction, similar to Al, and this is the case for samples from other European coastal sites highlighted in Table 4.20. However, this is not the case for the current work and this might be explained by the life history of the aerosol. As the aerosol population is transported to the site from its source ageing in the atmosphere will occur and the aerosol will be

subjected to a series of wetting and drying cycles (Spokes et al. 1994; Baker et al., 2006b) during cloud formation and dissipation. These cycles will lead to a lowering in pH (enhanced acidity) which will attack more refractory solid phases such as the aluminosilicate lattice. This reaction may then release the element from the more residual solid speciation phase into the 'exchangeable' or the 'oxide/carbonate' fraction.

(ii) Elements whose solid state speciation signal is dominated by the "exchangeable" phase included Cd, Pb and Mn. For example, the average % of this phase contributing to the aerosol populations were 81%, 72% and 66% respectively. Previous studies (Chester et al., 1989; Chester et al., 1994; Wells, 1999; see Table 4.20) have also indicated high average % "exchangeable" or "soluble" phase associations for elements such as Pb and Cd although there is a significant degree of variability for these elements (e.g. Pb has quoted ranges of ca 5 – 97 % ; Chester et al. 1994), this variability also being detected in samples collected from the current sampling site. In this study Pb and Cd predominately originated from anthropogenic sources (EF_{crust} 187 and 227 respectively for the selected samples). High exchangeable fractions are consistent with such material being generated from high temperature processes (Chester et al., 1989).

(iii) For the remaining elements, Mo, Co and Ni, the majority of the total concentrations are associated with the exchangeable and residual fractions, with relatively minor contribution from the oxide/carbonate solid phase. There is very limited data regarding the solid state speciation for these elements, the only published work being that for LUAP (Chester et al., 1989). LUAP associated Co shows similar trends to that observed for the Plymouth aerosol, however Ni clearly indicated a proportionally higher exchangeable fraction (57 %) with that observed in LUAP. There are no literature data available for Mo aerosol solid state speciation and therefore no comparison may be made.

Therefore the differences, in the portioning of the elements between the three stages can potentially be related to the contributing elemental source either anthropic or crustal, and/or mechanisms which modify the solid state speciation during transport.

4.5.1 Elemental solid state speciation signal associated with aerosol populations derived from different wind sectors

Recent studies (Koçak et al., 2007) have clearly shown that the chemical speciation signal exhibited by an element is dependent upon the amount of and type of sources contributing to the aerosol samples (i.e. anthropogenic or natural) along with aerosol modification during atmospheric transport. Using samples from different air mass types collected from the South Eastern Turkish coastline, they were able to illustrate statistical differences between the elemental solid state speciation signals for Al, Fe, Pb and Cd, with lower exchangeable fractions and higher residual fractions in aerosol populations associated with air masses from the south of the region compared with those from the north. This was explained by Southerly air masses passing over the Saharan desert, hence being loaded with a proportionally higher amounts of crustal material compared with anthropogenically derived material.

Owing to the already stated differences in the chemical characteristics (section 4.3.6) of the two different air mass types, it is of interest to investigate if there are any differences in the elemental solid state speciation for aerosol populations associated with (i) the Atlantic air masses and (ii) the UK+European air masses. The major difference between the two air masses is that the aerosol material associated with Atlantic air masses would have had more time to experience population modification during transport as a result of (i) sequential deposition of large, crustal particles and (ii) chemical modifications as a result of cycles of evaporation and condensation. Table 4.21 highlights the % contribution of each sequential leach stage as a % of the total aerosol metal concentration for Plymouth

samples associated with the two different wind sectors (Atlantic, UK+Europe). A Mann-Whitney test with a confidence level of 95 % has been applied to test the differences between the two wind sectors. There were no significant statistical differences in the percentage of elemental solid phase associations with air mass origins.

Table 4.21 and the associated statistical analysis clearly highlight the relatively consistent solid state speciation character of the two aerosol populations, even though there are differences associated with their respective concentrations (Section 4.3.6).

This indicates that the aerosol material transported through both air mass sectors has reached equilibrium in terms of the impact of any chemical modifications which might have occurred during transport (such as evaporation/condensation cycles). A similar consistent trace elemental chemical speciation signal was observed by Nimmo (pers. comm) for Irish Sea aerosol populations derived from contrasting wind sectors.

4.6 Total atmospheric dry depositional fluxes to the English Channel

The impact of particulate trace metals on the biogeochemical cycle of the English Channel can be assessed by calculating the trace metal dry depositional fluxes can using aerosol data and assigned elemental settling velocities (see Table 4.22).

The flux and input of aerosol associated trace metals to the English Channel sea surface were calculated using the following equations:

$$F = (C * V * T) \cdot 10^{-4} \quad (4.3)$$

Where:

F: dry deposition flux (ng cm⁻² yr⁻¹)

C: concentration of element in ambient the air (ng m⁻³)

V: settling velocity (m s⁻¹)

T: number of seconds in a year (31,536,000)

Table 4.20. Comparison of sequential leach result of the Plymouth aerosol with other European marine aerosols in wt %.

Element and Stage	English Channel ¹ Plymouth	English Channel ²	Irish Sea ³	North Sea ⁴	LUAP ⁵	LUAP ¹	Western Med ⁶	Eastern Med. ⁷	Saharan Crust ⁵
Al-S1	1.2±1.2	0.4±0.4	5±4	5	5.6±4.8	1.3±0.26	4.3±2.5	2.4±1.8	0.05±0.015
Al-S2	14.6±7.8	4.1±7.8	11±5	13.5	12.1±5.8	11.9±3.1	4.2±1	3.6±2.2	14.4±2
Al-S3	84.2±8.3	95.5±7.6	85±7	81.5	82.3±7.2	83.7±22	91.5±2.4	94.0±2.5	85.6±2
Cd-S1	71.7±10.2	82±26.7	72±11			25.4±5.0	79.7±134	84.6±14.2	
Cd-S2	0.6±0.5	11±14.7	15±6	-	-	67.8±18.1	8.8±8.0	7.9±7.7	-
Cd-S3	27.8±10.5	0.3±0.7	13±7			6.78±1.8	11.7±8.4	7.5±7.5	
Co-S1	39.6±18.0		-			26.8±7.0			
Co-S2	2.5±2.1	-		-	-	N.D	-	-	-
Co-S3	58.1±18.6					73.2±11			
Fe-S1	2.2±1.9	N.D	1.0±1.2	6.5	9.9±6.2		8.3±8.1	1.7±1.2	0.03±0.003
Fe-S2	41.8±14.9	3.3±5.8	21±12	11	31.9±11.8	-	0.3±8.1	4.9±3.3	9.5±2
Fe-S3	56.0±15.3	96.7±7.6	78±12	82.5	58.2±12.2		91.4±8.1	93.4±3.9	90.5±2
Mn-S1	66.2±15.4	69.4±15.4	45±10	56	44.2±13.2	45.7±0.17	63.3±7	43.5±10.0	22.8±1.1
Mn-S2	3.31±2.7	15.5±9.6	13±6	7	22.7±12.3	17.7±0.1	nd	13.4±8.4	34.2±2.6
Mn-S3	30.5±15.8	15±8.4	42±12	37	33.1±13.7	36.6±0.23	36.7±7	43.5±5.8	43±2.7
Mo-S1	36.8±20.6								
Mo-S2	2.0±1.4	-	-	-	-	-	-	-	-
Mo-S3	61.2±20.6								
Ni-S1	57.3±16.0					16.1±3.0			
Ni-S2	13.1±5.9	-	-	-	-	41.7±8.2	-	-	-
Ni-S3	29.6±12.3					42.3±13			
Pb-S1	80.8±7.8	54.5±31.2	79±9	77	81.5±6.9	57.1±6.0	97.3±3.5	72.0±20.0	5.7±5.1
Pb-S2	2.0±0.5	19.4±15.8	16±6	15.5	11.1±6.7	29.2±9.0	N.D	22.0±14.8	28.8±5.7
Pb-S3	17.3±8.1	26±21.2.	5±4	7.5	7.4±4	13.7±2.7	2.7±3.4	6.0±7.0	65.5±6.2

1: current study; 2: Wells, (1999); 3: Laes, (1999); 4: Chester *et al.*, (1994); 5: Chester *et al.*, (1989); 6: Nimmo (personal communication); 7: Koçak *et al.*, (2005).

Table 4.21. Statistical summary of the three stage sequential leach (standard deviation in parentheses) for the different wind sources, (geometric mean in % for all elements).

Elament	Atlantic Wind Source			UK+European Wind Source		
	Stage 1	Stage 2	Stage 3	Stage 1	Stage 2	Stage 3
Al	1.4(0.69)	13.4(5.6)	85.4(6.1)	1.5(1.4)	16.3(7.9)	83.6(9.2)
Cd	67.5(10.6)	0.87(0.56)	31.9(11.1)	73.3(9.84)	0.97(0.44)	26.1(10.1)
Co	41.2(16.9)	4.41(2.15)	55.1(18.9)	38.9(18.9)	2.3(1.65)	59.2(19)
Fe	1.7(0.8)	38.5(19.7)	59.7(19.6)	2.41(2.18)	43.3(13)	54.3(13.6)
Mn	62(13.3)	4.08(3.2)	34.5(12.7)	67.8(16.2)	4.09(2.12)	28.9(16.9)
Mo	30.6(18.2)	2.64(1.6)	66.8(18.3)	39.3(21)	1.9(1.2)	58.9(21.6)
Ni	60(21.8)	11.9(6.72)	28.1(17.1)	56.2(13.9)	13.6(5.7)	30.2(10.4)
Pb	81.9(368)	2.02(0.35)	16.1(3.71)	80.3(9.1)	1.97(0.6)	17.7(9.4)

The flux and input of aerosol associated trace metals to the English Channel sea surface were calculated using the following equations:

$$F = (C * V * T) \cdot 10^{-4} \quad (4.3)$$

Where:

F: dry deposition flux (ng cm⁻² yr⁻¹)

C: concentration of element in ambient the air (ng m⁻³)

V: settling velocity (m s⁻¹)

T: number of seconds in a year (31,536,000)

The factor 10⁻⁴ was applied to normalise units.

$$I = (F * SA) \cdot 10^{-5} \quad (4.4)$$

Where:

I: trace metal input (tonnes yr⁻¹)

F: dry deposition flux (ng cm⁻² yr⁻¹)

SA: surface area of the body of the water (km²) (For the English Channel this is 77,000 km²)

The main uncertainty in Equation 4.3 when calculating the dry depositional flux is the choice of the settling velocity and the method used to determine it. In the literature there are a wide range of quoted settling velocities. These have been determined using both experimental and modelling techniques, including; (i) mathematical modelling, (ii) mass-size distributions (using a cascade impactor), (iii) subtraction of the wet deposition flux from the total deposition flux and (iv) using surrogate surfaces. The settling velocities used in the current study have been adapted from the literature as there was no size segregation of the aerosol population or the deployment of surrogate collection surfaces. Table 4.22 represents the adopted settling velocities taken from Spokes et al., (2001) and Duce et al., (1991). Spokes et al., (2001) calculated mass weighted settling velocities for Al, Mn, Zn and Pb using the settling velocities from Duce et al., (1991), and aerosol size fractionated data (coarse/fine) for the Atlantic and southerly + easterly wind sector (UK+Europe) to calculate weighted settling velocities, which have been used in this study. When settling velocities were not available from Spokes et al., (2001), settling velocities from Duce et al., (1991) were used. Although no V_d values were calculated for Fe by Spokes et al., (2001), it was assumed that the V_d would be similar to that calculated for Al. These values are limited in that they are not exactly from the collection area, however they represent the best approximate value (Duce et al., 1991) in the literature and consequently are used widely. The elements have been categorized into two groups according to Duce et al., (1991): 1) elements found primarily on particles in the accumulation ($<1 \mu\text{m}$) mode (Pb, Cd, Zn, and Ni) mostly produced by anthropogenic processes, 2) elements found primarily on particles in the coarse ($>1 \mu\text{m}$) mode (Al and Fe) mostly produced naturally. The settling velocity used for group 1 elements was 0.1 cm s^{-1} whereas 2 cm s^{-1} was used for group 2 elements.

A more refined version of Equation 4.3 was used (Equation 4.5) to take into account the influence of contrasting wind sectors (Atlantic and UK+Europe) and settling velocities. Including the effect of different air sectors is important as the air mass derived from the

UK+ Europe is considered to be more predominantly influenced by anthropogenic and natural sources (i.e. higher aerosol trace metal loadings). The relative temporal influence of the Atlantic and UK+Europe air masses was 0.58 and 0.42 respectively (see Section 4.3.6).

Table 4.23 summarises settling velocities adopted for European coastal regions. Different authors have reported a diverse range of settling velocities which highlights the uncertainty in these velocities and as a result the input of trace metals. Air mass weighted and un-weighted dry fluxes calculated according to the Equations 4.3 and 4.5 are presented in Table 4.24.

Table 4.22. Elemental settling velocities used in the calculation of (V_d) dry deposition adopted from the literature for the current study (Spokes et al., 2001 and Duce et al., 1991).

Element	V_d (cm s ⁻¹)		Reference
	Atlantic wind source	UK+European wind source	
Al	1.3	2	Spokes et al., 2001-Duce et al., 1991
Cd	0.1	0.1	Duce et al., 1991
Co	2	2	Duce et al., 1991
Fe	1.3	2	Spokes et al., 2001-Duce et al., 1991
Mn	1.1	1.4	Spokes et al., 2001
Mo	0.1	0.1	Duce et al., 1991
Na	3	3	Duce et al., 1991
Ni	0.1	0.1	Duce et al., 1991
Pb	0.36	0.63	Spokes et al., 2001
V	0.1	0.1	Duce et al., 1991
Zn	0.71	0.92	Spokes et al., 2001

The refined equation used to calculate the air mass weighted dry flux values is as follow:

$$F = [(C_{At} * V_{d At} * 0.58) + (C_{UK+EU} * V_{d UK+EU} * 0.42)] * T \quad (4.5)$$

Where:

F: dry deposition flux ($\text{ng m}^{-2} \text{yr}^{-1}$)

C: concentration (ng m^{-3}) of element in Atlantic and UK+Europe air masses respectively

$V_{d At}$; $V_{d UK+EU}$: deposition velocity (m s^{-1}) of elements in Atlantic and UK+Europe air masses respectively; see Table 4.22

T: number of seconds in a year (31,536,000)

A comparison of the dry deposition fluxes calculated for the Western English Channel (Plymouth) with values from the literature is presented in Table 4.25. Direct comparison of current fluxes with those from the literature are a little misleading as different settling velocities have been adopted by the different authors. For example, values calculated by Wells (1999) show variation between Fe, Cd, Co, Ni and Zn and those for the current study due to the fact that Wells (1999) applied contrasting settling velocities. The settling velocities used were calculated with dry deposition collected samples using a surrogate surface and the corresponding aerosol metal concentrations. The comparatively higher values observed for Al and Fe in the Eastern Mediterranean atmosphere may be attributed to the higher aerosol concentrations observed in this area being impacted by crustal material during Saharan dust events from North Africa.

Literature values (Chester et al., 1990; Ottley and Harrison, 1993) also have higher Pb fluxes due to its relatively higher aerosol concentration (see chapter 2). Therefore it is clear from the comparison that calculations of the atmospheric trace metal dry depositional fluxes is fraught with problems and inaccuracies, mainly derived from the uncertainty associated with the choice of the settling velocity. Therefore there is an urgent need to better define, in a regional study, the element settling velocities.

However, using dry depositional flux it is possible to calculate the dissolved atmospheric trace metal flux as this is an estimate for the component of the particulate fraction that may be incorporated into the marine biological cycle. This is calculated using the flux calculations presented in Table 4.26 and the percentage of the element in the exchangeable fraction (see Table 4.19.) of the sequential leach. The total dry and “dissolved” inputs for trace metals to the English Channel were calculated using Equation 4.4 and compared with those for trace metals calculated by Wells (1999). Table 4.27 shows the calculated input in the current study and the input calculated by Wells (1999). The differences in the inputs between the two studies are due to variance in the applied fluxes (due to the variation in concentration and settling velocities between the two sites) which have been discussed above.

Table 4.27 compares the calculated inputs using current study aerosol concentration and the settling velocities reported by Wells (1999). Using the same settling velocities improves the correlation between elemental inputs (e.g. Pb and Ni). However, settling velocities calculated by Wells are not very convincing as some values contradict each other and are not consistent with model values. For example Al has a settling velocity of 1.08 whereas Fe is 0.08 which is not geochemically consistent. Zn has a settling velocity of 0.09 which not consistent with the Zn mainly has a local source. However, Pb and Cd have more reliable values for settling velocities (0.04 and 0.02) which are consistent with the conclusion that Cd and Pb have long range transport anthropogenic sources.

Table 4.23. Literature elemental settling velocities (cm s^{-1}) for European coastal regions.

Element	Fones 1996 Irish Sea	Dulac et al., 1989 Western Med.	Remoudaki et al., 1992 Mediterranean Sea	Ottley and Harrison 1993 North Sea	Rojas et al., 1993 North Sea	Migon et al., 1997 Ligurian Sea	InjUK et al., 1998 North Sea	Guerzoni et al., 1999a and Guerzoni et al., 1999b Mediterranean	Wells (1999), English Channel	Spokes et al. (2001), N. Atlantic	Sakata and Marumoto (2004), Lake Michigan	Koçak et al. (2005), Eastern Med.
Al	0.46	0.69–3.8	—	0.46	—	—	—	2	1.08	1.3	—	1.73–1.8
Cd	0.38	0.053	—	0.38	0.39	0.42	—	0.2	0.04	—	0.21–0.82	0.1
Cu	0.70	—	1.1	0.70	0.48	1.19	0.21–0.5	—	0.44	—	1.2–3	1.1–1.4
Fe	0.45	—	—	0.45	—	—	0.32–0.55	2	0.08	—	—	1.73–1.8
Mn	0.60	—	—	—	—	—	0.21–0.53	—	0.69	1.1–1.4	1–4.6	1.48–1.7
Pb	0.17	0.041	1.9	0.17	0.25	0.19	0.07–0.11	0.2	0.02	0.36–0.63	0.35–1.7	0.8
Zn	0.52	—	—	0.52	0.35	4.38	0.20–0.4	—	0.09	0.71–0.92	0.73–2.7	0.99–1.11

Table 4.24. The flux (expressed as $\mu\text{g m}^{-2} \text{yr}^{-1}$ except for Al, Fe, Mn and Na which are expressed as $\text{mg m}^{-2} \text{yr}^{-1}$) of aerosol associated trace metals to the English Channel. mass influence (see text for further discussion).

Element	Air mass weighted flux
Al	88.7
Cd	3.46
Co	108
Fe	121
Mn	2.22
Mo	16.6
Na	7165
Ni	81.6
Pb	863
V	73.8
Zn	2392

Table 4.25. A comparison of dry deposition fluxes from Plymouth (current study) with other European regions (fluxes are expressed as $\mu\text{g m}^{-2} \text{yr}^{-1}$ except for Al, Fe, Mn and Na which are expressed as $\text{mg m}^{-2} \text{yr}^{-1}$).

Element	Irish Sea Fones 1996	English Channel Current study	English Channel, C. Wells 1999	North Sea Otley and Harrison 1993	W.Mediterranean Chester et al., 1990	E. Mediterranean Koçak et al., 2005
Al	30.43	88.7	78.3	28.54	93.8	320
Cd	22.7	3.46	1.5	149	49	3.8
Co	37.5	108	14.5		18	
Cu	1000		321	1520	895	2600
Fe	22.5	121	2.96	26.03		230
Mn	0.779	2.22	1.72		1.56	3.8
Na	546	7165	762	1822		
Ni	701	81.6	330		240	
Pb	809	863	8.6	1560	1410	5650
V		73.8				
Zn	4140	2392	575	12210		5330

Table 4.26. Bio-available and air mass weighted fluxes (expressed as $\mu\text{g m}^{-2} \text{yr}^{-1}$ except for Al, Fe, Mn and Na which are expressed as $\text{mg m}^{-2} \text{yr}^{-1}$).

Element	"Dissolved" flux	Air mass weighted flux
Al	1.28	88.7
Cd	2.45	3.46
Co	43.4	108
Fe	2.60	121
Mn	1.42	2.22
Mo	5.81	73.8
Ni	47.6	81.6
Pb	697	863

Table 4.27. Dry and dissolved trace metal inputs to the English Channel (t yr^{-1}).

Element	Current study		Current study (using Wells 1999 settling velocities)		Wells (1999)	
	Dissolved	Dry	Dissolved	Dry	Dissolved	dry
Al	98.6	6830	65.7	4381	116	6029
Co	3.34	8.32	0.627	1.58	0.755	1.12
Ni	3.67	6.28	2.52	4.40	13.3	25.4
Pb	53.67	66.45	2.07	2.56	0.323	0.662

4.7 Conclusions

This study has revealed the factors which affect the variability in the trace metal aerosol chemical composition of the Plymouth coastal and semi-urban aerosol. Local, regional and long distance sources have an effect on the aerosol trace metal concentrations, furthermore air mass transport and associated removal mechanisms are also significant. To define this variability the following factors have been discussed; (i) aerosol source types, (ii) aerosol emission strengths, (iii) proximity of aerosol source, (iv) air mass transport processes and (v) removal processes.

The Plymouth coastal and semi-urban aerosol concentrations for all elements were lower (2-13x) than aerosol elemental concentrations observed at other comparative UK urban sampling locations. The Plymouth coastal and semi-urban aerosol population has no major regional industrial sources, and is influenced more by long range transported anthropogenically derived material from the UK and Western Europe. In addition, the Plymouth aerosol undergoes dilution by more pristine maritime air masses from the west and south-west, leading to lower observed trace elemental concentrations. Periodically, however, the sampling area has been subject to the impact of immediate local construction activity, leading to elevated concentrations for all elements, with some elements exhibiting intense diurnal patterns (i.e. Al, Fe, Mn).

EF_{crust} analysis indicated that Fe, Mn, Co and V have low EF_{crust} values (<10) which indicates increasing crustal source contributions, whereas the remaining elements have high (> 10) EF_{crust} values. However, calculation the % of crustal contribution indicates that $EF_{\text{crust}} < 2$ represents the transition from predominantly anthropogenic to crustal source contributions. Hence, Fe, Mn, Co, V and Ni have calculated crustal contributions with an average of 57, 41, 38, 22 and 12 % respectively. The rest of the elements have percentage crustal contributions <5 .

Apart from the initial influence from local construction activities, the variation in the Plymouth aerosol trace metal concentrations did not exhibit diurnal changes, but did exhibit a high degree of temporal variation, consistent with the literature. Seasonal (winter/summer) differences were found for Na, Mo, Co, Cd and Zn such that the winter concentrations were higher except for Zn.

Air mass transport was a significant influence on the variation in the elemental concentrations, with enhanced concentrations (about 2x) in air masses associated with the

UK and European air mass (statistically significant for Al, Fe, Mn, Cd, Mo and Pb at $p < 0.05$). This impact was also apparent when inter-elemental relationships were considered. Significant correlations between anthropically and crustally derived trace metals were found, indicating that air mass movement is a major factor influencing the variation in the aerosol elemental concentrations. Lower statistical significance between the anthropic and crustal inter-elemental relationships for the Atlantic air sector compared with those associated with the UK+European sector would, in addition, suggest that during air mass movement there is a sequential change in the chemical character of the aerosol population owing to removal processes. Zn concentrations were not statistically different ($p < 0.05$) in the two air mass sectors, suggesting regional sources. The re-suspension of material from dis-used and abandoned mine wastes from historical mining activities in the South West being a possibly source for Zn.

Sequential leach analysis showed that Al and Fe are present predominantly in the combined refractory and oxide / carbonate fractions (>95%). Elements for which the solid state speciation signal is dominated by the exchangeable phase were Cd, Pb and Mn. For the remaining the elements (Mo, Co and Ni) the majority of the total concentrations are associated with the exchangeable and residual fractions, with relatively minor contributions from the oxide/carbonate solid phase.

Using dry deposition fluxes (air mass weighted and dissolved fluxes), elemental inputs have been calculated for the western English Channel (Table 4.27). However, it is clear from comparison with the literature that calculation of dry depositional fluxes and inputs is fraught with problems and uncertainties, mainly derived from the uncertainty of settling velocities.

Modelling trace metal budgets in the English Channel has been carried out by Wells (1999) a simplified conceptual model is presented on Figure 4.9.

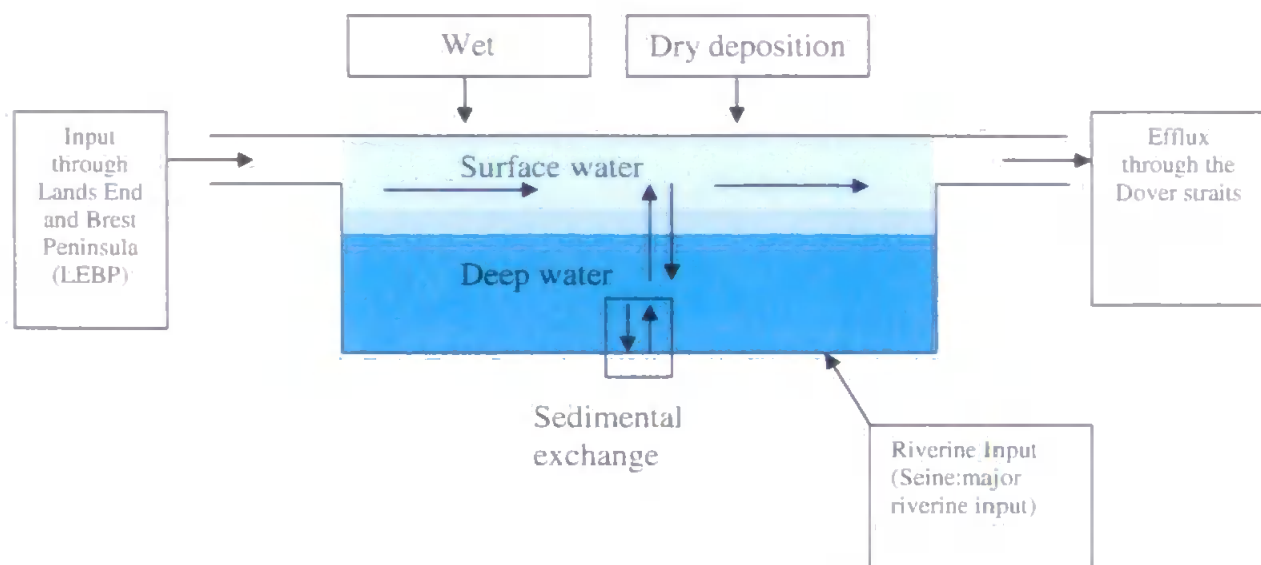


Figure 4.9. Simplified model of the trace metal fluxes in the English Channel

Using total dry atmospheric input values of trace metals calculated in this study; revised budgets for Ni and Pb in the English Channel have been calculated (Table 4.28).

Table 4.28. Geochemical budget of Ni and Pb (t y^{-1}) in the English Channel.

	Lead budget			Nickel budget		
	Current study with adopted settling velocities	Current study using Wells 1999 settling velocities	Wells (1999)	Current study with adopted settling velocities	Current study using Wells 1999 settling velocities	Wells (1999)
Metal inputs						
Rivers	81	81	263	23	23	23
LEBP transect	104	104	104	1040	1040	1040
Atmosphere (wet & dry)	298	242	240	251	249	270
Total	483	427	607	1314	1312	1314
Metal Outputs (Dover straits)						
Overall	-687	-743	-563	171	169	190

The budget calculations are explained in more detail by Wells, (1999). The budget uses a simple box model of the English Channel, assuming a flux of water of $4 \times 10^{12} \text{ m}^3 \text{ yr}^{-1}$ (Wells, 1999) across the Lands End and Brest Peninsular (LEBP) which is balance by water flow through the Straits of Dover. Trace metal fluxes across the Straits of Dover were estimated by Statham et al. (1993), whereas the trace metal transport across LEBP were estimated from the Quality Status Report (Reid et al., 1993) as were the riverine inputs for Ni whereas more recent Pb riverine inputs were calculated from data obtained from the Quality Status Report (2000). Unfortunately no information for Ni riverine inputs are included in this report. Table 4.28 summarises the inputs and outputs along with the net balance of the metal budgets (Ni and Pb) for the English Channel using the dry deposition inputs from the current study. These are compared with the metal balances calculated by Wells (1999) as well as atmospheric inputs using the contrasting settling velocities quoted in Wells (1999) to serve as a sensitivity check on the model. A negative balance would indicate that sediments are a source of trace metals whereas a positive balance would indicate that the English Channel sediments would be a geochemical sink. The revised inputs yielded from this study made little difference to the overall budget calculations (around 10% and 20% for Pb). Overall the revised budget calculations do not change the conclusions presented by Wells (1999), who showed that the output of Pb was higher than the inputs to the English Channel, suggesting that there is an unaccounted source which is likely to be the sediments. In contrast the output of Ni is lower than its input to the English Channel, suggesting that the sediment is a geochemical sink for Ni.

Further work is necessary, however, to better constrain fluxes of trace elements to the western English Channel and consequently allow more accurate trace metal budgets for the marine system. The uncertainty in trace metals fluxes arise from the lack of accuracy in the adopted settling velocities, therefore there is an urgent need to better define, on a regional scale, more accurate elemental settling velocities.

Chapter 5

Aerosol trace metal trace metal concentrations at a Red Sea coastal site (Jeddah)

5.1 Introduction

This chapter will discuss the variability in the aerosol trace metal concentrations (Al, Fe, Mn, Ni, Co, Cd, Pb, Zn,) observed at an eastern Red Sea coastal site (Jeddah), over a seventeen month sampling period (August 2002 to January 2004). Long (seasonal) variability in the aerosol chemical composition will be defined. The observed variability will be discussed in the context of the following factors (i) aerosol source types (ii) aerosol emission strengths (iii) proximity of aerosol source (iv) air mass transport processes (v) and removal processes. In addition, this section will also present the atmospheric total and “bioavailable” trace elemental dry deposition into the eastern Red Sea. Full details of sampling and analytical methods employed have previously been discussed (sections 3.2.1 and 3.3).

5.2. Background

5.2.1. Red sea coastal environment

More than 50 percent of the population of Saudi Arabia (26.7 million; 19.7 million Saudis and 7 million foreign nationals) reside within 100 km of the Saudi Arabian coastline. Off shore, the waters of the Red Sea and Arabian Gulf support a vital fishing industry and provide recreation facilities.

The Red Sea developed 20-30 million years ago when the tectonic plates of Arabia and East Africa separated, and hence is one of the youngest oceans in the world. It has an elongated shape which is due to slow seafloor spreading occurring over the last 4-5 Million years. Countries sharing the Red Sea coastline are Egypt, Sudan, Eritrea Djibouti, Israel, Jordan and Yemen. It is connected to two Seas; in the South, the Indian Ocean via the Gulf of Aden and in the north the Eastern Mediterranean via the Gulf of Suez and the Suez Canal.

The length of the Red Sea is ~1900 km with a maximum width of ~ 306 – 354 km (at Massawa, Eritrea) and a minimum width of ~ 27 km at the Strait Bab al Mandeb (Yemen); with an average depth of 490 m. The maximum depth is 2850 m. Approximately 40 % of the Red Sea is shallow (under 100 m) whereas about 25 % of the Red Sea is under a depth of 50 m deep. The rest is over 1000 m depth, forming deep axial troughs. Famous troughs include the Atlantis, Discovery and the Oceanographer Deeps. These are areas of metalliferous sediments and salt deposits.

The total surface area is $438 - 450 \times 10^3 \text{ km}^2$, with a total volume of $215 - 251 \times 10^3 \text{ km}^3$. The average surface water temperature during the summer ranges between 26-30 °C, and has about a 2 °C variation during the winter months. The Red Sea salinities range between 36 and 38. The tidal height ranges between 0.6 m (in the north) and 0.9 m (in the south), with the central Red Sea (Jeddah area) being essentially tideless. Current velocities data are severely lacking as they are generally weak and variable, being governed predominantly by air flow. Generally during the summer months NW winds move surface water towards the southern Red Sea, whereas during winter the flow is reversed resulting in the inflow of water from the Gulf of Aden into the Red Sea.

Water mass exchange with the Arabian Sea (see section 5.9), Indian Ocean is via the Gulf of Aden. These physical factors reduce the effect of high salinity caused by evaporation.

Unique to the Red Sea and relevant to the current study of metal inputs, is that there are no fluvial inputs. Restricted inputs may occur via wadis (valley) (which are seasonal in nature) mainly in the southern region, however input of continental material to the Red Sea will be mainly via atmospheric deposition.

5.2.2. Regional Climatology

The Southern Red Sea experiences two monsoon seasons. Monsoon winds occur because of the differential heating between the land surface and sea. The rainfall over the Red Sea is on average 6 cm yr^{-1} . The scarcity of rainfall and no major source of fresh water to the Red Sea results in an excess evaporation as high as 205 cm yr^{-1} and high salinity with minimal seasonal variation.

With the exception of the northern part of the Red Sea, which is dominated by persistent north-west winds with speeds ranging between 7 and 12 km hr^{-1} , the rest of the Red Sea and the Gulf of Aden are subjected to the influence of regular and seasonally reversible winds. The wind regime is characterized by both seasonal and regional variations in speed and direction with average wind speeds generally increasing northward.

During the winter period (November - April), Asiatic highs over Siberia and the Azores, shifts westward out of the Mediterranean Basin. Overall wind flow changes to Northerlies. Cold fronts may reach as far south as the Gulf of Aden, producing rain showers and thunderstorms.

Transition towards the summer begins in mid-March with a strengthening of the Azores high, with dissipation of the Saharan high. This is normally replaced by the Saharan low. These features close the winter storm track. This ends the wet season by the end of April.

There are number of characteristic wind systems for the coastal region, both land / sea winds existing, with peak gusts of generally $45\text{-}65$ knots. The Shamal is the strong north westerly wind and persists from $1\text{-}5$ days at any time of the year. However, during the summer a Shamal may even persist for upto 40 days, with maximum strength occurring in June and July. The wind being stronger during the daytime. Often the Shamal is dust

loaded (El Sayed et al., 2004). In contrast the Kaus winds are moderate to gale force south easterly winds on the Arabian Gulf, being most frequent during December – April.

5.2.3. Aerosol trace element concentrations in the Red Sea Marine Aerosol (RSMA)

The biogeochemistry of aerosol trace metals in the RSMA is still poorly defined. Studies are very limited in numbers, being those of Behairy et al., (1985), El sayed et al., (2004) and Chester et al., (1991). The earliest study was that carried out by Behairy et al., (1985). Trace metal (Fe, Mn, Cu and Cd) concentrations in dust falling over six months were investigated by collecting dry deposited samples at Jeddah (Faculty of Marine Science) at six different sampling locations using the American Standard Deposit Gauge. The concentrations of the elements followed the order: Fe>Mn>Cu>Cd, although the data did not present actual atmospheric concentrations (ng m^{-3}), only trace metal concentrations in the collected dust ($\mu\text{g g}^{-1}$) were determined. Fe concentrations did not show variations during the six months of sampling. For Mn, Cu and Cd the concentrations were variable with the highest values being detected in December for Mn and January for Cu and Cd. The abnormally high concentration of Cd ($23 \pm 8 \mu\text{g g}^{-1}$) in comparison to that in the literature was attributed to a local source i.e. a cement factory to the north of Jeddah (which now has subsequently been closed down).

El sayed et al., (2004) have also reported (for the Jeddah area) the following order in metal concentrations in deposited dust: Fe>Al>Mn>Zn>Cu>Ni>Pb>Cd. Over a period of 13 months they collected monthly dry deposition samples using simple plastic funnels (which may be lacking in accuracy owing to the possible re-suspension of dust). Comparing the concentration of elements reported by Behairy et al., (1985) and El sayed et al., (2004) the concentration values despite samples being collected from the similar location, were higher by factors of 41 and 1.3 for Cd and Mn respectively for those determined by Behairy et al., (1985). However, Fe concentrations were lower by a factor of 2.6 whereas Cu

concentrations were comparable. For Cd a 10 year interval since the closure of a cement factory close to the site may have explained the higher values (41 times higher), as stated by El sayed et al., (2004), whereas, for the other elements no explanation for the observed variability was presented.

However, Chester et al., (1991) have reported trace metal concentrations in the Arabian marine aerosol (17 high volume samples were collected) in which the aerosol concentrations followed the order: Al>Fe>Mn>Zn>V>Pb>Cu>Ni>Co>Cd. In comparison (with other coastal sea locations in the Atlantic and Pacific Ocean) the aerosol concentrations of Al, Fe and Mn measured in the Arabian Sea were intermediate in value (lower than North East Atlantic and but higher than the Pacific aerosol concentration). Moreover, Sanders (1983) report concentration of aerosol associated trace metals for samples (n=3) collected in research cruise in the Red Sea.

Chester et al., (1991) clearly stated that the Arabian Sea aerosol trace metal concentrations are affected by the surrounding arid regions. However, it is the monsoon wind system (impact on the wind direction and hence dust transport) which yields seasonality in aerosol trace metal concentrations. During the northeast monsoon, the wind direction is from North Easterly direction crossing over arid landmasses to the north. Whereas, during the South west monsoon, no such dust transport will occur. The study by Chester et al., (1991) involved the collection of aerosol samples during the Northeast monsoon (October-November) which would explain the relatively high observed concentrations of crustal dominated elements (Al 1227 and Fe 790 ng m⁻³). Table 5.1 summarises and compares the results observed from the three studies discussed above. In the literature there are many studies defining aerosol trace metal concentration for marine systems influenced by arid regions, such as the Eastern Mediterranean atmospheric aerosol (e.g. Kubilay and Saydam 1995; Kubilay et al., 1997; Kubilay et al., 2000; Kocak et al., 2004 and Koçak et al., 2005).

Table 5.1 Concentration of trace metal in the marine aerosol from samples collected from the Arabian Sea (Chester et al., 1991; expressed as ng m^{-3}) and trace metal concentration in dust fall from the Red Sea coast (Behairy et al., 1985; expressed as $\mu\text{g g}^{-1}$) and El sayed et al., (2004; expressed as $\mu\text{g g}^{-1}$).

Element	Chester et al., (1991)	Behairy et al., (1985)	El sayed et al., (2004)
Al	1127	-	25449
Fe	790	13600	35796
Mn	17	755	589
Cd	0.045	23	0.555
Co	0.38	-	-
Cu	2.6	203	214
Ni	2.0	-	67
Pb	4.3	-	28
Zn	10	-	371
V	6.3	-	-

However, for the Arabian Peninsula as described above few studies have been carried out (Behairy et al., 1985 (Jeddah); El sayed et al., (2004) (Jeddah); Al-Rajhi et al., 1996 and Modaihsh 1997 (Riyadh)). Therefore, a long term programme designed to investigate the importance and the biogeochemical cycle of the Red Sea aerosol trace metals was instigated.

5.2.4. Aerosol sampling location.

The aerosol sampling location was positioned towards the North of Jeddah which is located on a narrow coastal plain, with the Red Sea to the west and the mountain chain (Alsaraawat Mountains) of the Arabian Shield to the east. Jeddah is the major urban centre of Saudi Arabia. The general characteristics of the sampling area is an arid region with low rainfall (ca 60 mm yr^{-1}), experiencing predominantly NW (Morcos 1970) wind directions. This area of Saudi Arabia has been subject to rapid urbanization and industrilisation over

the last twenty years. Industry in and around Jeddah is mainly petroleum industries or light industries. Yanbu is an industrial city located to the north of Jeddah (about 300 km) and it is one of the two main industrial cities build by the government of Saudi Arabia for the oil industry. Two oil refineries are located in Yanbu; Petromin-Mobil and Kefi-Aramco. In Rabigh an Aramco refinery is situated to the north of Jeddah (120 km).

In Jeddah, an industrial area comprising of approximately 300 small and medium-sized industries is situated in the southern part of the city. These include oil refineries, a power plant, food industry and other small industries such as painting, plastic ware, pressurised gas and carpets (UNEP report 166).

Local mineral reserves which contain Zinc ores are associated with gold, extraction lie toward the east of Jeddah in the Samran mineral belt and copper deposits to the NE of Jeddah at Jabal Sambran.

5.3 The trace metal chemical composition of the RSMA

5.3.1 The overall chemical characteristics of the aerosol trace metals in the Jeddah urban aerosol.

A summary of the aerosol trace metal loadings (ng m^{-3}) observed at the coastal site at Jeddah, during the sampling period is presented on Table 5.2, as arithmetic and geometric means along with the range of values observed during the sampling period. This is, for the current study, referred to as the Red Sea marine aerosol (RSMA). From a consideration of Table 5.2, it is apparent that the elemental concentrations exhibit a wide range of values, consistent with literature aerosol databases of the marine atmosphere (Dulac, 1987; Chester et al., 1991; Kubilay, 1995; Kocak et al., 2004). Geometric means will be used in subsequent comparisons and discussions owing to the log-normality for all elements in the aerosol populations. The log-normality of the datasets was verified by applying the Kolmogorov-Smirnov test at the 95% confidence level (see section 4.3.1 for further

details). These values also are compared on Table 5.2 with trace metal aerosol loadings found in other marine systems whose atmospheres are significantly influenced by crustal material (i.e. Eastern Mediterranean, Kubilay and Saydam 1995; Herut et al., 2001; Kocak et al., 2004; Kocak et al., 2005; Western Mediterranean, Giueu et al., 1997; Arabian Sea, Chester et al., 1991). Table 5.2 comparing data set from Jeddah to other coastal regions which are influenced by arid land masses (i.e. the western and eastern Mediterranean; Atlantic North East Trades and the Arabian Sea). From Table 5.2 a number of general observations may be made. For the current study area high aerosol loadings of the predominantly crustally derived elements are observed (Al, Mn and Fe; crustal source contributions >70%, section 5.3.2.).

For example they are in excess of those observed in the Southern Levantine basin of the Eastern Mediterranean (Tel Shikmona, Herut et al., 2000; Kocak et al., 2005) by a factor of between 2.7-3.1 (Al-2.7x; Fe-3.1x; Mn-3.0x) and the Northern Levantine Basin by a factor of between 4.5-6.2 (Al-4.5x; Fe-5.5x; Mn-6.2x). Similarly, the ratio of the Al, Mn and Fe concentrations in the RSMA and their equivalents observed in the Arabian Sea marine aerosol (Chester et. al., 1991) amounted to 2.1, 2.9 and 2.9 respectively. The comparatively elevated concentrations of the crustally derived elements in the RSMA are not unexpected owing to the sampling location being surrounded by arid continental regions. However, they are lower than those quoted in Murphy (1985) for the North East Trades in the Atlantic Ocean (ANET). These elemental concentrations represent a restricted sample population number (n=7), documenting an individual intense Saharan dust event, and as such are likely not representative of the overall annual aerosol concentrations in this location, although the intensity of Saharan dust plumes occurring in the open Atlantic Ocean are exhibited by these data.

Table 5.2. The trace metal concentrations (ng m^{-3}) in the Red Seas Marine Aerosol (RSMA); Comparison with values from the literature of coastal systems bordered by arid regions.

Element	Red Sea Marine Aerosol (RSMA) (current study)			Southern Levantine Basin Eastern Mediterranean Tel Shikmona (n=185) (Kocak et al., 2004; 2005)	Northern Levantine Basin Eastern Mediterranean Erdemli (n=436) (Kocak et al., 2004)	Southern Levantine Basin Eastern Mediterranean Tel Shikmona (Herut et al., 2001)	Arabian Sea (n=17) (Chester et al., 1991)	Western Mediterranean (Guieu et al., 1997)	Atlantic North East Trades (n=7) (Murphy, 1985)	Red Sea (n=3) (Sanders, 1983)
	Arithmetic mean	Geometric Mean	Min. – Max.	Geometric Mean	Geometric Mean	Geometric Mean	Geometric Mean	Geometric Mean	Geometric Mean	Geometric Mean
Al	3736±3889	2589	8-34715	952 (1143)*	567	865	1227	370	5925	1864
Fe	3397±5050	2262	279-55274	724 (891)*	407	787	790	320	3865	1365
Mn	75±83	49.3	4-527	16.7 (19.9)*	7.9	15.7	17	11	65	25.6
Ni	9.6±7.5	7.4	0.6-58.6	-	-	-	2	2.8	6.6	7.64
Co	1.89±2.4	1.1	n.d. – 1.89	-	-	-	0.38	-	2.1	0.94
Cu	10.4±7.9	7.95	n.d.-44	5.9 (7.4) *	8.9	5.7	2.6	6.2	4.5	5.53
Pb	12.9±12	9.8	0.7-111	24.9 (27.4)	21.5	34.2	4.3	58	6.9	8.46
Zn	38.6±30.5	31.9	5-344	22.4 (27.4)*	15.9	-	10	41	16	5.37
Cd	0.17±0.12	0.12	n.d.-0.7	0.22 (0.24) *	0.17	0.24	0.045	0.36	0.12	0.06
Mo	0.36±0.26	0.28	n.d. -1.8	-	-	-	-	-	-	-
V	23.7±19.5	14.7	n.d – 145	-	-	-	6.3	-	15	-

(*) Geometric means for air masses derived from the SW (i.e. Saharan events). See Kocak et al., (2004) for further details.

For those elements whose average anthropogenic contributions are in excess of 80% (see section 5.3.2., for further information) of their total concentrations (i.e. Cd, Pb and Zn) the following trends were apparent;

(i) Cd detected over the Arabian Sea (Chester et al., 1991) was around 30% of that determined in the current study, which in turn was consistently lower than the observed concentrations in both the Eastern and Western Mediterranean marine atmospheres (0.12 ng m^{-3} compared to $0.17\text{-}0.24 \text{ ng m}^{-3}$ and 0.36 ng m^{-3} respectively). The comparatively lower values observed in the Arabian Sea being explained by the more remote marine character of the sampling location to that of the RSMA which itself is likely to be less influenced by long range transported Cd from industrial activities occurring in eastern European nations, accounting for the elevated values in the Eastern and Western Mediterranean atmospheres.

(ii) Pb also exhibits similar regional trends, again being due to the comparative lower influence of long range transport anthropic material and the lack of regional intense industrial activities,

(iii) Zn, however was elevated in the RSMA being the highest at any of the considered sites, indication of regional Zn inputs. Zinc deposits in Saudi Arabia are widespread, although zinc is mainly produced as a by product of gold mining. The local market has a significant demand for zinc (estimated to be 27,706 tonnes in 2003). The majority of zinc occurrences in Saudi Arabia are hosted by low-grade volcanosedimentary rocks in the neoproterozoic volcanic-arc terrain of the Arabian Shield (Saudi Geology Survey; web page within references). A substantial belt lies to the N / NE of Jeddah in the Samran field, where Zn bearing minerals are processed. Enhanced aerosol Zn levels might, therefore be due to one or more of the following (i) the extraction and (ii) processing activities as well

as (iii) enriched crustal material being present in the region. This will be investigated further when we consider the trace metal characteristics for contrasting air masses. Co and Ni concentrations have not been quoted for the Levantine Basin of the Eastern Mediterranean, so only a limited comparison with the literature may be made to sites within the influence of the arid regions, however Ni seems to be in excess to that which is detected along the Western Mediterranean coast (Chester et al., 1993; Guieu et al., 1997) and is around 3 x higher than those determined in the Arabian Sea, a consistent enhancement factor as observed for the other elements. Cu was found in concentrations consistent with those determined at other coastal sites, even though recent mining for Cu has taken place, indicating little or no impact on region aerosol concentration as a result of this activity. For V there is very little comparative data (Arabian Sea and ANET). The current range of values are in excess of that observed in Arabian sea. The V concentrations are also well in excess of those observed in Western European marine aerosols (i.e. the Plymouth coastal and semi-urban aerosol being 2.1 ng m^{-3} ; Liverpool and Preston aerosol concentrations being 7.7 and 7.3 ng m^{-3} respectively, see Table 4.5). Owing to the occurrence of regional crude oil refining, then it is possible that enhanced RSMA concentrations are as a result of these activities. The enhanced V concentrations observed in the NW of England (compared to that of the Plymouth aerosol) were also attributed to local crude oil refining (see section 4.3.2).

5.3.2 Evaluation of the Jeddah aerosol trace metal sources; Application of the crustal enrichment factor (EF_{crust})

To gain an indication of the sources contributing to the elemental aerosol concentrations of the RSMA, the EF_{crust} were calculated (Chester et al., 1993; Chester et al., 1994b; Herut et al., 2001) as discussed in section 4.3.3 to indicate the degree of crustal source influence. Table 5.3 presents the EF_{crust} for the RSMA and for comparative marine aerosols.

Table 5.3. A comparison of the EF_{crust} (calculated using $(E/Al)_{\text{crust}}$ ratios from Taylor 1964) for the RSMA with those determined at other marine systems

Element	RSMA *			% non-crustal	Southern Levantine	Arabian Sea	Western Mediterranean	Atlantic North East
	current study			elemental aerosol	Basin	(Chester et al.,	(Chester et al., 1999)	Trades
	Arithmetic mean	Geometric Mean	Min. – Max.	Geometric Mean	(Herut et al., 2001)	1991)		(Chester et al., 1991)
Fe	1.4±0.9(1.7±1.1)	1.3(1.6)	0.6-10.6(0.8-13.4)	19±20(33±20)	2.3	1.0	1.2	1.1
Mn	1.9±1.5(2.5±1.9)	1.6(2.1)	0.2-12.7(0.2-17)	31±27(43±38)	2.4	1.4	2.9	1.0
Ni	3.8±2.4(4.9±3.1)	3.2(4.1)	0.4-14.7(0.5-19)	63±23(71±18)	-	2.3	10	0.73
Co	2.1±1.9(2.1±1.9)	1.8(2.1)	0.-12.0(0-12)	33±30(34±30)	-	2.1	2.3	0.9
Cu	5.0±5.1(12.7±10.1)	4.5(9.4)	0.1-32.4(0.2-68)	70±21(85±32)	21	7.2	27	1.3
Pb	38.1±56.2(31±45)	25(20.5)	3.8-524(3-428)	94±5(93±5)	159	27	1129	7.4
Zn	19.3±16.4(20±17)	14.6(15.2)	1.8-10.1(1.9-105)	99±7(91±7)	117	18	167	3.1
Cd	29.1±27.4(55±52)	20.1(38)	0.3-176(0.5-336)	91±13(95±15)	228	18	-	3.2
Mo	8.1±8.2(10.5±5.8)	6.0(7.7)	0.5-74(0.6-96)	77±20(83±14)	-	-	-	-
V	5.4±4.3(7.2±5.8)	3.5(4.7)	0.1-32.6(0-46)	68±19(76±19)	-	-	-	1.3

* Values in brackets represent the EF_{crust} and % non-crustal elemental aerosol contribution values calculated using element /Al ratios from Wedpohl (1995)

Table 5.3 also highlights the non-crustal contribution as a % of the total elemental concentrations. These were calculated in the same manner as Herut et al., (2001) which have been described previously in section 4.3.4.

With the consideration of the EF_{crust} values for the current study, the E_f is increasing in the following order $Fe < Mn < Co < Ni < V < Cu < Mo$ and all are classed as being “non-enriched” elements, i.e. they all have $EF_{\text{crust}} < 10$, using the tradition definition. As shown in the literature (e.g. Murphy, 1985; Chester et al., 1999; Herut et al., 2001; Kocak et al., 2005) Fe, Mn, Co are generally shown to be “non-enriched” in most marine atmospheres, whereas Cu may exhibit both anomalously enriched behavior (Western Mediterranean, Chester et al., 1999; Atlantic Westerlies, Murphy, 1985) as well non-enriched behavior, as observed for the current study and in other crustal rich populations (i.e. ATNET, Murphy, 1985).

The rest of the elements, Zn, Cd and Pb are all classed as anomalously enriched elements, which indicate their non-crustal origins. Comparison with the literature the EF_{crust} values for the RSMA are all higher than those found in the North Atlantic aerosol (see Table 5.3) but equivalent to those observed for the Arabian Sea (Chester et al., 1991), indicating the same general chemical character of the aerosol population except that the RSMA has a higher loading of aerosol material which is not surprising owing to the relative locations of the two sampling sites. The RSMA EF_{crust} are generally lower than those observed for both the Western and Eastern Mediterranean aerosol (Chester et al., 1999; Herut et al., 2001). Lower EF_{crust} than those in the Mediterranean aerosol would be expected, owing to lower proximity of the RSMA to anthropic activities as well as lower intensity regional anthropic sources (except for Zn; see earlier) and more importantly a higher contribution to the aerosol population of crustal material (~3-6x), leading to ‘dilution’ effect on the anthropogenically derived material.

When we consider the elemental % non-crustal contributions it is interesting to note that elements with EF_{crust} lower than 10 still have, in some cases, a predicated predominating non-crustal source (i.e. >50% contributions). This was also the case for the Plymouth aerosol as well (see section 4.3.4). Table 5.3 also compares the EF_{crust} and % non-crustal contributions calculated using more recent elemental:Al ratios suggested by Weddhpohl (1995). Generally, values for each element were slightly greater, again illustrating that caution should prevail during the use of the EF_{crust} value. However the same general conclusions would have been derived in terms of elemental classification with the use of the Weddhpohl (1995) elemental:Al ratios. To gain a better appreciation of the representative nature of the global elemental ratios there is an urgent need to compile elemental ratios of the local and region crustal material to enable a more accurate definition of the EF_{crust} to be made and hence a more representative calculation of the contributions of sources to the aerosol trace metal pool. This approach has recently been adopted by Kocak et al., (2007), who used the composition of a Saharan dust end-member to define the appropriate crustal elemental / Al ratios to be used in the calculation for the EF_{crust} . Unfortunately such information is currently not available for the crustal precursor material for the RSMA.

5.4 Temporal variations in the trace metal concentration in the RSMA

The temporal variability in the RSMA of all trace metal concentrations are highlighted in Figures 5.1-5.3. Sample number 1 represents the commencement of the sampling regime (i.e. 8th August 2002) whereas the final presented sample number (370) represents the termination of sampling activities (i.e. 11th January 2004). The current section will define and explain the temporal variability in the RSMA (Jeddah) trace metal concentrations over the whole period (from 8th August 2002 to 11th January 2004). As was discussed in section 4.3.5 it is normally the case that aerosol trace metal concentrations exhibits very large temporal variability, this was the case for the Plymouth marine aerosol as well as those

observed in other marine aerosol populations. The RSMA is no exception. Figures 5.1-5.3 clearly highlight the high temporal variability exhibited by the RSMA. Seasonality in the aerosol trace metal concentration was investigated by categorising the data set into two populations; summer and winter. The summer period being classed as that covering the months from early April to August whereas the winter covers the months from September to early February (Tanaka and Chiba 2006). Referring to Figures 5.1-5.3, sample number from 100 to 309 represent the samples collected during the summer period, whereas sample numbers 56-99 and 310-370 represent the winter period. The statistical summary of the two populations is presented on Table 5.4. To evaluate any statistically significant differences between the two seasons, the Mann-Whitney test (the equivalent non-parametric t-test) at the 95% confidence limits was applied, owing to the log-normal distribution characteristics of the two populations. From this test, statistical differences were detected for all elements between the two defined sampling periods, except for Co.

Comparison of the elevated concentrations during the summer with those encountered during the winter clearly illustrates the effect of seasonal processes such that the elemental enhancement ranged from 1.3 (Mo) to 3.1 (V).

The predominantly crustally derived trace metals (Al, Mn and Fe: % non-crustal source contribution amounted <50%, see section 5.3.2) exhibited concentrations during the summer period (June-July) which were consistently around 2x (Table 5.4) those observed during the winter season. Such elevated concentrations may be explained by enhanced dust movement in the Nubian desert (covering several potential source areas from central Egypt to central Sudan (Engelstaedter et al., 2006) and local sources (i.e. Arabian Peninsula) which have been shown to exhibit a summer peak in dust events (AWS/FM-100/009, 1980).

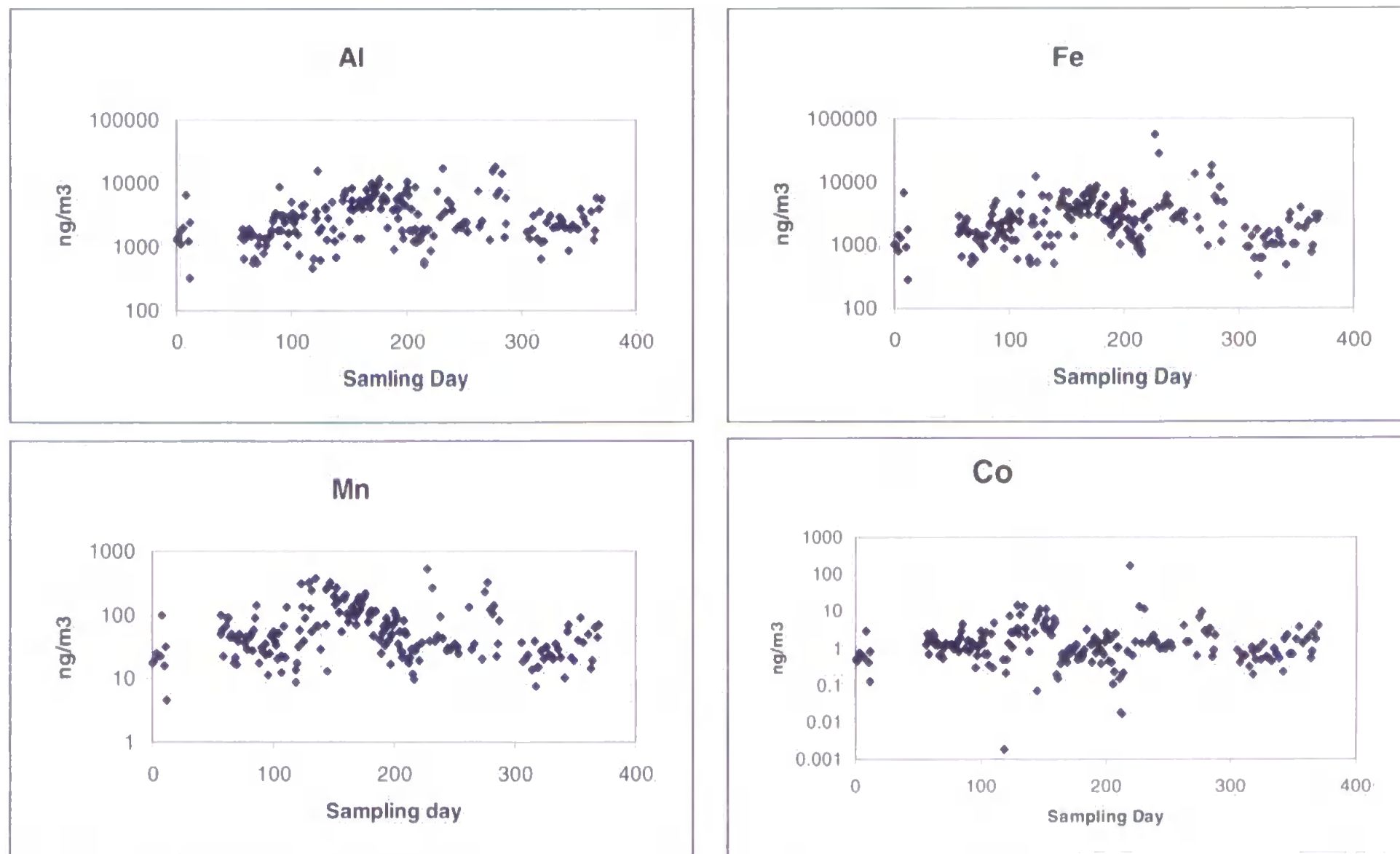


Figure 5.1 Temporal variability of (a) Al (b) Fe (c) Mn and (d) Co concentrations (log10) in the Red Sea marine aerosol. All the above elements have $EF_{crust} < 2$

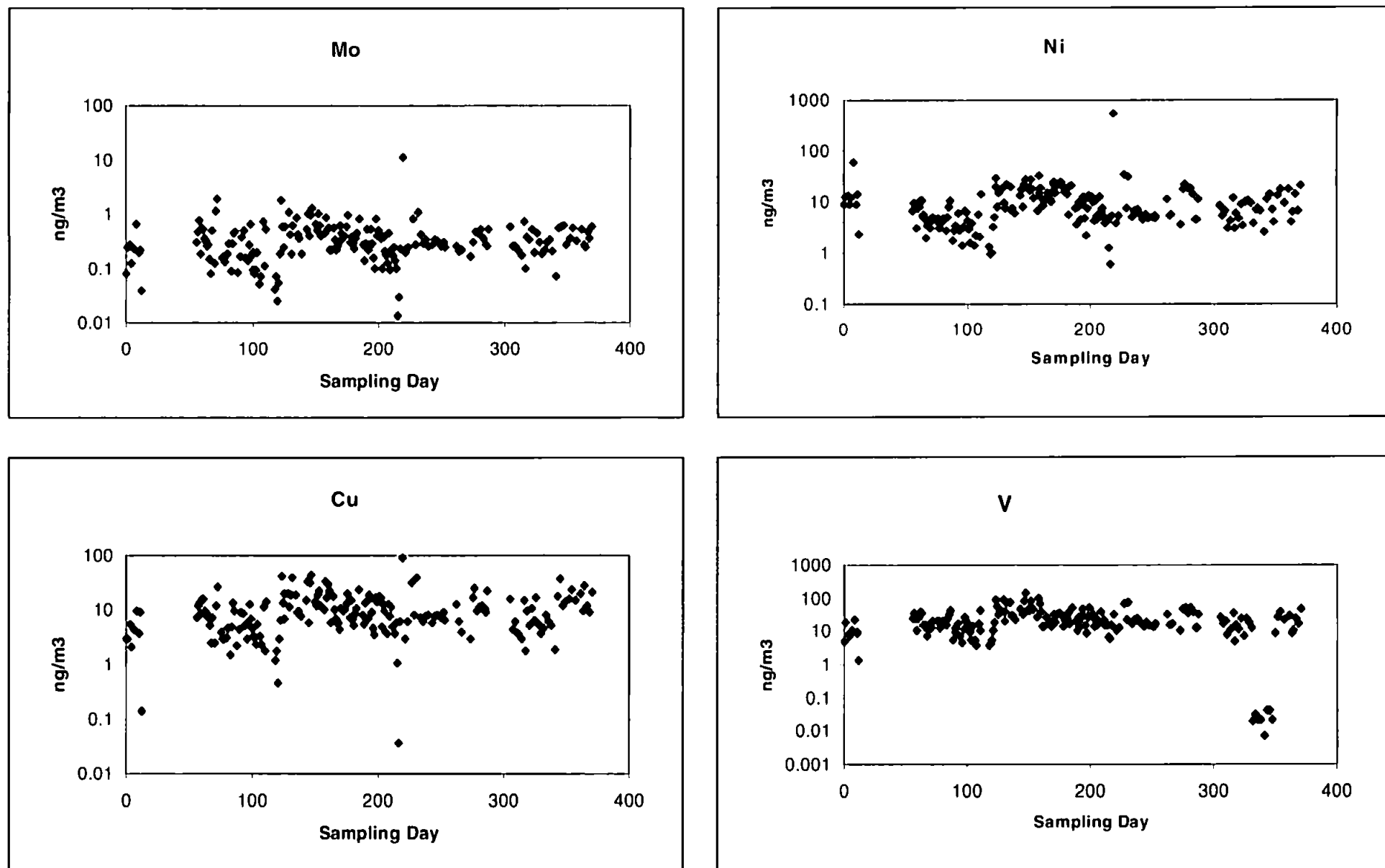


Figure 5.2 Temporal variability of (a) Ni (b) Cu (c) Mo and (d) V concentrations (log₁₀) in the Red Sea marine aerosol. All the above elements have EF_{crust} values between 3 and 6

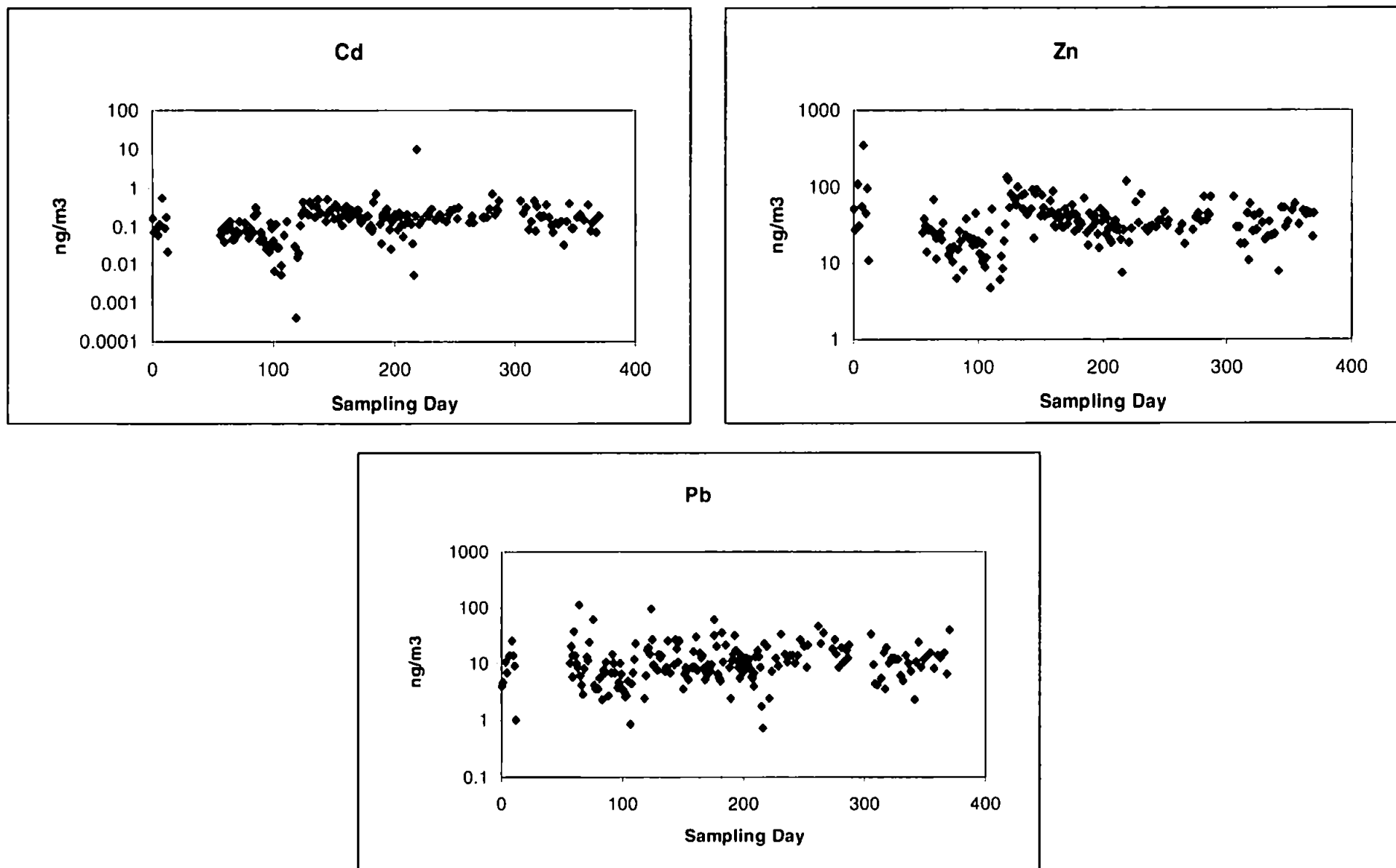


Figure 5.3 Temporal variability of (a) Pb (b) Zn and (c) Cd concentrations (log10) in the Red Sea marine aerosol. All the above elements have EF_{crust} values between 14 and 25

Table 5.4. Geometric mean aerosol trace metal concentrations (expressed as ng m⁻³ except for Al, Fe and Mn expressed as µg m⁻³) in the RSMA for winter and summer period.

Element	Winter	Summer	Summer/Winter
Al	1.7	3.57	2.1
Fe	1.47	3.15	1.9
Mn	0.04	0.07	1.8
Ni	5.23	8.96	1.7
Co	1.04	1.17	1.1
Cu	6.66	9.11	1.4
Pb	8.5	11.8	1.4
Zn	24.2	37.8	1.6
Cd	0.08	0.18	2.3
Mo	0.24	0.31	1.3
V	7.9	24.4	3.1

The Nubian desert sources are mostly active in the summer between April and August with the highest values of the Total Ozone Mapping Spectrometer Aerosol Index (TOMS AI) at the eastern Sudanese coast in June-July (See figure 5.4; Engelstaedter et al., 2006). This is clearly highlighted when the monthly mean TOMS AI (X10) between 1980-1992 are considered (Engelstaedter et al., 2006). The TOMS was a detection system onboard the Nimbus 7 polar-orbiting satellite which was active from November 1978 to May 1993. The TOMS was designed to provide global estimates of total column ozone using backscattered UV radiance measured in six bands. Aerosol measurements were made in the three longest wavelengths where gaseous absorption is weak and where the backscattered radiation is primarily controlled by scattering from aerosol and clouds (Prospero et al., 2002).

Peak activity and dust re-suspension in the Arabian Peninsula occurs during June-July (refer to Figure 5.5). Haboobs (dust activity) are often a product of strong convective outflow, which occur as the ITZC (Intertropical Convergence Zone; a zone of trade wind

convergence) and migrates north over the summer months (Fett, 1983). A hot and dry southerly wind (identified as an, Aziab) transports dust from southern Saudi Arabia northward this is most common in the spring when soil conditions are very dry (Walters, 1988).

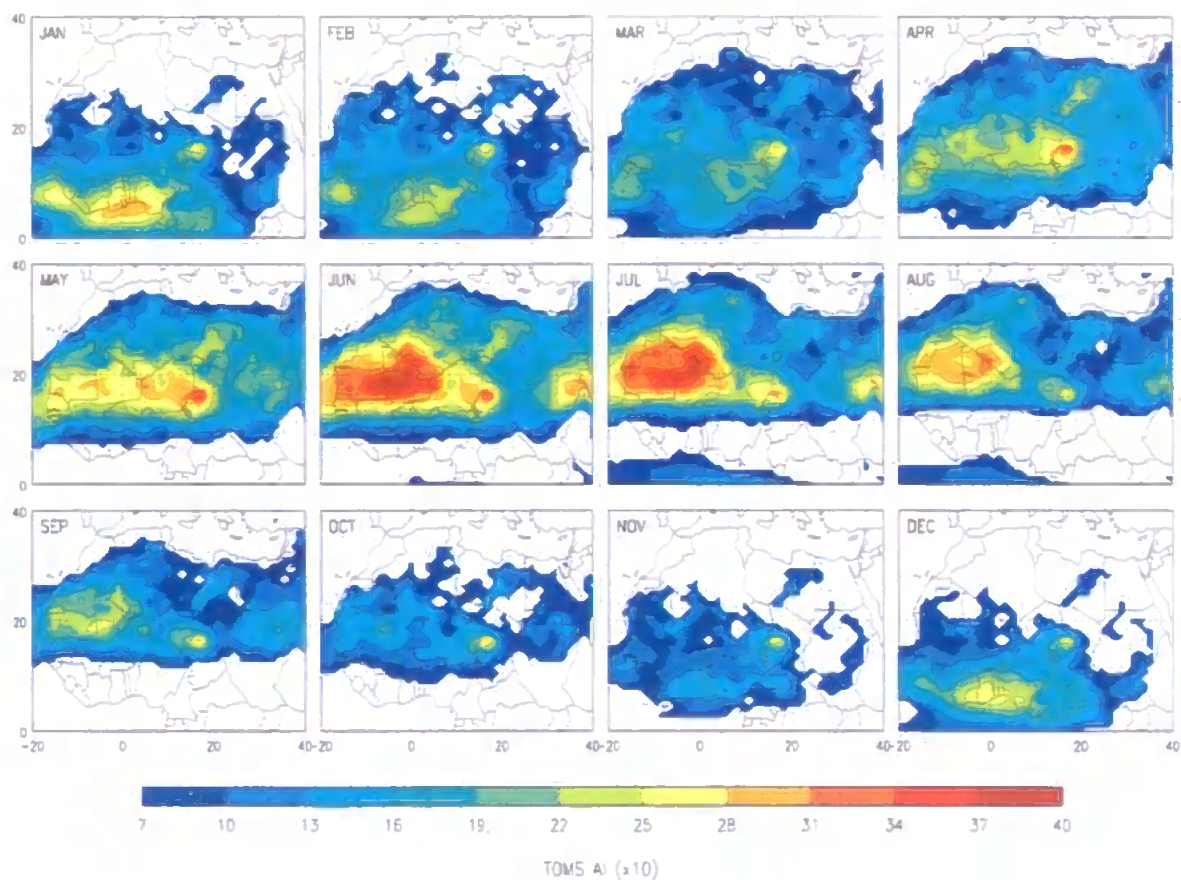


Figure 5.4. Monthly mean TOMS AI ($\times 10$) (1980–1992). After Engelstaedter et al., (2006).

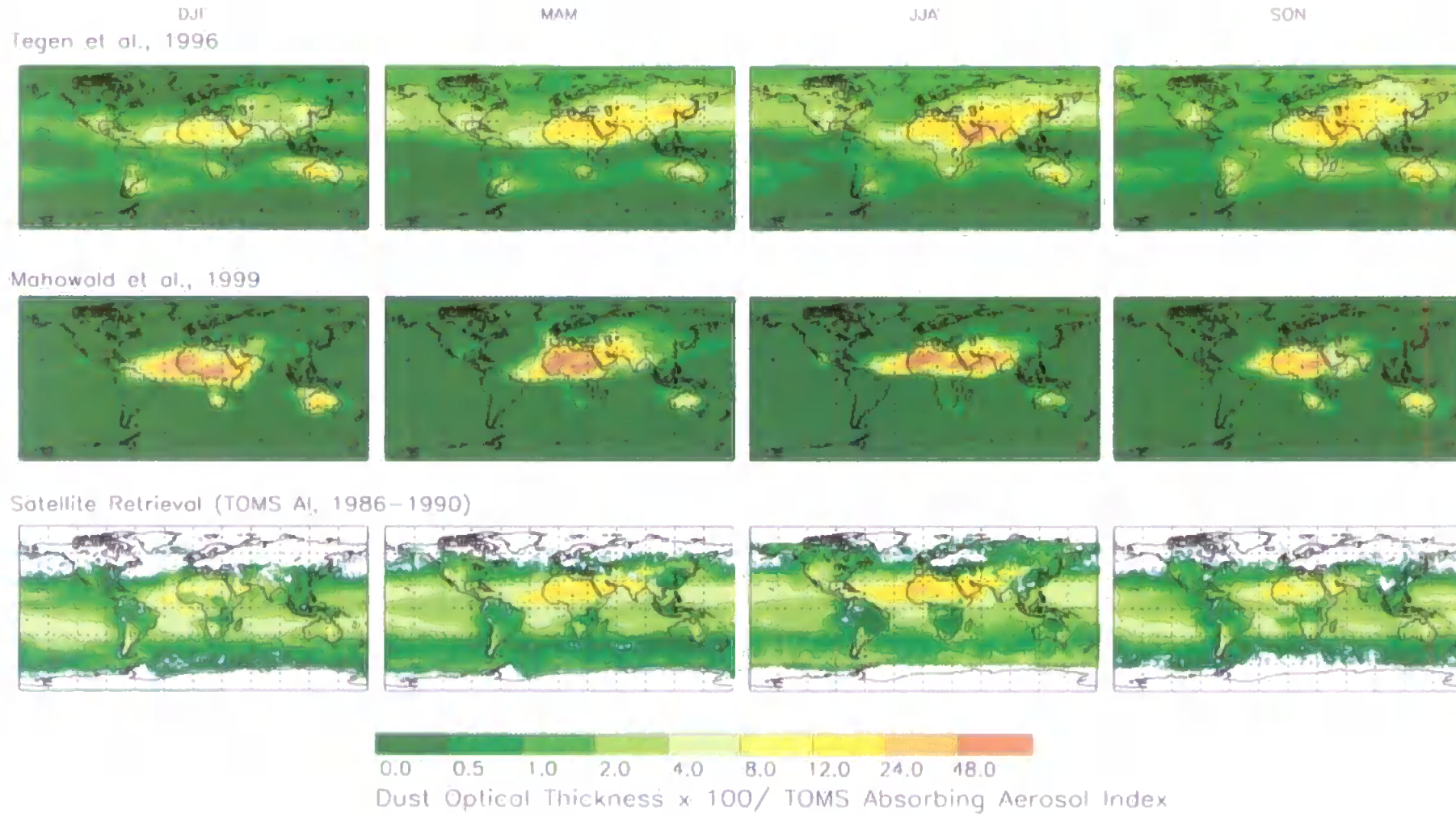


Figure 5.5. Comparison of seasonal of dust (Tegen et al., 1996 and Mahowald et al., 1999) and remotely sensed absorbing Aerosol Index from the Total Ozone Mapping Spectrometer (TOMS AI) average of 5 years (1986-1990).

Therefore the well documented seasonal dust transport in the region would explain the enhanced concentrations for Al, Fe and Mn in the Summer period. Hence it is also possible that elements which have a significant crustal contribution will also exhibit a seasonal difference in their concentrations as a result of this process. Of those elements presented in Table 5.3, Ni, Mo, Cu and V have significant crustal contributions (i.e. > 20%). Whether the crustal contribution is significant enough to lead to a seasonal variation in these elemental summer and winter concentrations could be tested by calculating (i) the theoretical elemental crustal component and (ii) the equivalent anthropogenic component contribution for each sample in the two seasonal populations, and then determining whether each of the two elemental sources for each element exhibit a statistically significant seasonal difference. This was carried out for Ni, Mo, V and Cu.

The two source contributions made to each aerosol sample elemental concentration was calculated using the following equations:

$$\text{Elemental crustal contribution (EF}_{\text{crust}}) = (C_{\text{Alp}}) * (C_{\text{xc}} / C_{\text{Alc}}) \quad (5.1)$$

$$\text{Elemental anthropic contribution (E}_{\text{anthrop.}}) = C_{\text{xp}} - [(C_{\text{Alp}}) * (C_{\text{xc}} / C_{\text{Alc}})] \quad (5.2)$$

where (C_{xp} and C_{Alp}) are the concentrations of a trace metal x and Al, respectively, in the individual aerosol samples, and (C_{xc} and C_{Alc}) are their comparable concentrations in average crustal material (Taylor, 1964).

The above calculation was made for all individual samples and each fraction was tested for any statistically significant seasonal differences. Of those considered V and Ni exhibited seasonal differences between the summer and winter for both their anthropogenic and crustal fractions (Mann-Whitney test; 95 % confidence level). Therefore, for these two

elements the seasonal difference is not only attributed to enhanced summer dust transport within the region, but also as a result of enhanced summer anthropogenic emissions. This might be as a result of greater fossil fuel burning in the summer to meet the demands of enhanced power requirements. There is a large seasonal variation in the regional electricity production due to the huge consumption during the hot summer season (the NEEP National Energy Efficiency Program web page within references). Power generation plants in Saudi Arabia use different types of fuel for the electricity generation; (i) diesel (ii) diesel + gas (iii) gas, the more common plants being types (i) and (ii) (electricity company web page within references). Vanadium emissions are also associated with crude oil refining. Therefore the enhanced seasonal power generation may not be the only explanation for the observed seasonal variability. Crude oil refining will also lead to V atmospheric emissions associated with the breakdown of porphyrin complexes in the crude oil. These emissions may, if emitted in sufficient quantities, enrich the local terrestrial environment. Clearly where you have then natural seasonal re-suspension of crustal material then any associated contaminants would also be re-suspended. Therefore it is possible that the seasonality might be, in part, as a result of natural crustal re-suspension which has historically been enriched from regional anthropic V emissions. One way this might be investigated would be to determine the V/Al ratio in local and regional desert dusts and then compare these with natural background ratios. As Ni is also known to be associated with crude oil refining and fossil fuel burning the seasonal variations in the $Ni_{anthrop}$ concentrations may also be as a result of the processes described above (e.g. Singh et al., 2002).

In contrast, the Mo and Cu anthropogenic contributions exhibited no difference between summer and winter whereas crustal contributions, as expected, did. Therefore, it is more likely that crustal movement and transport accounts for the seasonal variation for these elements, rather than non-crustal anthropogenic sources.

The exhibited seasonality in their concentration may be attributed to the seasonal variation in dust activity as a result of mobilisation of mine waste containing remnants of Zn ore. As discussed in section 5.3.1 the regional mining of Zn is well documented (Poldervaart 1955, 1956) and may explain the generally higher Zn aerosol concentration in the region.

As Pb and Cd are primarily derived from anthropogenic source, it might be conclude that contrasting seasonal anthropogenic emission influence the RSMA. However, as their concentrations are comparatively low, the observed variability in their concentrations is likely to be influenced by more distant anthropic sources. No difference in winter and summer for both Pb and Cd aerosol concentrations were detected in the South and Northern Levantine region of the Eastern Mediterranean, a potential source region of the Pb/Cd to the Red Sea atmosphere (Koçak et. al., 2004). However, for both these basins enhancement in Pb and Cd were detected during Saharan dust events (concentrations were corrected to take into account crustal material contribution). It was speculated that this enhancement during such events was due to the following:

- (i) association and transport by high dust concentration and/or
- (ii) contamination from land based anthropogenic sources in the South and South-eastern region of the Mediterranean Basin (i.e. Egypt) where a seasonal variation has been detected (Ali et. al., 1986; Hassanien et. al., 2001).

It is possible that mineral dust might act as a transport mechanism for anthropogenically derived material. Uptake of pollutants by mineral dust has been shown to occur at several locations around the world, including pollutants originated in European sources detected on Saharan dust (Formenti et. al., 2001; Falkovich et. al., 2004).

5.5 Impact of air mass source on the aerosol trace metal concentrations in the RSMA

Previous studies have classified aerosol samples into contrasting air mass types, influencing a sampling site, in order to investigate the impact of different regional sources on aerosol trace metal concentrations (Yaaqub et. al., 1991; Spokes et al., 2001; Kocak et al., 2004). This was also carried out for the Plymouth coastal and semi-urban aerosol as highlighted in section 4.3.6. For the current study four air mass types were defined. For the RSMA these were (i) Egyptian (E), (ii) Northern Saudi Arabia (NSA), (iii) Southern + middle Saudi Arabia (SSA) and (iv) Red Sea (RS), (Figure 5.6).

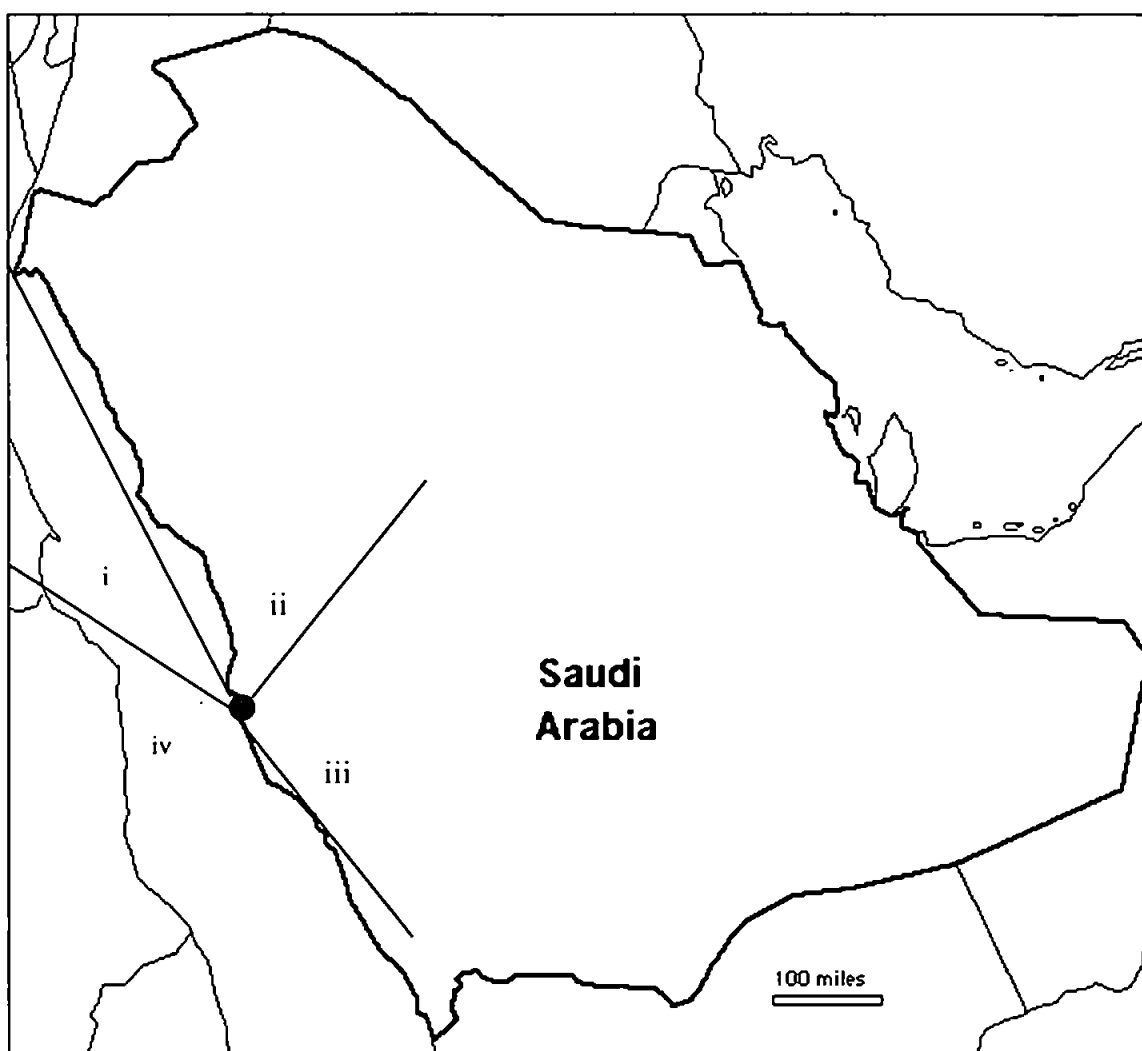


Figure 5.6. Air mass sectors of (i) Egyptian (E) (ii), Northern Saudi Arabia (N) (iii), Southern + middle Saudi Arabia (SSA) (iv) and Red Sea (RS).

However the categorisation of individual air mass types during the period for each individual collected sample was challenging. Owing to the narrow width of the Red Sea, the majority of air masses which had travelled over the Red Sea would have been influenced, to differing degrees, by terrestrial inputs. Therefore, the Red Sea population was defined as those samples whose air mass trajectories had not passed over any continental regions during the defined trajectories history (3 days). Where air mass trajectories for the same sample could be categorized into >1 sector owing to contrasting back trajectories at different pressure levels, allocation into an air mass sector was determined on the ground level air mass trajectory. Table 5.5 highlights the proportions of the total sample population allocated into each of the defined air mass categories.

Table 5.5. The % influence of each air mass back trajectory category during the sampling period.

Egypt	Northern Saudi Arabia	Middle and Southern Saudi Arabia	Red Sea	Unclassified
38 (43)	21 (24)	19 (21)	11 (12)	11

*Values in % in brackets did not include the “unclassified” air masses .

Table 5.5 clearly highlights the strong influence of both air masses derived from Egypt and those from the Northern areas of the Jeddah sampling site, amounting to around 50% of the air mass influence compared with only 19% from the southern and middle regions of Saudi Arabia.

Following from the air mass trajectory classification, the respective aerosol elemental concentrations for each sector were calculated and a statistical summary is presented on Table 5.6.

To investigate any statistical significant differences between air mass sectors the aerosol trace metal concentrations observed in each sector was compared with each of the other defined sectors and a Mann Whitney test was applied, at the 95% confidence level. If we refer to Table 5.6 it is apparent that inter-air mass sector aerosol elemental concentrations can be very significant. This is particularly the case for those elements for which the % crustal contributions are in excess of 50%, i.e. Al, Fe, Mn and Co. For all these elements the concentrations are greatest in the air masses derived from the Middle and Southern Saudi Arabian (SSA) regions, whereas the lowest concentrations are detected in air masses from the Red Sea (RS) region, the ratio of SSA: RS concentrations for Al, Fe, and Mn being 3.4, 2.0, and 2.8 respectively. Considering the statistical differences between the four air mass sectors, it was clear that in the Red sea aerosol Al, Fe, Mn and Co concentrations were all statistically the lowest ($p < 0.05$), compared to all the other sectors. For Al, Fe and Mn, SSA concentrations were statistically higher than those observed in the N air mass sector, but not between the N and E air mass sectors.

The above observations are logical in that the aerosol population loadings associated with the Red Sea air sector are likely to be lower, in contrast to those associated with the other sectors, as the aerosol material would have been subject to progressive dry deposition over the marine surface, with minimal terrestrial inputs of these elements, for at least 72 hours prior to their transport to the sampling location. Whereas aerosol populations associated with the other sectors are all influenced to a lesser or greater degree by crustal inputs, with those associated with the SSA sector receiving the greatest quantity of crustal material, the concentrations being significantly larger ($p < 0.05$) than those for the N as well as those of the RS.

Table 5.7 summarises these findings with statistically significant differences being highlighted with an “*”.

Table 5.7. Summary of statistical differences between air sector elemental aerosol concentrations. Differences are highlighted with an “*”. (SSA = Middle and Southern Saudi Arabia; N= Northern Saudi Arabia; E= Egyptian ; RS= Red Sea).

Al	Fe	Mn	V
SSA vs E	SSA vs E	SSA vs E	SSA vs E
SSA vs N*	SSA vs N*	SSA vs N*	SSA vs N*
SSA vs RS*	SSA vs RS*	SSA vs RS*	SSA vs RS*
N vs E	N vs E	N vs E	N vs E
N vs RS*	N vs RS	N vs RS*	N vs RS*
E vs RS*	E vs RS*	E vs RS*	E vs RS*
Co	Ni	Cu	Zn
SSA vs E	SSA vs E*	SSA vs E*	SSA vs E
SSA vs N	SSA vs N*	SSA vs N	SSA vs N
SSA vs RS*	SSA vs RS*	SSA vs RS*	SSA vs RS*
N vs E	N vs E	N vs E	N vs E
N vs RS*	N vs RS*	N vs RS*	N vs RS*
E vs RS*	E vs RS*	E vs RS*	E vs RS*
Mo	Cd	Pb	
SSA vs E*	SSA vs E	SSA vs E	
SSA vs N	SSA vs N	SSA vs N*	
SSA vs RS*	SSA vs RS	SSA vs RS*	
N vs E	N vs E	N vs E	
N vs RS*	N vs RS	N vs RS	
E vs RS*	E vs RS*	E vs RS*	

Zn and Co exhibit a similar trend in their concentration in the following order: SSA, N and E having no significant differences, but all are significantly greater than those observed in the RS aerosol. The fact that there are no differences between the SSA, N and E air sectors can generally be explained by the influence of more local / regional sources rather than distant sources, such that air mass source becomes progressively less significant in influencing elemental aerosol concentrations. In the section 5.3.1 it was suggested that the regionally elevated aerosol Zn concentrations may be attributed to the Samran mineral belt (Moore 1975) and from the mineral mining to the N E region of the sampling site, in particular the Mahd adh Dhahab region. Zinc is currently extracted from the Mahd adh Dhahab gold mine as a by-product concentrate (amounting to about 3,000 t Zn per year).

This is further suggested as the Zn EF_{crust} (N=16.7; E=13; SSA=11.2) for the N sector which is the highest of all sector other than the RS.

V exhibited a similar trend in air sector concentrations to the crustal dominated elements. This is likely owing to the significant crustal contribution (~30%) made to the total V concentrations. However it is important to evaluate any differences in the air mass sector concentrations of the concentrations of V_{anthrop} (as calculated by equation 5.1). This was carried out, producing geometric mean concentrations of V_{anthrop} of 13.7 ng m^{-3} ; 14.5 ng m^{-3} ; 19.8 ng m^{-3} and 10.5 ng m^{-3} respectively for the four air mass sectors E, N, SSA, and RS. What was of interest was that there were no statistical differences between the air sectors V_{anthrop} concentrations in the E, N and SSA but all of these sectors were significantly greater than the V_{anthrop} concentration in the RS sector. This confirms that the observed difference in total aerosol V concentrations between the air sectors SSA and N was a result of the greater crustal contribution made to the SSA aerosol population. In the previous section seasonality in both vanadium anthropic and crustal aerosol concentration contributions were detected, with the variation in the anthropic contributions being attributed to either enhanced burning of fossil fuels in the summer period and / or enrichment of surface soils as a result of crude oil refining. As both activities lie to the north, south and east of the sampling site determination of the specific sources would be difficult and hence would likely lead to little regional air sector differences in concentrations as illustrated by the trends in the $V_{\text{anthropic}}$ concentrations.

Cu concentrations indicated that E, N and SSA sectors were significantly greater compared with the RS population, with the SSA population also being greater than the E sector but not the N sector. When the Cu_{anthrop} concentrations were calculated for all section E and RS sectors were no longer different, indicating that the background aerosol $Cu_{\text{anthropic}}$ concentrations were the same. However the SSA population $Cu_{\text{anthropic}}$ concentrations were

still significantly greater than those in both the N and E sectors, indicating a clear $Cu_{anthropic}$ source from the Middle to south of Saudi Arabia.

Ni total concentrations exhibited significant differences in all air sectors, except between N and E, in the following order $SSA > N = E > RS$, such that SSA had the highest Ni concentrations which is a characteristic behaviour of the crustally derived elements. Calculation of the $Ni_{anthropic}$ and assessment of the air mass sectors differences, showed that the only change to that as presented on Table 5.7 was that the $Ni_{anthropic}$ concentrations between the E and RS sectors were not significantly different, indicating that regional anthropic sources located to the north, east and south of the sampling site were enhancing the background $Ni_{anthropic}$ concentrations influencing the E and RS air sectors.

Cd exhibits similar concentrations in all wind sectors except between the RS, however, the only significant difference is between the E and RS wind sector. This is most likely explained by long range transport of material from the North, i.e. Eastern Mediterranean regions. This is also supported by the comparative data on Table 5.2, highlighting the lower Cd concentrations in the RSMA compared with those observed in the Eastern Mediterranean (Southern and Northern Mediterranean). Therefore it would appear that there is little influence of regional sources on the Cd aerosol concentrations.

Pb, as with the majority of the elements, exhibited lowest concentrations in the RS sector (6.10 ng m^{-3}) and highest in the SSA (13.2 ng m^{-3}), the difference being statistically significant. Although Pb concentrations in the N sector were lower than those of SSA and E (statistically significant for SSA) a higher EF_{crust} (28; compared to 23.6 for both the E and SSA sectors) was calculated, which is indicative of additional noncrustal sources. The enhanced Pb concentrations in the SSA may have been accounted for by the higher crustal

influence of the aerosol population. This was investigated by calculating the $Pb_{anthrop}$ concentrations for each of the sectors. These amounted to 9.4, 9.2, 12.8, and 6.9 $ng\ m^{-3}$ for air sectors E, N, SSA and RS respectively. The trends in air mass sector differences for the total Pb were unaltered (except that there was no significant difference between air sectors E and RS) for $Pb_{anthrop}$ concentrations, indicating that the enhanced SSA Pb concentrations were not as a result of enhanced crustal contributions and therefore anthropic /sources lie to the east and south of the sampling site. As highlighted in an earlier section there lies to the south of the sampling site the industrial area of Jeddah which might explain the enhanced Pb concentrations. As there were no differences between RS, E and N for $Pb_{anthrop}$ concentrations it would further suggest that there exists a background Pb concentration which is perturbed by anthropic sources only to the east and south of the sampling site.

5.5.1 Seasonality of aerosol trace metal concentration associated with different air masses.

The seasonality of the aerosol traces metal concentrations were considered for each of the four defined air sectors. Table 5.8 states whether there are any statistical differences between summer and winter aerosol elemental concentrations for the different wind sectors. What is striking is the similarity in seasonality for all air mass sectors, other than the Red Sea sector, with summer concentrations being greater, for the majority of elements, than those observed in the winter. However, for Cu and Pb there was no seasonal difference for the SSA air sector which would imply regular rates of emissions from sources influencing this sector which are not influenced by seasonal dust remobilisation, further supporting a local distinct anthropogenic emission source influence. It was also apparent from the last section that Cu and Pb aerosol concentrations in the SSA air sector were statistically greater than those in the Egyptian and northern sectors respectively. Aerosol samples derived from the Red Sea sector exhibited no difference in their summer/winter

concentrations except for Fe. The lack of seasonality in the trace metals concentration of the Red Sea population might be as a result of the manner in which the Red Sea air mass populations were defined (i.e. air masses that had resided for at least 3 days over the Red Sea exclusively). During this defined time (3 days) it is possible that aerosol particle size distribution would change as aerosol associated trace metals which associated with the large particle size fraction (crustal material) may have undergone deposition lowering their concentration in the air mass which led to no significant different in seasonal variations for this aerosol population.

Table 5.8. Summary of statistical differences (at 95 % confidence level) between summer and winter trace metals aerosol concentration dataset for the four defined air mass sectors (Y= statistical differences; N= no statistical differences).

Element	Egypt	N	SSA	RS
Al	Y	Y	Y	N
Mn	Y	Y	Y	N
Fe	Y	Y	Y	Y
V	Y	Y	Y	N
Co	N	N	N	N
Ni	Y	Y	Y	N
Cu	Y	Y	N	N
Zn	Y	Y	Y	N
Mo	Y	N	Y	N
Cd	Y	Y	Y	N
Pb	Y	Y	N	N

5.6 Inter-elemental relationships within the RSMA

A statistically significant correlation between different elements will give an indication of common processes (source origins, factors affecting concentration during transportation, i.e. wet and dry deposition as well as aerosol chemical processes) that affect elemental concentrations in an aerosol population. A Pearson's correlation test has been used (using the statistical package Minitab) to investigate any relationships between elements. The p value indicates the statistical significance of the correlation i.e. for a p value < 0.05 a statistical significance at the 95% confidence level is indicated. Since the aerosol trace

metals exhibited log-normal distributions, correlation coefficients between the trace elements were determined after taking their logarithms. The total sample dataset and the categorised samples from different back trajectories (1-Egypt 2-North Saudi 3-South and middle of Saudi) were tested. The results are presented in Table 5.9. It is important, as has been mentioned in section 4.4, to bear in mind that this test should be taken as a first approximation and not as absolute indication of causes/effects between the two variables (but as a tool to aid in data interpretation). The complete sample population correlation coefficient matrix is presented in Table 5.9a. The correlation coefficients with * represent non-statistically significant relationships.

Table 5.9 Pearson correlation coefficients between log transformed aerosols trace metal concentrations in the RSMA. *indicates a non-significant Person's correlation (at $p < 0.05$; 95% confidence level).

(a) All aerosol samples

	Al	Mn	Fe	V	Co	Ni	Cu	Zn	Mo	Cd
Mn	0.700									
Fe	0.819	0.840								
V	0.338	0.511	0.438							
Co	0.413	0.676	0.560	0.370						
Ni	0.594	0.739	0.648	0.382	0.623					
Cu	0.501	0.691	0.572	0.354	0.653	0.758				
Zn	0.404	0.587	0.456	0.358	0.509	0.782	0.749			
Mo	0.472	0.640	0.538	0.349	0.641	0.795	0.853	0.716		
Cd	0.346	0.448	0.403	0.308	0.494	0.724	0.643	0.697	0.654	
Pb	0.347	0.382	0.402	0.265	0.241	0.481	0.591	0.583	0.547	0.525

(b) Egypt

	Al	Mn	Fe	V	Co	Ni	Cu	Zn	Mo	Cd
Mn	0.742									
Fe	0.921	0.780								
V	0.597	0.886	0.614							
Co	0.548	0.755	0.608	0.688						
Ni	0.653	0.868	0.648	0.940	0.644					
Cu	0.502	0.755	0.537	0.839	0.629	0.873				
Zn	0.320	0.613	0.340	0.774	0.453	0.796	0.841			
Mo	0.433	0.676	0.457	0.812	0.572	0.810	0.864	0.789		
Cd	0.292	0.498	0.320	0.675	0.508	0.731	0.669	0.757	0.685	
Pb	0.169*	0.138*	0.240	0.281	0.036*	0.329	0.316	0.543	0.336	0.487

(C) North Saudi Arabian

	Al	Mn	Fe	V	Co	Ni	Cu	Zn	Mo	Cd
Mn	0.708									
Fe	0.914	0.886								
V	0.346	0.489	0.392							
Co	0.264*	0.636	0.461	0.417						
Ni	0.712	0.872	0.793	0.385	0.515					
Cu	0.481	0.623	0.609	0.398	0.584	0.664				
Zn	0.510	0.628	0.558	0.440	0.537	0.785	0.803			
Mo	0.456	0.588	0.569	0.411	0.626	0.603	0.808	0.692		
Cd	0.566	0.608	0.552	0.402	0.308*	0.802	0.542	0.691	0.439	
Pb	0.560	0.559	0.580	0.427	0.417	0.596	0.812	0.751	0.656	0.511

(d) South and Middle of Saudi Arabian

	Al	Mn	Fe	V	Co	Ni	Cu	Zn	Mo	Cd
Mn	0.598									
Fe	0.859	0.804								
V	0.402	0.614	0.662							
Co	0.039*	0.605	0.196*	0.368						
Ni	0.709	0.837	0.762	0.506	0.469					
Cu	0.214*	0.543	0.279*	0.441	0.715	0.586				
Zn	0.412	0.644	0.419	0.354	0.648	0.747	0.890			
Mo	0.406	0.669	0.511	0.393	0.660	0.674	0.838	0.796		
Cd	0.416	0.159	0.427	0.275	0.056	0.353	0.368	0.427	0.484	
Pb	0.251	0.292	0.306	0.358	0.300	0.339	0.467	0.342	0.539	0.368

(e) Red Sea

	Al	Mn	Fe	V	Co	Ni	Cu	Zn	Mo	Cd
Mn	0.330*									
Fe	0.452	0.741								
V	0.447	0.868	0.612							
Co	0.158*	0.613	0.499	0.364*						
Ni	0.309*	0.800	0.565	0.877	0.391*					
Cu	0.164*	0.619	0.447	0.590	0.292*	0.838				
Zn	0.040*	0.463	0.303*	0.531	0.098*	0.726	0.716			
Mo	0.189*	0.661	0.516	0.697	0.492	0.879	0.751	0.609		
Cd	0.044*	0.506	0.375*	0.584	0.237*	0.810	0.847	0.691	0.760	
Pb	-0.049*	0.264	0.030*	0.415*	0.029*	0.530	0.596	0.459	0.516	0.693

Trace elemental aerosol concentrations for the whole dataset are significantly correlated (Table 5.9a) highlighting the dominance of the crustal source influence on trace metal aerosol concentrations in this region. Similar findings for the Egyptian and Northern Saudi sample sets were observed. With the exception for Co and Cd in the North Saudi trajectory

samples as Co is not correlated significantly with Al and Cd is not correlated significantly with Co. However, Pb did not have a statistically significant correlation with both Al and Mn in the Egyptian sample set whereas in the North Saudi Arabian sample set Pb is significantly correlated with Al, Mn and Fe. It has been stated in section 5.3.1 that Pb is, to a certain extent, affected by long-range transport and exhibits a seasonal variability in its concentration (with higher concentrations in the summer than the winter, section 5.4) which is similar to that for Al and Fe. Seasonality in the Pb concentration is unlikely to be as a result of a higher input of the crustal material in the summer owing to its dominant anthropogenic source. However, this seasonality in the Egyptian sample set could be due to the fact that during winter in the potential source area (North Eastern Europe) aerosol Pb concentrations may be lower in the atmosphere owing to rain and snow scavenging, Ali and Bacso (1994). Moreover, a seasonal variation in Pb concentration in Egypt (with higher Pb concentrations in summer compared to those in winter) has been reported by Ali and Bacso (1994). However, Hassanien et al., (2001) have reported a contradictory behaviour for Pb as the concentration of Pb in winter is higher than that observed in the summer owing to temperature inversions occurring in the Egyptian atmosphere, mainly around Cairo, entrapping pollutants in the local atmosphere. This could result in a lower long range transport flux in the winter from Egypt compared to that during the summer, possibly explaining the seasonally enhanced Pb concentration observed in the Egyptian air sector at Jeddah during the summer period.

In the North Saudi Arabian air mass sector sample seasonality in Pb concentrations seemed to be affected by the mineral dust input as the Pb concentration co-varies with the concentration of crustally derived elements (i.e. Al and Fe). Therefore seasonality in this sample set could be due to:

- (i) anthropogenic input (e.g. suspended of contaminated Pb soil)

(ii) interaction of anthropogenic Pb aerosol with Saharan dust (impact on dust surface) rather than anthropogenic source inputs.

However, for the samples associated with the Middle and Southern Saudi origin Al, Fe and Mn exhibit significant co-variance whereas Co, Cu, Cd and Pb do not co-vary with any crustally derived elements. This would indicate that Pb, Cd, Co and Cu have unique sources to the south of Jeddah, most likely arising from the southern industrial area of Jeddah and associated anthropogenic activities.

For the Red Sea aerosol population, as expected, the crustal source was not the dominate source. This is illustrated by the insignificant relation between crustally derived elements and Al, in contrast with the other air sectors (e.g. SSA) where crustally derived elements had a high correlation with Al as shown earlier in this section. However, Ni and Mn have the most prominent correlation which co-varies significantly with all elements except Al (along with Co which do not co-varies significantly with Ni).

5.7 The elemental solid state speciation of the RSMA

The statistical summary of the elemental solid state speciation signal is presented in Table 5.10. In addition, the elemental solid state speciation signals are compared in Table 5.11 with those determined from other aerosol populations, including those from the Plymouth aerosol described in Chapter 4.

Al and Fe are associated predominantly with the residual fraction (Stage 2), amounting to on average $94 \pm 3.1\%$ and $97 \pm 1.6\%$ for Al and Fe, respectively. Compared with the Plymouth aerosol population the contribution to the total speciation of the exchangeable fraction was lower, being 0.3 % for both elements compared to 1.5 % and 2.2 % for Al and Fe respectively.

Table 5.10 Summary of the elemental aerosol solid state speciation in the RSMA

Element	Stage 1		Stage 2		Stage 3	
	% (S.D.)	Range	% (S.D.)	Range	% (S.D.)	Range
Al	0.3 (0.28)	<0.1-1.4	6.0(2.9)	1.9-16.8	93.7 (3.1)	82.3-97.7
Co	43.2 (28.7)	<1 -97	33.6 (29.3)	<1-87	23.2 (16.3)	2.5-59.8
Fe	0.3 (0.3)	<0.1-1.6	3.2 (1.4)	0.9-6.4	96.5 (1.6)	91.9-99.0
Mn	62.7 (11.6)	35.9-89.5	29.5 (12.8)	<1-62.3	7.8 (6.8)	0.5-22.5
Pb	36.0 (15.6)	13.6-82.5	59.2 (16.8)	<1- 85.7	4.8 (5.9)	<1-23.8
Zn	53.5 (13.4)	22-73.7	31.3 (12.2)	<1-64.9	15.7 (12.4)	9.2-52.9

It was also clear that the contribution to the oxide/carbonate phase for Fe was much lower (3.2%) than that observed at Plymouth (42%). This is most likely due to the lower anthropogenic and correspondingly higher crustal contributions to the RSMA, leading to the lower potential for inter-aerosol interactions during atmospheric transport when evaporation/condensation cycles occur, such as those suggested by Spokes et. al, (1994). During these cycles the pH of the surface micro-layer of the aerosol particulates may experience a significant decrease which may re-distribute the Fe to a more soluble solid phase (i.e. stage 3 to stages 1 and /or 2; stage 2 to stage 1) in a similar manner to that previously discussed by Spokes et al., (1994). These observations are consistent when we compare the speciation signal for Al and Fe in the two “end-member” aerosols, Saharan dust and LUAP. Both speciation signals of Al and Fe for Saharan dust and LUAP are similar to those observed in the RSMA and Plymouth aerosol samples respectively.

For Pb and Zn, as would be expected, there are lower associations with the exchangeable fraction in the RSMA compared with that in the Plymouth aerosol population and indeed compared with most anthropogenically influenced aerosol populations (Table 5.11). What is surprising is that for the RSMA, the oxide and carbonate phases appear to be much more important than the residual phase, in comparison with the Plymouth coastal and semi-urban

aerosol. This is further illustrated on Figure 5.7 where the elemental solid state speciation signals are presented and compared graphically between a Saharan dust end-member (Chester *et al.*, 1989) and the RSMA samples. However, for both Zn and Pb the speciation signal is similar to that observed in the Eastern Mediterranean aerosol which is also strongly influenced by crustal inputs.

Table 5.11. Comparison of the elemental solid state speciation determined in European and Saharan influenced aerosol populations (expressed as a % of the total)

Element and Stages	RSMA ¹	Saharn ²	Eastern Med. ³	Western Med ⁴	LUAP ⁵	Plymouth Aerosol ⁶
Al-S1	0.3	0.05±0.015	2.4±1.8	4.3±2.5	5.6±4.8	1.5
Al-S2	6.0	14.4±2	3.6±2.2	4.2±1	12.1±5.8	15.4
Al-S3	93.7	85.6±2	94.0±2.5	91.5±2.4	82.3±7.2	84.2
Fe-S1	0.3	0.03±0.003	1.7±1.2	8.3±8.1	9.9±6.2	2.2
Fe-S2	3.2	9.5±2	4.9±3.3	0.3±8.1	31.9±11.8	41.8
Fe-S3	96.5	90.5±2	93.4±3.9	91.4±8.1	58.2±12.2	55.9
Mn-S1	62.7	22.8±1.1	43.5±10.0	63.3±7	44.2±13.2	66.2
Mn-S2	29.5	34.2±2.6	13.4±8.4	nd	22.7±12.3	3.3
Mn-S3	7.8	43±2.7	43.5±5.8	36.7±7	33.1±13.7	30.5
Zn-S1	53.5	0.2±0.35	51.1±18.4	82±6.8	77.9±9.8	-
Zn-S2	31.3	8.4±3.7	26.7±6.6	0.5±1.6	8.8±6.1	-
Zn-S3	15.7	91.4±3.8	22.2±16.1	17.5±6.5	13.2±8.6	-
Pb-S1	36	5.7±5.1	72.0±20.0	97±3.5	81.5±6.9	80.8
Pb-S2	59.2	28.8±5.7	22.0±14.8	nd	11.1±6.7	2
Pb-S3	4.8	65.5±6.2	6.0±7.0	2.7±3.4	7.4±4	17.3

¹ Current study; ²Chester *et al.*, (1989). ³Kocak *et al.*, (2007); ⁴Nimmo (unpublished); ⁵Chester *et al.*, (1989); LUAP= Liverpool urban particulate material; ⁶Current study

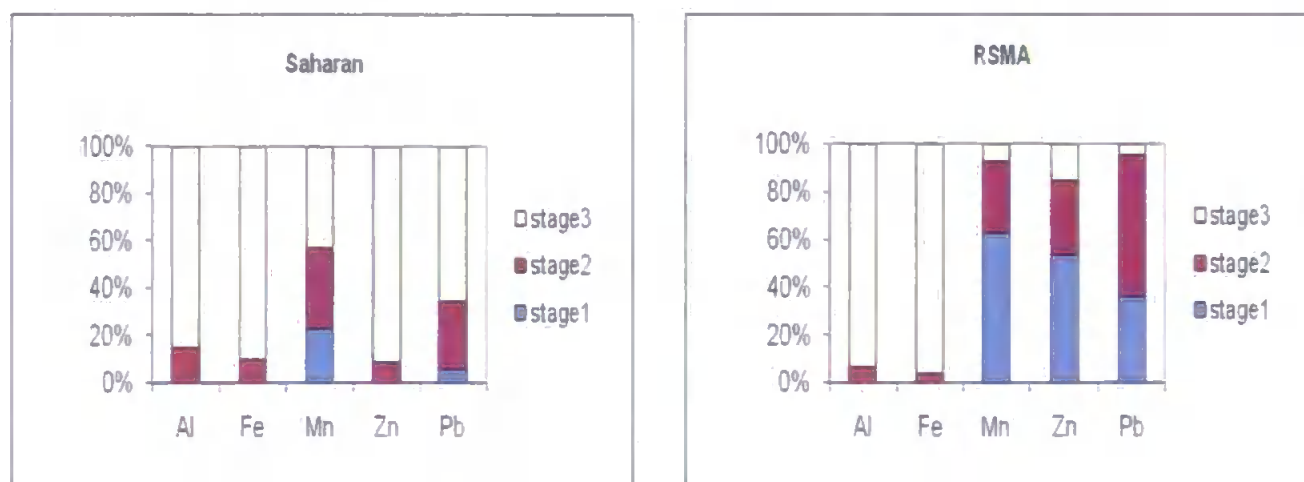


Figure 5.7 Comparison of the elemental solid state speciation signal for the RSMA population and that of the Saharan aerosol end member population (Chester *et al.*, 1989).

For the former, the exchangeable phase associated metal may be mobilised into the particle surface aqueous film and may subsequently re-adsorb on to adsorptive sites on the aerosol particle surfaces (such as oxide surfaces, mineral lattices) or form complexes of lower solubility in the aqueous film. Mechanisms of re-adsorption on the surface of aerosol material (which happened during the transport of dust in the atmosphere) which include dissolution of elements followed by condensation and finally re-adsorption (see Spokes et. al., 1994) are more likely with interactions of anthropogenic material with increasing crustal material due to the increase of the reaction area. Such a similar solid phase shift for Pb has been recorded by Chester et al., (1995). It is also clear that there is a strong negative relationship ($r=-0.937$) between % stages 1 and 2 which would further support the phase transfer of Pb during atmospheric transport.

As has already been stated Zn is enriched in the RSMA, hence the chemical character of the local source material might have had an influence on the solid state speciation of the aerosol Zn. The majority of zinc occurrences in Saudi Arabia are hosted by low-grade volcanosedimentary rocks in the Arabian Shield. However, along the Red Sea coast, Zn also occurs in sandstone and carbonate minerals, as well as sphalerite occurrences in carbonate intersects in deep boreholes east of the Arabian shield (Saudi Geological Survey; web page within references) which might explain the importance of the carbonate phase for Zn. In addition Zn might be associated with the iron sulphide in sphalerite minerals being released in stage 2 during the sequential leach procedure. However no significant relationship ($r=0.205$) was detected between stage 2 of Zn and Fe, suggesting this is not an important mechanism / source.

Manganese appears to be distributed between the three stages (see Table 4.20 and Table 5.9) with stage one dominating in aerosol populations affected by the anthropogenic

contributions (LUAP) and to a lesser extent samples affected by crustal input (Eastern Mediterranean) where it is distributed between the three stages in the Saharan aerosol.

Two possible explanations for the Pb speciation signal might be considered; (i) as Pb could have undergone significant long range transport aerosol from the North, chemical modifications may have taken place during transport, liberating a higher proportion of Pb from the exchangeable phase and / or (ii) a contribution of local crustal material containing higher carbonate minerals.

However, in the RSMA the third stage has a low percentage (ca. 8 %). Co is distributed between the three stages with a comparatively low third stage percentage (23%) compared with a typically higher percentage in the literature.

5.8 Atmospheric dry deposition of trace metal to the Red Sea

The dry deposition of aerosol associated trace metal is usually calculated using the equation presented in section 4.6, i.e.

$$F = (C \times V_d \times T) \times 10^{-4}$$

Where F is the dry depositional flux ($\text{ng cm}^{-2} \text{ yr}^{-1}$), V_d is the elemental aerosol settling velocity (m s^{-1}) and C is the geometric trace metal aerosol concentrations (expressed as ng m^{-3}), preferably taken from a large data base of sample collection spanning at least an annual period and T is the number of seconds per year. The major limitation of such a calculation, as emphasised in section 4.6, is the chosen value for the elemental V_d which is being influenced by the aerosol particle size, humidity and wind speed. Therefore this component of the calculation is more open to error. Duce et al. (1990) suggested the application of a V_d of 1 cm s^{-1} for elements associated predominantly with crustally derived material, whereas for those associated with anthropic derived material, a settling velocity of 0.1 cm s^{-1} would be more suitable. Table 4.23, in Chapter 4, highlights the range of V_d 's that have been used in the literature for contrasting European coastal

systems. Kocak et al., (2005), recently calculated a size weighted settling velocity using two stage size fractionated aerosol data for the metals Al, Fe, Mn, Cu, Zn and Pb yielding V_d of 1.73, 1.73, 1.43, 1.1, 1.11 and 0.8 cm s^{-1} respectively for the Eastern Mediterranean atmosphere. It is clear that the allocated values for metals such as Zn and Pb are significantly larger (0.8 - 1.1 cm s^{-1}) than those suggested by Duce et al., (i.e. 0.1 cm s^{-1}) and other literature values (Flament 1985; Ottley and Harrison, 1993; Injuk et al., 1998; Rojas et al., 1998; see Table 4.23). V_d for the anthropically derived elements being lowest in the North Sea atmosphere, compared with the Western and Eastern Mediterranean atmosphere. The higher elemental V_d values calculated for the Eastern Mediterranean atmosphere (Kocak et al., 2005), for the traditionally anthropogenically derived elements are likely to be due to (i) a more significant crustal (i.e. comparative lower EF_{crust} values) contribution made to the aerosol concentrations of the trace metals owing to a greater influence of the surrounding arid land masses (ii) crustal particles acting as a surface on which adsorption of finer anthropic derived particles may take place, via impaction during atmospheric transport, which would lead to a greater observed settling velocities than that predicted or modelled owing to co-deposition. This is supported by the recent work by Falkovich et al., (2004) who observed the interaction of mineral dust originating from the Sahara with semi-volatile organic compounds (along Israel's coastal plain), and identified as specific tracers for urban air pollution. This would suggest that dusts may provide surfaces for uptake of anthropogenic material, which would then lead to potential chemical interactions and modifications during transport of the combined aerosol material. Unfortunately, for the current study, no size fractionated aerosol sampling was carried out, so an approximation of the elemental settling velocities in a similar manner to that carried out by Kocak et al., (2005) and Spokes et al., (2001) could not be carried out. However, given the RSMA elemental concentrations and corresponding EF_{crust} , it is clear that the RSMA is more strongly influenced by crustal sources and hence the aerosol population is likely to have a larger size particle spectrum than other reported aerosol populations.

Therefore for the current study, owing to the lack of local V_d 's, those recently calculated for the Eastern Mediterranean aerosol, (Kocak et al., 2005) were considered to be the most representative literature values for the RSMA, although if in error they are likely to be an underestimation. For those elements for which V_d wasn't calculated by Kocak et al., (2005) for the Eastern Mediterranean atmosphere (i.e. Ni, Co, Mo, V, Cd) using their EF_{crust} (Table 5.3), a V_d was allocated to them based on a comparison with the EF_{crust} of those elements which had an allocated Kocak et al., (2005) V_d . Therefore, the following V_d 's were allocated ; Co-1.48 cm s⁻¹; Ni, V and Mo were all allocated a V_d of 1.1 cm s⁻¹; and Cd was allocated a V_d of 0.1 cm s⁻¹, whilst Pb was given a V_d of 0.8 cm s⁻¹.

Chester et al., (1991) defined the elemental V_d for the Arabian Sea marine aerosol, based on their EF_{crust} and MMD (mass medium diameter). Therefore, elements which (i) had $EF_{crust} < 10$ with a MMD $> 2.5\mu m$ were allocated a V_d of 1.5cm s⁻¹ (Al, Fe, Mn, Ni, Co Cr, V and Cu) and (ii) had an $EF_{crust} > 10$ and a MMD $< 0.55\mu m$ were allocated a V_d (Zn, Pb, and Cd) of 0.5 cm s⁻¹. Hence for the current study we used comparatively higher V_d 's for Al, Fe, Zn and Pb, but a similar value for Mn and a lower value for Cu.

These were then used, along with the elemental geometric aerosol concentrations for each of the air mass sectors (Table 5.6) and the appropriate temporal weightings (Table 5.5), to take into account the temporal contribution made by each of the air mass sectors during the course of the collection period. This allowed the calculation of the air mass weighted total elemental dry deposition fluxes to the Red Sea, expressed as $\mu g m^{-2} yr^{-1}$ ($mg m^{-2} yr^{-1}$ for Al, Fe and Mn). These are presented on Table 5.12 and compared with a selection of elemental total dry deposition fluxes presented in the literature for other coastal regions. Two sets of data are presented for the Red Sea; those calculated as described above and those using the overall aerosol trace metal concentrations (Table 5.2), instead of the air mass sector weighted concentrations. It is clear that very little difference is observed in the

dry depositional fluxes calculated by the two different approaches (< 3 % for Al, Fe, Ni, Co, Cu, Pb, Zn, Cd, Mo and around 5 % difference for Mn and V).

Clearly, as we have seen for the aerosol concentrations, the total dry deposition fluxes for the crustally derived elements (Al, Fe, Mn, and Co) increased in the following order; North Sea < Western Mediterranean < Eastern Mediterranean (Northern Levantine basin) < Eastern Mediterranean (Southern Levantine basin) < RSMA. This is not unexpected as the trends represent the progressive greater geographical influence of arid land masses on marine aerosol populations and hence the progressively increased re-suspension of crustal material into the atmosphere.

Comparing the total dry depositional fluxes of the predominantly anthropogenically derived elements between sites is a little more challenging owing to the differences in the applied V_d 's in the flux calculations. Lower V_d 's were adopted for Western Mediterranean aerosol dry deposition fluxes (typically 0.1 cm s^{-1}), which were probably underestimates of the real V_d 's. What we can be reasonably sure of is that the dry depositional fluxes in the RSMA for these elements are (i) lower than those calculated for the two Levantine basins of the Eastern Mediterranean for Pb, (ii) comparable for Cd and (iii) enhanced in the RSMA for Zn (as the same settling velocities were adopted for both these studies).

Table 5.12 also highlights the total deposition of trace metals to the Arabian Sea, calculated by Chester et al., (1991). These figures include an estimate for wet deposition as well as dry depositional fluxes. In addition, different V_d 's were adopted (see above). However, comparing the two sets of fluxes would indicate that for Al, Fe, Mn, Cu, Ni and Co the fluxes are around twice as great for the RSMA. This clearly is due to the less remote location of the RSMA sampling site compared with that adopted by Chester et al., (1991). Of the remaining metals Zn had the highest ratio of Arabian : RSMA fluxes, being

4.5, most likely as a result of the Zn enriched region around the Eastern Red Sea coastline, whereas for Cd, the ratio was 0.5, indicative of a progressively lower transport of Cd to the Arabian Sea from the Northern industrialised nations.

However, it is clear that the greatest uncertainty in dry depositional fluxes is the choice of the elemental V_d . For the RSMA we have assumed a similar rate of deposition as that for the Eastern Mediterranean, a crustally influenced aerosol. However it is likely that owing to the RSMA being more dominated by crustal contributions it is likely that the real V_d 's are greater. Therefore there is an urgent need to define the V_d 's at this location by (i) the collection of size fractionated aerosol samples (using cascade impactor samplers) enabling the size fraction spectrum of the aerosol population to be defined and (ii) collection in parallel of dry deposition samples.

Recently dry deposition estimates have been carried out at sites in and around Jeddah by El-Sayed et al., (2004), during 2002 and 2003. The dust was collected in intervals using surrogate samples, followed by the weighing of collected dust and its acid total digestion (HNO_3 / HF) followed by spectroscopic analysis of the acid digests for a suite of trace elements. The average annual dry depositional fluxes observed for this study are presented in Table 5.12. The ranges presented on Table 5.12 represent the lowest and highest annual mean dry depositional fluxes. Typically the lowest depositional fluxes were associated with a site located to the North of Jeddah – not far from the current sampling site, whereas the highest fluxes were generally observed at the sampling site located in the southern area of Jeddah. Given the likely errors associated with such a calculation the current agreement would suggest that an acceptable choice of settling velocities was made. However, Cd dry deposition fluxes for the current study were lower than the range calculated by El-Sayed (2004) which would suggest that the adopted settling velocity for Cd for the current study maybe too small.

5.8.1 Atmospheric trace metal total dry and “bioavailable” inputs into the Red Sea

The total dry deposition input (tons yr⁻¹) of trace metals to the Red Sea may be calculated using the dry depositional fluxes presented in Table 5.6, along with the known surface area of the Red Sea (438 – 450 x 10³ km²) using the following equation;

$$\text{Total dry atmospheric inputs (tons yr}^{-1}\text{)} = \text{dry deposition flux (mg m}^{-2}\text{ yr}^{-1} * 1/1,000) \text{ (air mass weighted) } \times \text{surface area (km}^2\text{)}$$

The total dry elemental atmospheric inputs are presented on Table 5.13 and the order of increasing inputs are as follows; Cd < Mo < Co < Pb = Ni < Cu < V < Zn < Mn < Fe < Al.

Section 5.4 highlighted the seasonal differences between the trace elemental concentrations. The concentrations for the different seasons were then used to calculate the inputs for each metal for each of the two seasons. Al, Fe, Cd and V had > 60 % of their total annual inputs (Al and Fe 61 %; Cd – 61 % and V – 68 %) occurring over the summer season, whereas the remaining elements, the inputs were equally split between the two seasons (Mn – 56 %; Ni – 55 %; Co – 45 %; Cu and Pb - 50 %; Zn – 52 %; Mo – 48 % for the summer).

This might sound surprising owing to the higher summer aerosol elemental concentrations, however it has to be remembered that in our definition the summer months lasted for five month whereas the remaining part of the year was classed as the winter period. Hence the seasonal inputs had to be weighted accordingly, lowering the relative importance of the enhanced summer concentration effect on the seasonal inputs of most of the trace metals.

Table 5.13. The atmospheric total dry inputs (tons yr⁻¹) of trace metals to the Red Sea. The “bioavailable” fraction is quoted in brackets for selected elements. (* after Koçak et. al., 2006; § Saharan samples carried out in this study).

Element	Minimun	Maximun
Al	630,000 (1890)	647,000 (1941)
Fe	533,000 (1559)	548,000 (1644)
Mn	10,200 (6426)	10,500 (6615)
Cu	1610 (579.6)*	1660 (597.6)*
Zn	4780 (2533)	4910 (1718)
Pb	1540 (554)	1580 (569)
Cd	13 (10.1)*	14 (10.9)*
Ni	1100 (66)§	1140 (68.4)§
Co	220 (95)	227 (98)
Mo	44	45
V	2360	2420

As with the atmospheric depositional budgets made for the English Channel (section 4.7), using the sequential leach data for the RSMA it is also possible to calculate the “bioavailable” fraction of the total atmospheric dry deposition by assuming that the “bioavailable” fraction is that which is associated with the “exchangeable” fraction as determined using the sequential leach approach. The “bioavailable” fraction of the total dry deposition input of Al, Fe, Mn, Co, Pb and Zn would therefore be 0.3 %, 0.3 %, 63 %, 36 % and 54 % respectively. The “bioavailable” dry depositional inputs are also presented on Table 5.13. The “bioavailable” or exchangeable fraction is an operational definition, and for the current study is based upon the first stage (ammonium acetate) of the sequential leach scheme (e.g. Chester et. al., 1989). However, different definitions have been reported in the literature, for example Turner et. al., (2001) used the Pepsin enzyme to quantify the “bioavailable” fraction in sediments. Other adopted approaches included those by Fernandez et al., (2002) and Voutsas and Samara, (2002), with the applied technique being

dependent upon the scientific context within which the data is to be applied. This has been the case more recently for various studies carried out to define the “solubility” of Fe associated with the marine aerosol (e.g. Chen and Siefert, 2003; Bonnet and Guieu, 2004; Hand et al., 2004; Desboeufs et al., 2005; Baker et al., 2006a, b), leading to non-comparable datasets. Therefore there is an urgent need to assess the relative efficiencies of the different extraction stages of these techniques to facilitate more informed comparisons. In addition, it is crucial to show how a metal’s aerosol solid state speciation relates to its actual seawater solubility. A limited number of previous studies have attempted to do this (Chester et al., 1993, 1994b) and these suggest that the exchangeable fraction represents an upper limit of their seawater solubilities.

5.9 Trace metal budget within the Red Sea

The Red Sea is a long narrow basin connected to the Indian Ocean (Arabian Sea) via the Strait of Bab Al-mandeb, it stretches from 30°N to 12.5 ° N (2000 km) with a typical width of 250 km (Morcos 1970) and average depth of 450 m (Degens and Ross, 1969) (see section 5.2.1 for more details) Figure 5.8 presents a simplified model of the trace metal fluxes in the Red Sea with exchange / transport depicted by arrows. From this study we have atmospheric input estimates which we will assume is the same for all the regions of the Red Sea surface. Red Sea water exchange with the Indian Ocean occurs through three layers (Bethoux, 1988), (i) incoming surface layer from the Gulf of Aden (ii) a seasonal sub-surface water which is incoming from July-September and out going from October-December and finally (iii) outgoing Red Sea Deep water. However, due to the lack of data of trace metal concentrations (particulate and dissolved) for the Red Sea a two layer model only will be considered in calculating the trace metal budget for the Red Sea. Generally, the circulation pattern in the Red Sea is as follows: the surface water moves toward the north, whilst travelling north the surface water loses buoyancy, mostly due to evaporation, leading to an increase in its density (Sofianos and William, 2003). The down-welling of the

Ideally, to calculate the trace metal budget within the Red Sea accurate data of water mass movement as well as reliable dissolved and particulate trace metal concentrations for representative water masses are required. In addition, estimates of trace metal sediment exchange between deep waters and the surface sediments are required, in addition to atmospheric inputs.

Dissolved trace metals concentrations used in the current study in surface seawaters have been adopted from Al-shiwafi et al., (2005) whereas deep water concentrations of dissolved trace metals has been adopted from Shridah et al., (2004). Al-shiwafi et al., (2005) carried out their study in the South of the Red (Yemen) whereas, Shridah et al., (2004) carried their study in the north of the Red Sea (Egypt). Shridah et al., (2004) collected seawater samples from the northern Red Sea and Gulf of Aqaba at different depths on board RV/METEOR cruise 44. They filtered each of the 2L seawater sample using a 0.45 μm nitrocellulose membrane filter. Filtrates were acidified with nitric acid to pH 2 and subsequently metals were pre-concentrated prior to analysis. Pre-concentration of the metals was carried out by complexation with ammonium pyrrolidine dithiocarbamate (APDC) and then extracted using methylisobutylketone (MIBK) and back extracted into an acidic aqueous solution. Atomic absorption spectroscopy was used to measure metal concentrations. A certified reference seawater (NASS-5) was used to monitor the quality of the analytical data. However, Al-shiwafi et al., (2005) measured trace metals in the southern Red Sea (cost of Yemen) the samples were collected in a pre-cleaned 2.5 L about 10 cm below seawater surface (to avoid floating materials) then the samples were filtered through 0.45 μm Millipore filters. Pre-concentration of the metals was carried out using a column of Chelex-100 resin. The metals were eluted using silica distilled 2 M HNO_3 followed by evaporation of the solution near dryness. Finally one mL of 6 M HNO_3 was added and the volume was made up to 25 mL using deionized water, followed by analysis using flame atomic absorption spectroscopy.

The filtration procedure used in these two studies involved the use of a 0.45 μm membrane filter, however particularly for soluble Fe, unless a pore size of $< 0.03 \mu\text{m}$ (Hurst and Bruland 2006) or $< 0.02 \mu\text{m}$ (Cullen et al., 2006) is used, the operational fraction $< 0.45\mu\text{m}$ will not only include dissolved Fe but also a colloidal fraction. This might explain the relatively high concentrations (23.9 nM) reported by Shridah et al., (2004). The ‘dissolved’ high Fe concentrations reported by Shridah et al., (2004) could also be due to sedimental release of reduced Fe followed by its complexation by organic ligands, enhancing its solubility above its inorganic solubility product ($\sim 0.7\text{nM}$; Hiemstra and van Riemsdijk, 2006) and release via the bacterial regeneration of falling biotic material.

Table 5.14 presents the detected dissolved concentrations ($\mu\text{g L}^{-1}$) of trace metal in deep and surface water and Table 5.15 highlights the water mass layer transport at Bab Al-mandeb. The influx, efflux ($\text{m}^3 \text{s}^{-1}$) and budget (t yr^{-1}) of trace metals at Bab Al-mandab have been calculated using the dataset in Tables 5.14 and 5.15 using the budget equations (see Appendix C).

To calculate the budget the following assumptions had to be made:

- (i) The concentration at the north Red Sea (deep layer) is equal to that in Southern Red Sea deep waters.
- (ii) The Red Sea is consistently of a two layer (surface and deep) system.

In addition, the limitations were as follows:

- (i) The lack of metal concentrations (dissolved and particulate) at Bab Al-Mandab (at different depths; surface, subsurface and bottom layer).
- (ii) Data for metal input from the sediment to benthic water layers were not available.

Table 5.14. Dissolved trace metal concentrations in surface and deep waters of the Red Sea, expressed as $\mu\text{g L}^{-1}$ (nM).

Elment	Surface layer Al-shiwafi et al., (2005)	Deep layer Shridah et al., (2003)
Fe	0.095 (1.7)	1.34 (23.9)
Cu	0.060 (0.95)	0.10 (1.58)
Mn	0.035 (0.64)	0.09 (1.64)
Co	0.665 (11.3)	0.12 (2.03)
Ni	0.075 (1.29)	0.09 (1.55)
Zn	0.047 (0.73)	0.17 (2.66)
Cd	0.950 (8.33)	0.33 (2.89)
Pb	0.070 (0.34)	0.27 (1.3)

Very few studies have been carried out to measure the water mass exchange at Bab Al-mandab (Vercelli, 1927; Siedler, 1968 and Maillard and Soliman, 1986). However, indirect measurements have been carried out (Patzert, 1974 and Bethoux, 1988) using ship's drift observations and atlas and hydrographic data at the straits. Patzert, (1974) used an evaporation rate of about 2.1 m yr^{-1} to estimate the annual mean surface transport to be $33 * 10^{-4} \text{ m}^3 \text{ s}^{-1}$. However, Bethoux (1988) used an evaporation rate of 2.4 m yr^{-1} and estimated the annual mean surface transport to be $38 * 10^{-4} \text{ m}^3 \text{ s}^{-1}$. The Bethoux (1988) layer transport at Bab Al-mandeb strait (Table 5.15) has been adapted for the calculation of the trace metal flux through the strait as it more recent than the estimates of Patzert, 1974. A summary of the water mass balance values presented in the literature are presented in Table 5.15.

Table 5.15. Literature estimates of the layer transport (surface, sub-surface and deep layer) at Bab Al-mandeb (inflow +, Outflow -, in $10^{-4} \text{ m}^3 \text{ s}^{-1}$).

Month	Flux ($10^4 \text{ m}^3 \text{ s}^{-1}$)	Vercelli (1927)	Siedler (1968)	Patzert (1974)	Maillard and Soliman (1986)	Bethoux (1988)
01	F_{surface}			57		72
	$F_{\text{sub-surface}}$			0		0
	F_{deep}			-54		-67
02	F_{surface}			40		70
	$F_{\text{sub-surface}}$			0		0
	F_{deep}			-37		-67
03	F_{surface}	58		57		69
	$F_{\text{sub-surface}}$	0		0		0
	F_{deep}	-49		-54		-67
04	F_{surface}			42		68
	$F_{\text{sub-surface}}$			0		0
	F_{deep}			-39		-67
05	F_{surface}			38		67
	$F_{\text{sub-surface}}$			0		0
	F_{deep}			-35		-67
06	F_{surface}			-06		67
	$F_{\text{sub-surface}}$			09		0
	F_{deep}			0		-67
07	F_{surface}			-20	-16	-26
	$F_{\text{sub-surface}}$			23	25	35
	F_{deep}			0	-06	-09
08	F_{surface}			-21	-25	-23
	$F_{\text{sub-surface}}$			24	33	35
	F_{deep}			0	-05	-09
09	F_{surface}			-09	-14	-20
	$F_{\text{sub-surface}}$			12	20	35
	F_{deep}			0	-03	-09
10	F_{surface}			52		54
	$F_{\text{sub-surface}}$			0		-35
	F_{deep}			-49		-09
11	F_{surface}		58	57		50
	$F_{\text{sub-surface}}$		0	0		-35
	F_{deep}		-42	-54		-09
12	F_{surface}			51		49
	$F_{\text{sub-surface}}$			0		-35
	F_{deep}			-48		-09

Table 5.16 shows the budget for the different elements in the Red Sea calculated using atmospheric dry deposition (“bioavailable”) dissolved concentrations of trace metals in surface (input) and deep (efflux) Red Sea waters with the annual layer transport.

Table 5.16. Elemental fluxes to and from the Red Sea (t yr^{-1}).

Element	Atmospheric (dry input) "bioavailable" flux (+)	Input from the Arabian Sea (+)	Efflux to the Arabian Sea (-)	Total input (+)	Net flux	% Atmospheric / Net fluxes
Fe	1644	14889	192697	16533	-176164	0.93
Cu	598	9404	14380	10002	-4378	14
Mn	6615	5486	12942	12101	-841	786
Co	98	104228	17256	104326	87070	0.11
Ni	68	11755	12942	11823	-1119	6
Zn	1718	7366	24447	9084	-15363	11
Cd	11	148897	47455	148908	101453	0.01
Pb	569	10971	38827	11540	-27287	2.1

From the calculated estimated budget (net flux), Table 5.16, it would appear that the Red Sea is a net source of elements to the Arabian Sea for most of the considered elements except for Co and Cd. The excess quantities of the elements are likely to have been derived from undefined sediment inputs. This input from sediments across the Red Sea axis seems to be a much more significant source than the atmospheric input for Fe which is contradictory to what would have been anticipated in a semi-enclosed basin surrounded by arid areas.

The current study has defined the atmospheric component of the trace metal budgets of the Red Sea. However sediment exchange with the deep water as well, as the direct input of trace metals through the hydrothermal discharge, have not been defined. Clearly there is a need for future studies to define the exchange of trace metals through the Straits of Bab Al-mandab and in particular between the sediments and the deep waters of the Red Sea, before realistic trace metals budgets for the Red Sea can be presented.

5.10 Conclusions

The following points may be concluded from this study at the Jeddah site:

- High aerosol loadings of the predominantly crustally derived elements are observed (Al, Mn and Fe). They are in excess of those observed in the Southern and Northern Levantine basin of the Eastern Mediterranean and the Arabian Sea. However, they are lower than those observed by Murphy (1991) for the North East Trades in the Atlantic Ocean. Cadmium detected over the Arabian Sea is lower than that determined in the current study, which in turn was consistently lower than the observed concentrations in both the Eastern and Western Mediterranean marine atmospheres. Lead also exhibits similar regional trends. However Zn shows comparatively high regional values, being attributed to locally enriched mineralogy.
- The influence of contrasting sources has been defined from the calculated the % of noncrustal contribution, using $(E/Al)_{\text{crust}}$ ratios from Taylor (1964). Elements with about 70% crustal contribution (Fe, Mn and Co) were considered to be crustally derived elements. The rest of the elements (Cd, Cu, Mo, Ni, Pb, V, Zn) were classified as anthropogenically derived elements as their % of non-crustal contribution is < 70%.
- For all elements, concentrations are greatest in the air masses derived from the SSA regions, whereas the lowest concentrations are detected in air masses from the RS, with the exception of Cd, where it is comparable in the E and N regions.
- Al, Fe, Mn, Cu, Mo and Zn show seasonal variations which are due to the enhanced seasonal dust transport occurring in the summer. For Ni and V the seasonality in their concentrations is more likely to be due to the increase in fossil fuel usage

during the summer, whereas the seasonality for Pb and Cd will be due to anthropogenic source inputs and/or its interaction with crustal material movement.

- A first approximation of the trace metal budget in the Red Sea highlights the potential importance of the sediment input. Unexpectedly, atmospheric input was not a key source for some elemental inputs to the Red Sea, notably “bioavailable” Fe. The net flux for trace elements shows that there is a deficit in the budget for all elements except for Cd and Co where the annual influx concentration is higher than the annual efflux.

Chapter Six

Conclusions and future work

6.1 The aerosol trace metal chemical characteristics of the Plymouth urban aerosol and RSMA

The current study has provided both novel and timely data on the trace metal chemical character of two contrasting aerosol populations (i) Plymouth urban aerosol (ii) Red Sea Marine Aerosol (RSMA). Using this data the variability of these populations can be attributed to (i) aerosol source types, (ii) aerosol emission strengths, (iii) proximity of aerosol source, (iv) air mass transport processes and (v) removal processes.

6.1.1 The Plymouth urban aerosol population

Aerosol trace metal concentrations in the Plymouth urban aerosol were much lower (2-13X) than other UK urban sampling locations. The Plymouth urban aerosol population was influenced more by long range transported anthropogenically derived material from the UK and Western Europe which subsequently undergoes dilution by more pristine maritime air masses originating the west of the UK. However, elevated concentrations of aerosol trace metals (at the beginning of sampling campaign) were due to local construction activities. This influence leads to diurnal variability in the monitored aerosol concentrations.

EF_{crust} analyses indicated that Fe, Mn, Co and V were “non-enriched” (i.e. $EF_{crust} < 10$) which would indicate an increasing crustal source contribution, whereas the remaining elements have high (> 10) EF_{crust} values. However, calculation of the % crustal contribution indicates that $EF_{crust} < 2$ represents the transition from predominantly anthropogenic to crustal source contributions. Hence, Fe, Mn, Co, V and Ni have calculated crustal contributions with an average of 57, 41, 38, 22 and 12

% respectively. The rest of the elements (Cd, Mo, Na Pb and Zn) have percentage crustal contributions <5.

Using air mass back trajectories, the influence of the source area on aerosol trace metal concentrations was evident. Two source areas were considered, (i) Atlantic air masses and (ii) UK + European air masses. Generally, enhanced concentrations (about 2x) were observed in the UK and European air masses (statistically significant for Al, Fe, Mn, Cd, Mo and Pb at $p < 0.05$). This impact was also apparent when inter-elemental relationships were considered. Significant correlations between anthropically and crustally derived trace metals were apparent, indicating that air mass movement was a major factor influencing the variation in the aerosol elemental concentrations. Lower statistical significances between the anthropic and crustal inter-elemental relationships for the Atlantic air sector compared with those associated with the UK+European sector would, in addition, suggest that during air mass movement there is a sequential change in the chemical character of the aerosol population owing to wet and dry removal processes. Zinc concentrations were not statistically different ($p < 0.05$) in the two air mass sectors, suggesting regional sources. The re-suspension of material from disused and abandoned mines in the South West being a possible source for Zn.

The solid state speciation of aerosol trace metals (subsequently used to predict the fate of the element in seawater post deposition) was investigated using a three stage sequential leach. The sequential leach procedure revealed that Al and Fe were predominantly present in the combined refractory and oxide / carbonate fractions (>95%). Whereas Cd, Pb and Mn were dominant in the exchangeable phase which

indicates that high fractions of these elements will be labile post-deposition in sea water. For the rest of the elements (Mo, Co and Ni) the total concentrations were associated with the exchangeable and residual fractions and relatively minor contributions from the oxide/carbonate solid phase.

Elemental dry deposition inputs have been calculated for the western English Channel and compared with literature values. However, it was apparent that the calculation of dry depositional fluxes and inputs is fraught with limitations and inaccuracies, mainly as a result of the uncertainty of elemental settling velocities. However, accepting these limitations, total dry atmospheric input of trace metals calculated in this study were used to calculate a revised budget (budget calculated by Wells, 1999) for Ni and Pb in the English Channel. The revised inputs were very similar to those (around 11%) previously calculated by Wells (1999) and do not change the conclusions presented by Wells (1999), who suggested that the efflux of Pb was higher than the inputs to the English Channel. It was proposed that the unaccounted source within the English Channel was likely to be the sediments. In contrast the efflux of Ni was lower than its input suggesting that the sediments are a geochemical sink for Ni in the English Channel.

6.1.2 The Red Sea Marine Aerosol (RSMA)

In comparison to other coastal regions which are influenced by inputs from arid land masses (i.e. the western and eastern Mediterranean; Atlantic North East Trades and the Arabian Sea) the RSMA clearly exhibited high aerosol loadings of the predominantly crustally derived elements (Al, Mn and Fe; crustal source contributions >70%). The observed concentrations were higher than those of the Eastern

Mediterranean, Northern Levantine Basin and the Arabian Sea marine aerosol by factors of between 2.1-6.2. However, they were lower than those quoted in Murphy, (1985) for the North East Trade in the Atlantic Ocean. For elements with a high anthropogenic contribution (> 80%) Cd, Pb and Zn exhibited the following trends;

Cadmium concentrations were lower than Eastern and Western Mediterranean marine atmospheres (0.17-0.22 and 0.36 ng m⁻³ respectively), but higher than that observed at the Arabian Sea by a factor of 2.6, explained by the more remote marine character of the sampling site in the Arabian Sea. Lead exhibits similar regional trends (except for the Southern air mass sector), again due to the comparative lower influence of long range transport anthropic material and the lack of regional intense industrial activities. Zinc, however, was elevated in the RSMA being the highest at any of the considered sites with the exception of western Mediterranean (Table 5.2), indicative of regional and local Zn inputs. The sampling site is surrounded by the Arabian shield where Zn is found in low-grade volcanosedimentary rocks or mainly produced as a by product of gold mining.

Seasonal variability in the RSMA trace metal concentrations was detected. Predominantly crustally derived trace metal (Al, Mn and Fe) concentrations during the summer period (June-July) were consistently around 2x higher than those observed during the winter season. Such elevated concentrations can be explained by enhanced dust re-suspension and transport in the Nubian desert and local sources (i.e. Arabian Peninsula) which have been shown in the literature to exhibit a summer peak in dust events.

At Jeddah the EF_{crust} analysis indicated that the crustal source influence is prominent and follows the order $Fe < Mn < Co < Ni < V < Cu < Mo$, these elements being classed as “non-enriched” elements, i.e. they all have $EF_{\text{crust}} < 10$. The remaining elements, Zn, Cd and Pb are all classed as anomalously enriched, highlighting their non crustal origins. In comparison with the literature, the EF_{crust} values for the RSMA are all higher than those found in the North Atlantic aerosol but equivalent to those observed for the Arabian Sea indicating the same general chemical character of the aerosol population except that the RSMA has a higher loading of metal. The RSMA EF_{crust} are generally lower than those observed for both the Western and Eastern Mediterranean aerosol. This is logical due to the fact that Jeddah is less impacted by regional anthropic sources.

Using air mass back trajectories, elemental concentration variability associated with different air masses was noted. This was particularly the case for those elements whose % crustal contributions were in excess of 50%, i.e. Al, Fe, Mn and Co. For all these elements the concentrations were greatest in air masses derived from the Middle and Southern Saudi Arabian (SSA) regions, whereas the statistically lowest concentrations were detected in air masses derived from the Red Sea (RS) region. For Al, Fe and Mn concentrations in the SSA air mass trajectory were the highest, which illustrates the fact that the effect of the local desert is more important than regional sources. However, V, Zn and Co show a similarity in all air mass trajectories (with the exception being the RS sector, which has the lowest values) which would indicate that a local source is the dominating factor. Lead concentration was highest at the SSA air mass trajectory due to the effect of the local industrial area to the south of Jeddah.

The solid state speciation signature for the RSMA highlights the prominent influence of crustal material. The exchangeable fraction was 0.3 % for both Al and Fe compared with 1.5% and 2.2% for Al and Fe respectively found in the Plymouth aerosol population. A similar trend was observed for the oxide/carbonate phase of Fe, being much lower (3.2%) than that observed at Plymouth (42%). This could be explained by the greater contribution from crustal material in the RSMA population than that in the Plymouth aerosol population. For Pb, as would be expected, there is a lower associations with the exchangeable fraction compared with the Plymouth aerosol population and indeed compared with most anthropogenically influenced aerosol populations. This would clearly impact upon its solubility post-deposition in seawater.

Atmospheric dry deposition of trace metal to the Red Sea was calculated. Generally, the total dry deposition fluxes for the crustally derived elements (Al, Fe, Mn, and Co) increased in the following order; North Sea < Western Mediterranean < Eastern Mediterranean (Northern Levantine basin) < Eastern Mediterranean (Southern Levantine basin) < RSMA. The total dry depositional fluxes of the predominantly anthropogenically derived elements in the RSMA are lower than those calculated for the two Levantine basins sites for Pb, however comparable fluxes for Cd were calculated and enhanced fluxes of Zn were detected in the RSMA. However, it is clear that the greatest uncertainty in dry depositional fluxes is the choice of the elemental V_d .

A first order trace metal budget within the Red Sea was calculated using the elemental dry deposition fluxes calculated in the current study. Although a number of assumptions were made in calculating the budget, it was apparent that the net flux of

the dissolved metals out of the Red Sea, via the strait of Bab Al-mandab, suggest that the sediments are an important source for all elements except for Co and Cd.

Both set of samples (Jeddah and Plymouth) have a high variability shown by the large standard deviation regardless of the difference in sampling location or time of sampling. In general, the crustally derived elements (with lower than 10 EF_{crust}) Al, Fe Mn and Co have the greatest variability at Jeddah whereas the non-crustal derived elements (with higher than 10 EF_{crust}) such as Ni, Cd, Pb and Co have the greatest variability at Plymouth. The aerosol trace metal concentrations of the crustally derived elements at Jeddah (Al: 2589 ng m⁻³; Fe: 2262 ng m⁻³; Mn: 49.3 ng m⁻³) are much higher than at Plymouth (Al: 187 ng m⁻³; Fe: 250 ng m⁻³; 6.2 ng m⁻³) which indicates the significant effect of the hyper arid area surrounding Jeddah.

6.2 Future work

(1) To better constrain trace elemental fluxes to the western English Channel and consequently allow a more accurate budget to be constructed, the uncertainty of elemental settling velocities has to be lowered. Therefore there is an urgent need to better define, on a regional scale, more accurate elemental settling velocities. This might be achieved by collection of (i) dry deposited material using surrogate collectors whilst collecting simultaneously aerosol samples or (ii) collection of size fractionated aerosol samples (using cascade impactor samplers) and applying models such as that proposed by Slinn and Slinn (1980) to assign settling velocities. For the case of the English Channel, the collection of rainwater and its subsequent analysis

for trace metals would allow an estimate of the trace metal wet deposition input. This would further enhance the accuracy of a trace metal budget for the English Channel.

(2) To gain a better appreciation of the representative nature of the global elemental ratios it is essential to map the elemental/Al ratios of local and regional crustal material to allow a more accurate definition of the EF_{crust} and hence a more representative calculation of contrasting sources contributions to the aerosol trace metal pool.

(3) The Red Sea requires extensive future research efforts to allow for a better understanding of the internal biogeochemical cycles of trace elements. For example, constrained fluxes of trace elements within, to and out of the Red Sea would consequently allow for a more accurate trace metal budget for this marine system. The uncertainty in trace metals fluxes arises from the lack of accurate trace metals concentrations (particulate and dissolved) at various locations and depths within the Red Sea. This dearth of knowledge needs to be addressed as soon as possible. Regular seasonal depth profiles of dissolved and particulate trace metal concentrations in the strait of Bab Al-mandab are critical if an accurate water mass balance of trace metals to and out of the Red Sea is to be constructed.

(4) To better define the impact of dry deposition inputs the aerosol trace metal seawater solubilities should be defined. Moreover, factors controlling trace metal seawater solubility, including particle concentration, the presence of organic ligands, aerosol source and seawater temperature need to be evaluated.

(5) Finally, the current study has highlighted temporal and air mass factors which influence the seasonal trace metal concentration in the RSMA. To better define dry deposition inputs of trace metals, a network of aerosol sampling stations around the Red Sea coastline is recommended.

References

Aberg, G., Charalampides, G., Fosse, G. and Hjelmseth, H. 2001. The use of Pb isotopes to differentiate between contemporary and ancient sources of pollution in Greece. *Atmospheric Environment* 35, 4609-4615.

Alfaro, S. C., Gomes, L., Rajot, J. L. Lafon, S., Gaudichet, A., Chatenet, B., Maille, M. Cautenet, G. Lasserre, F. Cachier, H. Zhang, X. Y. 2003. Chemical and optical characterization of aerosols measured in spring, 2002 at the ACE-Asia supersite, Zhenbeitai, China. *Journal of Geophysical Research* 108, (D23), 8641, doi:10.1029/2002JD003214, 2003.

Ali, A. E. and Bacso, J. 1994. Trace and major elements in atmospheric deposition in Debrecen city. *Journal of Radioanalytical and Nuclear Chemistry Letters* 188, 199-210.

Ali, A. E. Nasralla, M. M. and Shakour, A. A. 1986. Spatial and seasonal variation of lead in the Cairo atmosphere. *Environmental Pollution* 11, 205-210.

Al-Masri, M.S., Al-Kharfan, K. and Al-Shamali, K. 2006. Speciation of Pb, Cu and Zn determined by sequential extraction for identification of air pollution sources in Syria. *Atmospheric Environment* 40, 753-761.

Al-Rajhi, M. A. Al-Shayeb, S. M. Seaward, M. R. D. and Edward, H. G. M. 1996. Particle size effect for metal pollution analysis of atmospherically deposited dust. *Atmospheric Environment* 30, 145-153.

Al-Shiwafi, N., Rushdi, A. I. and Ba-Issa, A. 2005. Trace metals in surface seawaters and sediments from various habitats of the Red Sea coast of Yemen. *Environmental Geology* 48, 590-598.

Apsimon, H. M., Kruse, M. and Bell, J. N. B. 1987. Ammonia emissions and their role in acid deposition. *Atmospheric Environment* 21, 1939-1946.

Arimoto, R., Duce, R.A., Ray, B.J. and Tomza, U. 2003. Dry deposition of trace elements to the western North Atlantic. *Global Biogeochemical Cycles* 17, 1010. doi:10.1029/2001GB001406.

Arimoto, R. and Duce, R. A. 1986. Dry deposition models and the air/sea exchange of trace elements. *Journal of Geophysical Research* D91, 2787-2792.

Arimoto, R., Duce, R. A., Ray, B. J., Hewitt, A. D. and Williams, J. 1987. Trace elements in the atmosphere of American Samoa: Concentrations and deposition to the tropical south Pacific. *Journal of Geophysical Research* D92, 8465-8479.

Austin, L. S. and Millward, G. E. 1986. Atmosphere-coastal ocean fluxes of particulate arsenic and antimony. *Continental Shelf Research* 6, 459-474.

AWS/FM-100/009. 1980. Climate and Weather of the Arabian Peninsula. Air force weather station.

- Azam, F. 1998. Microbial control of oceanic carbon flux: The plot thickens. *Science* 280, 694-696.
- Baeyens, W., Dehairs, F. and Dedeurwaerder, H. 1990. Wet and dry deposition fluxes above the North Sea. *Atmospheric Environment* 24A, 1693–1703.
- Baker, A. R., French, M. and Linge, K. L. 2006a, Trends in aerosol nutrient solubility along a west–east transect of the Saharan dust plume. *Geophysical Research Letters* 33, L07805, doi:10.1029/2005GL024764.
- Baker, A.R. Jickells, T.D., Witt, M. and Linge, K.L. 2006b. Trends in the solubility of iron, aluminium, manganese and phosphorus in aerosol collected over the Atlantic Ocean. *Marine Chemistry* 98, 43-58.
- Baker, A. R., Kelly, S. D., Biswas, K. F., Witt, M. and Jickells, T. D. 2003. Atmospheric deposition of nutrients to the Atlantic Ocean. *Geophysical Research Letters* 30, 2296, doi:10.1029.
- Barry, R. G. and Chorley, R. J. 1992. *Atmosphere, Weather and Climate* (6th Edition) 392pp. Routledge.
- Behairy, A. K. A., El-Sayed, M. Kh. and Durgaprasada Rao, N. V. N. 1985. Aeolian dust in the coastal area north of Jeddah, Saudi Arabia. *Journal of Arid Environments* 8, 89-98.
- Bergametti, G. 1987. Apports de matiere par voie atmospherique a la mediterrannee Occidental. Ph.D. thesis, University of Paris, France.
- Bergametti, G., Dutot, A. L., Buat-Menard, P., Losno, R. and Remoudaki, E. 1989. Seasonal variability of the elemental composition of atmospheric aerosol particles over the northwestern Mediterranean. *Tellus* 41B, 353-361.
- Berry, A. 1990. Solid state speciation and seawater solubility studies and trace metal chemistry of the Indian Ocean Aerosol. Ph.D. thesis, University of Liverpool, UK.
- Bertho, M. L., Deboudt, K., Flament, P., Puskaric, E., 1998. The lead content of atmospheric aerosols above the eastern channel: seasonal variability and solubility in a coastal seawater. *Hydrobiologia* 374, 317-332.
- Bethoux, J. P. 1988. Red Sea geochemical budgets and exchanges with the Indian Ocean. *Marine Chemistry* 24, 83-92.
- Biscombe, A. 2004. Factors influencing the seawater solubility of aerosol associated trace metals. Ph.D. thesis, University of Plymouth, UK.
- Bonnet, S. and Guieu, C. 2004. Dissolution of atmospheric iron in seawater. *Geophysical Research Letters* 31, L03303, doi:10.1029/2003GL018423.
- Borer, P. M., Sulzberger, B., Reichard, P. and Kraemer, S. M. 2005. Effect of siderophores on the light-induced dissolution of colloidal iron(III) (hydr)oxides. *Marine Chemistry* 93, 179-193.

- Borg, H., Andersson, P. and Johnsson, K. 1989. Influence of acidification on metal fluxes in Swedish forest lakes. *The Science of Total Environment* 87/88, 241-253.
- Boutron, C. F. 1995. Historical reconstruction of the earth's past atmospheric environment from Greenland and Antarctic snow and ice cores. *Environmental Reviews* 3, 1-28.
- Bowie, A.R., Whitworth, D.J., Achterberg, E.P., Mantoura, R.F.C. and Worsfold, P.J. 2002. Biogeochemistry of Fe and other trace elements (Al, Co and Ni) in the upper Atlantic Ocean. *Deep-Sea Research I*, 49, 605-636.
- Bruland, K.W. 1992. Complexation of cadmium by natural organic ligands in the central North Pacific. *Limnology and Oceanography*. 37, 1008-1017.
- Buat-Menard, P. and Chesselet, R. 1979. Variable influence of the atmospheric flux on the trace metal chemistry of oceanic suspended matter. *Earth and Planetary Science Letters* 42, 399-411.
- Buma, A. G. J., de Barr, H. J. W., Nolting, R. F. and van Bennekom, A. J. 1991. Metal enrichment experiments in the Weddell Sea: effects of Fe and Mn on various plankton communities. *Limnology and Oceanography* 36, 1865-1878.
- BUWAL. 1995. Vom Menschen verursachte Luftschadstoffe Emissionen in der Schweiz von 1900 bis. Bundesamt Fur Umwelt, Wald und Landschaft, Bern, Switzerland.
- Caputo, M., Giménez, M. and Schlamp, M. 2003. Intercomparison of atmospheric dispersion models. *Atmospheric Environment* 37, 2435-2449.
- Cave, R. R., Andrews, J. E., Jickells, T. and Coombes, E. G. 2005. A review of sediment contamination by trace metals in the Humber catchment and estuary, and the implications for future estuary water quality. *Estuarine, Coastal and Shelf Science* 44, 547-557.
- Cawse, P.A. 1981. AERE Harwell Rep. R9886, H.M.S.O., London.
- Chan, Y. C., Vowles, P. D., McTainsh, G. H., Simpson, R. W., Cohen, D. D., Bailey, G. M. and McOrist, G. D. 2000. Simultaneous collection of airborne particulate matter on several collection substrates with a high-volume cascade impactor. *Atmospheric Environment* 34, 2645-2651.
- Chen, Y. Siefert, R. L. 2003. Determination of various types of labile atmospheric iron over remote oceans. *Journal of Geophysical Research.*, 108 (D24), 4774, doi:10.1029/2003JD003515.
- Chen, Y., Street, J. and Paytan, A. 2006. Comparison between pure water and seawater soluble nutrient concentrations of aerosols for the Gulf of Aquaba. *Marine Chemistry* 101, 141-305.

Chester, R., Bradshaw, G.F. and Corcoran, P.A. 1994b. Trace metal chemistry of the North Sea particulate aerosol concentration, source and seawater fates. *Atmospheric Environment* 28, 2873-2883.

Chester, R., Lin, F. J. and Basaham, A. S. 1994a. Trace metal solid state speciation changes associated with the down-column fluxes of oceanic particulates. *Journal of the Geological Society* 151, 351-360.

Chester, R. and Murphy, K. J. T. 1986. Oceanic sources of copper to the Atlantic aerosol. *Science of the Total Environment* 49, 325-338.

Chester, R. 2000. *Marine Geochemistry*. Blackwell Science. Oxford, UK.

Chester, R., Berry, A. S. and Murphy, K. J. T. 1991. The distribution of particulate atmospheric trace metals and mineral aerosols over the Indian Ocean. *Marine Chemistry* 34, 261-290.

Chester, R., Bradshaw, G. F., 1991. Source control on the distribution of particulate trace metals in the North Sea atmosphere. *Marine Pollution Bulletin* 22, 30-36.

Chester, R., Lin, F. J. and Murphy, K. J. T. 1989. A three stage sequential leaching scheme for the characterisation of the sources and environmental mobility of trace metals in the marine aerosol. *Environmental Technology Letters* 10, 887-900.

Chester, R., Murphy, K. J. T., Lin, F. J., Berry, A. S., Bradshaw, G. A., and Corcoran, P. A. 1993. Factors controlling the solubilities of trace metals from non-remote aerosols deposited to the sea surface by the 'dry' deposition mode. *Marine Chemistry* 42, 107-126.

Chester, R., Nimmo, M. and Keyse, S. 1996. The influence of Saharan and Middle Eastern desert-derived dust on the trace metal composition of Mediterranean aerosols and rainwaters: An overview. In 'The impact of desert derived dust across the Mediterranean'. Guerzoni, S. and Chester, R. (eds.), Kluwer Academic Publishers, 253-273.

Chester, R., Nimmo, M. and Nicolas, E. 1990. Atmospheric trace metals transported to the Western Mediterranean: Data from a station on Cap Ferrat. *Water Pollution Report* 20, 597-612.

Chester, R., Nimmo, M. and Preston, M. R. 1999. The trace metal chemistry of atmospheric dry deposition samples collected at Cap Ferrat: A coastal site in the Western Mediterranean. *Marine Chemistry* 68, 15-30.

Chester, R., Nimmo, M., Fones, G. R., Keyse, S. and Zhang, Z. 2000. Trace metal chemistry of particulate aerosols from the UK mainland coastal rim of the NE Irish Sea. *Atmospheric Environment* 34, 949-958.

Chester, R., Nimmo, M., Murphy, K. J. T. and Nicolas, E. 1990. Atmospheric trace metals transported to the Western Mediterranean: Data from a station in Cap Ferrat. 597-612. *Water Pollution Research Report* 20, European Commission.

- Chester, R., Sharples, E.J., Sanders, G. S. and Saydam, A. C. 1984. Saharan dust incursion over the Tyrrhenian Sea. *Atmospheric Environment* 18, 929-935.
- Chiapello, I., Bergametti, G., Chatenet, B., Bousquet, P., Dulac, B. and Santos Soares E. 1997. Origins of African dust transported over the northeastern tropical Atlantic. *Journal of Geophysical Research*. 102, (D12), 13,701-13,709.
- Church, T. M., Tramontano, J. M., Whelpdale, D. M., Andreae, M. O., Galloway, J. N., Keene, W. C., Knap, A. H. and Tokos, J. J. 1991. Atmospheric and precipitation chemistry over the North Atlantic Ocean: Shipboard results from April-May 1984. *Journal of Geophysical Research* 96(D10), 18705-18725.
- Church, T. M., Tramontano, J. M., Scudlark, J. R., Jickells, T. D., Tokos, J. J. and Knap, A. H. 1984. The wet deposition of trace metals to the western Atlantic ocean at the mid-Atlantic coast and on Bermuda. *Atmospheric Environment* 18, 2657-2664.
- Cimino, G. and Toscano, G. 1998. Dissolution of trace metals from lava ash: influence on the composition of rainwater in the Mount Etna volcanic area. *Environmental Pollution* 99, 389-393.
- Coale, K. H., Johnson, K. S., Fitzwater, S. E., Gordon, R. M., Tanner, S., Chavez, F. P., Ferioli, L., Sakamoto, C., Rogers, P., Millero, F., Steinberg, P., Nightingale, P., Copper, D., Cochlan, W. P., Landry, M. R., Constantinou, J., Rollwagen, G., Trasvina, A. and Kudela, R. 1996. A massive phytoplankton bloom induced by an ecosystem –scale iron fertilization experiment in the equatorial Pacific Ocean. *Nature* 383, 495-501.
- Conner, T. L. and Williams, R. W. 2004. Identification of possible sources of particulate matter in the personal cloud using SEM/EDX. *Atmospheric Environment* 38, 5305-5310.
- Crecelius, E.A. 1980. The solubility of coal fly ash and marine aerosols in seawater. *Marine Chemistry* 8, 245-250.
- Croot, P. L., Laan, P., Nishioka, J., Strass, V., Cisewski, B., Boye, M., Timmermans, K. R., Bellerby, R. G., Goldson, L., Nightingale, P. and de Barr, H. J. W. 2005. Spatial and temporal distribution of Fe(II) and H₂O₂ during EisenEx, an open ocean mesocoscale iron enrichment. *Marine Chemistry* 95, 65-88.
- Cullen, J. T. Bergquist, B. A. and Moffett, J. W. 2006. Thermodynamic characterization of the partitioning of iron between soluble and colloidal species in the Atlantic Ocean. *Marine Chemistry* 98, 295-303.
- Dabek-Zlotorzynska, E., Aranda-Rodriguez, R. and Buykx, S.E.J. 2002. Development and validation of capillary electrophoresis for the determination of selected metal ions in airborne particulate matter after sequential extraction. *Analytical and Bioanalytical Chemistry*. 372, 467-472.

Dabek-Zlotorzynska, E., Kelly, M., Chen, H. and Chuni, L.C. 2003. Evaluation of capillary electrophoresis combined with a BCR sequential extraction for determining distribution of Fe, Zn, Cu, Mn, and Cd in airborne particulate matter *Analytica Chimica Acta*, 498, 175-187.

Dabek-Zlotorzynska, E. Kelly, M. Chen H. and Chuni L.C. 2005. Application of capillary electrophoresis combined with a modified BCR sequential extraction for estimating of distribution of selected trace metals in PM_{2.5} fractions of urban airborne particulate matter. *Chemosphere*, 58, 1365-1376

de Barr, H. J. W., Buma, A. G. J., Nolting, R. F., Cadée, G. C., Jacques, G. and Treguer, P. 1990. On iron limitation of the Southern Ocean: experimental observations in the Weddell and Scotia Seas. *Marine Ecology Progress Series* 65, 105-122.

de Barr, H. J. W., de Jong, J. T. M., Bakker, D. C. E., Loscher, B. M., Veth, C. and Bathmann, U. 1995. Importance of iron for plankton blooms and carbon dioxide drawdown in the Southern Ocean. *Nature* 373, 412-415.

de Barr, H. J. W., de Jong, J. T. M., Nolting, R. F., Timmermans, K. R., van Leeuwe, M. A., Bathmann, U., van der Loeff, R. M. and Sildam, J., 1999. Low dissolved Fe and the absence of diatoms blooms in remote Pacific waters of the Southern ocean. *Marine Chemistry* 66, 1-34.

Deboudt, K., Flament, P., Weis, D., Mennessier, J. P., Maquinghen, P., 1999. Assessment of pollution aerosols sources above the Straits of Dover using lead isotope geochemistry. *Science of the Total Environment* 236, 57-74.

Degens, E. T. and Ross, D. A. 1969. Hot Brines and recent heavy metal deposition in the Red Sea. Springer-Verlag, New York, USA.

Desboeufs, K. V., Sofikitis, A., Losno, R., Colin, J. L. and Ausset, P. 2005. Dissolution and solubility of trace metals from natural and anthropogenic aerosol particulate matter. *Chemosphere*, 58, 195-203.

Desboeufs, K. V., Losno, R., and Colin, J. L. 2001. Factors influencing aerosol solubility during cloud processes. *Atmospheric Environment* 35, 3529-3537.

Dixon, J.L. 1998. Trace metal-particle water interactions in the western North Sea. Ph.D. thesis, University of Plymouth, UK

Dockery, C., Pope, X., Xu, J., Spengler, J., Ware, M., Fay, B. Ferris, B. and Speizer, F. 1993. Mortality Risks of Air Pollution A Prospective Cohort Study. *New England Journal of Medicine* 329, 1753-1759.

Dolske, D. A. and Gatz, D. F. 1985. A field intercomparison of methods for the measurement of particle and gas dry deposition. *Journal of Geophysical Research*, 90, D1, 2076-2084.

- Dordevic, D., Vukmirovic, Z., Totic, I. and Unkasevic, M. 2004. Contribution of dust transport and resuspension to particulate matter levels in the Mediterranean atmosphere. *Atmospheric Environment* 38, 3637-3645.
- Duce, R. A., Arimoto, R., Ray, B. J., Unni, C. K. and Harder, P. J., 1983. Atmospheric trace metals at the Enewatak Atoll. I. Concentrations, sources and temporal variability. *Journal of Geophysical Research* 88, 5321-5342.
- Duce, R. A., Liss, P. S., Merrill, J. T., Atlas, E. L., Buta-Menard, P., Hicks, B. B., Miller, J. M., Prospero, J. M., Arimoto, R., Church, T. M., Ellis, W., Galloway, J. N., Hansen, L., Jickells, T. D., Knap, A. H., Reinhardt, K. H., Scheneider, B., Soudine, A., Tokos J. J., Tsunogai, S., Wollast, R. and Zhou, M. 1991. The atmospheric inputs to the world ocean. *Global Biogeochemical Cycles* 5, 193-259.
- Dulac, F., Buat-Menard, P., Arnold, M. and Ezat, U. 1987. Atmospheric input of trace metals to the Western Mediterranean Sea: I. Factors controlling the variability of atmospheric concentrations. *Journal of Geophysical Research* 92, 8437-8453.
- Dulac, F., Buat-Menard, P., Ezat, U. Melki S. and Bergametti, G. 1989. Atmospheric input of trace metals to the western Mediterranean: uncertainties in modeling dry deposition from cascade impactor data, *Tellus* 41B, 362-378.
- Ebert, M., Weinbruch, S., Hoffmann, P. and Ortner, H. M. 2000. Chemical characterization of North Sea aerosol particles by total reflection X-ray fluorescence analysis and high-resolution scanning electron microscopy. *Journal of Aerosol Science* 31 613-632.
- El Sayed, M. A., Basaham, A. S., Rifaat, A. E., Turki, A. J. and El-Mamney, M. H. 2004. Study of the composition of Aeolian dust in the coastal area of Jeddah. *King Abdulaziz University Scientific Research, Council Project* 253/422.
- Engelstaedter, S., Tegen, I. And Washington, R. 2006. North African dust emission and transport. *Earth Science Reviews* 79,73-100.
- Falkovich, A. H., Schkolnik, G., Ganor, E. and Rudich, Y. 2004. Adsorption of organic compounds pertinent to urban environments onto mineral dust particles. *Journal of Geophysical Research* 109, D02208, doi:10.1029/2003JD003919.
- Fernández, A. J. Rodríguez, E. M. Francisco, T. de la Rosa, J. B. and Jiménez Sánchez, J. C. 2002. A chemical speciation of trace metals for fine urban particles. *Atmospheric Environment* 36, 773-780.
- Fernández, A. J., Ternero, M. F. Barragán, J. and Jiménez, J. C. 2000. An approach to characterization of sources of urban airborne particles through heavy metal speciation *Chemosphere - Global Change Science* 2, 123-136.
- Fett, R. W., Bohan, W. A. And Englebreton R. E. 1983. Navy tactical applications guide. Vol 5 part 1 (NEPRF/TR-83-03).

- Fine, R., Warner, M. and Weiss, R. 1988. Water mass modification at the Agulhas retroflection: Chlorofluoromethane studies. *Deep Sea Research* 35 (A), 311-332.
- Fitzgerald W. J. 1991. Marine aerosols: A review. *Atmospheric Environment* 25, 533-545.
- Flament, L. 1985. Métaux-traces associés aux aerosols atmosphériques: apports au milieu marin du littoral Nord-Pas-de-Calais. Ph.D. thesis, Université des Sciences et Techniques de Lille, France.
- Flament, P. Auger, Y., Leprêtre, A. and Noël, S. 1987. Coastal aerosols in the northern Channel. *Oceanologica Acta* 10, 49-61.
- Flament, P., Bertho, M. L., Deboudt, K., Véron, A. and Puskaric, E. 2002. European isotopic signatures for lead in atmospheric aerosols: a source apportionment based upon $^{206}\text{Pb}/^{207}\text{Pb}$ ratios. *Science of the Total Environment* 296, 35-57.
- Fones, G. R. 1996. Atmospheric Deposition of trace metals to urban and coastal environments. Ph.D. thesis, University of Central Lancashire, Preston, UK.
- Formenti, P., Andreae, M. O., Andreae, T. W., Ichoku, C., Schebeske, G., Kettle, J., Maenhaut, W., Cafmeyer, J., Ptasiński, J., Karnieli, A. and Lelieveld, J. 2001. Physical and chemical characteristics of aerosols over the Negev Desert during summer 1996. *Journal of Geophysical Research* 106, 4871-4890.
- Fuchtjohann, L., Jakubowski, N., Gladthe, D., Barnowski, C., Klockow, D. and Broekaert, J. A. C. 2000. Determination of soluble and insoluble nickel compounds in airborne particulate matter by graphite furnace atomic absorption spectrometry and inductively coupled plasma mass spectrometry. *Fresenius Journal of Analytical Chemistry* 366, 142-145.
- Gehlen, M., Heinze, C., Maier-Remier, E. and Measures, C. I. 2003. Coupled Al-Si geochemistry in an ocean general circulation model: A tool for the validation of oceanic dust deposition fields. *Global Biogeochemical Cycles* 17, 1028.
- GESAMP. 1989. The atmospheric input of trace species to the world oceans. UNEP.
- Gong, F., Bo-Tang, W., Ying-Sing, F. and Foo-Tim, C. 2005. Chemometric characterization of the quality of the atmospheric environment in Hong Kong. *Atmospheric Environment*, 39, 6388-6397.
- Gordon, A. S., Donat, J. R., Kango, R. A., Dyer, B. J. and Stuart, L. S. 2000. Dissolved copper-complexing ligands in cultures of marine bacteria and estuarine water. *Marine Chemistry* 70, 149-160.
- Graham, W. F. and Duce R. A. 1982. The atmospheric transport of phosphorus to the western North Atlantic. *Atmospheric Environment* 16, 1089-1097.

Guerzoni, S., Molinaroli, E. and Chester, R. 1997. Saharan dust inputs to the western Mediterranean Sea: Depositional patterns, geochemistry and sedimentological implications. *Deep-Sea Research II* 44, 631-654.

Guerzoni, S., Chester, R., Dulac, F., Herut, B., Loye-Pilot, M., Measures C., Migon, C., Molinaroli, E., Moulin, C., Rossini, P., Saydam, C., Soudine, A. and Ziveri, P. 1999. The role of atmospheric deposition in the biogeochemistry of the Mediterranean Sea. *Progress in Oceanography* 44, 147-190.

Guerzoni, S., Molinaroli, E., Rossini, P., Rampazzo, G., DeFalco, G. and Cristini, S. 1999. Role of desert aerosol in the metal fluxes in the Mediterranean area. *Chemosphere* 39, 229-246.

Guieu, C. and Thomas, A. 1996. Saharan aerosol: from the soil to the ocean, In: the impact of desert dust across the Mediterranean. Guerzoni, S. and Chester, R. (eds.), Kluwer Academic Publishers, 207-216.

Guieu, C., Chester, R., Nimmo, M., Martin, J. M., Guerzoni, S., Nicolas, E., Mateu, J. and Keyse, S. 1997. Atmospheric input of dissolved and particulate metals to the northwestern Mediterranean. *Deep Sea Research (II)* 44, 655-674.

Guieu, C., Martin, J. M., Thomas A. J. and Elbaz-Poulichet, F. 1991. Atmospheric versus river inputs of metals to the Gulf of Lions, *Marine Pollution Bulletin* 22, 176-183.

Halstead, M. J. R., Cunninghame, R. G. and Hunter, K. A. 2000. Wet deposition of trace metals to a remote site in Fiordland, New Zealand. *Atmospheric Environment* 34, 665-676.

Hand, J. L., Mahowald, N. M., Chen, Y., Siefert, R. L., Luo, C., Subramaniam, A. and Fung, I. 2004. Estimates of atmospheric-processed soluble iron from observations and a global mineral aerosol model: Biogeochemical implications. *Journal of Geophysical Research* 109, D17205, doi:10.1029/2004JD004574.

Harrison, R. M. and Yin, J. 2000. Particulate matter in the atmosphere: which particle properties are important for its effects on health. *Science of the Total Environment* 249, 85-101.

Hassanien, M. A., Rieuwerts, J., Shakour, A. A. and Bittó, A. 2001. Seasonal and annual variations in air concentrations of Pb, Cd and PAHs in Cairo, Egypt. *International Journal of Environmental Health Research* 11, 13-27.

Heal, M. R., Hibbs, L. R., Agius, R. M. and Beverland, I. J. 2005. Total and water-soluble trace metal content of urban background PM₁₀, PM_{2.5} and black smoke in Edinburgh, UK. *Atmospheric Environment* 39, 1417-1430.

Helmerts, E. and Schrems, O. 1995. Wet deposition of metals to the tropical north and south Atlantic ocean. *Atmospheric Environment* 29, 2475-2484.

- Herut, B., Nimmo, M., Medway, A., Chester, R. and Krom, M. D. 2001. Dry atmospheric inputs of trace metals at the Mediterranean coast of Israel (SE Mediterranean): sources and fluxes. *Atmospheric Environment* 35, 803-813.
- Hicks, B. B. and Williams, R. M. 1980. Transfer and deposition of particles to water surfaces In *Atmospheric Sulfur Deposition*, Shriner D. S., Richmond, C. R. and Lindberg, S. E. (eds.) 237-244.
- Hiemstra, T. and van Riemsdijk, W. H. 2006. Biogeochemical speciation of Fe in ocean water. *Marine Chemistry* 102, 181-197.
- Hodge, V., Johnson, S. R. and Goldberg, E. D. 1978. Influence of atmospherically transported aerosols on surface ocean water composition. *Geochemistry Journal* 12, 7-20.
- Hodzic, A., Vautard, R., Bessagnet, B., Lattuati, M. and Moreto, F. 2005. Long-term urban aerosol simulation versus routine particulate matter observations. *Atmospheric Environment* 39, 5851-5864.
- Hoffmann, T. L. 2000. Environmental implications of acoustic aerosol agglomeration. *Ultrasonics* 38, 353-357.
- Hoffman, R., Laskin, A. and Finlayson-Pitts, B. J. 2004. Sodium nitrate particles: physical and chemical properties during hydration and dehydration, and implecations for aged sea salt aerosols. *Aerosol Science* 35, 869-887.
- Huang, S., Arimoto, R. and Rahn, K. A. 1996. Changes in atmospheric lead and other pollution elements at Bermuda. *Journal of Geophysical Research* 101, D15. 21,033–21,040.
- Huang, S., Arimoto, R. and Rahn, K. A. 2001. Sources and source variations for aerosol at Mace Head, Ireland. *Atmospheric Environment* 35, 1421-1437.
- Hurst M. P. and Bruland, K. W. 2006. An investigation into the exchange of iron and zinc between soluble, colloidal, and particulate size-fractions in shelf waters using low-abundance isotopes as tracers in shipboard incubation experiments. *Marine Chemistry* 103, 211-226.
- Injuk, J., van Grieken R. and de Leeuw, G. 1998. Deposition of atmospheric trace elements into the North Sea: coastal, ship, platform measurements and model predictions, *Atmospheric Environment* 32, 3011–3025.
- Injuk, J., Otten, Ph., Laane R., Maenhaut, W., and Van Grieken, R. 1992. Atmospheric concentrations and size distributions of aircraft-sampled Cd, Cu, Pb and Zn over the southern bight of the North Sea. *Atmospheric Environment* 26, 2499-2508.

- Jickells T. D., Knap A., Church T., Galloway J. and Miller, J. 1982. Acid Rain in Bermuda. *Nature*, 297, 55-57.
- Jickells, T. D. 1995. Atmospheric inputs of metals and nutrients to the oceans: their magnitude and effects. *Marine Chemistry*, 48, 199-214.
- Jickells, T. D. and Spokes, L. J. 2001. Atmospheric iron inputs to the oceans, in *Biogeochemistry of Iron in Seawater* Turner, D. and Hunter, K. A. (eds.) 85-121. (John Wiley New York).
- Jickells, T. D., Kelly, S. D., Baker, A. R., Biswas, K., Dennis, P. F., Spokes, L. J., Witt, M. and Yeatman, S. G. 2003. Isotopic evidence for a marine ammonia source. *Geophysical Research Letters* 30, 1374, doi:10.1029.
- Kahl, J. D., Harris, J. M., Herbert, G. A. and Olson, M. P., 1989. Intercomparison of three long-range trajectory models applied to Arctic haze. *Tellus* 41B, 524-536.
- Kane, M. M., Rendell A.R. and Jickells T. D. 1991. Atmospheric scavenging processes over the North Sea. *Atmospheric Environment* 28, 2523-2530.
- Kasparian, J., Frejafon, E., Rambaldi, P., YU, J., Vezin, B., Wolf, J. P., Ritter, P. and Viscard, P. 1998. Characterization of urban aerosols using SEM-Microscopy, X-Ray analysis and Lidar measurements. *Atmospheric Environment* 32, 2957-2967.
- Keyse, S. 1995. Trace metal chemistry of Mediterranean rain waters. Ph.D. thesis, University of Liverpool, UK.
- Kim, E., Kalman, D. and Larson, T. 2000. Dry deposition of large, airborne particles onto a surrogate surface. *Atmospheric Environment* 34, 2387-2397.
- Koçak, M. 2001. Investigation of the chemical composition of the lower tropospheric aerosols in the eastern Mediterranean region: Implications regarding sources and long range transport. M.Sc. Thesis. Middle East Technical University, Erdemli, Turkey.
- Kocak, M., Kubilay, N., Herut, B. and Nimmo, M. 2005. Dry atmospheric fluxes of trace metals (Al, Fe, Mn, Pb, Cd, Zn, Cu) over the Levantine Basin: A refined assessment. *Atmospheric Environment* 39, 7330-7341.
- Kocak, M., Kubilay, N., Herut, B. and Nimmo, M. 2007. Trace Metal solid state speciation in aerosols of the Northern Levantine Basin, East Mediterranean. *Journal of Atmospheric Chemistry* 56, 239-257.
- Kocak, M., Nimmo, M., Kubilay, N. and Herut, B. 2004. Spatio-temporal aerosol trace metal concentrations and sources in the Levantine Basin of the Eastern Mediterranean. *Atmospheric Environment* 38, 2133-2144.
- Kramer, J., Laan, P., Sarthou, G., Timmermans, K. R. and de Baar, H. J. W. 2004. Distribution of dissolved aluminium in the high atmospheric input region of the subtropical waters of the North Atlantic Ocean. *Marine Chemistry* 88, 85-101.

Kubilay, N. N. and Saydam, A. C. 1995. Trace elements in atmospheric particulates over the Eastern Mediterranean; concentrations, sources, and temporal variability. *Atmospheric Environment* 29, 2289-2300.

Kubilay, N. N., Saydam, A. C., Yemenicioglu, S., Kelling, G., Kapur, S., Karaman, C., and Akca, E. 1997. Seasonal chemical and mineralogical variability of atmospheric particles in the coastal region of the Northeast Mediterranean. *Catena* 28, 313-328.

Kubilay, N., Nickovic, S., Moulin, C. and Dulac, F., 2000. An illustration of the transport and deposition of mineral dust onto the eastern Mediterranean. *Atmospheric Environment* 34, 1293-1303.

Kuma, K., Nishioka, J. and Matsunaga, K. 1996. Control on iron (III) hydroxide solubility in seawater: The influence of pH and natural organic chelators. *Limnology and Oceanography* 41, 396-407.

Kuo, Y. H., Skumanich, M., Haagenson, P. L. and Chang, J. S. 1985. The accuracy of trajectory models as revealed by the observing system simulation experiments. *Monthly Weather Review* 113, 1852-1867.

Kwon, S. B., Lim, K. S., Jung, J. S., Bae, G. N. and Lee, K. W. 2003. Design and calibration of a 5-stage cascade impactor (K-JIST cascade impactor). *Journal of Aerosol Science* 34, 289-300.

Lamb, H. H. 1950. Types and spells of weather around the year in the British Isles: Annual trends, seasonal structure of the year, singularities. *Quarterly Journal of the Royal Meteorological Society* 76, 393-438.

Lammel, G., Rohrl, A. and Schreiber, H. 2002. Atmospheric lead and Bromine in Germany—post abatement levels, variabilities and trends. *Environmental Science and Pollution Research* 9, 397-404.

Lantzy, R. J. and Mackenzie, F. T. 1979. Atmospheric trace metals: Global cycles and assessment of man's impact. *Geochimica et Cosmochimica Acta* 43, 511-525.

Lee, D. S. Garland, J. A. and Fox, A. A. 1994. Atmospheric concentrations of trace elements in urban areas of the United Kingdom. *Atmospheric Environment* 28, 2691-2713.

Le Gall, A. C., Statham, P. J., Morley, N.H., Hydes, D.J. and Hunt, C.H. 1999. Processes influencing distributions and concentrations of Cd, Cu, Mn and Ni at the North West European shelf break. *Marine Chemistry* 68, 97-115.

Li, Z., Hopke, P. H., Qureshi, L. H. S., Dutkiewicz, V. A., Schwab, J. J., Drewnick, F. and Demerjian, K. L. 2004. Sources of fine particle composition in New York city. *Atmospheric Environment* 38, 6521-6529.

Lim, B. 1991. Trace metals in the North Atlantic precipitation. Ph.D. thesis, University of East Anglia, UK.

Lim, B. and Jickells, T. D. 1990. Dissolved, particulate and acid leachable trace metal concentrations in North Atlantic precipitation collected on the Global Change Expedition. *Global Biogeochemical Cycles* 4, 445-458.

Lim, B., Jickells, T. D., Colin, J. L. and Losno, R. 1994. Solubilities of Al, Pb, Cu and Zn in rain sampled in the marine environment over the North Atlantic and Mediterranean Sea. *Global Biogeochemical Cycles* 8, 349-363.

Lim, M. C.H. Godwin A. A., Lidia M., Zoran, D. R. and Jayaratne, E. R. 2005. Effect of fuel composition and engine operating conditions on polycyclic aromatic hydrocarbon emissions from a fleet of heavy-duty diesel buses. *Atmospheric Environment* 39, 7836-7848.

Lim, M. C. H., Godwin, A., A., Lidia, M., Zoran, D. R., Jayaratne, E., R. and Kokot, S. 2006. A comparative study of the elemental composition of the exhaust emissions of cars powered by liquefied petroleum gas and unleaded petrol. *Atmospheric Environment* 40, 3111-3122.

Lion, L. W. and Leckie, J. O. 1981. Chemical speciation of trace metals at the air-sea interface: the application of an equilibrium model. *Environmental Geology* 3, 293-314.

Liu, X. and Millero, F. J. 1999. The solubility of iron hydroxide in sodium chloride solutions. *Geochimica et Cosmochimica Acta* 63, 3487-3497.

Liu, X. and Millero, F. J. 2002. The solubility of iron in seawater. *Marine Chemistry* 77, 43-54.

Losno, R., Bergametti, G. and Buat-Menard P. 1988. Zinc partitioning in Mediterranean rainwater. *Geophysical Research Letters*. 15, 1389-1392.

Losno, R., Bergametti G., Carlier P., and Mouvier G. 1991. Major ions in marine rainwater with attention to sources of alkaline and acidic species. *Atmospheric Environment* 25, 763-770.

Lowenthal, D. H. and Rahn, K. A. 1987. The use of Whatman 41 filter papers for high volume aerosol sampling. *Atmospheric Environment* 21, 2732-2734.

Lum, K. R., Betteridge, J. S. and Macdonald, R. R. 1982. The potential availability of P, Al, Cd, Co, Cr, Fe, Mn, Ni, Pb and Zn in urban particulate matter. *Environmental Technology Letters* 3, 57-62.

Lyamani, H., Olmo, F.J. and Alados-Arboledas, L. 2004. Saharan dust outbreak over southeastern Spain as detected by sun photometer. *Atmospheric Environment* 39, 7276-7284.

Mahowald, N., Kohfeld, K. E., Hansson, M., Balkanski, Y., Harrison, S. P., Prentice, I. C., Schulz, M. and Rohde, H. 1999. Dust sources and deposition during the Last Glacial Maximum and current climate: a comparison of model results with paleodata from ice cores and marine sediments. *Journal of Geophysical Research* 104, 15895-16436.

Mahowald, N. M., Baker, A. R. Bergametti, G. Brooks, N. Duce, R. A. Jickells, T. D. Kubilay, N. Prospero, J. M. and Tegen, I. 2005. Atmospheric global dust cycle and iron inputs to the ocean. *Global Biogeochemical Cycles* 19, GB4025, doi:10.1029/2004GB002402.

Maillard, C. and Soliman, G. 1986. Hydrography of the Red Sea and exchanges with the Indian Ocean in summer. *Oceanologica Acta* 9, 249-269.

Maring, H. B. and Duce, R. A. 1987. The impact of atmospheric aerosols on trace metal chemistry in open ocean surface seawater, I, Aluminum. *Earth and Planetary Science Letters* 84, 381-392.

Maring, H. B., and Duce, R. A. 1989. The impact of atmospheric aerosol on trace metal chemistry in open ocean surface seawater, II, Copper, *Journal of Geophysical Research* 94, 1039-1045.

Maring, H. B. and Duce, R. A. 1990. The impact of atmospheric aerosols on trace metal chemistry in open ocean surface seawater, III, Lead. *Journal of Geophysical Research* 95, 5341-5347.

Martin J. H., Fitzwater, S. E. and Gordan, R. M. 1990. Iron deficiency limits phytoplankton growth in Antarctic waters. *Global Biogeochemical Cycles* 4, 5-12.

Martin, J. H. and Gordon, R. M., 1988. Northeast Pacific iron distributions in relation to phytoplankton productivity. *Deep-Sea Research (A)* 177-196.

Martin, J. H., Gordon, R. M. and Fitzwater, S. E., 1991. The case for iron. *Limnology and Oceanography* 36, 1793-1802.

Martin, J. M., Elbaz-Poaulichet, F., Guieu, C., Loye-Pilot, M. D., and Han, G., 1989. River versus atmospheric inputs of material to the Mediterranean Sea: an overview. *Marine Chemistry* 28, 159-182.

Merrill, J. T., Bleck, R. and Avila, L., 1985. Modeling atmospheric transport to the Marshall islands. *Journal of Geophysical Research* 90, 12,927-12,936.

Methven, J., Evans, M., Simmonds, P. and Spain, G. 2001. Estimating relationship between air mass origin and chemical composition. *Journal of Geophysical Research* 106, D5, 5005-5019.

Migon, C. and Nicolas, E. 1998. Effects of anti-pollution policy on anthropogenic lead transfers in the Ligurian sea. *Marine Pollution Bulletin* 36, 775-779.

Migon, C., Alleman, L., Leblond, N., and Nicolas, E. 1993. Evolution of atmospheric lead over the northwestern Mediterranean between 1986 and 1992. *Atmospheric Environment* 27, 2161-2167.

Migon, C., Journel, B., and Nicolas, E. 1997. Measurement of trace metal wet, dry and total atmospheric fluxes over the Ligurian sea. *Atmospheric Environment* 31, 889-896.

- Miller, J.N. and Miller, J.C. 2001. *Statistics and Chemometrics for Analytical Chemistry*. Prentice Hall. Dorset, UK.
- Millero, F. J. 1996. *Chemical Oceanography*, second edition. CRC Press, New York.
- Mills, M. M., Ridame, C., La Roche, M. D. J. and Geider, R. J. 2004. Iron and phosphorus co-limit nitrogen fixation in the eastern tropical North Atlantic. *Nature* 429, 292-294.
- Modaihsh, A. S. 1997. Characteristics and composition of the falling dust sediments on Riyadh city, Saudi Arabia. *Journal of Arid Environments* 36, 211-223.
- Morcos, S. A. 1970. Physical and chemical oceanography of the Red Sea. *Oceanography and Marine Biology Annual Review* 8, 73-202.
- Moore, M. 1975. A major lineament in the Arabian Shield and its relationship to mineralization. *Mineralium Deposita* 11, 323-328.
- Moore R. M., Milley J. E., and Chatt A. 1984. The potential for biological mobilization of trace elements from Aeolian dust in the ocean and its importance in the case of iron. *Oceanologica Acta* 7, 221-228.
- Morel, F. M. M., and Price, N. M., 2003. The biogeochemical cycles of trace metals in the Oceans. *Science* 300, 944-947.
- Moreno, T., Jones T. and Richards R. 2004. Characterisation of aerosol particulate matter from urban and industrial environments: examples from Cardiff and Port Talbot, South Wales, UK. *Science of the Total Environment* 334-335, 337-346.
- Muller, K., Spindler, G., Maenhaut, W., Hitzenberger, R., Wieprecht, W., Baltensperger, U. and Brink, H. 2004. A campaign to assess the comparability of methods in use in Europe for measuring aerosol composition. *Atmospheric Environment* 38, 6459-6466.
- Murphy, K. J. T. 1985. The trace metal chemistry of the Atlantic aerosol. Ph.D. thesis, University of Liverpool, UK.
- Nair, P. R. Parameswaran, K. Abraham, A. and Jacob, S. 2005. Wind-dependence of sea-salt and non-sea-salt aerosols over the oceanic environment. *Journal of Atmospheric and Solar-Terrestrial Physics* 67, 884-898.
- Nair, P. R. Parameswaran, K. Sunilkumar, S. V. Abraham, A. and Jacob, S. 2004. Chemical composition of atmospheric aerosols over the Indian Ocean: impact of continental advection. *Advances in Space Research* 34, 828-832.
- Niemi, V. J., Tervahattu, H., Vehkamäki, H., Kulmala, M., Koskentalo, T., Sillanpää, M. and Rantamäki, M. 2004. Characterization and source identification of a fine particle episode in Finland. *Atmospheric Environment* 38, 5003-5012.

Nimmo, M., Van den Berg, C. M and Brown, J. 1989. The chemical speciation of dissolved nickel, copper, vanadium and iron in Liverpool Bay, Irish Sea. *Estuarine Coastal and Shelf Science* 29, 57-74.

Nriagu, J. O., 1979. Global inventory of natural and anthropogenic emissions of trace metals to the atmosphere. *Nature* 279, 409-411.

Oikonomou, M. C., Koçak, M., Kouvarakis, G., Kubilay N. and Mihalopoulos, N. 2003. Atmospheric deposition of inorganic phosphorus in the Levantine Basin, eastern Mediterranean: spatial and temporal variability and its role in seawater productivity. *Limnology and Oceanography* 48, 1557-1568.

Otten, P. Injuk, J. and Van Grieken, R. 1994. Elemental concentrations in atmospheric particulate matter sampled on the North Sea and the English Channel. *Science of the Total Environment* 155, 131-149.

Ottley, C.J. and Harrison, R.M. 1993. Atmospheric dry deposition flux of metallic species to the North Sea, *Atmospheric Environment* 27A, 685-695.

Owen, F. and Jones, R. 1990. *Statistics*. 3rd Edition, Pitman publishing Co.

Ozturk, M., Croot, P. L., Bertilsson, S., Abrahamsson, K., Karlson, B., David, R., Fransson, A. and Sakshaug, E. 2004. Iron enrichment and photoreduction of iron under UV and PAR in the presence of hydroxycarboxylic acid: implications for phytoplankton growth in the Southern Ocean. *Deep Sea Research (II)* 51, 2841-2856.

Pacyna, J.M., Vitols, V. and Hanssen, J. E. 1984. Size-differentiated composition of the arctic aerosol at NY-Ålesund, Spitsbergen. *Atmospheric Environment* 18, 2447-2459

Pacyna, J.M., Munch, J., Axenfeld, F. 1991. European inventory of trace metal emissions to the atmosphere. In: Vernet, J.P. (eds), *Heavy Metals in the Environment*. Elsevier, Amsterdam, Netherlands, 1-20.

Paoletti, L., De Berardis, B., Arrizza, L., Passacantando, M., Inglessis, M. and Mosca, M. 2003. Seasonal effects on the physico-chemical characteristics of PM_{2.5} in Rome: a study by SEM and XPS. *Atmospheric Environment* 37, 4869-4879.

Patterson, C. C. and Settle, D. M., 1987. Review of data on eolian fluxes of industrial and natural lead to the lands and seas in remote regions on a global scale. *Marine Chemistry* 22, 137-162.

Patzert, W. C. 1974. Volume and heat transports between Red Sea and Gulf of Aden, notes on the Red Sea heat budget, in *L'oceanographie physique de la Mer Rouge* pp 191-201, CNEXO, Paris.

Pease, P. P. Tchakerian, V. P. and Tindale, N. W. 1998. Aerosol over Arabian Sea: geochemistry and source areas for Aeolian desert dust. *Journal of Arid Environments* 39, 477-496.

Pickering, K. E., Thompson, A. M., McNamara, D. P. and Schoeberl, M. R., 1994. An intercomparison of isentropic trajectories over the South Atlantic. *Monthly Weather Review* 122, 864–879.

Pickering, K. E., Thompson, A. M., McNamara, D. P., Schoeberl, M. R., Fuelberg, H. E., Loring Jr., R. O., Watson, M. V., Fakhruzzaman, K. and Bachmeier, A. S., 1996. TRACE A trajectory intercomparison. 1. Effects of different input analyses. *Journal of Geophysical Research* 101, 23,903–23,925.

Plahn, O., Baschek, B., Badewien, T. H., Walter, M. and Rhein, M. 2002. Importance of The Gulf of Aqaba for the formation of bottom water in the Red Sea. *Journal of Geophysical Research* 107, 3108, doi: 10.1029/2000JC000342.

Poldervaart, A. 1955. Zircons in rocks. *American Journal of Science* 253, 433-461.

Poldervaart, A. 1956. Zircons in sedimentary rocks. *American Journal of Science* 254, 521-554.

Pope, M., Thun, M., Manbooditi, D., Dockery, J., Evans, Speizer, F. and Heath, C. 1995. Particulate air pollution as a predictor of mortality in a prospective study of U.S. adults, *American Journal of Respiratory and Critical Care Medicine* 151, 669–674.

Profumo, A. Spini, G. Cucca, L. and Pesavento, M. 2003. Determination of inorganic nickel compounds in the particulate matter of emissions and workplace air by selective sequential dissolutions. *Talanta* 61, 465-472.

Prospero, J. M., Charlson, R. W., Mohnen, V., Jeanicke, R., Dealny, A. C., Moyers, J., Zoller, W., and Rahan, K., 1983. The atmospheric aerosol system: an overview. *Reviews of Geophysics and Space Physics*. 21, 1607-1629.

Prospero, J. M., Ginoux, P., Torres, O., Nicholson, S. E. and Gill, T. E. 2002. Environmental characterization of global sources of atmospheric soil dust identified with the Nimbus 7 Total Ozone Mapping Spectrometer (TOMS) absorbing aerosol product. *Reviews of Geophysics* 40, 1-31.

Ramsay, C. R., Basahel, A. N. and Jaacson, N. J. 1981. Petrography, geochemistry and origion of the volcan-sedimentry succession between jabal Ibrashim and Al-Aqiq, Saudi Arabia. *Bulletin of the Faculty of Earth Science* 4, 1-24 (King AbdulAziz University, Jeddah).

Reid, P. C. Auger, C. Chaussepied, M. and Burn, M. 1993. The Channel. Quality Status Report: Report on Sub-Region 9. UK, Department of the Environment.

Reimann, C. and de Caritat, C. 2000. Intrinsic flaws of element enrichment factors (EFs) in environmental geochemistry. *Environmental Science and Technology* 34, 5084-5091.

Remoudaki, E. 1990. Etude des processus controlant la variabilite temporelle des fluxes atmospheriques de polluants et de poussières minérales en Méditerranée occidentale. Ph.D. thesis, University of Paris, France.

Ridame, C., Guieu, C., and Loye-Pilot, M. D. 1999. Trend in total atmospheric deposition fluxes of aluminum, iron and trace metals in the northwestern Mediterranean over the past decade (1985-1997). *Journal of Geophysical Research* D104, 30127-30138.

Rijkenberg, M.J.A., Fischer, A.C., Kroon, J.J., Gerringa, L.J.A., Timmermans, K.R., Wolterbeek, H.Th. and de Baar, H.J.W. 2005. The influence of UV irradiation on the photoreduction of iron in the Southern Ocean. *Marine Chemistry* 93, 119-129.

Rojas, C., Injuk, J., van Grieken A. and Laane, R.W. 1993. Dry and wet deposition fluxes of Cd, Cu, Pb and Zn into the southern bight of the North Sea, *Atmospheric Environment* 27A, 251–259.

Rolph G. D. and Draxler, R. R., 1990. Sensitivity of three-dimensional trajectories to the spatial and temporal densities of the wind field. *Journal of Applied Meteorology* 29, 1043–1054.

Sakata, M. and Marumoto, K. 2004. Dry deposition fluxes and deposition velocities of trace metals in the Tokyo Metropolitan area measured with a water surface sampler. *Environmental Science and Technology* 38, 2190-2197.

Samet, F., Dominici, F., Curriero, I. C. and Zeger, S. 2000. Fine particulate air pollution and mortality in 20 U.S. cities, 1987-1994., *S. Cities. New England Journal of Medicine* 343, 1742–1749.

Sanders, G.S. 1983. Metals in marine atmospheric particles. Ph.D. thesis, University of Liverpool, UK.

Sarthou, G., Baker, A. R., Blain, S., Achterberg E. P., Boye, M., Bowie, A. R., Croot, P., Laan, P., de Baar, H. J. W., Jickells, T. D. and Worsfold, P. J. 2003. Atmospheric iron deposition and sea-surface dissolved iron concentrations in the eastern Atlantic Ocean. *Deep-Sea Research (I)* 50, 1339-1352.

Sarthou, G., Baker A. R., Kramer, J., Laan, P., Laes A., Ussher, S., Achterberg E. P., de Baar, H. J. W., Timmermans, K. R., and Blain, S. 2007. Influence of atmospheric input on the iron distribution in the subtropical North-East Atlantic Ocean. *Marine Chemistry* 104, 186-202.

Saydam, A. C. 1981. The elemental chemistry of Eastern Mediterranean atmospheric particulates. Ph.D. thesis, University of Liverpool, UK.

Saydam, A. C. and Senyuva, H. C. 2002. Deserts: Can they be the potential suppliers of bioavailable iron. *Geophysical Research Letters* 29, 1524, doi:10.1029/2001GL013562.

Seibert, P. 1993. Convergence and accuracy of numerical methods for trajectory calculations. *Journal of Applied Meteorology* 32, 558–566.

Shriadah, M. A., Okbah, M. A. and El-Deek, M. S. 2004. Trace metals in the water columns of the Red Sea and the Gulf of Aqaba, Egypt. *Water Air and Soil Pollution* 153, 115-124.

Shotyk, W. 1996. Peat bog archives of atmospheric metal deposition: Geochemical assessment of peat profiles, natural variations in metal concentrations, and metal enrichment factors. *Environmental Reviews* 4(2):149-183.

Siedler, G. 1968. Schichtungs- und Bewegungsverhältnisse am Sudausgang des Roten Meeres. *Meteor Forschungsergeb (Reihe A)* 4, 1-76.

Siefert, R. L. Johansen, A. M. Hoffmann, M. R. 1999. Chemical characterization of ambient aerosol collected during the southwest monsoon and intermonsoon seasons over the Arabian Sea: Labile-Fe(II) and other trace metals. *Journal of Geophysical Research* 104(D3), 3511-3526, 10.1029/1998JD100067.

Singh, M., Jaques, P. A. and Sioutas, C. 2002. Size distribution and annual characteristics of Particle-bound metals in source and receptor sites of the Los Angeles Basin. *Atmospheric Environment* 36, 1675-1689.

Slejkovec, Z., Salma, I., van Eletren, J. T. and Zemplen-Papp, E. 2000. Speciation of arsenic in coarse and fine urban aerosols using sequential extraction combined with liquid chromatography and atomic fluorescence detection. *Journal of Analytical Chemistry* 366, 830-834.

Slinn, S.A. and Slinn, W.G.N. 1980. Prediction for particle deposition on natural waters. *Atmospheric Environment* 14, 1013-1016.

Sofianos, S. S. and William E. J. 2003. An oceanic general circulation model (OGCM) investigation of the Red Sea circulation: 2. Three-dimensional circulation in the Red Sea. *Journal of Geophysical Research* 108, 3066, doi: 10.1029/2001JC001185.

Spindler, G., Müller, K., Brüggemann, E., Gnauk T. and Herrmann, H. 2004. Long-term size-segregated characterization of PM₁₀, PM_{2.5}, and PM₁ at the IfT research station Melpitz downwind of Leipzig (Germany) using high and low-volume filter samplers. *Atmospheric Environment* 38, 5333-5347.

Spokes, L. J. and Jickells, T. D. 1996. Factors controlling the solubility of aerosol trace metals in the atmosphere and on mixing into seawater. *Aquatic Geochemistry* 1, 355-374.

Spokes, L. J., Jickells, T. D. and Lim, B. 1994. Solubilisation of aerosol trace metals by cloud processing: A laboratory study. *Geochimica Cosmochimica Acta*. 58, 3281-3287.

Spokes, L., Jickells, T. D. and Jarvis, K., 2001. Atmospheric inputs of trace metals to the northeast Atlantic Ocean: the importance of southeasterly flow. *Marine Chemistry* 76, 319-330.

- Stafford, R. G. and Ettinger, H. J. 1972. Filter efficiency as a function of particle size and velocity. *Atmospheric Environment* 6, 353-362.
- Statham, P. J. and Chester, R. 1988. Dissolution of manganese from marine atmospheric particles into seawater and rainwater. *Geochimica et Cosmochimica Acta* 52, 2433-2437.
- Stohl, A. 1998. Computation, accuracy and applications of trajectories—A review and bibliography. *Atmospheric Environment* 32, 947-966.
- Stohl, A. and Seibert, P. 1998. Accuracy of trajectories as determined from the conservation of meteorological tracers. *Quarterly Journal of the Royal Meteorological Society* 125, 1465-1484.
- Stohl, A., Eckhardt, S., Forster, C., James, P., Spichtinger, N. and Seibert, P. 2002. A replacement for simple back trajectory calculations in the interpretation of atmospheric trace substance measurements. *Atmospheric Environment* 36, 4635-4648.
- Stohl, A., Wotawa, G., Seibert, P. and Kromp-Kolb, H., 1995. Interpolation errors in wind fields as a function of spatial and temporal resolution and their impact on different types of kinematic trajectories. *Journal of Applied Meteorology* 34, 2149-2165.
- Sulzberger, B. and Laubscher, H., 1995. Reactivity of various types of Iron(III) (hydr)oxides towards light-induced dissolution. *Marine Chemistry* 50, 103-115.
- Sunda, W. G. and Huntsman, S. A., 1995. Iron uptake and growth limitation in oceanic and coastal phytoplankton. *Marine Chemistry* 50, 189-206.
- Sunda, W. G. and Huntsman, S. A., 1995. Cobalt and zinc interreplacement in marine phytoplankton: Biological and geochemical implications *Limnology and Oceanography* 40, 1404-1417.
- Tanaka, T. Y. and Chiba, M. 2006. A numerical study of the contributions of dust source regions to the global dust budget. *Global and Planetary Change* 52, 88-104.
- Taylor, S. R. 1964. Abundance of chemical elements in the continental crust: A new table. *Geochimica et Cosmochimica Acta* 28, 1237-1285.
- Tegen, I. and Lacis, A. A. 1996. Modeling of particle size distribution and its influence on the radiative properties of mineral dust aerosol. *Journal of Geophysical Research* 101, 19237-19244.
- Tindale, N. W. and Pease, P. P. Aerosol over the Arabian Sea: Atmospheric transport pathways and concentrations of dust and sea salt. *Deep-Sea Research II* 46, 1577-1595.
- Toyoda, M., Kaibuchi, K., Nagasono, M., Terada, Y., Tanabe, T., Hayakawa, S. and Kawai, J. 2004. X-ray analysis of a single aerosol particle with combination of

scanning electron microscope and synchrotron radiation X-ray microscope. *Spectrochimica Acta Part B: Atomic Spectroscopy* 59, 1311-1315.

Tucker, W. G. 2000. An overview of PM_{2.5} sources and control strategies. *Fuel Processing Technology* 65-66, 379-392.

Turner, A., Henon, D. N. and Dale, J. L. L. 2001. Pepsin-digestibility of contaminated estuarine sediments. *Estuarine, Coastal and Shelf Science* 53, 671-681.

UNEP. 1997. Assessment of Land-based Sources and Activities Affecting the Marine Environment in the Red Sea and Gulf of Aden. UNEP Regional Seas Reports and studies No.116.

van den Berg, C. M. G. 1985. Direct determination of molybdenum in seawater by adsorption voltametry. *Analytical Chemistry* 57, 1532-1536.

van den Berg, C. M. G. 1995. Evidence for organic complexation of iron in seawater. *Marine Chemistry* 50, 139-157.

Var, F., Narita, Y. and Tanaka, S. 2000. The concentration, trend and seasonal variation of metals in the atmosphere in 16 Japanese cities shown by the results of National Air Surveillance Network (NASAN) from 1974 to 1996. *Atmospheric Environment* 34, 2755-2770.

Vercelli, E. 1927. *Richerche di oceanografia fisica eseguite della R. N. AMMIRAGLIO MAGNAGHI (1923-24)*, 4, La temperature e la salinita. *Ann. Idrogr.* 11, 1-66.

Veron, A.J., Church, T.M., Flegal, A.R., Patterson, C.C., Erel, Y. 1993. Response of lead cycling in the surface Sargasso Sea to changes on tropospheric input. *Journal of Geophysical Research* 98, 18269–18276.

Voutsas, D. and Samara, C. 2002. Labile and bioaccessible fractions of heavy metals in the airborne particulate matter from urban and industrial areas. *Atmospheric Environment* 36, 3583-3590.

Wai, Ka-Ming and Tanner, P. A. 2004. Wind-dependent sea salt aerosol in a Western Pacific coastal area. *Atmospheric Environment* 38, 1167-1171.

Walsh, P. R. and Duce, R. A. 1976. The solubilisation of anthropogenic atmospheric vanadium in seawater. *Geophysical Research Letters* 3, 375-378.

Walters, K. R. and Sjoberg, W. F. 1988. The Persian gulf region a climatological study. USAFETAC/TN-88/002.

Wang, H. and Shooter, D. 2002. Coarse–fine and day–night differences of water-soluble ions in atmospheric aerosols collected in Christchurch and Auckland, New Zealand. *Atmospheric Environment* 36, 3519-3529.

- Wedepohl, K. H. 1995. The composition of the continental crust. *Geochimica et Cosmochimica Acta* 59, 1217-1232.
- Wells, C. L. 1999. Atmospheric trace metal biogeochemistry and fluxes to shelf seas. Ph.D. thesis , University of Plymouth, UK.
- Wen, Liang-Saw Jiann, Kuo-Tung and Santschi, P. H.. 2006. Physicochemical speciation of bioactive trace metals (Cd, Cu, Fe, Ni) in the oligotrophic South China Sea. *Marine Chemistry* 101, 104-129.
- Wesely, M. L. and Hicks, B. B. 2000. A review of the current status of knowledge on dry deposition. *Atmospheric Environment* 34, 2261-2282.
- Whitby, K. T. 1977. The physical characteristics of sulphur particles. *Atmospheric Environment* 12, 135-159.
- Whitfield, M. 2001. Interactions between phytoplankton and trace metals in the ocean. *Advances in Marine Biology* 41, 1-128.
- Wieprecht, W., Acker, K., Müller, K., Spindler, G., Brüggemann, E., Maenhaut, W., Chi, X., Hitzengerger, R., Bauer, H. and Brink, H. T., 2004. Ionic constitution and comparison of filter and impactor. *Atmospheric Environment* 38, 6477-6486.
- Williams, M. R., Millward, G. E., Nimmo, M., and Fones, G. R. 1998. Fluxes of Cu, Pb and Mn to the North-Eastern Irish Sea: The importance of sedimental and atmospheric inputs. *Marine Pollution Bulletin* 36, 366-375.
- Wollast, R. and Chou, L. 1985. Kinetics of the dissolution of albite with a continuous flow-trough fluidised bed reactor, In: the chemistry of weathering, Drever J. I. (eds). Reidel, Norwell, Mass.
- Wu, J. F., Boyle, E., Sunda, W. and Wen, L. S. 2001. Soluble and colloidal iron in the oligotrophic North Atlantic and North Pacific. *Science* 293, 847-849.
- Wu, J. F. and Boyle, E. 1997. Lead in the western North Atlantic Ocean: Completed response to leaded gasoline phaseout. *Geochimica et Cosmochimica Acta*, 61, 3279-3283.
- Xie, R. K., Seip, H. M., Leinum, J. R., Winje, T. and Xiao, J. S. 2005. Chemical characterization of individual particles (PM₁₀) from ambient air in Guiyang city, China. *Science of the Total Environment* 343, 261-272.
- Xie, Y. and Berkowitz, C. M. 2006. The use of positive matrix factorization with conditional probability functions in air quality studies: An application to hydrocarbon emissions in Houston, Texas. *Atmospheric Environment* 40, 3070-3091.
- Yaaqub, R. R., Davies, T. D., Jickells, T. D. and Miller, J. M., 1991. Trace elements in daily collected aerosols at a site in Southeast England. *Atmospheric Environment* 25A, 985-996.

Yee, D. and Morel, F. M. M., 1996. In vivo substitution of zinc by cobalt in carbonic anhydrase of a marine diatom. *Limnology and Oceanography* 41, 573-577.

Yin, J., Allen, A.G., Harrison, R.M., Jennings, S.G., Wright, E., Fitzpatrick, M., Healy, T., Barry, E., Ceburnis, D. and McCusker, D. 2005. Major component composition of urban PM₁₀ and PM_{2.5} in Ireland. *Atmospheric Research* 78, 149-165.

Yip, F. Y., Keeler, G. J., Dvonch, J. T., Robins, T. G., Parker, E. A., Israel, B. A. and Brakefield-Caldwell, W. 2004. Personal exposures to particulate matter among children with asthma in Detroit, Michigan. *Atmospheric Environment* 38, 5227-5236.

Yuan, H., Kenneth, A. R. and Guoshun, Z. 2004. Graphical techniques for interpreting the composition of individual aerosol particles. *Atmospheric Environment* 38, 6845-6854.

Zatka, V. J., Warner, J. S. and Maskery, D. 1992. Chemical speciation of nickel in airborne dusts: analytical methods and results of an interlaboratory test program. *Environmental Science and Technology*. 26, 138-144.

Zhu, X. Prospero, J. M. Millero, F. J. Savoie, D. L. and Brass, G. W. 1992. The solubility of ferric ion in marine mineral aerosol solutions at ambient relative humidities. *Marine Chemistry* 38, 91-107.

Zhuang, G., Duce R. A., and Kester D. R. 1990. The solubility of atmospheric iron in surface seawater of the open ocean. *Journal of Geophysical Research* 95, 16207-16216.

World Wide Web Pages:

1-(Saudi Geology Survey: <http://www.sgs.org.sa/index.cfm?sec=74&sub=195&sub2=200&page=>)

2- (the NEEP National Energy Efficiency Program: <http://www.neep.org.sa/>)

3- (electricity company web page within references:<http://www.se.com.sa/semain>)

Appendix

Appendix A. Samples concentrations, date and Enrichment Factors at Plymouth and Jeddah

(1) Plymouth:

Sample Number	Date of Collection	Sample Number	Date of Collection
1	10.12-11.12.01	56	13.6.02
2	11.12-12.12.01	57	13.6-14.6.02
3	12.12-13.12.01	58	14.6.02
3	13.12-14.12.01	59	21.6.02
4	13.12.01	60	24.6.02
5	15.12-17.12.01	61	24.6-25.6.02
6	17.12.01	62	25.6.02
7	17.12-18.12.01	63	25.6-26.6.02
8	18.12.01	64	26.6.02
9	18.12-19.12.01	65	26.6-27.6.02
10	19.12.01	66	27.6.02
11	19.12-20.12.01	67	27.6-28.6.02
12	20.12.01	68	28.6.02
13	20.12-21.12.01	69	28.6-31.6.02
14	21.12.01	70	1.7.02
15	3.1.02	71	1.7-2.7.02
16	3.1-4.1.02	72	2.7.02
17	4.1.02	73	3.7.02
18	4.1-5.1.02	74	3.7-4.7.02
19	7.1.02	75	4.7.02
20	7.1-8.1.02	76	4.7-5.7.02
21	8.1.02	77	5.7.02
22	8.1-9.1.02	78	5.7-8.7.02
23	10.1.02	79	8.7.02
24	10.1-11.1.02	80	9.7.02
25	11.1.02	81	9.7-10.7.02
26	11.1-12.1.02	82	10.7.02
27	14.1.02	83	10.7-11.7.02
28	14.2.02	84	11.7.02
29	15.2.02	85	11.7-12.7.02
30	14.2-15.2.02	86	15.7.02
31	15.2-16.2.02	87	16.7.02
32	18.2.02	88	16.7-17.7.02
33	18.2-19.2.02	89	17.7.02
34	12.3.02	90	17.7-18.7.02
35	1.5.02	91	18.7.02
36	2.5.02	92	18.7-19.7.02
37	3.5.02	93	19.7.02
38	3.5-4.5.02	94	23.7.02
39	8.5.02	95	23.7-24.7.02
40	8.5-9.5.02	96	24.7.02
41	24.5-25.5.02	97	24.7-25.7.02
42	28.5-29.5.02	98	25.7.02
43	29.5-30.5.02	99	25.7-26.7.02
44	30.5.02	100	26.7.02
45	30.5-31.5.02	101	26.7-29.7.02
46	31.5.02	102	29.7.02
47	31.5-5.6.02	103	29.7-30.7.02
48	5.6.02	104	12.8.02
49	5.6-6.6.02	105	12.8-13.8.02
50	6.6.02	106	13.8.02
51	6.6-7.6.02	107	13.8-14.8.02
52	10.6-11.6.02	108	14.8.02
53	11.6.02	109	14.8-15.8.02
54	12.6.02	110	15.8.02
55	12.6-13.6.02	111	15.8-16.8.02

Sample Number	Date of Collection	Sample Number	Date of Collection
112	19.8.02	177	4.11.02
113	19.8-20.8.02	178	12.11.02
114	29.8-30.8.02	179	12.11-13.11.02
115	30.8.02	180	13.11-14.11.02
116	2.9.02	181	14.11-15.11.02
117	12.9-13.9.02	182	15.11.02
118	13.9.02	183	15.11-18.11.02
119	13.9-16.9.02	184	18.11.02
120	16.9.02	185	21.11-22.1.02
121	16.9-17.9.02	186	22.11-25.11.02
122	17.9.02	187	2.12-3.12.02
123	17.9-18.9.02	188	3.12-4.12.02
124	18.9.02	189	4.12-5.12.02
125	18.9-20.9.02	190	5.12-6.12.02
126	20.9-23.9.02	191	6.12-9.12.02
127	23.9-24.9.02	192	13.12.02
128	24.9.02	193	13.12-16.12.02
129	24.9-25.9.02	194	17.12.02
130	25.9.02	195	17.12-18.12.02
131	25.9-26.9.02	196	19.12-20.12.02
132	26.9.02	197	28.1-30.1.03
133	26.9-27.9.02	198	30.1-2.2.03
134	27.9.02	199	2.2-10.2.03
135	27.9-30.9.02	200	11.2-14.2.03
136	30.9.02	201	14.2-26.2.03
137	30.9-1.10.02	202	28.2-3.3.03
138	1.10.02	203	13.3-17.03.03
139	1.10-2.10.02	204	17.03-21.3.03
140	2.10-3.10.02	205	21.3-24.3.03
150	3.10.02	206	24.-27.3.03
151	3.10-4.10.02	207	27.3-30.3.03
152	4.10.02	208	16.4-19.4.03
153	4.10-7.10.02		
154	7.10.02		
155	7.10-8.10.02		
156	8.10.02		
157	8.10-9.10.02		
158	9.10.02		
159	9.10-10.10.02		
160	10.10.02		
161	10.10-11.10.02		
162	11.10.02		
163	14.10.02		
164	14.10-15.10.02		
165	15.10-16.10.02		
166	16.10-17.10.02		
167	17.10-18.10.02		
168	18.10.02		
169	18.10-21.10.02		
170	23.10.02		
171	23.10-24.10.02		
172	24.10.02		
173	25.10.02		
174	25.10-28.10.02		
175	25.10-28.10.02		
176	28.10-29.10.02		

Concentration (ng m⁻³)

	Al	Mn	Fe	Na	V	Ni	Co	Zn	Mo	Cd	Pb
41	172		119	778471	0.80	3.40	0.13	1.87	*	0.082	2.67
42	380	2.62	52.2	15248	1.60	*	0.10	90.22	0.12	0.18	1.34
43	211	3.78	180	10574	2.60	1.05	0.13	30.71	0.39	0.05	2.38
44	276	4.91	308	8284	4.11	*	0.20	36.94	0.67	0.11	4.25
45	242	2.96	255	6423	2.23	0.17	0.08	38.31	0.35	0.12	4.82
46	245	4.24	286	3553	6.24	1.23	0.40	24.87	0.65	0.09	4.34
49	175	4.33	275	1418	1.84	*	0.12	19.82	0.23	0.07	2.70
50	210	7.65	353	1298	3.33	4.38	0.33	*	0.69	0.38	11.66
51	63.4	1.82	93.2	8404	3.15	2.14	0.09	84.0	0.21	0.04	1.80
52	253	10.3	272	10465	2.38	11.97	0.39	*	0.50	0.11	5.17
53	212	11.6	199	3857	2.48	18.01	0.60	*	0.47	0.16	5.62
54	269	7.50	287	2852	1.26	8.15	0.33	169	0.67	0.08	5.17
55	69.8	1.86	39	1330	2.97	1.87	0.11	158	0.08	0.03	1.04
56	129	1.24	176	753	5.22	1.16	0.13	65.7	0.55	0.05	2.39
57	100	2.61	68.0	998	19.9	11.70	0.31	*	0.24	0.09	2.90
58	95.3	3.95	99.2	5609	6.94	8.74	0.24	153	0.27	0.05	1.62
59	239	3.16	210	3938	10.7	4.47	0.20	64.0	0.59	0.03	2.86
60	70.3	1.17	87.0	351	0.25	*	0.07	7.39	0.17	0.02	1.43
61	154	2.54	181	3330	1.77	*	0.07	15.7	0.30	0.20	8.92
62	229	7.70	295	654	1.19	*	0.20	20.0	0.73	0.05	4.86
63	121	4.53	369	998	3.62	*	0.12	14.3	0.49	0.06	3.82
64	328	9.03	425	1271	1.44	*	0.26	22.1	0.70	0.06	4.89
65	147	4.94	284	2687	1.54	*	0.10	10.7	0.35	0.03	2.16
66	465	14.4	391	1274	1.22	0.26	0.28	23.5	0.40	0.03	6.51
67	324	8.31	425	2676	1.63	0.19	0.17	14.5	0.37	0.07	4.78
68	512	11.7	514	3016	1.58	0.06	0.31	20.7	0.41	0.06	6.05
69	198	6.30	387	2298	1.62	0.67	0.13	15.2	0.62	0.17	5.02
70	133	4.22	218	2694	*	1.49	0.08	12.5	0.36	0.033	3.91
72	135	1.59	91.2	12207	2.07	1.58	0.03	6.43	0.19	0.012	1.17

73	186	6.53	274	6623	0.51	6.38	0.23	151	0.63	0.128	4.73
74	248	7.07	364	2465	0.01	2.33	0.12	16.4	0.42	0.055	4.60
75	114	3.85	230	3726	1.55	2.49	0.07	15.2	0.38	0.049	3.73
76	164	3.46	182	2231	0.40	1.73	0.07	15.1	0.38	0.030	2.51
77	29.5	1.58	32.5	3200	1.87	3.73	0.07	30.7	0.12	0.017	0.49
78	222	7.56	435	646	0.20	4.18	0.17	29.0	0.93	0.071	4.64
79	58.1	2.86	129	1989	1.90	4.07	0.12	36.4	0.28	0.039	3.24
80	56.9	2.12	113	852	0.40	2.09	0.05	28.4	0.36	0.030	1.67
81	198	6.33	363	1520	0.195	2.81	0.114	31.5	0.810	0.070	6.22
83	211	5.97	335	2316	1.52	2.98	0.15	27.8	0.68	0.069	9.39
84	83.7	2.79	169	4250	1.35	1.65	0.03	9.81	0.36	0.056	1.84
85	225	6.71	350	2623	0.74	2.95	0.14	34.6	0.80	0.062	4.70
87	359	10.5	418	*	0.15	3.19	0.17	21.1	0.34	0.086	8.50
88	461	12.0	546	*	1.41	4.36	0.32	25.3	0.35	0.092	26.1
89	107	15.5	290	575	6.21	12.0	0.51	36.5	0.89	0.168	11.4
90	538	15.0	604	57	0.20	4.56	0.38	24.3	0.35	0.078	16.0
91	163	6.67	392	101	0.66	3.14	0.11	14.0	0.22	0.180	8.37
92	476	14.8	517	239	0.97	4.15	0.31	37.4	0.61	0.339	14.3
93	318	18.0	433	774	9.73	7.15	0.22	24.2	0.81	0.297	10.6
95	284	30.3	359	4339	*	53.6	1.86	*	0.66	0.424	8.84
96	68.7	3.47	191	2183	0.23	1.76	0.07	9.44	0.16	0.041	10.5
97	267	8.61	385	917	*	2.79	0.14	16.3	0.46	0.057	6.54
101	66.9	2.62	139	13867	5.161	1.78	0.060	0.946	0.257	0.033	2.28
103	*	10.0	423	1531	1.61	*	0.177	5.12	0.336	0.142	5.31
105	68.9	3.46	203	27886	2.54	0.849	0.073	0.943	0.209	0.057	2.48
107	361	5.91	261	19475	13.3	6.12	0.204	3.86	0.352	0.018	2.30
109	120	4.40	193	11063	13.5	5.39	0.219	1.56	0.472	0.090	3.69
111	*	5.73	379	48073	0.89	0.428	0.100	0.92	0.400	0.161	1.92
113	*	4.19	281	18914	1.78	2.15	0.109	0.808	0.321	0.071	5.00
114	59.0	3.44	91.4	8260	5.25	6.43	0.168	22.9	0.345	0.147	3.46
117	564	23.5	685	24521	12.6	5.26	0.379	6.86	1.46	0.655	22.6
119	445	11.2	370	48633	5.97	2.42	0.192	3.15	0.747	0.281	6.36

121	783	13.5	481	25643	4.93	2.25	0.259	6.22	0.835	0.514	24.8
123	263	19.0	253	44708	8.55	3.07	0.216	3.63	0.573	0.279	8.28
125	469	20.5	490	44147	10.4	4.25	0.446	3.85	1.43	0.281	11.5
126	384	13.9	484	32933	5.77	4.84	0.258	3.95	0.933	0.447	20.0
127	557	9.64	424	27325	1.42	0.819	0.205	2.38	0.453	0.399	17.8
129	516	12.9	597	15549	2.57	1.40	0.250	4.80	0.747	1.14	31.1
131	346	12.8	675	18353	5.22	2.77	0.299	2.48	0.976	0.219	14.8
133	122	7.99	402	35736	2.31	1.88	0.182	9.17	0.540	0.185	6.53
135	519	12.7	452	64521	9.1	3.75	0.280	5.18	0.983	0.364	13.1
137	340	9.6	349	16671	10.1	4.13	0.432	4.07	0.787	0.300	11.4
139	160	5.27	198	1531	2.10	0.88	0.083	4.05	0.558	0.162	10.02
151	194	9.76	641	45830	1.56	1.43	0.147	5.77	1.29	0.394	10.43
153	80.9	3.90	232	64521	2.04	1.03	0.076	1.40	0.509	0.141	5.44
155	255	7.09	248	29568	6.32	2.42	0.178	1.65	0.516	0.243	8.33
157	346	10.2	280	31250	3.20	1.49	0.193	5.21	0.560	0.542	13.5
159	378	36.8	448	37979	8.6	4.63	0.411	6.93	1.82	0.564	23.4
164	124	8.37	220	30363	4.36	2.47	0.751	4.18	0.722	0.239	7.37
169	74.9	7.27	268	36643	1.82	3.81	0.323	6.96	0.758	0.186	6.41
171	*	8.24	232	36643	0.823	1.38	0.555	3.92	0.729	0.358	10.8
174	2.03	1.14	46.6	56621	0.397	0.485	0.175	0.415	0.197	0.067	0.99
176	764	23.19	483	115264	5.55	4.62	0.937	8.32	0.631	0.536	8.91
179	89.7	4.68	172	64613	2.70	1.79	0.637	0.663	0.318	0.051	1.36
183	427	8.56	336	64042	3.48	1.93	0.359	4.35	0.861	0.365	26.0
186	52.6	2.06	55.6	412091	5.07	1.99	0.210	0.809	0.306	0.080	4.92
193	203	7.09	188	36072	4.46	3.73	0.320	3.19	1.81	0.393	16.4
195	289	6.38	204	49771	2.16	1.55	0.399	2.16	0.812	0.207	11.6

	Al	Mn	Fe	Na	V	Ni	Co	Zn	Mo	Cd	Pb
1	723	24.4	*	*	10.1	5.72	1.10	54.7	1.37	0.509	22.9
2	530	11.1	*	*	3.11	2.50	0.440	21.0	0.621	0.172	11.0
3	357	6.91	*	*	3.05	1.95	0.291	22.9	0.554	0.177	12.1
4	1032	21.3	*	*	3.27	3.49	0.902	24.7	0.359	0.115	6.08
5	1265	20.2	*	*	8.89	5.05	0.776	40.7	0.987	0.315	21.6
6	758	16.9	*	*	2.03	4.06	1.650	24.3	0.470	0.104	8.31
7	137	5.26	*	*	1.28	1.57	0.133	23.9	0.552	0.370	16.0
8	880	15.7	*	*	1.78	3.45	0.704	23.8	0.633	0.063	11.1
9	144	4.06	*	*	0.901	1.30	0.146	15.1	0.348	0.410	11.8
10	633	15.8	*	*	3.13	3.50	0.302	24.8	0.830	0.123	14.5
11	128	3.09	*	*	1.08	1.55	0.064	8.18	0.357	0.086	5.09
12	773	15.9	*	*	1.86	3.65	0.523	26.1	0.654	0.091	7.73
13	181	5.86	*	*	1.85	1.80	0.323	15.4	0.658	0.178	9.74
14	*	*	*	*	0.025	1.83	0.327	11.2	0.527	0.039	4.03
15	1097	22.5	743	33193	6.08	1.30	21.9	135	1.11	0.640	28.4
16	277	5.26	228	51231	9.20	0.33	7.50	46.2	0.66	0.748	21.3
17	448	11.2	364	33193	6.38	0.47	6.68	57.2	0.94	1.27	22.6
18	68.3	6.58	85.3	145436	7.70	0.41	10.6	46.0	0.34	0.219	7.35
19	3520	88.8	2591	9081	25.09	4.12	19.8	148	2.30	0.710	44.1
20	246	12.3	257	20296	7.02	0.20	4.44	30.3	1.07	0.248	11.8
21	2021	54.5	1250	14689	13.55	4.14	9.74	76.4	1.68	0.587	23.9
22	318	10.2	314	29268	3.29	0.36	4.09	52.6	0.83	0.339	15.7
23	1322	30.6	1679	44408	6.63	1.65	6.83	86.2	3.08	0.644	84.3
24	682	21.5	1608	2352	2.77	0.57	15.9	91.4	3.20	0.627	83.2
25	4600	56.7	2823	4595	8.79	7.04	10.8	191	5.58	2.08	63.8
26	820	13.7	457	184781	7.17	0.62	14.7	66.2	0.61	0.205	11.8
27	371	10.5	201	63006	4.90	0.70	18.7	131	0.55	0.298	5.83
28	1040	23.9	842	24782	2.19	0.86	51.0	51.0	0.91	0.276	20.0
29	1084	22.0	774	6278	2.52	0.81	35.8	35.8	0.83	0.235	16.0
30	357	89.6	795	632677	1.80	7.56	*	256	0.86	0.880	40.1
31	1146	207	3168	756041	11.12	15.56	*	603	6.49	4.40	157

	378	6.58	382	4035	0.90	0.16	2.78	20.1	0.53	0.069	5.57
33	121	1.86	147	531742	0.29	0.12	1.91	9.27	0.50	0.040	2.57
34	3128	95.8	2025	33754	9.09	3.54	38.9	486	1.11	0.626	29.6
35	4597	35.6	602	14689	2.61	0.33	4.24	35.6	0.86	0.313	10.8
36	317	9.16	730	41604	2.61	0.25	5.36	43.1	0.61	0.315	10.9
37	575	10.2	540	14689	2.41	12.36	0.31	3.63	28.0	0.159	8.35
38	218	7.34	383	36090	2.64	7.50	0.17	1.89	63.6	0.507	11.3
39	1510	37.4	1070	1792	4.97	35.94	2.77	6.43	105	0.789	24.9
40	885	19.0	815	2352	4.40	19.43	0.46	6.09	542	0.955	28.0

(2) Jeddah

Sample Number	Date of Collection	Sample Number	Date of Collection
1	10.8-11.8.02	57	3.2-4.2.03
2	11.8-12.8.02	58	4.2-5.2.03
3	12.8-13.8.02	59	5.2-6.2.03
4	13.8-14.8.02	60	6.2-7.2.03
5	14.8-15.8.02	61	8.2-9.2.03
6	15.8-16.8.02	62	9.2-10.2.03
7	16.8-17.8.02	63	10.2-11.2.03
8	17.8-18.8.02	64	11.2-12.2.03
9	18.8-19.8.02	65	12.2-14.2.03
10	19.8-20.8.02	66	14.2-15.2.03
11	20.8-21.8.02	67	15.2-17.2.03
12	21.8-22.8.02	68	17.2-18.2.03
13	22.8-23.8.02	69	18.2-19.2.03
14	24.8-25.8.02	70	19.2-20.2.03
15	25.8-26.8.02	71	20.2-21.2.03
16	26.8-27.8.02	72	21.2-22.2.03
17	27.8-28.8.02	73	22.2-23.2.03
18	28.8-29.8.02	74	23.2-24.2.03
19	29.8-30.8.02	75	24.2-25.2.03
20	30.8-31.8.02	76	25.2-27.2.03
21	31.8-1.9.02	77	27.2-28.2.03
22	1.9-2.9.02	78	1.3-2.3.03
23	2.9-3.9.02	79	2.3-3.3.03
24	3.9-4.9.02	80	3.3-4.3.03
25	7.9-8.9.02	81	4.3-11.3.03
26	8.9-9.9.02	82	11.3-12.3.03
27	9.9-10.9.02	83	12.3-13.3.03
28	10.9-11.9.02	84	13.3-14.3.03
29	14.9-15.9.02	85	14.3-15.3.03
30	23.9-24.9.02	86	15.3-16.3.03
31	28.9-29.9.02	87	16.3-17.3.03
32	29.9-30.9.02	88	17.3-18.3.03
33	30.9-1.10.02	89	18.3-19.3.03
34	6.1-7.1.03	90	19.3-22.3.03
35	7.1-8.1.03	91	22.3-23.3.03
36	8.1-9.1.03	92	23.3-24.3.03
37	9.1-10.1.03	93	24.3-25.3.03
38	10.1-11.1.03	94	26.3-28.3.03
39	13.1-14.1.03	95	28.3-29.3.03
40	11.1-12.1.03	96	29.3-30.3.03
41	12.1-13.1.03	97	30.3-1.4.03
42	14.1-15.1.03	98	1.4-5.4.03
43	15.1-16.1.03	99	5.4-6.4.03
44	16.1-17.1.03	100	6.4-7.4.03
45	17.1-18.1.03	101	7.4-8.4.03
46	18.1-19.1.03	102	8.4-9.4.03
47	19.1-20.1.03	103	9.4-12.4.03
48	20.1-21.1.03	104	12.4-13.4.03
49	21.1-22.1.03	105	13.4-14.4.03
50	22.1-23.1.03	106	14.4-15.4.03
51	23.1-24.1.03	107	15.4-16.4.03
52	27.1-28.1.03	108	16.4-19.4.03
53	28.1-29.1.03	109	19.4-20.4.03
54	29.1-30.1.03	110	20.4-21.4.03
55	30.1-1.2.03	111	21.4-22.4.03
56	1.2-2.2.03	112	22.4-23.4.03

Sample Number	Date of Collection	Sample Number	Date of Collection
113	23.4-24.4.03	169	24.6-25.6.03
114	24.4-26.4.03	170	25.6-28.6.03
115	26.4-27.4.03	171	28.6-29.6.03
116	27.4-28.4.03	172	29.6-30.6.03
117	28.4-29.4.03	173	30.6-1.7.03
118	29.4-30.4.03	174	1.7-2.7.03
119	30.4-1.5.03	175	2.7-3.7.03
120	1.5-2.5.03	176	3.7-4.7.03
121	2.5-3.5.03	177	4.7-5.7.03
122	3.5-4.5.03	178	5.7-8.7.03
123	4.5-5.5.03	179	6.7-7.7.03
124	6.5-7.5.03	180	7.7-8.7.03
125	7.5-8.5.03	181	8.7-9.7.03
126	8.5-10.5.03	182	9.7-10.7.03
127	10.5-11.5.03	183	10.7-12.7.03
128	11.5-12.5.03	184	12.7-13.7.03
129	12.5-13.5.03	185	13.7-14.7.03
130	13.5-14.5.03	186	14.7-15.7.03
131	14.5-15.5.03	187	15.6-16.7.03
132	16.5-17.5.03	188	16.7-17.7.03
133	17.5-20.5.03	189	17.7-18.7.03
134	20.5-21.5.03	190	19.7-20.7.03
135	21.5-22.5.03	191	20.7-21.7.03
136	22.5-23.5.03	192	21.7-22.7.03
137	23.5-24.5.03	193	22.7-23.7.03
138	24.5-25.03	194	23.7-29.7.03
139	25.5-26.5.03	195	29.7-30.7.03
140	26.5-27.5.03	196	30.7-2.8.03
141	27.5-28.5.03	197	2.8-3.8.03
142	28.5-29.5.03	198	3.8-4.8.03
143	29.5-30.5.03	199	4.8-5.8.03
144	30.5-31.5.03	200	5.8-6.8.03
145	31.5-1.6.03	201	6.8-7.8.03
146	1.6-2.6-.03	202	7.8-9.8.03
147	2.6-3.6.03	203	9.8-10.8.03
148	3.6-4.6.03	204	10.8-11.8.03
149	4.6-5.6.03	205	11.8-12.8.03
150	5.6-6.6.03	206	12.8-13.8.03
151	6.6-7.6.03	207	13.8-14.8.03
152	7.6-8.6.03	208	14.8-16.8.03
153	8.6-9.6.03	209	16.8-17.8.03
154	9.6-10.6.03	210	17.8-19.8.03
155	10.6-11.6.03	211	19.8-20.8.03
156	11.6-12.6.03	212	20.8-21.8.03
157	12.6-13.6.03	213	21.8-22.8.03
158	13.6-14.6.03	214	22.8-23.8.03
159	14.6-15.6.03	215	23.8-24.8.03
160	15.6-16.6.03	216	24.8-25.8.03
161	16.6-17.6.03	217	25.8-26.8.03
162	17.6-18.6.03	218	26.8-27.8.03
163	18.6-19.6.03	219	27.8-30.8.03
164	19.6-20.6.03	220	30.8-31.8.03
165	20.6-21.6.03	221	16.9-17.9.03
166	21.6-22.6.03	222	17.9-18.9.03
167	22.3-23.6.03	223	18.9-19.9.03
168	23.6-24.6.03	224	19.9-20.9.03

Sample Number	Date of Collection	Sample Number	Date of Collection
225	20.9-21.9.03	281	24.11-25.11.03
226	21.9-22.9.03	282	25.11-26.11.03
227	22.9-23.9.03	283	26.11-27.11.03
228	23.9-25.9.03	284	27.11-28.11.03
229	25.9-27.9.03	285	28.11-29.11.03
230	27.9-28.9.03	286	29.11-30.11.03
231	28.9-29.9.03	287	30.11-1.12.03
232	29.9-30.9.03	288	1.12-3.12.03
233	30.9-1.10.03	289	3.12-6.12.03
234	1.10-2.10.03	290	6.12-7.12.03
235	2.10-3.10.03	291	7.12-8.12.03
236	3.10-4.10.03	292	8.12-9.12.03
237	4.10-5.10.03	293	9.12-10.12.03
238	5.10-6.10.03	294	10.12-12.12.03
239	6.10-7.10.03	295	12.12-13.12.03
240	7.10-8.10.03	296	13.12-14.12.03
241	8.10-9.10.03	297	14.12-15.12.03
242	9.10-10.10.03	298	15.12-16.12.03
243	10.10-11.10.03	299	16.12-17.12.03
244	11.10-12.10.03	300	17.12-24.12.03
245	12.10-13.10.03	301	24.12-25.12.03
246	13.10-14.10.03	302	25.12-27.12.03
247	15.10-16.10.03	303	27.12-28.12.03
248	16.10-17.10.03	304	28.12-29.12.03
249	17.10-18.10.03	305	29.12-30.12.03
250	18.9-19.10.03	306	30.12-31.12.03
251	19.10-20.10.03	307	4.1-5.1.04
252	20.10-21.10.03	308	5.1-6.1.04
253	21.10-22.10.03	309	6.1-7.1.04
254	22.10-23.10.03	310	7.1-8.1.04
255	23.10-25.10.03	311	8.1-10.1.04
256	25.10-26.10.03	312	10.1-11.1.04
257	26.10-27.10.03		
258	27.10-28.10.03		
259	28.10-29.10.03		
260	29.10-30.10.03		
261	30.10-1.11.03		
262	1.11-2.11.03		
263	2.11-3.11.03		
264	3.11-4.11.03		
265	4.11-5.11.03		
266	5.11-7.11.03		
267	7.11-8.11.03		
268	8.11-9.11.03		
269	9.11-10.11.03		
270	10.11-12.11.03		
271	12.11-14.11.03		
272	14.11-16.11.03		
273	16.11-17.11.03		
274	17.11-18.11.03		
275	18.11-19.11.03		
276	19.11-20.11.03		
277	20.11-21.11.03		
278	21.11-22.11.03		
279	22.11-23.11.03		
280	23.11-24.11.03		

Concentration (ng m⁻³)

Sample	Al	Mn	Fe	V	Co	Ni	Cu	Zn	Mo	Cd
1	1277.7	17.2	1036.0	4.82	0.50	8.69	2.94	50.30	0.08	0.16
2	1440.0	18.2	1001.0	17.52	0.46	12.53	2.84	27.49	0.24	0.07
4	1821.8	24.3	1456.5	8.14	0.77	13.30	5.48	107.28	0.27	0.09
5	1113.9	22.9	797.7	6.86	0.60	9.10	2.06	30.74	0.12	0.06
7	1954.0	22.4	1283.9	10.39	0.60	12.06	4.28	55.85	0.23	0.12
9	6287.5	98.0	6505.4	21.38	2.96	58.66	9.70	344.61	0.66	0.56
10	34714.6	527.5	26609.6	296.09	12.92	289.49	132.25	1462.65	6.36	3.25
11	1190.0	16.0	901.6	8.45	0.41	8.71	3.70	45.33	0.19	0.09
12	2376.5	31.8	1718.7	9.57	0.81	14.37	8.96	95.83	0.21	0.18
13	322.3	4.6	279.6	1.34	0.12	2.28	0.14	10.87	0.04	0.02
14	17210.8	194.3	10498.8	200.0	12.8	192.9	24.7	2150.4	13.13	14.10
35	1431.9	48.3	1478.0	24.31	1.19	6.86	7.32	24.65	0.29	0.06
36	1936.0	96.5	2826.5	33.65	2.38	9.24	11.67	37.99	0.45	0.08
37	1305.7	56.2	1885.0	24.56	1.53	7.40	13.23	31.27	0.74	0.07
38	649.6	22.4	640.2	10.27	0.66	3.08	8.24	13.89	0.18	0.04
39	1602.9	90.9	2356.5	36.92	2.54	10.35	9.67	27.77	0.35	0.08
40	1684.7	62.2	1763.6	24.62	1.77	7.50	16.00	27.26	0.54	0.10
41	1582.3	67.1	1983.2	27.52	1.77	8.08	15.28	27.10	0.52	0.11
42	1856.7	87.2	2612.5	35.92	2.20	10.63	8.87	26.28	0.32	0.11
43	1466.8	44.8	1564.4	15.49	1.26	5.10	7.62	68.02	0.25	0.13
44	1459.7	49.8	1474.5	13.54	1.44	5.63	7.32	24.05	0.27	0.08
45	1547.1	45.2	1603.5	15.60	1.28	4.84	5.12	21.31	0.15	0.04
46	542.9	17.9	500.4	7.20	0.62	1.93	2.43	11.13	0.08	0.05
47	635.2	21.6	665.6	11.80	0.69	3.53	7.24	23.31	0.49	0.05
49	555.2	16.5	576.9	12.10	0.55	3.01	2.52	24.88	0.12	0.07
50	1053.2	38.0	1258.4	13.56	1.05	4.20	11.77	20.19	1.13	0.06
51	1380.0	48.4	1583.2	19.84	1.30	5.22	26.54	33.00	1.83	0.13
52	774.5	37.0	1013.2	20.67	1.21	4.81	3.80	12.65	0.15	0.13
53	1324.5	43.9	1399.7	20.09	1.23	4.07	2.98	15.60	0.16	0.08

54	1045.7	28.3	872.4	12.74	0.93	3.02	2.90	14.85	0.13	0.07
55	1381.4	45.5	1454.1	19.12	1.20	4.06	3.13	10.38	0.18	0.05
56	1516.3	48.1	1414.6	18.90	1.47	4.84	4.66	16.58	0.27	0.09
57	1837.1	26.8	2021.7	14.41	0.83	2.72	1.46	6.30	0.09	0.07
58	2491.4	57.2	2250.7	23.03	1.91	5.15	4.88	15.38	0.28	0.19
59	2918.3	87.1	3019.0	32.61	2.92	8.05	13.51	26.47	0.42	0.29
60	3399.0	137.1	4075.6	41.66	4.55	10.60	9.36	19.83	0.47	0.22
61	1782.3	17.7	1159.6	5.25	1.00	1.77	2.15	8.04	0.08	0.04
62	8628.2	0.0	4922.1	*	*	*	*	*	*	*
63	3048.7	30.0	2028.1	9.50	1.53	2.70	4.32	22.63	0.16	0.07
64	1834.7	26.5	1494.6	12.34	0.81	3.41	9.15	37.97	0.36	0.05
65	3045.1	35.5	2282.7	17.08	1.51	5.99	8.27	21.68	0.48	0.04
66	2376.0	23.5	1687.2	7.03	1.18	2.74	5.02	21.66	0.15	0.02
67	1063.2	11.4	883.7	4.54	0.30	1.40	2.83	17.04	0.13	0.02
68	1603.6	24.4	1283.6	10.83	0.65	3.23	6.20	20.70	0.26	0.03
69	2941.6	46.1	2426.0	26.98	1.00	6.59	12.71	45.73	0.66	0.12
70	3112.8	46.9	2401.3	20.29	1.24	6.35	6.73	18.20	0.17	0.09
71	4952.3	55.4	3378.0	16.81	2.98	4.20	4.50	19.62	0.19	0.04
72	3420.7	39.3	2345.8	11.96	1.81	3.09	3.29	13.59	0.09	0.01
73	2407.3	33.1	1766.9	9.10	1.35	2.97	3.05	13.11	0.08	0.11
74	1730.3	20.4	1207.6	5.52	0.68	1.59	2.35	10.50	0.09	0.03
75	2955.9	51.7	2740.1	14.00	2.73	3.82	5.50	17.82	0.19	0.03
76	1520.4	22.7	1155.5	5.50	0.66	1.43	3.25	8.87	0.05	0.01
77	760.9	12.2	605.5	3.85	0.34	2.22	2.39	11.91	0.07	0.01
78	4264.9	67.9	3248.7	16.48	2.39	5.80	10.95	26.17	0.70	0.06
79	3029.1	21.8	2363.0	10.78	0.29	2.11	1.75	4.72	0.11	*
80	4464.6	134.9	6361.8	40.31	4.98	14.17	14.15	50.79	0.52	0.13
81	461.5	13.5	610.2	3.73	0.48	1.34	1.17	5.97	0.04	0.03
82	657.4	8.9	514.7	4.02	0.00	0.93	1.71	12.47	0.07	0.00
83	2697.6	17.4	2084.9	5.61	0.21	1.02	0.44	8.53	0.02	0.02
84	3638.4	31.0	2788.7	10.04	0.50	3.24	2.88	19.26	0.05	0.02
85	2796.2	58.3	2088.9	17.69	1.31	5.22	6.27	31.89	0.18	0.10

86	15470.2	306.9	12018.1	91.45	7.53	28.52	41.19	132.43	1.79	0.20
87	1714.3	132.4	1379.8	52.89	2.72	19.38	12.97	122.54	0.58	0.43
88	615.3	38.2	525.2	32.90	1.09	7.88	6.89	53.00	0.24	0.23
89	1971.4	91.3	1450.0	47.33	2.69	14.52	19.69	80.01	0.57	0.26
90	4001.7	314.0	5926.3	85.89	14.46	18.34	19.14	74.88	1.04	0.21
91	4131.7	125.4	2282.9	38.45	3.28	9.42	10.90	67.22	0.42	0.44
92	1288.3	53.7	956.4	19.55	2.45	7.75	18.47	58.05	0.18	0.35
93	2775.5	235.6	3572.5	74.05	7.80	22.49	38.87	102.02	0.60	0.35
94	4924.4	366.5	5692.0	75.76	13.21	19.56	18.63	78.45	0.83	0.17
95	1918.1	65.4	1412.4	28.76	3.55	7.17	9.08	51.85	0.40	0.32
96	1218.9	66.6	972.1	28.11	2.12	7.64	9.25	81.84	0.35	0.52
97	673.1	28.3	499.1	22.64	0.83	6.03	7.50	44.04	0.17	0.21
98	1483.5	70.1	1429.2	45.30	2.72	13.57	15.13	51.05	0.51	0.13
99	5276.0	249.6	4042.3	43.15	5.74	17.23	31.76	92.69	1.02	0.20
100	6425.7	12.7	4670.8	32.13	0.07	7.89	5.60	21.54	0.38	0.49
101	6593.3	271.8	5535.7	82.38	7.71	22.27	31.45	82.57	0.97	0.23
102	7573.9	325.4	7017.8	145.13	11.58	27.59	43.62	91.27	1.23	0.25
103	2528.5	195.9	4019.8	52.47	4.54	20.15	14.03	42.38	0.66	0.16
104	4009.7	144.6	2870.4	42.56	3.47	16.67	11.84	43.48	0.50	0.37
105	8237.2	269.1	6629.2	81.17	11.05	26.86	18.41	78.29	1.03	0.30
106	5265.3	157.9	3879.1	51.74	6.29	17.51	22.14	52.55	0.61	0.28
107	3709.2	106.6	2463.6	44.91	3.16	11.52	11.53	41.61	0.38	0.16
108	1319.6	54.5	1366.0	26.67	2.24	6.92	10.04	44.57	0.42	0.10
109	4344.8	182.6	3398.0	97.95	3.72	33.10	31.83	64.83	0.87	0.19
110	5214.9	173.9	4646.7	67.50	6.07	14.71	16.51	46.40	0.53	0.26
111	1357.3	208.5	4104.9	39.71	4.69	18.17	29.40	87.09	0.54	0.32
112	5034.5	102.9	4362.4	13.35	0.19	11.80	21.58	30.60	0.22	0.24
113	3996.8	75.7	2955.3	13.73	0.15	8.38	5.58	29.16	0.21	0.16
114	5182.8	102.5	4041.9	27.22	0.37	11.35	17.23	40.26	0.55	0.17
115	7972.6	131.8	5965.2	23.97	0.68	14.70	10.11	44.92	0.33	0.26
116	5032.7	96.8	4153.6	15.97	0.55	11.43	6.75	37.90	0.24	0.22
117	5918.9	113.3	4508.7	17.32	0.59	11.40	5.60	31.28	0.21	0.23

118	5528.1	97.8	4054.3	13.42	0.56	9.91	5.84	29.82	0.25	0.21
119	4107.8	70.4	3011.3	17.96	0.41	15.76	4.37	29.99	0.30	0.26
120	9861.1	161.8	7005.2	33.12	0.88	21.36	10.44	52.02	0.61	0.27
121	8267.7	183.0	7540.3	30.19	0.93	24.81	10.13	43.42	0.44	0.17
122	6435.0	117.0	4855.5	18.44	0.73	14.92	9.66	32.63	0.36	0.12
123	7194.3	143.5	5616.0	30.82	0.90	21.19	9.87	40.00	0.40	0.14
124	9494.8	182.4	7337.4	34.91	1.02	23.49	13.38	45.18	0.57	0.16
125	11442.2	217.8	8613.9	32.22	1.26	23.98	19.60	57.12	0.93	0.18
126	3974.8	76.3	2946.2	13.08	0.51	19.25	7.33	25.84	0.29	0.18
127	5186.4	103.0	3874.1	21.00	0.64	15.74	15.07	42.90	0.37	0.09
128	6047.1	114.7	4563.1	25.88	0.65	17.47	6.71	35.33	0.28	0.10
129	5699.8	104.5	4207.4	23.93	0.52	13.64	5.16	28.13	0.22	0.07
130	5314.0	113.3	4309.8	33.97	0.64	19.18	8.53	35.08	0.35	0.09
131	2003.4	47.0	2440.6	16.17	0.91	5.81	10.63	32.84	0.43	0.42
132	8729.9	114.7	5898.2	50.57	3.13	20.27	23.46	72.66	0.81	0.69
133	3795.6	41.3	2176.9	20.39	1.26	7.54	8.00	25.55	0.26	0.11
134	893.1	24.4	1407.6	10.22	0.42	3.56	5.26	17.44	0.14	0.04
135	3972.5	52.1	2713.2	19.99	1.38	7.95	13.00	45.05	0.28	0.18
136	5569.6	66.2	3543.9	27.02	1.85	9.98	14.21	42.71	0.51	0.20
137	2866.2	33.6	1852.0	13.53	0.72	4.46	6.74	29.59	0.21	0.18
138	4010.3	62.2	3060.9	27.11	1.30	8.92	18.04	40.55	0.27	0.24
139	6201.7	88.8	4105.6	45.13	1.52	12.86	16.22	42.82	0.53	0.28
140	5359.6	71.5	3464.1	29.48	0.98	10.57	9.09	34.92	0.28	0.17
141	1789.4	39.6	2157.3	15.32	0.39	4.80	4.67	23.88	0.15	0.08
142	1310.2	16.9	1033.7	8.41	*	2.24	3.43	15.62	0.10	0.02
143	4661.7	50.2	2786.5	25.38	0.69	7.36	16.78	50.24	0.78	0.13
144	7034.5	68.4	3841.2	48.19	1.48	13.43	13.94	35.22	0.39	0.15
145	10295.5	114.5	6834.2	38.15	2.68	11.79	14.89	41.88	0.48	0.21
146	8076.2	100.3	5390.2	31.32	2.63	12.23	17.81	47.09	0.42	0.17
147	6562.4	86.4	4661.9	26.22	2.05	10.07	16.40	45.11	0.35	0.17
148	1828.8	34.8	1759.9	13.50	0.43	4.23	4.89	24.24	0.10	0.08
149	3915.4	54.7	2585.4	25.37	1.72	10.35	12.23	37.88	0.38	0.23

150	1775.5	27.9	1331.6	14.88	0.41	5.31	9.28	28.11	0.20	0.19
151	1236.8	21.6	1262.6	16.46	0.10	4.45	3.90	20.13	0.17	0.11
152	1898.5	26.0	1529.4	18.33	0.24	5.11	3.61	18.55	0.12	0.05
153	8685.0	81.3	4559.3	36.62	2.39	12.57	12.80	32.04	0.43	0.11
154	1142.7	53.6	2090.1	18.37	1.02	6.21	7.43	28.67	0.09	0.12
155	3300.0	48.2	2500.5	22.12	1.00	7.53	10.91	37.38	0.21	0.19
156	1456.6	20.8	1075.5	17.31	0.15	5.04	4.89	27.05	0.17	0.21
157	1295.2	17.3	889.9	14.67	0.02	3.83	5.16	30.23	0.23	0.15
158	1529.7	21.2	1029.8	14.79	0.02	4.64	3.63	29.72	0.13	0.13
159	1870.4	28.8	1313.6	14.57	0.21	4.40	5.64	26.88	0.10	0.12
160	590.8	12.1	707.6	6.47	*	1.26	1.08	20.30	0.01	0.03
161	523.6	9.7	817.6	5.74	*	0.62	0.04	7.41	0.03	0.01
162	1799.1	27.4	2461.6	15.31	0.81	5.51	6.07	27.72	0.23	0.19
164	1899.4	31.1	2965.3	32.22	170.20	538.88	89.10	119.19	10.73	10.11
166	853.8	19.0	1831.5	10.43	0.60	3.92	2.94	18.56	0.19	0.11
168	1481.5	37.4	3392.8	12.68	1.41	5.52	5.97	28.20	0.24	0.14
170	7622.7	514.4	55274.3	66.23	12.81	35.10	30.75	63.73	0.78	0.21
172	2968.8	38.4	3771.0	22.28	1.32	7.51	7.85	34.21	0.27	0.18
174	17489.4	260.0	27922.2	70.26	11.61	30.52	37.98	80.86	1.04	0.28
176	3586.5	39.5	4145.8	16.09	1.37	5.10	7.14	28.66	0.41	0.14
178	5218.1	46.7	4977.8	21.90	1.69	6.83	6.04	26.06	0.27	0.17
180	4772.3	91.6	6035.6	23.05	2.29	7.26	7.44	29.93	0.32	0.20
182	3681.9	43.1	4153.9	18.82	1.45	5.73	7.99	31.12	0.25	0.15
184	1867.5	27.1	2553.9	13.62	0.97	4.53	5.85	29.09	0.26	0.14
186	2087.4	29.9	2825.3	18.84	1.06	5.80	7.49	36.76	0.32	0.20
188	2021.4	28.4	2719.9	15.38	0.99	4.73	8.03	37.34	0.31	0.26
190	2454.6	35.8	3376.8	14.17	1.34	5.05	6.94	47.16	0.25	0.27
192	2416.4	32.0	3326.0	13.37	1.34	4.93	8.71	31.45	0.29	0.16
193	1683.9	25.2	2310.2	16.67	1.00	5.53	6.26	36.43	0.24	0.32
196	7514.2	131.3	13449.1	30.82	3.99	11.35	12.34	26.15	0.25	0.12
198	2112.5	28.3	2673.2	14.78	1.42	5.27	6.01	31.74	0.20	0.19
200	2548.5	34.5	1742.3	17.12	1.41	5.60	3.76	18.14	0.21	0.13

202	1277.3	20.2	963.5	10.60	0.61	3.58	2.97	26.87	0.16	0.18
204	15840.5	223.3	12324.2	46.74	6.83	17.68	16.76	39.94	0.29	0.17
206	17709.9	321.1	17487.4	52.24	9.57	21.88	24.32	44.45	0.46	0.18
208	6365.4	118.8	5755.0	35.16	2.83	18.96	9.43	35.24	0.43	0.28
210	7601.3	101.4	4856.4	50.32	2.50	18.97	11.12	75.24	0.50	0.70
212	14345.0	141.9	8160.7	39.75	3.38	13.74	12.08	36.47	0.35	0.21
214	1384.3	22.0	1144.9	12.00	0.56	4.58	10.79	45.31	0.26	0.27
216	2264.2	35.1	2027.1	12.49	0.88	4.58	8.85	43.61	0.25	0.26
218	5930.9	79.7	4764.6	31.25	2.29	11.31	21.93	74.76	0.51	0.46
219	1690.5	37.3	1877.1	25.10	0.90	8.36	15.80	75.65	0.58	0.46
220	1331.1	18.0	929.1	15.85	0.41	5.27	4.41	29.09	0.24	0.23
222	1930.5	20.0	936.9	19.56	0.63	6.59	5.89	30.12	0.25	0.31
224	3121.6	23.1	1334.0	8.06	0.64	3.11	3.68	17.99	0.21	0.08
226	1333.6	13.5	624.0	11.08	0.31	4.39	2.96	18.01	0.17	0.13
228	3571.9	38.1	1788.6	35.11	1.04	11.85	14.66	45.77	0.71	0.45
230	656.6	7.7	332.9	4.95	0.20	3.14	1.71	10.97	0.10	0.07
232	1151.5	15.3	610.4	15.33	0.78	6.01	9.23	59.32	0.37	0.34
234	1201.7	15.4	629.6	11.32	0.48	4.95	5.13	25.66	0.34	0.19
236	2419.2	27.0	1291.9	24.96	0.94	8.84	10.71	40.82	0.50	0.17
238	8.4	20.3	948.5	7.43	0.48	3.51	6.26	27.83	0.19	0.19
240	3044.0	31.9	1585.5	23.41	1.40	10.06	16.73	45.46	0.44	0.36
242	1972.1	23.1	1077.6	18.10	0.57	10.81	5.46	33.49	0.29	0.17
244	2056.8	21.9	1032.4	12.76	0.51	9.48	3.66	20.43	0.18	0.11
246	2059.4	19.9	993.3	0.02	0.46	3.86	4.47	21.74	0.21	0.07
248	2912.4	34.9	1660.2	0.03	0.92	7.21	8.05	34.88	0.30	0.12
250	2512.9	28.8	1337.8	0.02	0.70	7.76	6.07	22.64	0.33	0.11
252	1990.9	21.5	1010.1	0.02	0.53	6.92	5.06	24.03	0.20	0.13
254	881.7	10.1	475.1	0.01	0.24	2.66	1.87	7.75	0.07	0.03
256	1850.5	54.1	2473.7	0.04	1.72	11.35	17.70	52.70	0.55	0.14
258	2188.1	70.4	3206.7	0.04	2.27	14.33	35.55	53.69	0.58	0.40
260	1964.0	21.8	1025.5	0.02	0.69	7.30	11.94	29.93	0.62	0.09
262	1915.5	19.6	1020.9	8.83	0.67	4.06	13.95	35.34	0.26	0.09

264	3897.8	41.1	1976.7	25.77	1.68	12.96	15.63	48.57	0.36	0.17
266	2886.5	90.3	3828.5	36.52	3.64	17.66	23.63	59.79	0.55	0.20
268	2324.3	37.0	1835.4	21.48	1.30	9.45	14.98	32.58	0.31	0.14
270	3588.6	49.0	2315.4	27.97	1.84	17.98	19.95	48.80	0.51	0.37
272	1261.2	14.3	740.7	8.49	0.55	4.00	9.47	42.86	0.27	0.07
274	1837.9	18.9	963.6	9.95	0.79	6.38	27.71	47.22	0.24	0.13
276	5972.5	62.5	3004.5	24.06	2.61	13.95	12.08	45.81	0.45	0.15
278	3884.9	44.2	2421.7	16.72	1.70	6.77	8.71	22.28	0.35	0.07
280	5627.2	68.3	3061.2	44.32	4.03	21.12	20.20	44.92	0.58	0.18
282	3367.2	58.5	2647.1	18.24	2.39	13.26	27.87	56.99	1.44	0.23

Appendix B. The ICP-AES, ICP-MS operating conditions

ICP-AES applied operating conditions for the current study.

Int. Time	3 s
PMT Voltage	650 V
Power	1000 W
Plasma	15 L/min
Auxiliary	1.5 L/min
Pump	20
Sample Delay	10 s
Snout Purge	LOW
Stabilization time	15 s

ICP-MS applied operating conditions for the current study.

Power	1350 W
Plasma	13 l/min
Auxiliary	1 l/min
Nebuliser	1 l/min
Dwell time	10.2 ms (30 second acquire)
Sample uptake	1 ml/min

Appendix C . The equations used to calculate the trace metal budget in Red Sea.

Trace metal budget (t yr^{-1}) = (Surface water influx + Atmospheric dissolved dry deposition flux) – (Deep water efflux)

The flux (t yr^{-1}) were calculated as follows:

$$\text{Surface flux} = 497 * 315.36 * [M_{\text{sur}}]$$

$$\text{Deep flux} = 456 * 315.36 * [M_{\text{deep}}]$$

Atmospheric dissolved (“bioavailable”) flux (table 5.13)

Whereas;

$[M_{\text{sur}}]$: concentration of the metal in the surface layer in the Red sea ($\mu\text{g L}^{-1}$)

$[M_{\text{deep}}]$: concentration of the metal in the deep layer in the Red sea ($\mu\text{g L}^{-1}$)

$497 * 315.36 * 10^{12}$: the calculated surface influx (L yr^{-1}) using the estimates of the layer transport (Bethoux, 1988)

$456 * 315.36 * 10^{12}$: the calculated deep efflux (L yr^{-1}) using the estimates of the layer transport (Bethoux, 1988)

The product of the equation needs to be divided by 10^{12} to convert budget units from $\mu\text{g yr}^{-1}$ to t yr^{-1} .